

AD-A048 000

ROCKWELL INTERNATIONAL ANAHEIM CALIF AUTONETICS GROUP  
MICRO NAVIGATOR (MICRON) PHASE 2B VOLUME I. TECHNICAL REPORT.(U)  
AUG 77 J M MILLER, A P ANDREWS, T F BRASHER F33615-75-C-1301  
C75-787/201-VOL-1 AFAL-TR-77-138-VOL-1 NL

F/8 17/7

UNCLASSIFIED

1 OF 4  
AD  
A048000



AD 048000

AFAL-TR-77-138  
Volume I

①



# MICRO NAVIGATOR (MICRON) PHASE 2B

## Volume I — Technical Report

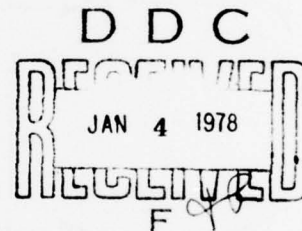
Autonetics Group  
Rockwell International  
3370 Miraloma Avenue  
Anaheim, CA 92803

August 1977

TECHNICAL REPORT AFAL-TR-77-138, VOLUME I

Final Report for the Period 5 August 1975 through 26 February 1977

Approved for public release; distribution unlimited.



**AIR FORCE AVIONICS LABORATORY  
AIR FORCE WRIGHT AERONAUTICAL LABORATORIES  
AIR FORCE SYSTEMS COMMAND  
WRIGHT-PATTERSON AFB, OHIO 45433**

NOTICE

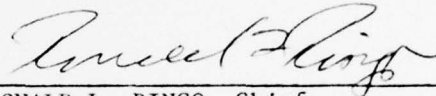
When Government drawings, specifications, or other data are used for any purpose other than in connection with a definitely related Government procurement operation, the United States Government thereby incurs no responsibility nor any obligation whatsoever; and the fact that the government may have formulated, furnished, or in any way supplied the said drawings, specifications, or other data, is not to be regarded by implication or otherwise as in any manner licensing the holder or any other person or corporation, or conveying any rights or permission to manufacture, use, or sell any patented invention that may in any way be related thereto.

This report has been reviewed by the Information Office (OI) and is releasable to the National Technical Information Service (NTIS). At NTIS, it will be available to the general public, including foreign nations.

This technical report has been reviewed and is approved for publication.



RONALD E. JANOSKO, Capt, USAF  
MICRON Project Manager, ADP-666A



RONALD L. RINGO, Chief  
Reference Systems Branch  
Reconnaissance & Wpn Delivery Div

FOR THE COMMANDER

"If your address has changed, if you wish to be removed from our mailing list, or if the addressee is no longer employed by your organization please notify AFAL/RWA, W-PAFB, OH 45433 to help us maintain a current mailing list".

Copies of this report should not be returned unless return is required by security considerations, contractual obligations, or notice on a specific document.

REPORT DOCUMENTATION PAGE		READ INSTRUCTIONS BEFORE COMPLETING FORM
1. REPORT NUMBER AFAL-TR-77-138, Volume I	2. GOVT ACCESSION NO.	3. RECIPIENT'S CATALOG NUMBER
4. TITLE (and Subtitle) MICRO NAVIGATOR (MICRON) PHASE 2B Volume I - Technical Report		5. TYPE OF REPORT & PERIOD COVERED Technical Report - Final, 5 Aug 1975 thru 25 Feb 1977
		6. PERFORMING ORG. REPORT NUMBER C75-787/201
7. AUTHOR(s) Joseph M. Miller, et al		8. CONTRACT OR GRANT NUMBER(s) F33615-75-C-1301
9. PERFORMING ORGANIZATION NAME AND ADDRESS Autonetics Group, Rockwell International 3370 Miraloma Avenue Anaheim, California 92803		10. PROGRAM ELEMENT, PROJECT, TASK AREA & WORK UNIT NUMBERS Project No. ADP 666A
11. CONTROLLING OFFICE NAME AND ADDRESS Air Force Avionics Laboratory Air Force Wright Aeronautical Laboratories Wright-Patterson AFB, Ohio 45433 AFAL/RWM-666A		12. REPORT DATE August 1977
		13. NUMBER OF PAGES 311
14. MONITORING AGENCY NAME & ADDRESS (if different from Controlling Office)		15. SECURITY CLASS. (of this report) Unclassified
		15a. DECLASSIFICATION DOWNGRADING SCHEDULE
16. DISTRIBUTION STATEMENT (of this Report)  Approved for public release, Distribution Unlimited.		
17. DISTRIBUTION STATEMENT (of the abstract entered in Block 20, if different from Report)		
18. SUPPLEMENTARY NOTES		
19. KEY WORDS (Continue on reverse side if necessary and identify by block number)		
Cost of Ownership	MICRON	
Engineering Prototype	MICRON	Navigation Performance
Mass Unbalance Modulation		Strapdown Inertial Navigator
Micro Electrostatic Gyro		Standard Navigator
Micro Navigator		Sure Start Gyro
20. ABSTRACT (Continue on reverse side if necessary and identify by block number)		
<p>The Micro Navigator (MICRON) is a low-cost, highly reliable, and moderately accurate strapdown inertial navigator. The heart of the MICRON system is the micro-electrostatic gyro (MESH), an instrument which incorporates an all-attitude, whole-angle readout from an electrostatically suspended rotor. Under previous Air Force contracts two developmental navigation systems (N57A-1 and N57A-2) were designed, fabricated, and flight tested. Two gyro subassemblies for developmental testing were designed, fabricated, and integrated.</p>		

The overall objective of the MICRON Phase 2B contract was to design, develop, fabricate, and integrate the Engineering Prototype MICRON (EPM) and its associated software and test equipment. The specific objectives were to develop a MICRON system resulting in high reliability, ease of maintenance, low acquisition cost, and moderate performance, and be a potential candidate as the inertial navigation unit (INU) for the F-16.

One EPM was designed, fabricated, assembled, and integrated. The EPM meets the performance requirements of the Phase 2B contract and the F-16 packaging envelope requirements. Spares were fabricated and tested to support maintenance of the EPM. Test Equipment, system software, and test station software were developed and verified.

System analyses, studies, and tradeoffs were made which resulted in improved accuracy, reliability, producibility, and life cycle costs. Design specifications were prepared and maintained.

Integration testing was conducted to establish system compatibility and operability. Seventeen navigation performance runs, including two demonstration runs, were made during integration testing. Position and velocity errors were well within (approximately one-half) the contract requirement.

ACCESSION for	
NTIS	White Section <input checked="" type="checkbox"/>
DDC	Buff Section <input type="checkbox"/>
UNANNOUNCED	<input type="checkbox"/>
JUSTIFICATION	
BY	
DISTRIBUTION/AVAILABILITY NOTES	
Dist.	OTAL
A	

B

CLASSIFICATION

## FOREWORD

This report was prepared under Air Force Contract F33615-75-C-1301, Project No. ADP 666A and covers work performed by the Autonetics Group of Rockwell International, 3370 Miraloma Avenue, Anaheim, Ca 92803, for the Air Force Avionics Laboratory, Wright-Patterson Air Force Base, Ohio. This final report consists of two volumes of which this is Volume I. The titles of the volumes are:

Volume I      Technical Report

Volume II     Appendices

The purpose of the MICRON Phase 2B contract was to design, develop, fabricate, and integrate the Engineering Prototype MICRON (EPM) and its associated software and test equipment. The MICRON is a low cost, highly reliable, moderately accurate inertial navigation system which utilizes electrostatic gyroscopes (ESG).

This program was conducted from 5 August 1975 through 25 February 1977. It was directed by the MICRON Program Manager, J. A. Schwarz; the MICRON Assistant Program Manager, J. E. Menzel; the Engineering Manager, A. P. Truban; and the Project Engineer, G. E. Runyon. The cognizant Air Force Project Managers on this phase of the MICRON program were Captain W. G. Peterson and Captain R. F. Janosko, AFAL/RWA-666A. The contractor submitted the draft of this report in May 1977. The contractor's final submittal date of this report was August, 1977.

The principal contributors to this report were A. P. Andrews, T. F. Brasher, H. L. Bump, J. D. Courtier, K. J. Gibson, F. J. Gulde, F. R. Hall, D. W. Holmes, K. K. Jin, L. E. Johnsen, J. Jurison, J. F. Klinchuch, and J. M. Miller.

This report has been assigned the Internal Rockwell Control Number, C75-787/201. All correspondence relating to this document should reference this number.

CLASSIFICATION TITLE

CLASSIFICATION



## TABLE OF CONTENTS

<u>Sections</u>	<u>Page</u>
I. Introduction and Summary .....	1
1.1 Introduction .....	1
1.2 Summary .....	2
1.2.1 Program Summary .....	2
1.2.2 Highlights and Conclusions .....	2
1.2.3 Summary by Statement of Work Tasks .....	2
II. Task 1, Prime Mission Product .....	7
2.1 Task 1.1, Inertial Navigation Unit (INU) .....	7
2.1.1 INU Error Analysis and Error Budget .....	7
2.1.2 INU CI Specification .....	20
2.1.3 INU Detail Design Specifications .....	21
2.1.4 MHU Design/Develop/Fab/Test .....	24
2.1.5 SEU Design/Develop/Fab/Test .....	36
2.1.6 IAU Design/Develop/Fab/Test .....	55
2.1.7 DPU Design/Develop/Fab/Test .....	85
2.1.8 IOU Design/Develop/Fab/Test .....	100
2.1.9 PSU Design/Develop/Fab/Test .....	116
2.1.10 Fabrication of MESSAGES for Second Source .....	124
2.2 Task 1.2, Inertial Navigation Battery Unit (INBU) .....	124
2.2.1 Detail Design Specification for Mount .....	124
2.2.2 Fab/Procure Mount .....	124
2.3 Task 1.3, Control/Navigation Panel (CNP) .....	124
2.4 Task 1.4, Software .....	127
2.4.1 INU Software .....	127
2.4.2 Test Station Software .....	160
2.5 Task 1.5, Integration .....	182
2.5.1 Test Equipment Checkout .....	183
2.5.2 Integrated Wiring Test .....	183
2.5.3 INU Mechanical Interface Test .....	183
2.5.4 Power Verification Test .....	183
2.5.5 Timing and Sequencing Test .....	183
2.5.6 DPU and System Electronics Verification .....	184
2.5.7 Flight Tape Checkout .....	186
2.5.8 Rotating EPM Integration .....	187
2.5.9 Thermal Control Tests .....	187

## TABLE OF CONTENTS (Cont)

<u>Section</u>	<u>Page</u>
2.5.10 BITE Verification .....	188
2.5.11 Spin Motor Electronics Checkout .....	188
2.5.12 MUM Demod and A/D Converter Checkout .....	189
2.5.13 Rotating IAU Integration .....	189
2.5.14 EMA Verification .....	190
2.5.15 Fast Warm-up Heater Checkout .....	190
2.5.16 System Computer Operation Without Control Panel .....	190
2.5.17 MESH Verification .....	191
2.5.18 Calibration and Navigation Software Checkout .....	192
2.5.19 Calibration Verification Testing .....	196
2.5.20 Initialization, Alignment, and Navigation Verification ..	196
2.5.21 Multi-Heading Navigation Testing .....	197
2.5.22 Fast Reaction Summary .....	199
2.5.23 Navigation Performance Summary .....	199
 III. Task 3, Test and Evaluation .....	 201
3.1 Task 2.1, Test Plans .....	201
3.2 Task 2.2, Developmental Test .....	202
3.2.1 Second Source Rotor and Cavity Tests .....	202
3.2.2 Non-destructible Rotor and Cavity Tests .....	212
3.3 Task 2.3, System Laboratory Test .....	212
3.4 Task 2.4, Mobile Test .....	212
3.5 Task 2.5, Contractor Flight Test .....	212
 IV. Task 3, Support Hardware .....	 213
4.1 Task 3.1, Engineering Test Equipment .....	213
4.1.1 Software Test Station .....	213
4.1.2 Electronics Test Equipment .....	217
4.1.3 DPU Engineering Test Equipment .....	222
4.2 Task 3.2, INU Test Station .....	225
4.2.1 STS Specification .....	225
4.2.2 EPM STS Configuration .....	225
4.3 Task 3.3, Repair .....	228
 V. Task 4, Air Force Flight Test .....	 233

**TABLE OF CONTENTS (Concluded)**

<u>Section</u>	<u>Page</u>
VI. Task 5, System Management .....	235
6.1 Task 5.1, Program Management .....	235
6.1.1 Design Reviews .....	235
6.1.2 Program Plans .....	248
6.1.3 Work Breakdown Structure .....	248
6.2 Task 5.2, Associate Contractor Support .....	248
6.2.1 Drawings and Specifications .....	248
6.2.2 Associate Contractor Visits to Autonetics .....	249
6.2.3 Support to Reliability Associate Contractor (Martin Marietta Corporation) .....	250
6.2.4 Other Associate Contractor Support Activities .....	250
6.3 Task 5.3, Cost of Ownership .....	251
6.3.1 Producibility .....	251
6.3.2 Reliability .....	252
6.3.3 Maintainability .....	255
6.4 Task 5.4, Parts Program .....	259
6.4.1 Parts Selection .....	259
6.4.2 A/D Converter MOS Circuit .....	260
6.4.3 Spin Motor MOS Circuit .....	262
6.4.4 INU MOS Circuits .....	262
VII. Task 6, Data .....	267
VIII. Changes in Key Personnel .....	271
IX. Trips, Meetings, and Conferences .....	273
X. Program Schedule .....	285
References .....	293

## LIST OF ILLUSTRATIONS

<u>Figures</u>	<u>Page</u>
1. EPM Functional Block Diagram .....	8
2. Peak Ensemble RMS Velocity Error Vs CEP Rate for LAX Flight Tests .	11
3. INU Major Components .....	22
4. INU Functional Diagram .....	23
5. INS Installation Control Drawing .....	25
6. N72 INU Inboard Profile .....	27
7. Master Interconnect Board (MIB) .....	28
8. INS Installation Control Drawing (10214-111 Rev B) .....	31
9. N73 INU Inboard Profile .....	33
10. N73 Mechanical Housing Unit (Front View) .....	34
11. N73 Mechanical Housing Unit (Back View) .....	34
12. Major Components of N73 INU .....	35
13. MLB Construction .....	37
14. Suspension and MUM Electronics Functional Block Diagram (SEU 1 and 2) .....	38
15. MUX Interconnect Diagram .....	40
16. Modulator Output and Preload Signals .....	41
17. Suspension Servo Charge Amplifier Pulse Amplitude Waveform .....	42
18. Suspension and MUM Electronics Module (SEU 1 and 2) .....	44
19. Timing and Sequencing Functional Block Diagram (SEU 3) .....	46
20. Timing and Sequencing Module (SEU 3) .....	50
21. Signal Generator and Memory Functional Block Diagram (SEU 4) .....	52
22. Signal Generator and Memory Module (SEU 4) .....	54
23. IAU Interface (Non-Rotating) .....	56
24. Rotating Instrument Assembly Unit (Exploded View) .....	57
25. IAU Functional Block Diagram .....	58
26. Rotating Instrument Assembly Unit (IAU) .....	59
27. High Voltage Waveforms .....	61
28. Charge Amplifier Module (Front Side) .....	62
29. Charge Amplifier Module (Back Side) .....	62
30. Spin Motor Electronics Subassemblies .....	64
31. Rotor Speed Vs Time, Rotor Brake Test .....	65
32. A77M EMA, MICRON Phase 2B .....	67
33. A77M EMA Outline and Electrical Interface .....	68
34. A77M-7602-002 Fast Reaction Tests .....	71
35. Fast Reaction from 0°F to 160°F at 0g Input .....	72
36. A77M EMA Threshold Test .....	73
37. Assembled A77 EMA .....	74
38. Exploded View of A77M EMA .....	75
39. EPM Electrostatic Gyro (ESG) Assembly .....	78
40. EPM ESG with Spin Motor Detached .....	78
41. Temperature Ramp Test .....	80
42. Z-Coil Heating Tests .....	82
43. Gap Vs Time, Rotor Heating Tests .....	83
44. DPU Functional Diagram .....	86
45. Central Processor Unit (Front Side) .....	87
46. Central Processor Unit (Back Side) .....	87

## LIST OF ILLUSTRATIONS (Cont)

<u>Figures</u>	<u>Page</u>
47. Processor Memory Module (Front Side) . . . . .	88
48. Processor Memory Module (Back Side) . . . . .	88
49. Processor Input/Output (Front Side) . . . . .	89
50. Processor Input/Output (Back Side) . . . . .	89
51. DPU Semiconductor Memory Organization . . . . .	92
52. MICRON DPU Test Flow . . . . .	96
53. Modified Test Fixture for DPU Temperature Testing . . . . .	98
54. Test Conditions for Voltage Extremes . . . . .	99
55. Digital/Synchro Converter Block Diagram . . . . .	104
56. Converter Module . . . . .	107
57. Data Terminal Organization . . . . .	109
58. DTU Input Z Vs Frequency . . . . .	110
59. Transmitter/Receiver Functional Block Diagram . . . . .	111
60. Encoding Logic Functional Block Diagram . . . . .	112
61. Decoding Logic Functional Block Diagram . . . . .	113
62. SSIU Functional Block Diagram . . . . .	114
63. Data Terminal Unit (Front Side) . . . . .	115
64. Data Terminal Unit (Back Side) . . . . .	115
65. Functional Diagram of Power Supply Configuration Selected for EPM . . .	117
66. Functional Diagram of Power Supply Configuration Evaluation for EPM . .	118
67. Functional Diagram of Power Supply Configuration Evaluated for EPM . .	119
68. EPM Power Supply Unit . . . . .	123
69. CDU/Memory Adapter . . . . .	126
70. EPM Fast Cycle - Normal Structure . . . . .	130
71. NAV Program Timing . . . . .	150
72. Read-Only Memory Utilization . . . . .	157
73. Read/Write Memory Utilization . . . . .	158
74. Start Mode Foreground Execution Times . . . . .	161
75. Align and Navigate Mode Foreground Execution Times . . . . .	162
76. Gyro No. 1 Drift Calibration Residuals Using Drift Model K46 . . . . .	166
77. Gyro No. 2 Drift Calibration Residuals Using Drift Model K46 . . . . .	167
78. Gyro No. 1 Drift Calibration Residuals Using Drift Model K73 . . . . .	170
79. Gyro No. 2 Drift Calibration Residuals Using Drift Model K73 . . . . .	171
80. Encoder Readouts - First Run . . . . .	180
81. Encoder Readout During Turnaround . . . . .	181
82. Polhode Signature Northrop N0009/NA11 . . . . .	203
83. Polhode Signature Northrop N0010/NA22 . . . . .	203
84. Polhode Signature MICRON A015Y Series . . . . .	203
85. Software Test Station Block Diagram . . . . .	214
86. Software Test Station . . . . .	215
87. Processor Control Panel . . . . .	216
88. Performance Card in Use with DATE . . . . .	223
89. DPU System Test Fixture with DPU and Interface Boards . . . . .	224
90. EPM System Test Station . . . . .	226
91. Power Supply Packaging Sensitivity Study . . . . .	257
92. Power Supply Redundancy Guidelines . . . . .	258
93. Life Cycle Cost Vs Calibration Stability . . . . .	258

LIST OF ILLUSTRATIONS (Concluded)

<u>Figures</u>	<u>Page</u>
94. Life Cycle Cost Vs Failure Rate .....	259
95. Functional Block Diagram of 65008 Chip .....	261
96. Functional Block Diagram of Spin Motor Control MOS Chip .....	263
97. Block Diagram of METG Device .....	265
98. Block Diagram of QRFG Device .....	266
99. Phase 2B MICRON Data Schedule .....	270
100. Program Schedule .....	286
101. Standard Milestone Symbols .....	292

## LIST OF TABLES

<u>Table</u>	<u>Page</u>
1. Summary of Phase 2B EPM Performance Requirements (to be Verified by Error Analysis) . . . . .	9
2. Summary of Phase 2A Performance Requirements . . . . .	10
3. Peak Ensemble RMS Velocity Errors, Phase 1A . . . . .	10
4. MESGA Error Budget . . . . .	13
5. EMA Error Budget . . . . .	13
6. Segments Approximating INS Route No. 6 . . . . .	15
7. MICRON Phase 2A Error Budget Updated . . . . .	16
8. Major Contributors to Peak Ensemble RMS velocity Error (Greatest to Least Significant) . . . . .	19
9. SMUM Self Test . . . . .	43
10. Test Results of "Halex Substrate" Digitizer . . . . .	69
11. A77M EDM Functional and Engineering Test Results . . . . .	70
12. A77M EMA, Power Interrupt Repeatability . . . . .	76
13. Results of Motor Tests . . . . .	82
14. MICRON CPU MOS Components . . . . .	90
15. Test Conditions . . . . .	95
16. Analog Outputs . . . . .	101
17. Analog Output Provisions . . . . .	102
18. DAC Accuracy Test Results . . . . .	105
19. Analog Input Provisions . . . . .	105
20. Discrete Inputs . . . . .	105
21. Discrete Input Provisions . . . . .	106
22. Discrete Outputs . . . . .	106
23. Discrete Output Provisions . . . . .	107
24. Power Characteristics and Consumptions . . . . .	121
25. Program Mode Control . . . . .	132
26. Program Commands . . . . .	134
27. Printer Control . . . . .	135
28. Start Mode Commands . . . . .	135
29. CDU Display During Start, Nav Standby, and Cal Data Collection . . . . .	136
30. CDU MODE STATUS Display . . . . .	136
31. PDO Discrete Output (OM Commands) . . . . .	137
32. RDO Discrete Output (WDO Command with PDO Enable) . . . . .	137
33. SDO Discrete Output (WDO Command With PDO Eanble) . . . . .	138
34. MDO Discrete Output (I/O Word 114) . . . . .	139
35. TDO Discrete Output (I/O Word 17) . . . . .	139
36. Discrete Inputs . . . . .	140
37. Status Input Discretets . . . . .	142
38. Interrupt Assignments . . . . .	144
39. Demod Frequency Usage . . . . .	146
40. Read-Only Memory Requirements . . . . .	159
41. Functional Formulas for Drift Model K73 . . . . .	169
42. EPM Navigation Performance Summary . . . . .	200
43. Northrop Items Received for Evaluation . . . . .	202
44. MESG Parameter Measurements . . . . .	203

**LIST OF TABLES (Concluded)**

<u>Table</u>	<u>Page</u>
45. Results of Angle and Drift Calibration Tests; Series of Four Consecutive Tests (Gyros NA0009 and NA0010) . . . . .	205
46. Drift Parameter Comparisons Between Successive Drift Calibrations, Gyro NA-0009 . . . . .	206
47. Drift Parameter Comparisons Between Successive Drift Calibrations, Gyro NA-0010 . . . . .	207
48. Overall Ranking of Parameters by RMS Drift Effect, Gyros NA-0009 and NA-0010 . . . . .	208
49. Equivalent Drift Rate Changes Between Successive Drift Calibrations, Gyro NA-0009 . . . . .	209
50. Equivalent Drift Rate Changes Between Successive Drift Calibrations, Gyro NA-0010 . . . . .	210
51. Overall Rankings of Parameters by Equivalent Drift Rate Changes, Gyros NA-0009 and NA-0010 . . . . .	211
52. Overall Summary of Angle and Drift Calibrations, Gyro NA0009 and NA0010 . . . . .	212
53. Special Tooling Fabricated for Module Assembly . . . . .	217
54. Hybrid and MLB Functional and Screen Test Equipment . . . . .	218
55. Test Aids . . . . .	225
56. Phase 2B Reliability MTBF Apportionment - MICRON (ACF) INU . . . . .	252
57. Reduced Module Size Impact on Life Cycle Cost . . . . .	257

## LIST OF ABBREVIATIONS

AB	Accumulator and Buffer
AC	Algorithm Control
ACF	Air Combat Fighter
A/D	Analog-to-Digital
ADC	Analog-to-Digital Converter
BCD	Binary-Coded Decimal
BITE	Built-in Test Equipment
BL	Beam Lead
BLSJ	Beam Lead Sealed Junction
BU	Battery Unit
CASC	Counter and Automatic Sequencer Control
CCP	Computer Control Panel
CCS	Calibration Constant Storage
CDRL	Contract Data Requirement List
CDU	Control Display Unit
CEB	Candidate Error Budget
CEP	Circle Error, Probable
CI	Configuration Item
CNP	Control/Navigation Panel
CPC	Ceramic Printed Circuit
CPU	Central Processor Unit
CSDL	Charles Stark Draper Laboratory
CU	Converter Unit
C&W	Chip and Wire
DAC	Digital-to-Analog Converter
DATE	Digital Automatic Test Equipment
DL	Decoding Logic
DMA	Direct Memory Access
DMAC	Direct Memory Access Control
DPU	Dedicated Processor Unit

LIST OF ABBREVIATIONS (Cont)

DTU	Data Terminal Unit
EAROM	Electrically Alterable Read Only Memory
EDM	Engineering Development Model
EL	Encoding Logic
EMA	Electromagnetic Accelerometer
EPM	Engineering Prototype MICRON
EPROM	Erasable PROM
ESG	Electrostatic Gyro
ESGM	Electrostatic Gyro Marine
ESWA	Engineering Shop Work Authorization
FET	Field - Effect Transistor
FRR	Form for Removal Reporting
GFE	Government Furnished Equipment
GSA	Gyro Subassembly
HAFB	Holloman Air Force Base
HGSA	HAFB Gyro Subassembly
IAU	Instrument Assembly Unit
IC	Integrated Circuit
IMU	Inertial Measuring Unit
INBU	Inertial Navigation Battery Unit
INS	Inertial Navigation Set
INT	Interrupt
INU	Inertial Navigation Unit
I/O	Input/Output
IR&D	Independent Research and Development
IUS	Interim Upper Stage
LAD	Logic and Adder
LAX	Los Angeles International Airport
LCC	Life Cycle Cost
LSB	Least Significant Bit
LSI	Large Scale Integration
MESG	Micro Electrostatic Gyro

### LIST OF ABBREVIATIONS (Cont)

MESGA	Micro Electrostatic Gyro Accelerometer
METG	MUM and EMA Timing Generator
MHU	Mechanical Housing Unit
MIB	Master Interconnect Board
MICRON	Micro Navigator
MLB	Multi-layer Board
MMC	Martin Marietta Corporation
MOS	Metal Oxide Semiconductor
M&P	Materials and Process
MPC	Micro Program Control
MSI	Medium Scale Integration
MSB	Most Significant Bit
MTBF	Mean-Time-Between-Failures
MTU	Multiplex Terminal Unit
MUAR	Mass Unbalance Attitude Readout
MUM	Mass Unbalance Modulation
MUX	Multiplexer
MXF	Multiplexer Four
NRZ	Non-Return-to-Zero
N77	Model number of ESG Inertial Navigation System developed by Autonetics prior to the Engineering Prototype Model (EPM)
PCB	Printed Circuit Board
PCT	Program Counter and Timer
PDO	Processor Discrete Output
PIO	Processor Input/Output
PM	Processor Memory
PMOS	P-Type Metal Oxide Semiconductor
PPM	Parts Per Million
PROM	Programmable Read Only Memory
PSU	Power Supply Unit
QRFG	Quasi-Reference Frequency Generator
RADC	Rome Air Development Center

CLASSIFICATION

**LIST OF ABBREVIATIONS (Concluded)**

RAM	Random Access Memory
RCA	Radio Corporation of American
RCP	Rotational Closure Point
R&D	Research and Development
RIW	Reliability Improvement Warranty
RLG	Ring Laser Gyro
RMS	Root-Mean-Square
ROM	Read Only Memory
RS	Register Storage
RSS	Root-Sum-Square
SAMUS	State Space Analysis of Multisensor Systems
SDO	Sequencer Discrete Output
SEU	System Electronics Unit
SF	Scale Factor
SMC	Spin Motor Control
SMPA	Spin Motor Power Amplifier
SMUM	Suspension and MUM
SOW	Statement of Work
SRU	Shop Replaceable Unit
SSI	Small Scale Integration
SSIU	Subsystem Interface Unit
SSM	Strapdown System Monitor
STS	System Test Station
TCI	Test Code Indicator
TD	Torque Disturbance
T/R	Transmitter/Receiver
TRCG	Timing and Reference Generator Control
T/S	Test Station
TSO	Time Sharing Option
TTL	Transistor-Transistor Logic
WBS	Work Breakdown Structure

## SECTION I

### INTRODUCTION AND SUMMARY

#### 1.1 INTRODUCTION

The objective of the MICRON Phase 2B contract was to develop the Engineering Prototype MICRON (EPM) and its associated electronics, software, and test equipment. The specific objectives were to develop a MICRON system resulting in high reliability, ease of maintenance, low acquisition cost, and moderate performance, and be a potential candidate as the inertial navigation unit (INU) for the F-16.

The MICRON Phase 2B EPM consists of an INU; an Inertial Navigation Battery Unit (INBU), which is a mount for the INU; a Battery Unit (BU); a Control/Navigation Panel (CNP), which provides the primary operator-to-MICRON interface; and a System Test Station (STS), which provides a secondary operator-to-MICRON interface. The INU consists of the Mechanical Housing Unit (MHU), the Systems Electronics Unit (SEU), the Dedicated Processor Unit (DPU), the Input/Output Unit (IOU), the Instrument Assembly Unit (IAU), and the Power Supply Unit (PSU).

The MICRON INU features two Micro Electrostatic Gyros (MESGs) and three Electromagnetic Accelerometers (EMAs) with associated electronics operating in a strapdown mode. When the MESG attitude data and the EMA delta velocity data are processed by the DPU, the system will provide accurate position, velocity, acceleration, attitude and other information to be used for guidance, navigation, weapon delivery, cargo delivery, reconnaissance, sensor pointing, and radar stabilization. Typical MICRON applications will include strategic cruise missiles, interceptors, fighter-bombers, transports, close air support aircraft, helicopters, drones, and remotely piloted vehicles.

Under previous Air Force contracts, gyro drift-rate calibration programs have been developed and performance tests of the gyro and its suspension and MUM pickoff electronics have been performed. Two developmental navigation systems (N57A-1 and N57A-2) were designed, fabricated, and flight tested. Two gyro subassemblies (GSA) were designed, fabricated, and integrated. One GSA was used for MESGA development testing and one was used for 4-plate gyro and electronics development.

Under the Phase 2B contract, the following tasks were performed:

1. Prime Mission Product - INU, INBU, CNP, Software, Integration
2. Test and Evaluation
3. Support Hardware
4. AF Flight Test (None specified)
5. System Management
6. Data

This report is arranged according to tasks.

## 1.2 SUMMARY

### 1.2.1 Program Summary

Phase 2B contract activities commenced on 5 August 1975. EPM integration testing began in early June 1976. Demonstration navigation runs were conducted in December 1976. Direction was received in a 10 February 1977 meeting at WPAFB to proceed in accordance with a revised contract statement of work. The contract requirements reflected in this report have been changed to reflect the revised statement of work as documented in Autonetics letter 77AN69052 dated 11 March 1977.

### 1.2.2 Highlights and Conclusions

A strapdown navigation system was designed, fabricated, and tested which meets the navigation performance requirements of the Phase 2B contract and the F-16 packaging envelope requirements. Two demonstration navigation runs were performed in accordance with the contract which verified the system met the performance requirements. Additional navigation performance runs were made which also demonstrated CEP rate and velocity error well within the contract requirements. The CEP error rate and velocity error for 17 navigation runs demonstrated actual errors of about one-half the allowable errors.

### 1.2.3 Summary by Statement of Work Tasks

Under Task 1, Prime Mission Product, the MICRON System Specification was prepared and submitted in November 1975 as CDRL Item A008. The EPM INU CI Development Specification and the DPU CI Development Specification were also prepared and submitted in November 1975 as CDRL Items A007 and A006, respectively. In addition, nine detail design specifications were prepared and maintained for appropriate subelements of the EPM INU.

INU error analysis and error budget activities were performed to predict the performance characteristics of the EPM and to allocate subsystem error budgets. The error analysis program (SAMUS) was modified to agree with the EPM design. The only new performance requirement that was difficult to meet was the peak ensemble rms velocity error. This requirement was met by implementing a rotating instrument cluster which was the most cost effective and least schedule perturbing means of meeting the velocity accuracy requirement.

During the design phase, tradeoff studies were conducted to determine the lowest cost and most reliable EPM configuration. Thermal analyses, stress analyses, and mass properties analyses were performed. The design and development of the INU underwent major changes from the initially proposed system in order to reflect the F-16 unique requirements. In particular, the F-16 system package size resulted in a total repartitioning of the system. The requirement for 115 v 400 Hz primary power and 28 vdc backup required power supplies to be completely redesigned. In addition to these initial changes, as noted in the above paragraph, rotation of the IAU was subsequently implemented to achieve the velocity accuracy requirements.

The MHU chassis, MIB, IAU, and INU electronics were designed and fabricated under this task. Thirty-one different hybrids were designed and a total of 138 hybrids, including spares, were fabricated, assembled, and tested. Sixteen

different electronic module assemblies were designed and a total of 34 of these assemblies, including spares, were fabricated, assembled, and tested. All hybrids and electronic modules were functionally and screen tested per ESWA documentation and all successfully met test requirements derived from the detail design specifications.

A total of six MESH's (including four spares) were assembled and tested for the EPM. In addition, Phase 2A instruments were upgraded to the EPM configuration. MESH Phase 2B activities included the development of the narrow groove cavity, small gap gyro, sure start gyro, fast reaction rotor, motor development, and heater incorporation. Fabrication of MESH's, rotors, and cavities to support second-source and non-destructible rotor and cavity efforts was also accomplished under this task.

Six EMA's (including three spares) were assembled and tested for the EPM. In addition, two EMA engineering development models were completed and functional and performance evaluation tests were conducted. EMA development activities addressed reduced costs, fast reaction performance, and improved stability and repeatability.

Under subtask 1.2, a detail design specification for the Inertial Navigation Battery Unit (INBU) was prepared. One INBU, including the Battery Unit, was assembled.

Under subtask 1.3, the CDU/Memory Adapter was designed, fabricated, assembled, and checked out. The CDU Memory Adapter provides the interface from the MICRON computer to the CDU. No modification to the N57A CDU was required for it to meet its function.

Under subtask 1.4, INU and test station software was developed. The INU software was designed according to the requirements in the INU CI Specification. INU program requirements were defined, coded, checked out, and verified in system integration testing. A new assembler and associated support software were developed, verified, and completely documented. The INU software is completely described in Para 2.4.1, including DPU memory allocation and software execution timing data. Detailed flow charts of all INU programs are presented in Appendices G through L.

During the course of Phase 2B, many diverse test station software programs were developed and implemented in the MICRON Lab HP2100 computer system. These programs were used in integration, calibration, and diagnosis of the EPM sensors, and for aiding INU software development. The various tasks which have been performed are described in detail in Para 2.4.2.

Under subtask 1.5, integration testing was conducted to establish compatibility and operability of the INU, INBU, BU, CDU, STS, and software. The detail design specifications were updated to reflect changes made during the test program. Two demonstration navigation runs required by the contract were performed. The position error CEP rate for these two runs was 0.71 nmph. This was within the 1.0 nmph allowable error. A total of 17 navigation performance runs were made during integration testing. Ensemble position and velocity errors were well within (approximately one-half) the contract requirement and goals. This performance is summarized below.

	Contract Requirement	Goal	EPM 1 Performance
Position Error Rate CEP (nmph)			
1st Hour	1.0	0.8	0.36
Total Run	1.5	1.0	0.41
Time RMS Velocity Error (FPS)			
North Channel	3.0	2.5	1.66
East Channel	3.0	2.5	1.06

Under Task 2, Test and Evaluation, test plans were prepared and submitted in April 1976 as CDRL Item A00D. The test plans were the MICRON EPM Integration Test Plan, the MESG Test Plan, and the A77M Accelerometer Test Plan. A test plan for EPM laboratory testing was prepared and a partial submittal made in February 1977 as CDRL Item A00D. Due to the revised contract statement of work, the remaining portion of this test plan activity was stopped. Under the Developmental Test subtask, all parts received from the second-source were evaluated. Component level evaluation showed that all parts were good for instrument use with regard to size, roundness, surface finish, and general integrity. Two gyros were assembled using second-source rotors and cavities. Prefunctional tests and four complete sets of angle and drift calibrations were performed on each of the two instruments. Both gyros successfully met the repeatability test requirements. Four rotors and two cavity sets were received from CSDL in February 1977. Assembly of these parts into the MESG configuration was initiated but further activity was terminated per the Ref 5 revised statement of work.

Under Task 3, Support Hardware, a cost effective tool for software development and checkout was created by converting the existing MICRON test console and processor to a Software Test Station. The station was completed in December 1975 and was successfully used for software development. Design, fabrication, and checkout of all the electronics test equipment for hybrid and MLB functional and screen testing was successfully completed. DPU test equipment and software was developed under this task as well as various test aids required to support integration. A CI specification was prepared to define the EPM System Test Station (STS). Design and fabrication of the STS was completed making maximum use of equipment from previous MICRON contracts. The STS was successfully used in integration testing of the EPM system. Repair activity included repair of N57A and Phases 2A and 2B hardware.

Under Task 4, Air Force Flight Test, no activity was planned for Phase 2B.

Under Task 5, System Management, 10 informal design reviews and one Phase 2B Fee Evaluation/Design Review meeting were conducted at Autonetics. The MICRON Phase 2B Program Plan was prepared and submitted in September 1975. A detailed work breakdown structure was prepared and submitted in August 1975 as CDRL Item A003.

Autonetics provided support to the associate contractors for MESH second-source and non-destructible rotor and cavity efforts. Revised drawings and specifications for MESH rotors and cavities were submitted as required. Drawings, specifications, and manuals describing the Autonetics owned Automatic Cavity Grinder were submitted in February 1976 as CDRL Item A00H.

During the period 5 August through 30 September 1975, contractual cost of ownership activities were performed in support of the EPM design task by trading off producibility, reliability, and maintainability parameters. A parts program was also conducted during this period to support the cost of ownership team in the selection of parts. Also under this task, the developments (initiated under Phase 2A) of the MOS A/D converter, spin motor control circuit, and INU MOS chips were completed.

Under Task 6, Data, 82 Phase 2B data items were submitted. A list of these data items, along with the submittal dates, is given in Section 7.

A complete schedule of the major milestones of the Phase 2B program, by task, is given in Section 10.



## SECTION II

### TASK 1. PRIME MISSION PRODUCT

#### TASK 1.0, MICRON SYSTEM SPECIFICATION

Under Task 1.0, Autonetics developed a MICRON System Specification which describes the general physical, electrical, and mechanical interfaces between the Inertial Navigation Unit (INU), Inertial Navigation Battery Unit (INBU), Battery Unit (BU), Control/Navigation Panel (CNP), and System Test Station (STS).

The MICRON System Specification (AJ00088) was submitted in November 1975 as CDRL Item A008. This specification was reviewed at the December 1975 informal design review and was found satisfactory.

The electrical interconnects between the INU, INBU, BU, CNP, and STS are shown in Figure 1. The detailed signal interface and mechanical interfaces are also included in the system specification; however, they are not reproduced here and the reader is referred to the specification for details.

#### 2.1 TASK 1.1, INERTIAL NAVIGATION UNIT (INU)

In Task 1.1, Autonetics conducted an error analysis and developed an error budget for the INU, developed an INU specification, designed and developed the INU, developed detail design specifications for the INU SRU's, and designed, developed, fabricated, and tested SRU's and spares for the INU. MESH parts to support second-source and non-destructible gyro efforts were also fabricated under this task. These activities are discussed in detail in the following sections.

##### 2.1.1 INU Error Analysis and Error Budget

###### 2.1.1.1 Objective

The objective of this task was to use the error analysis programs developed under previous contracts for accurately predicting the performance characteristics of the Engineering Prototype MICRON (EPM), and for allocating subsystem error budgets such that the EPM system will meet its performance requirements.

###### 2.1.1.2 Background

Under previous contracts, a computer program had been developed for error analysis of strapdown ESG navigation systems. This program utilizes the generalized error analysis program for State-space Analysis of Multi-sensor Systems (SAMUS), which had been developed at Autonetics. The specialized models for strapdown ESG errors had been developed for the specific application to MICRON under contracts in previous development phases. These models characterize the errors of an instrument configuration "strapped" to the airframe, but with the spin axes of the two ESG's unconstrained from maintaining fixed inertial directions. The models take into account random attitude variations about the flight path, and the changes in mean attitude with changes in the flight path. This error analysis program had been used in developing the N57A error budget, and in developing the error analysis for preliminary design under Phase 2A. However, the MICRON performance requirements were changed at the start of Phase 2B.

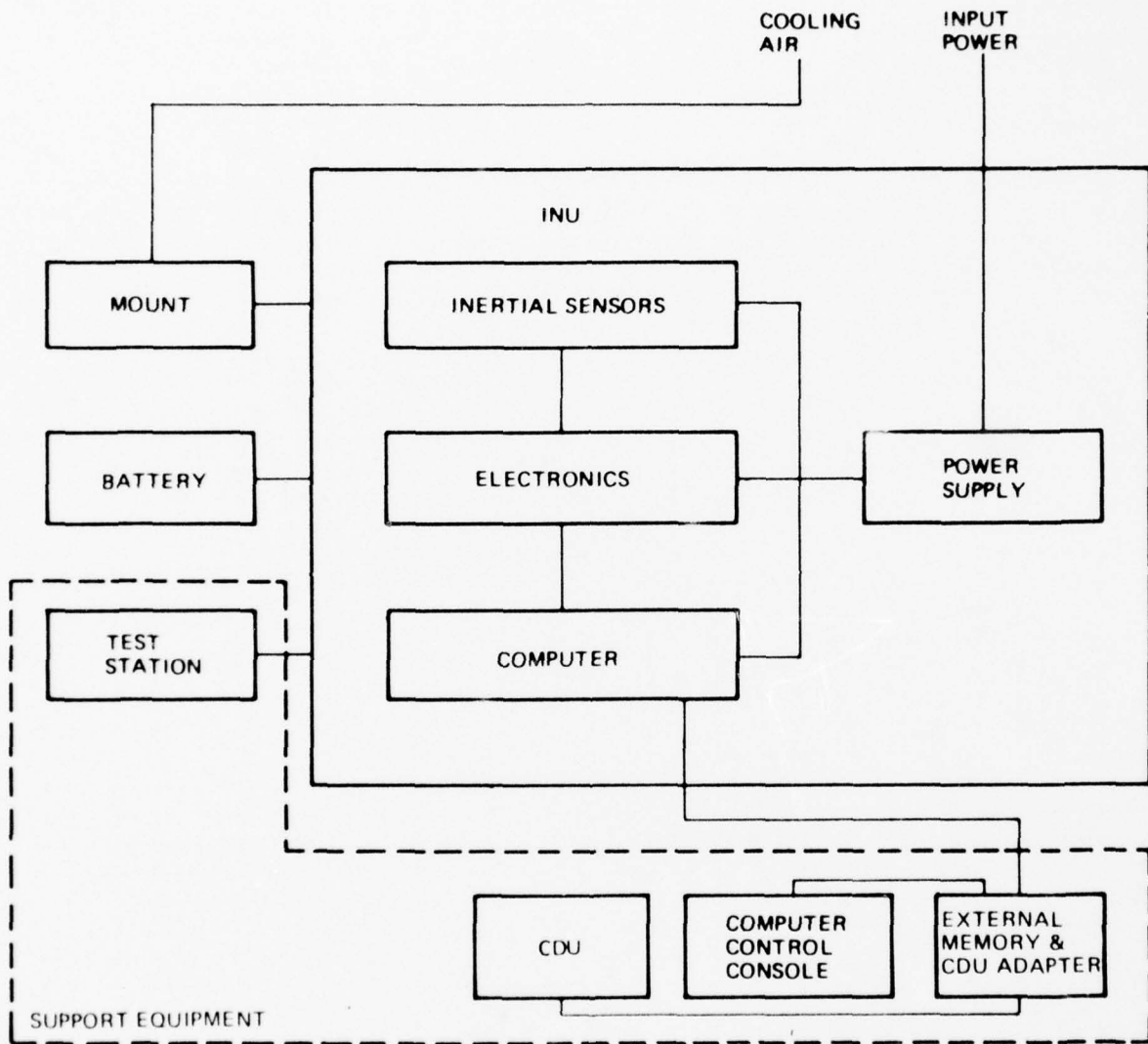


Figure 1. EPM Functional Block Diagram

The EPM performance requirements set forth in the Contract Statement of Work are summarized in Table 1. The position accuracy requirements are consistent with the requirements imposed during the MICRON Phase 2A design period, which are summarized in Table 2. The velocity accuracy requirement for Phase 2B is more severe, however. It is more severe in two respects:

1. The new requirement is for "peak ensemble rms velocity error", which is the peak value in the ensemble rms velocity error curve. The Phase 2A requirement was imposed on the "time-rms" value of the rms error curve, which will always be smaller than the peak value. The peak value on the rms velocity error curves (7.4 fps per axis) was about 40 percent larger than the time-rms value (5.2 fps per axis), 0-3 hr (Ref 2, p. 17). Consequently, 5 fps "time-rms" would correspond to about 7 fps "peak ensemble rms" velocity errors.
2. The new requirement is for 3.0 fps versus the Phase 2A requirement of 5.0 fps.

Combining effects of (1) and (2) yields an effective reduction of four-sevenths in allowed velocity errors (from 7 fps "peak ensemble rms" to 3 fps "peak ensemble rms," or 57 percent.

TABLE 1. SUMMARY OF PHASE 2B EPM PERFORMANCE REQUIREMENTS  
(to be Verified by Error Analysis)

System Accuracy Category	How Specified	Units	Specified Requirement	Time After Entering Navigate Mode
Position	CEP rate*	nmi/Hr	1.0	0-1 hr
			(0.8**) (3.5***)	0-1 hr
Velocity (Horizontal)	Peak Ensemble RMS	FPS per Axis	1.5	0-2.5 hr
			(1.0**) (3.0) (2.5**) (9.0***)	0-2.5 hr
Velocity (Vertical)	Pk Ensemble RMS	FPS per Axis	2.0 (3.0***)	0-2 hr

\*Interpreted as: least-squares straight line fit through origin.

\*\*Goal

\*\*\*After stored heading alignment. (Other requirements are after gyrocompass alignment)

TABLE 2. SUMMARY OF PHASE 2A PERFORMANCE REQUIREMENTS

System Accuracy Category	How Specified	Units	Requirement
Position	CEP Rate	nmi/Hr	1.0
Velocity (Horizontal)	Time-RMS	fps per Axis	5.0 (0-3 hr)

This 57 percent reduction in allowed velocity errors between Phase 2A and Phase 2B is the single most difficult requirement to meet through realistic error budgeting. The reason that this improvement is particularly difficult to achieve is, essentially, that 7 fps per axis peak ensemble rms velocity error is more consistent with 1 nautical mile per hour CEP rate for the error characteristics of a strapdown system such as MICRON. For example, the error analysis and error budget developed during Phase 1A development had predicted peak ensemble rms velocity errors in the range of 6 - 10 fps per axis, depending upon the flight profile, for performance consistent with 1 nautical mile per hour. These results are summarized in Table 3, and are taken from Ref 2. The first flight profile is a polygonal profile with 70-degree left turns every 30 minutes. The second flight profile has alternating right and left 70 deg turns every 30 minutes. The third flight profile assumes Poisson-distributed turns with 30 minutes mean time between turns, and heading changes normally distributed with standard deviation 70 degrees.

TABLE 3. PEAK ENSEMBLE RMS VELOCITY ERRORS, PHASE 1A

Flight Path	Peak Ensemble RMS Velocity Errors 0-2 Hr
1. (Circular)	9.6 fps per axis
2. (Zig-Zag)	9.2 fps per axis
3. (Random Turns)	6.6 fps per axis

The empirical relationship of peak ensemble rms velocity error to CEP rate is shown in Figure 2, in which the peak ensemble rms velocity error is plotted versus CEP rate for the two N57A systems tested by Rockwell Flight Test Operations at Los Angeles International Airport. The "sample sizes" for these statistics were the following:

- 7 flights with N57A-1
- 5 flights with N57A-2

These results indicate a ratio of peak ensemble rms velocity errors to CEP rate of about 10.0 fps (per axis) to 1.0 nautical mile per hour. On the basis of this, one might expect that the level of position accuracy performance consistent with 3.0 fps peak ensemble rms velocity error for N57A is about 0.3 nautical mile per hour, CEP rate.



Figure 2. Peak Ensemble RMS Velocity Error  
Versus CEP Rate for LAX Flight Tests

The primary reason for the inconsistency of 1 nautical mile per hour CEP rate with 3 feet per second peak ensemble rms velocity error (per axis) is that MICRON is a strapdown system. Its sensor input axes are body-fixed, so that their inputs change value with heading changes of the host vehicle. There are output error mechanisms (such as EMA or MESH scale factor error) which cause changes in the sensed acceleration under these conditions. Consequently, sensed acceleration errors are induced by heading changes. These small, random step changes in acceleration error have a more significant first integral (velocity error) than second integral (position). Also, a significant heading change is likely to occur between alignment and the cruise portion of flight. This heading change has an immediate effect upon velocity errors early in the navigation period. As a result, this type of error mechanism, which is characteristic of strapdown systems, has a more significant effect upon velocity errors than upon position errors.

By contrast, the sensor input axes in a gimballed inertial system are isolated from heading changes by the gimbals. This removes the error mechanisms which cause disproportionate velocity errors in the strapdown system. In these systems, the errors are more likely dominated by drift errors, which take longer to accumulate as a second integral to velocity errors. Consequently, the gimballed inertial systems can achieve a smaller ratio of velocity errors to position errors, with the added complexity and weight of the gimbal structure.

#### 2.1.1.3 Approach

During the previous contract phase the design of the EPM sensor hardware and electronics had been purposely directed to meet the Phase 2A performance requirements at the lowest estimated life-cycle cost. Consequently, there is little performance "over-design" that can be counted upon to help meet the reduced velocity error allowance. Instead, the only system changes that can be proposed are mechanization changes in the hardware or software. One such mechanization is the "self-calibration" mechanization which has been designed into the EPM hardware, but has not been tested or otherwise evaluated in terms of its impact upon velocity errors. Re-orientation of sensor axes is another possible mechanization change. A possible software mechanization change is to develop algorithms for detection and correction of errors which cause angle readout bias variations at twice the demodulator output "slip" frequency. (These are the error mechanisms modeled by the so-called "demod" calibration parameters.)

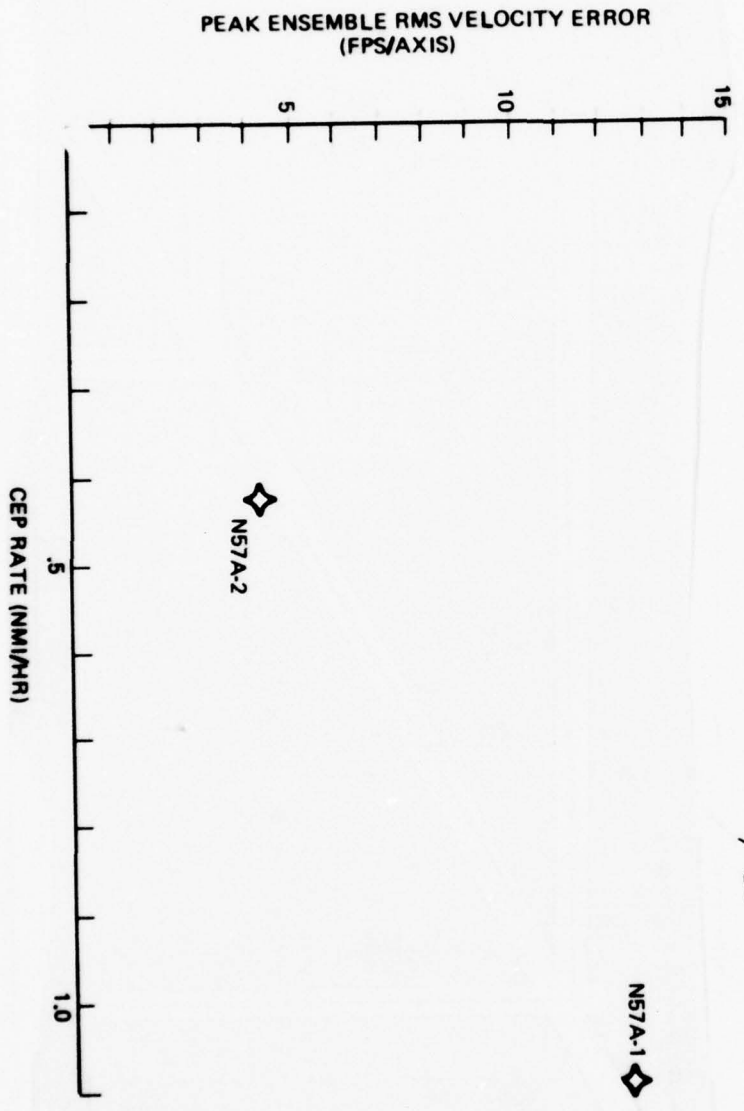


*Fig 2  
Pg 11*

*2 1/2*



*59%*

The proposed approach for meeting the velocity performance requirements was: (1) perform error analyses which identify the major error mechanisms producing the peak ensemble rms velocity errors, (2) investigate mechanization changes which would reduce the effects of the dominant error mechanisms, (3) perform error analyses to determine the impact of the improvements, (4) redetermine the dominant error mechanisms, and (5) return to step (2) and iterate until the objective has been achieved or until no further improvements can be made.

The basic tool used for error analysis and development of an error budget is the SAMUS program (Ref 3). This is a modularized, general-purpose program for error analysis of a wide variety of estimation and control problems. There is a subset of these modules which is specifically designed for implementing the state dynamics and sensor characteristics of strapdown systems in the aircraft "cruise" environment. This subset of modules had been compiled and executed on the IBM 370 operating system at the Corporate Computing Center, and the control deck setup had been developed for modeling MICRON errors. This effort had been completed under previous contracts, and the source decks for these modules had been saved on punched cards and on magnetic tape during Phase 2A. Also, a specialized "post processor" program for error budget evaluation and output formatting had been developed and saved on cards and tape.

The feasibility of implementing the SAMUS program on the computer systems in the MICRON laboratory was investigated, to see if the cost of conversion could be saved in direct charges for computer services. It appeared that the program size was within reason for implementing with "overlays" on the HP2100 system. However, there would be considerable recoding required for converting the IBM Fortran to ANSI Fortran, and some subroutines would have to be converted from IBM 370 assembly language to HP2100 assembly language. It was felt that the effort and risk required for recoding and checkout of a program of such size and complexity was not commensurate to the expected savings in computer charges. Consequently, the program was kept on the IBM 370 system.

The Phase 2A programs had been developed for error analysis of a system containing the MESGA (microelectrostatic gyroscope/accelerometer) multisensor. It was first necessary to modify the error models and post-processor to model the error characteristics of the three electromagnetic accelerometers (EMA) in place of the MESGA.

The MESGA error budget is shown in Table 4. Many physical error mechanisms are listed which cause acceleration error. These error mechanisms produce three types of effects on acceleration readout: - bias error, scalefactor error, and input axis misalignment error. These errors appear equally on the gyro x, y, and z axes. (Other effects are, of course present but are considered small and not included in the error budget.)

The EMA error budget is shown in Table 5. The same three effects are modelled. The EMA input axes are colinear with the gyro x, y, and z axes.

The sensed acceleration error on the *i*th axis (*i* = x, y, z) is

$$\delta A_i = \Delta_i + \delta K_i A_i - (\sin \phi_{ij}) A_k + (\sin \phi_{ik}) A_j$$

where

$$(i, j, k) = (x, y, z), (y, z, x), (z, x, y)$$

TABLE 4. MESGA ERROR BUDGET

Error Mechanism	Effect	
	Bias Repeatability	Scale Factor Repeatability
Preload Charge Variation	8.1 $\mu\text{g}$	20.4 ppm
Rotor Miscentering	8.1 $\mu\text{g}$	20.4 ppm
Gap Measurement	8.1 $\mu\text{g}$	20.4 ppm
Rotor Charge Measurement	8.1 $\mu\text{g}$	0
Stray Capacitance	8.1 $\mu\text{g}$	20.4 ppm
Propagation Delay	8.1 $\mu\text{g}$	0
Rise Time Variation	8.1 $\mu\text{g}$	0
Digitizer Electronics	10.0 $\mu\text{g}$	20.0 ppm
Subtotal (RSS of the above)	23.6 $\mu\text{g}$	45.4 ppm
Scale Factor Stability	15 ppm, $\tau = 20 \text{ min}^*$	
Axis Misalignment Repeatability	10 $\widehat{\text{sec}}$	
Bias Thermal Transient	8.1 $\mu\text{g}$ , $\tau = 75 \text{ sec}^{**}$	
Scale Factor Thermal Transient	20.4 ppm, $\tau = 75 \text{ sec}^{**}$	

TABLE 5. EMA ERROR BUDGET

<u>Error Effect</u>	<u>Magnitude</u>
Scale Factor Repeatability	56.3 ppm
Scale Factor Stability	15.0 ppm, $\tau = 20 \text{ min}^*$
Axis Misalignment Repeatability	2 $\widehat{\text{sec}}$
Bias Repeatability	37.5 $\mu\text{g}$
Bias Thermal Transient	3 $\mu\text{g}$ , $\tau = 90 \text{ sec}^{**}$
Scale Factor Thermal Transient	32 $\mu\text{g}$ , $\tau = 90 \text{ sec}^{**}$

\*First order Markov process

\*\*Exponential decay to zero

and  $\Delta_i$  = bias error

$\delta K_i$  = scale factor error

$\phi_{ij}, \phi_{ik}$  = input axis misalignments about axes j and k respectively.

Accelerometer bias, scale factor, and axis misalignments are estimated during system calibration and the resulting parameters are used to compensate the accelerometer data. Therefore, the whole value bias, scale factor, and axis misalignments do not produce acceleration errors under operational conditions. Acceleration errors are produced by errors in estimating the parameters during system calibration, by changes in the instrument parameter values after system calibration, or by an unpredictable, random variation in the true value of the parameters.

Repeatability errors listed in the error budget describe the parameter shift after system calibration and also the errors in measuring the parameters during system calibration. The parameter shift is assumed to occur at system turn on and the parameter values are constant during periods of system navigation.

Scale factor stability describes the random scale factor variation during periods of system navigation. It is modeled as a first order Markov process with an exponential autocorrelation function  $\phi(T)$ .

$$\phi(T) = E \left\{ \delta K_s(t) \delta K_s(t+T) \right\} = \sigma_s^2 e^{-|T|/\tau}$$

where  $\delta K_s(t)$  is scale factor stability error at time t,  $E \{ \cdot \}$  is "expected value of",  $\sigma_s^2$  is the scale factor stability variance, and  $\tau$  is the time constant. The error is modeled by the differential equation

$$\dot{\delta K}_s = \left( -1/\tau \right) \delta K_s + u$$

where u is white noise with power spectral density amplitude  $2\sigma_s^2/\tau$ . State variable  $\delta K_s$  is initialized with variance  $\sigma_s^2$ .

Bias and scale factor thermal transients describe errors that only persist for the first few minutes after system turn on and are due to thermal gradients that have not stabilized. The magnitude of the error decays exponentially to zero

$$\sigma_{\Delta T}(t) = \sigma_{\Delta T}(0) e^{-t/\tau_{\Delta T}}$$

$$\sigma_{sT}(t) = \sigma_{sT}(0) e^{-t/\tau_{sT}}$$

where  $\sigma_{\Delta T}(t)$  and  $\sigma_{sT}(t)$  are the variances of the bias scale factor thermal errors at time t and  $\tau_{\Delta T}$  and  $\tau_{sT}$  are their time constants, respectively. The errors are modeled by the differential equations

$$\dot{\Delta}_T = \left( -1/\tau_{\Delta T} \right) \Delta_T$$

$$\dot{s}_T = \left( -1/\tau_{sT} \right) s_T$$

These EMA error models were then implemented in the SAMUS deck setup and verified by repeating a segment of a flight profile used in N57A error analysis with EMA error models. In this way, the system performance sensitivities to the EMA error terms could be compared one-to-one to those obtained from the N57A results.

The post-processor program multiplies the error sensitivities generated by the SAMUS program with the rms error budget terms, computes the rss of the resulting errors, and formats and prints the results. The section of the post-processor which processes the acceleration sensing errors was reprogrammed to use the appropriate error sensitivity terms and error budget terms for the EMA models, and the output formatting was reprogrammed to agree with these conventions.

The flight profile assumed for the error analyses was not changed from Phase 2A. This is CIGTF INS Route 6, which originates at Holloman AFB. INS Route 6 normally returns to HAFB from Bakersfield, California. The flight profile was extended to Sacramento, California and back to HAFB in order to allow a longer navigation period. The resulting flight profile is summarized in Table 6.

TABLE 6. SEGMENTS APPROXIMATING INS ROUTE NO. 6

Segment	Duration (sec)	Heading (Deg)	Velocity (fps)	Destination
1	336	0	0	(Alignment, Holloman AFB)
2	60	165	220	(Enter Nav, Takeoff)
3	600	220	400	Las Cruces, New Mexico
4	1800	267	735	Tucson, Arizona
5	900	300	735	Gila Bend, Arizona
6	1800	269	735	Miramar NAS, California
7	3300	329	735	Sacramento, California
8	6900	33	735	Holloman AFB

#### 2.1.1.4 Results

The Phase 2A Error Budget was used as a starting point in evolving an error budget that would meet the Phase 2B performance requirements. This will be called a "candidate error budget" (CEB) because, at the start, it does not meet the system performance requirements.

After the SAMUS program had been modified for EMA sensors and checked out, the EMA error budget shown in Table 5 was substituted for the MESGA error budget in the CEB. Also, some of the thermal time constants and estimated rms magnitude of thermally sensitive error sources were updated to agree with results of thermal tests and changes in system thermal control requirements since the Phase 2A error budget had been completed. The resulting CEB is given in Table 7.

TABLE 7. MICRON PHASE 2A ERROR BUDGET UPDATED

Error Source	Units	Budgeted RMS Value (Per Axis)
<u>Gyro</u>		
1. <u>Drift Rate</u> (.01°/hr Total)		
Spherical Harmonic 0	°/Hr	0.005 ( $\tau = 3600 \text{ sec}$ )
Spherical Harmonic 1	°/Hr	0.005 ( $\tau = 3600 \text{ sec}$ )
Spherical Harmonic 3	°/Hr	0.005 ( $\tau = 7200 \text{ sec}$ )
Preload Unbalance, Rotor Oblateness	Parts/Part	0.0002
Axial Mass Unbalance	Parts/Part	0.01
Random Motion Effects	°/Hr/Hr	0.003
Random Drift Rate	°/Hr	0.003 ( $\tau = 600 \text{ sec}$ )
2. <u>Angle Readout</u>		
Spherical Harmonic 0	MRAD	0.042 ( $f = .7, W_n = 2.4 (10^{-4})$ )
Spherical Harmonic 1	MRAD	0.042 ( $f = .7, W_n = 1.9 (10^{-4})$ )
Spherical Harmonic 3	MRAD	0.042 ( $f = .7, W_n = 9.4 (10^{-5})$ )
Scale Factor (4-Space)	Parts/Part	0.0001
Rotor Miscentering	PPM	2.3
Third Harmonic Rotor Shape	Parts/Part	0.001
Random Motion Effect	MRAD	0.03 ( $\tau = 600 \text{ sec}$ )
Electronics Thermal Errors	MRAD	0.01 ( $\tau = 75 \text{ sec}$ )
Readout Thermal Errors	MRAD	0.04 ( $\tau = 75 \text{ sec}$ )
Random Noise	MRAD	0.3

TABLE 7. (Cont)

Error Source	Units	Budgeted RMS Value (Per Axis)
<u>EMA Acceleration</u>		
Scale Factor Repeatability	PPM	56.3
Scale Factor Stability	PPM	15.0 ( $\tau = 1200$ Sec)
Axial Misalignment	SEC	10.0
Bias Repeatability	ug	37.5
Bias Thermal Transients	ug	3.0 ( $\tau = 90$ Sec)
Scale Factor Thermal Transients	PPM	32.0 ( $\tau = 90$ Sec)
<u>Miscellaneous</u>		
Gravity Anomaly	Sec	5.0 ( $\tau = 50$ sec)
Altimeter	Ft	500 ( $\tau = 1800$ sec)
Measurement Noise	Ft	1.0 (White Noise)
<u>Initial Conditions</u>		
Position	Ft	1.0
Velocity	FPS	1.0
Level Alignment	Sec	36000
Az Misalignment	Sec	36000

The estimated peak ensemble rms velocity error in the first two hours of navigation with this error budget is 5.4 fps (per axis). This peak occurs at about 56 minutes after the start of navigation. By contrast, the estimated time-rms velocity error and CEP rate for this error budget are 4.5 fps and 0.73 nautical miles per hour, respectively, 0 - 4 hr. This level of performance in velocity clearly does not meet the Phase 2B requirements.

A tabulation of the CEB contributions to peak ensemble rms velocity was prepared, and reviewed for the purpose of identifying budgeted values that could reasonably be reduced. This review included the responsible EMA and MESG engineers and electronics designers. Considerable scrutiny was applied to all budgeted values, with the purposes of identifying how well all subsystems were capable of meeting their requirements, and of reducing the level of allowable tolerances wherever possible. The most significant contributions to peak ensemble rms velocity at that time were EMA errors. The most significant result of this review, and of subsequent internal reviews, was the finding that the demonstrated axis misalignment stability of EMAs (2 arc-sec) was considerably better than the error budget, while the scale factor stability requirement (56.3 ppm) may be difficult to achieve. In the Phase 2A design of the EMA "cluster", each EMA input axis is about 55 degrees from vertical. In this orientation, the output error is particularly sensitive to scale factor error (because the input is nominally about 0.6 g's); more so than to axis misalignment. However, if the cluster were tilted down, so that two EMA input axis were approximately horizontal, then the output errors would be slightly more sensitive to input axis misalignment instability and significantly less sensitive to scale factor instability.

The SAMUS deck setup was modified to evaluate the expected error characteristics of a MICRON system with the EMA cluster re-oriented in this manner. The error analysis predicted a decrease in the contribution of EMA errors to peak ensemble rms velocity from 3.55 fps per axis to 2.06 fps per axis. This resulted in a decrease in the expected peak ensemble rms velocity of the system from 5.4 fps per axis to 4.6 fps per axis; from 180 percent of target (3 fps) to 150 percent of target.

As a result of this analysis, the design change was recommended and implemented. That is, the EMA cluster was re-oriented with two input axes nearly horizontal. It is not desirable to have either input axis too close to horizontal, because the near-zero output rate causes quantization noise sufficient to degrade alignment.

After this change, the estimated CEP rate was 0.72 nmi per hour, although the velocity error was still outside its specified range. The SAMUS program was used for identification of the most significant contributors to the peak ensemble rms velocity. All error sources which contribute 0.5 fps or more to the rss total are shown in Table 8. The rss of the first 10 terms is 4.0 fps per axis. The rss of all other contributors is only about 1.5 fps per axis. Consequently, in order to meet the velocity requirement, some mechanization improvements had to be found which will reduce the rss of these "top 10" considerably (from 4.0 to 2.6 fps).

Continued review of the CEB for other mechanization improvements, including self-calibration resulted in no changes that were expected to yield the required one-third improvement in peak ensemble rms velocity errors (from 4.6 fps per axis to 3.0), other than rotation of the instrument cluster. This mechanization had been tested on N57A-2, by rotation of the entire system  $\pm 180$  deg at about six degrees per second. It resulted in position error performance in the order of 0.1 nmi per hour CEP rate and velocity performance in the order of two fps peak velocity error for the first 14 hours of navigation.

TABLE 8. MAJOR CONTRIBUTORS TO PEAK ENSEMBLE RMS VELOCITY ERROR  
(Greatest to Least Significant)

ERROR SOURCE	CEB RMS MAGNITUDE	CONTRIBUTION TO PEAK ENSEMBLE RMS VELOCITY (FPS Per Axis)
Angle Readout, Spherical Harmonic No. 0	0.042 mrad	2.09
EMA Bias Repeatability	37.5 $\mu$ g	1.96
Angle Readout, Scale Factor	0.00010 pts/pt	1.50
Angle Readout, Spherical Harmonic No. 1	0.042 mrad	1.16
Angle Readout, Spherical Harmonic No. 3	0.042 mrad	1.14
Drift Rate, Spherical Harmonic No. 0	0.005 deg/hr	0.85
Angle Readout Random Noise	0.300 mrad	0.79
Gravity Anomalies	5.0 arc-sec	0.78
Drift Rate Spherical Harmonic No. 1	0.005 deg/hr	0.76
Drift Rate Random Drift	0.003 deg/hr	0.57
Initial Heading Error	36000. arc-sec	0.54
Angle Readout and Random Aircraft Motion	0.015 mrad	0.53
EMA Axis Misalignment	2.0 arc-sec	0.50

Before pursuing a hardware design change, discussions were held with AFAL and in the Standard Navigator Open Forums on the firmness of the velocity requirements. The velocity requirement was considered very important and no relaxation was forthcoming. In fact, the Standard Navigator requirements were set at a slightly tighter value than the MICRON Phase 2B INU Specification (CDRL Item A007) requirements.

Since instrument rotation was the most cost effective and least schedule perturbing means of meeting the Phase 2B velocity requirement, a study was conducted to determine if the INU could be redesigned with a rotated instrument cluster. A design approach was developed which still permitted the INU to meet the F16 envelope requirements. Evaluations were made of effects on cost of ownership, weight, reliability, thermal design, schedule, and contract cost. As a result of these studies/evaluations, the error analysis results, and the unyielding velocity requirement, it was decided that the instrument cluster would be rotated.

With the change to the rotated mode, the system errors were no longer characterized by the error analysis program. The major program revisions (and derivations of error models for the rotated IAU) required to produce an error analysis for the rotated IAU were substantial. Since the N57 data provided confidence that the CEP rate and velocity performance requirements would be comfortably met with the rotated instrument cluster, it was concluded that it was not cost effective to update the error analysis program.

#### 2.1.1.5 Summary and Conclusions

The only performance characteristic which was expected to be outside the Phase 2B requirements was velocity accuracy. By making adjustments in the Phase 2A error models (to change from MESGA to EMA acceleration sensors) and error budgets (to reflect design improvements and testing results), the expected peak ensemble rms velocity error was reduced from 7 fps to 5.4 fps per axis. The requirement is 3.0 fps per axis. By taking advantage of observed EMA error characteristics and re-orientating the EMA cluster, this estimate was further reduced to 4.6 fps per axis. MESH self-calibration was not expected to result in a significant improvement in velocity accuracy, compared to the one-third improvement needed. The only other cost effective mechanization change that could be expected to yield sufficient velocity accuracy improvement was rotation of the Instrument Assembly Unit (IAU).

Based upon EPM test results with the rotated IAU, the performance is well within the Phase 2B (and Standard Navigator) requirements.

#### 2.1.2 INU CI Specification

An INU specification was developed which established detail INU functional, performance, electrical, and physical requirements and configuration. This included overall INU requirements as well as requirements for the various modules and subelements of the INU.

This task was accomplished by performing the necessary analyses, tradeoffs, evaluations, and partitioning tasks to establish the INU configuration and requirements.

This task was completed and the EPM INU CI Development Specification (AJ00089) was submitted as CDRL data Item A007 in November 1975. This specification was reviewed at the December 1975 informal design review and found satisfactory.

The INU CI Specification defines the EPM system partitioning, functional requirements and detailed external interfaces. The detailed requirements for each of the functional areas are enumerated in the detailed design specifications which are discussed in the following section. The system is partitioned into the following major functional areas:

1. Mechanical Housing Unit - MHU
2. System Electronics Unit - SEU
3. Instrument Assembly Unit - IAU
4. Dedicated Processor Unit - DPU
5. Input/Output Unit - IOU
6. Power Supply Unit - PSU

The relationship of these units and associated external interfaces are shown in Figure 3. A functional diagram of the INU is shown in Figure 4.

The INU CI specification combines the contract statement of work Appendix I requirements with available F-16 requirements into a unified set of requirements.

A major activity was the repartitioning of the system to accommodate the F-16 form factor and translating F-16 external interface requirements into design requirements.

Although not specifically a part of the INU CI specification, the area of definition of a BITE philosophy permeated the systems engineering activity. Maximum use was made of prior BITE analysis (based on detailed failure modes effects analysis of N77 electronics) to develop a BITE philosophy for the design areas to follow.

### 2.1.3 INU Detail Design Specifications

Based on the requirements and configuration established by the EPM INU specification, detailed design specifications were prepared for appropriate subelements of the EPM INU. These specifications establish functional, performance, electrical, and physical requirements and configuration. Detail design specifications were prepared for the following EPM subelements:

1. Mechanical Housing Unit
2. Suspension and MUM Electronics Module (SEU's 1 and 2)
3. Timing and Sequencing Module (SEU 3)
4. Signal Generator and Memory Module (SEU 4)
5. Instrument Assembly Unit
6. Accelerometer
7. Converter Module
8. Data Terminal Module
9. Power Supply Unit

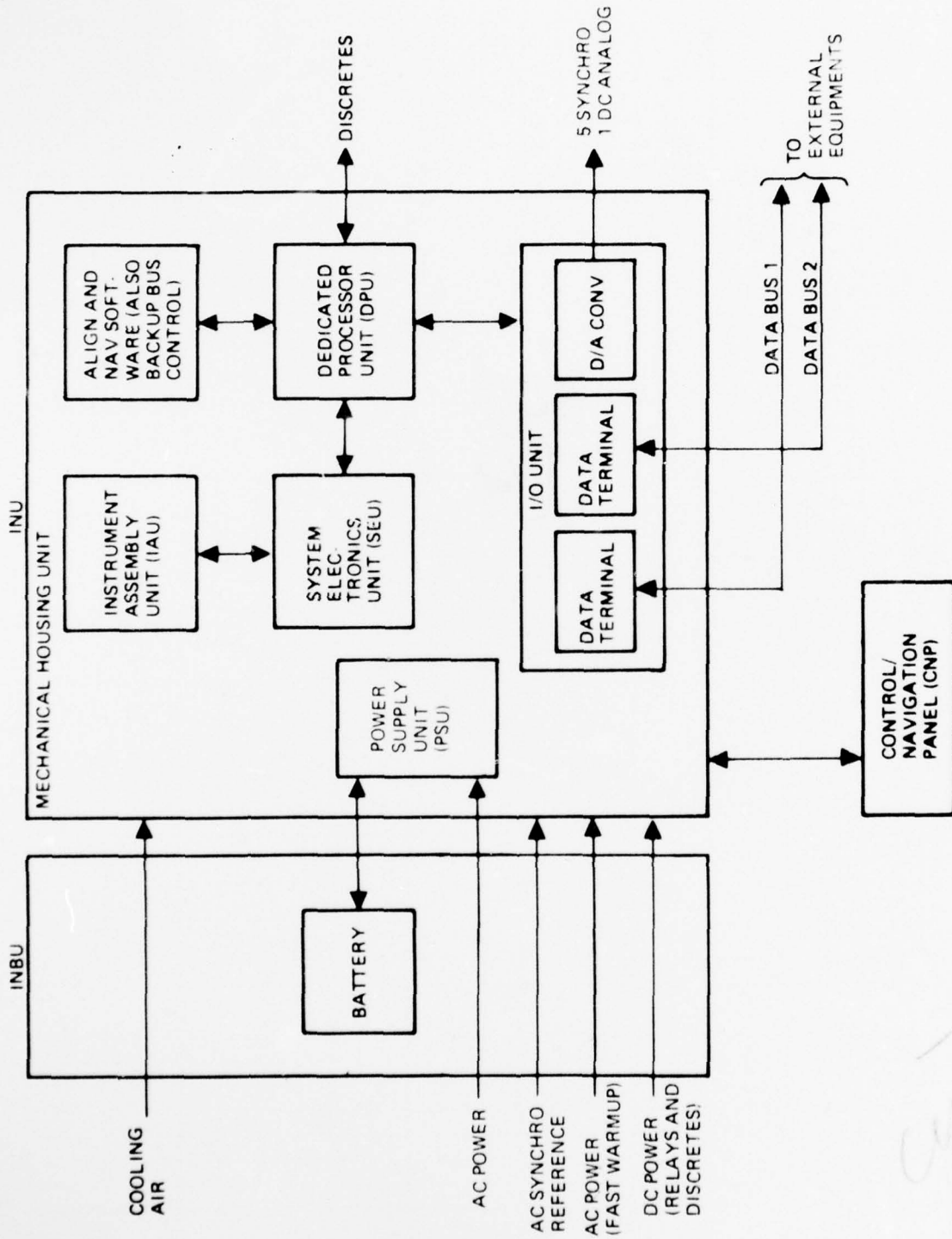


Figure 3. INU Major Components

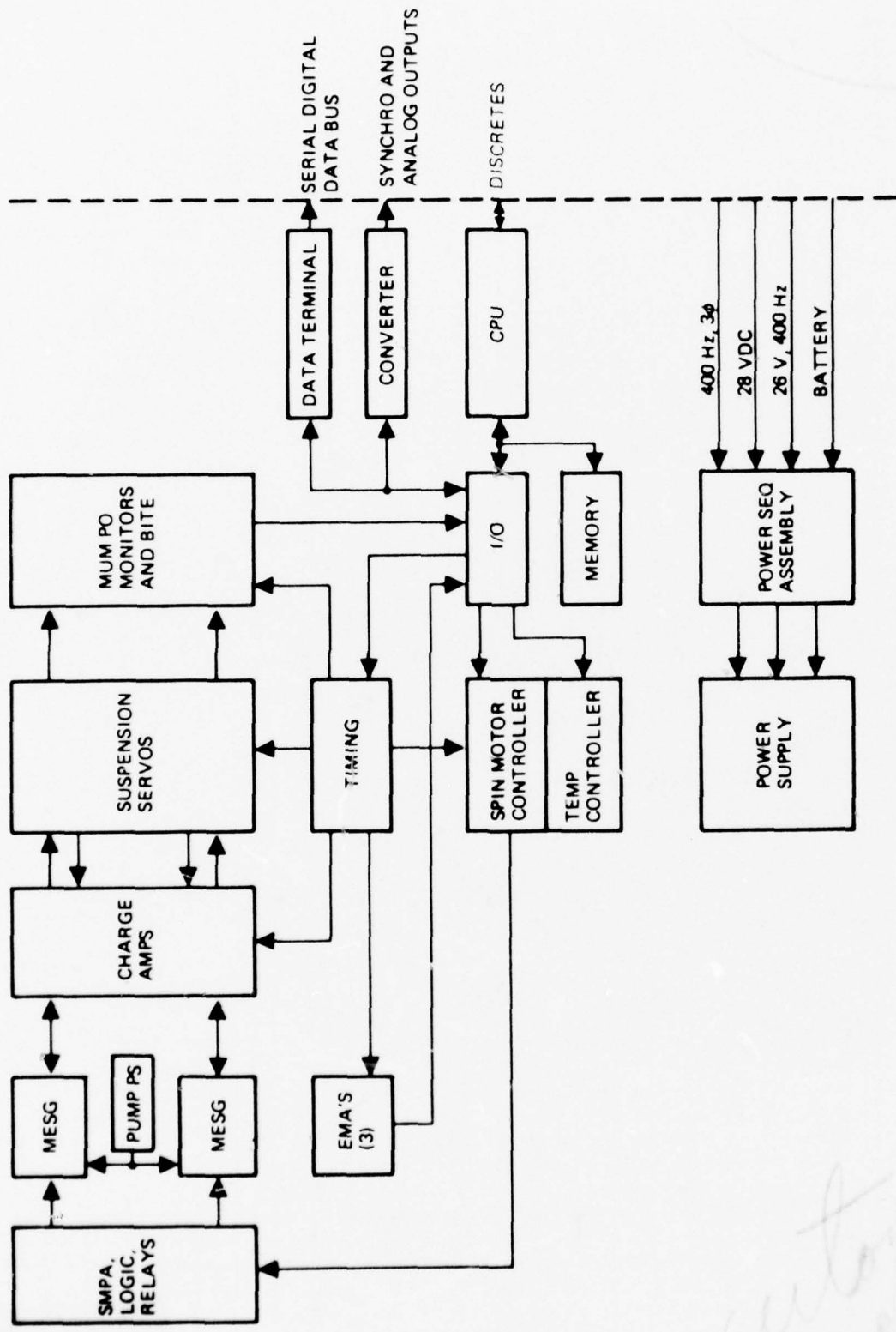


Figure 4. INU Functional Diagram

Preliminary detail design specifications were completed and distributed by internal letter during the period from 11 November 1975 through 1 January 1976. Final versions of the detail design specifications were completed and distributed during the period from 2 February 1976 through 29 April 1976.

During integration of the EPM, maintenance of these detail design specifications was performed on a continuous basis. This was accomplished by red-lining a master set of specifications used in the Integration Lab. The detail design specifications were used in conjunction with the INU CI Specification to evaluate INU performance and interface compatibility. The specifications were red-lined when corrective action was required on both hardware and specification requirements to achieve compatibility. The specifications were also red-lined when it was determined that improvements could be made in the specifications to more adequately or correctly specify requirements. This red-lining activity was completed in December 1976. The detail design specifications were re-typed and re-issued internally in January and February 1977.

A detail design specification was not prepared for the DPU because a CI development specification for the DPU (AJ00090) was prepared and submitted in November 1975 as CDRL data item A006.

#### 2.1.4 MHU Design/Develop/Fab/Test

Upon receipt of the MICRON Inertial Navigation Unit Preliminary Development Specification (Ref 4), Autonetics prepared an Installation Control Drawing (Drawing No. 10214-111) depicting all the physical interface characteristics of the MHU (Figure 5). The desired aspects of the design alternatives previously investigated during Phase 2A were incorporated into the new form factor and the inboard profile, Figure 6, was derived. The preliminary layout was reviewed and cost analyses indicated the design was on target.

Stress analysis, mass properties analyses, and thermal analyses were performed for the INU. The thermal analyses and the resulting EPM thermal design are discussed in detail in Appendix M. Early thermal analyses indicated that control of the SEU modules, required to meet design requirements, would be accomplished more efficiently if the heaters were installed on the SEU boards rather than on the MHU chassis. In addition, the SEU 1/2 and 3 boards were required to be electrically isolated from chassis ground potential while retaining the forced air heat exchanger capability in the MHU. This required a special fabrication procedure in the otherwise straightforward dip brazed chassis structure. With exception of the isolated rails for installing the SEU modules, the chassis is dip brazed together with an integral enclosed forced air heat exchanger.

The MHU chassis includes all the physical and electrical aircraft interfaces, mounting and alignment provisions and connectors prescribed by the aforementioned specification. The electrical interconnect for the INU is accomplished via a master Interconnection Board (MIB). This MIB is included in the MHU design effort and has all the internal interconnecting cabling attached. Figure 7 shows the MIB less cables.

A revision to the interface of the MHU was incorporated as a result of the Standard Navigator Appendix V, B revision received on 6 January 1976. This is reflected in the Installation Control Drawing 10214-111 "A." The configuration and form factor remained constant until 6 April 1976 when Autonetics became aware, by physically checking an F-16 aircraft, that a major interference existed between the

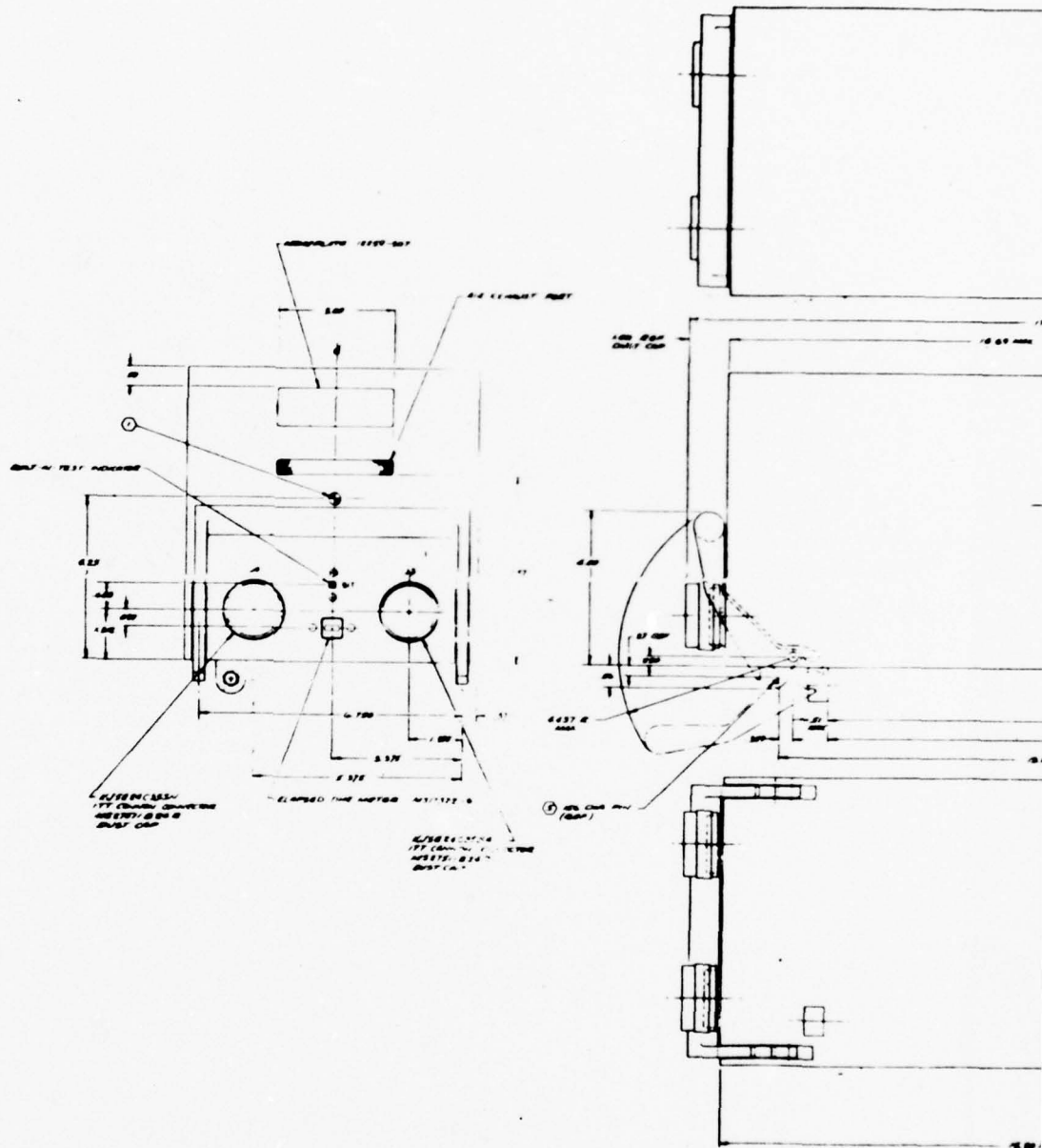
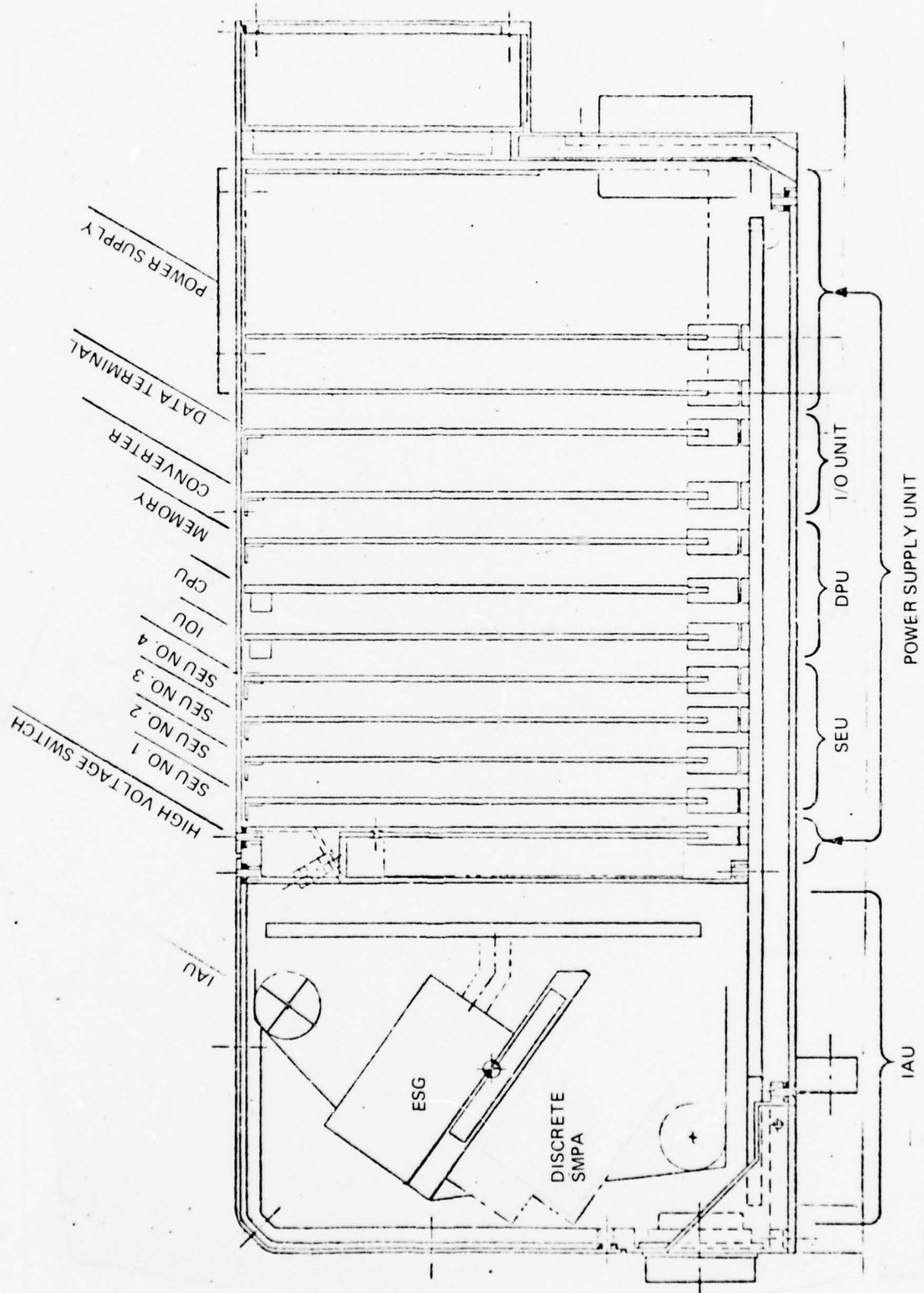


Figure 5. INS Installation Control Drawing





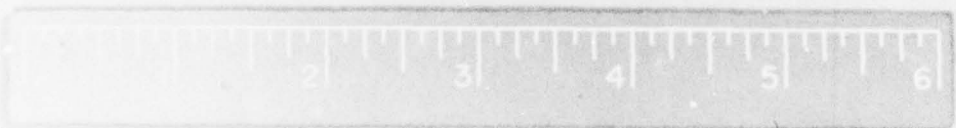
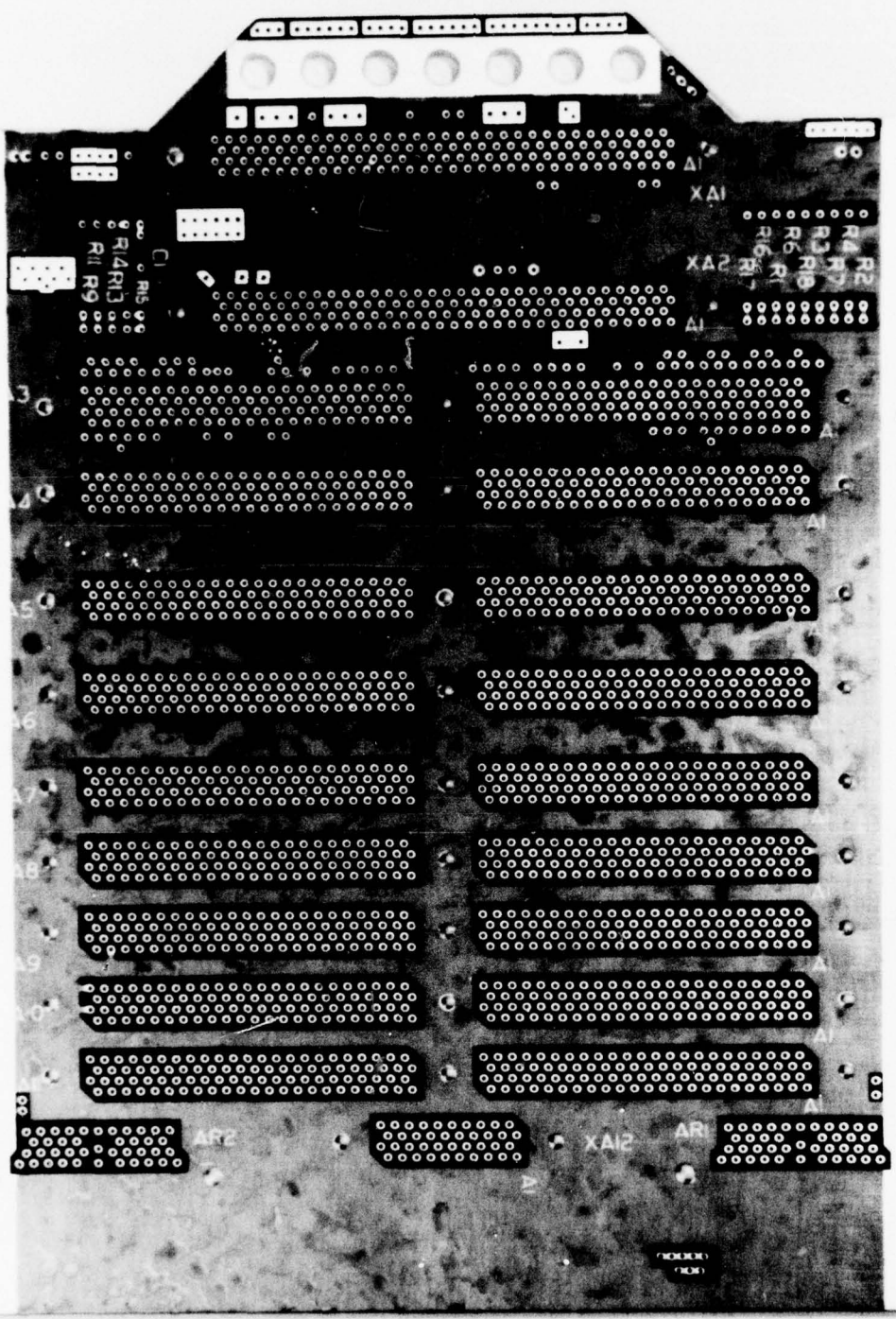
POWER SUPPLY UNIT

Figure 6. N72 INU Inboard Profile



Figure 7. Master Interconnect Board (MIB)

*Handwritten scribbles and markings on the right margin.*



5-12-76 07100008

MHU and aircraft structure. An immediate revision was implemented to the rear of the chassis which also improved maintainability of the MHU. The B revision of 10214-111 (Figure 8) reflects the form factor of the MHU fabricated to meet the installation required.

At approximately this same time (April 1976), the decision was made to proceed with the design and fabrication of a rotating MICRON (N73) to replace the non-rotating version (N72). The design impacted only the forward portion of the MHU which encloses the IAU. The non-rotating IAU was deleted and a rotating IAU was inserted. The Spin Motor Electronics had to be located in the forward section, but off the rotating IAU assembly. A twist capsule assembly was introduced as a means of easily providing the electrical interface between the MHU and the IAU without producing drag on the IAU and inhibiting the shock mount/insulator supporting the IAU. Figure 9 depicts the N73 MHU design with the IAU in place.

Fabrication, assembly, and wiring of the non-rotating (N72) MHU was completed in June 1976 and was used in EPM integration testing until completion of the rotating (N73) MHU.

Fabrication, assembly, and wiring of the rotating MHU was completed in August 1976. The completed MHU is shown in Figure 10 (front view) and Figure 11 (rear view). The MHU chassis, along with other major components of the N73, is shown in Figure 12.

The completed N73 MHU chassis, including the MIB, was delivered to the integration lab in August 1976. This activity completed the MHU task.

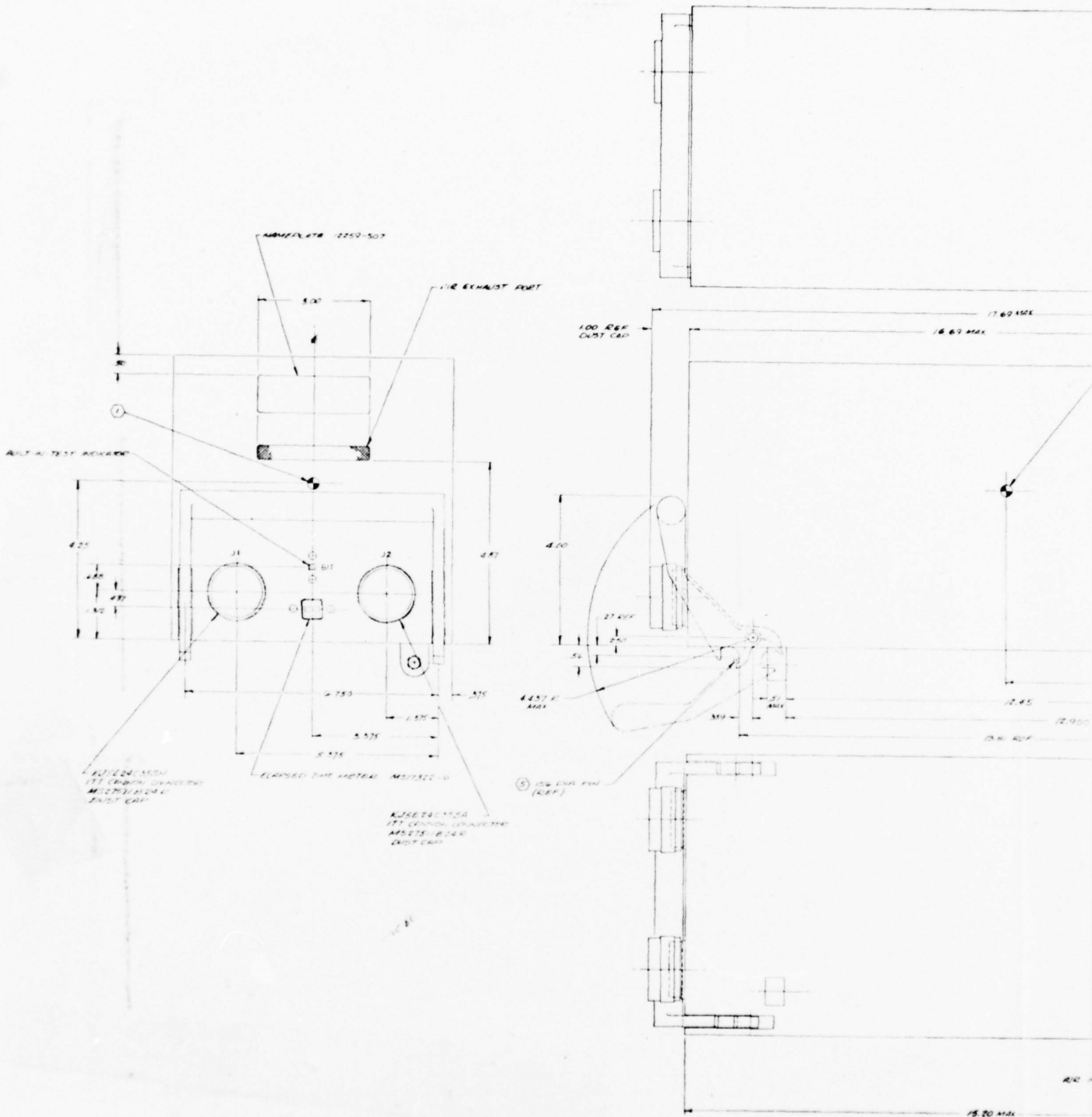
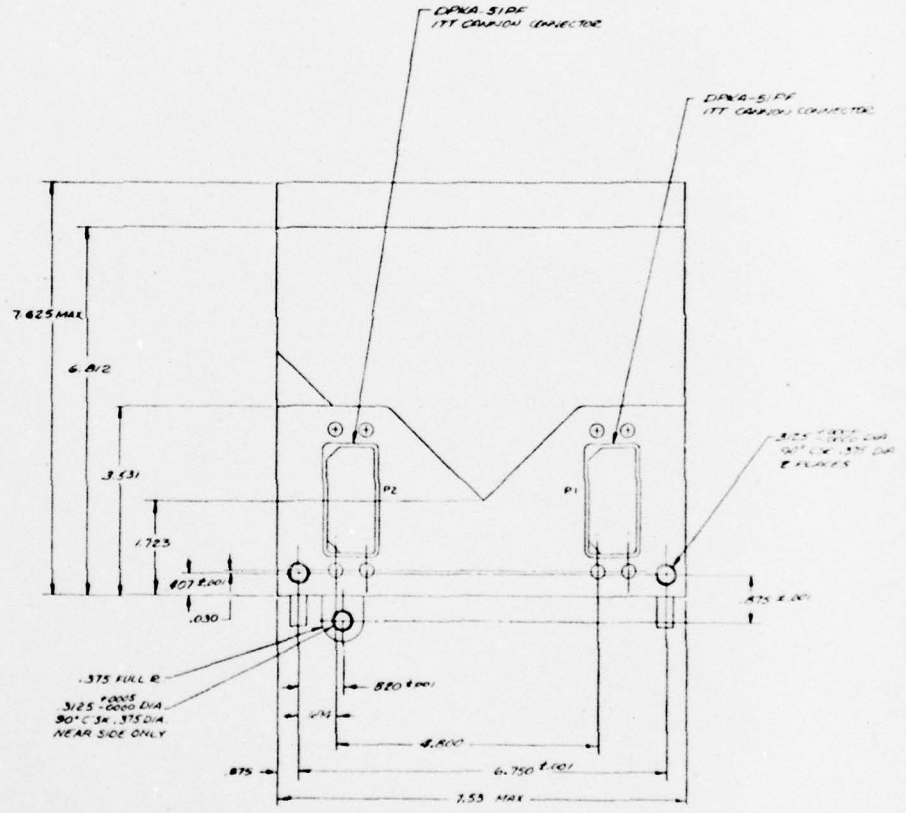
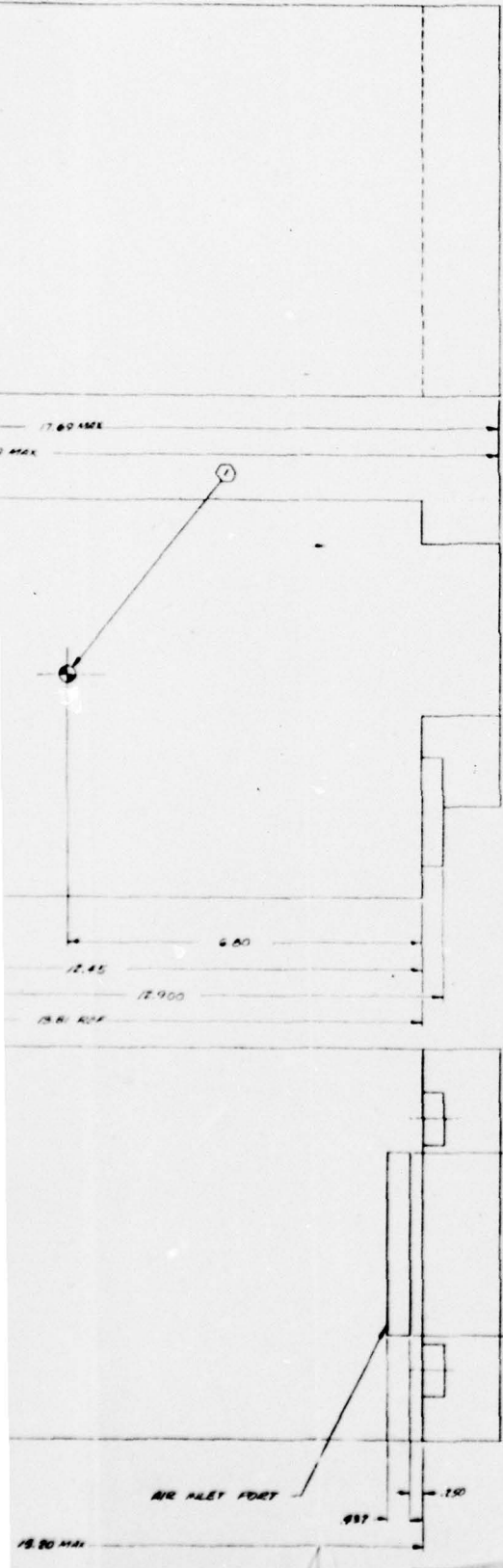


Figure 8. INS Installation Control Drawing (10214-111 Rev B)

NOTE: UNLESS OTHERWISE SPECIFIED

- ① CENTER OF GRAVITY
- ② WEIGHT TBD (SEE WEIGHT STATUS REPORT FOR FURTHER INFORMATION)
- ③ REFERENCE SPECIFICATION TBD
- ④ HANDLE LATCH TO CONFORM TO LATCH ASSEMBLY QWLZ-1-1, HANDLE POSITIONING CORP.
- ⑤ DATUM FPN IS PART OF QWLZ-1-1A KEEPER ASSEMBLY, CONTROL PADLOCK (REF. REFERENCE AUTOMATIC ENG. REF-1111, AND MOUNT INSTALLATION CONTROL)



2

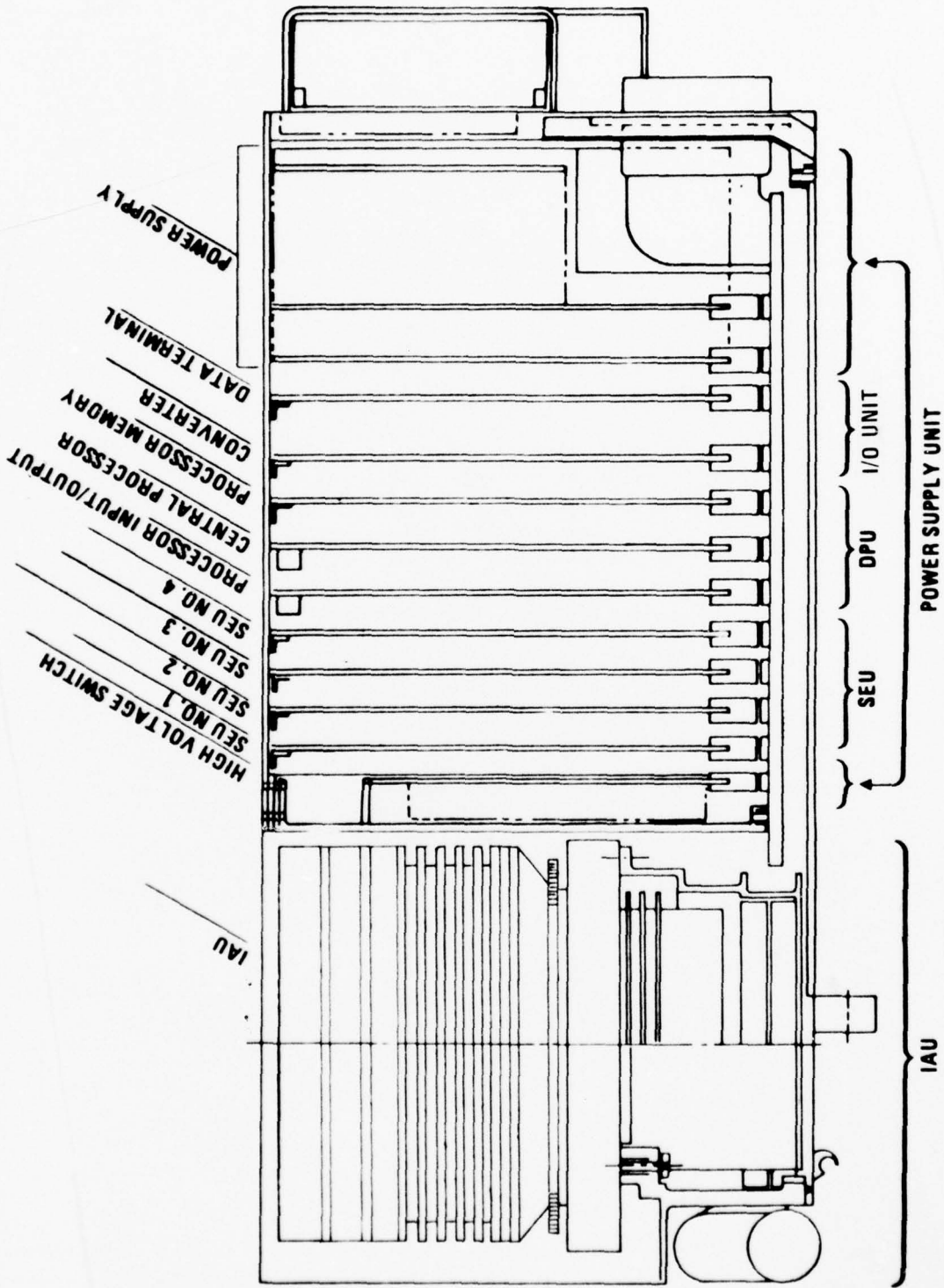


Figure 9. N73 INU Inboard Profile



Figure 10. N73 Mechanical Housing Unit (front view)

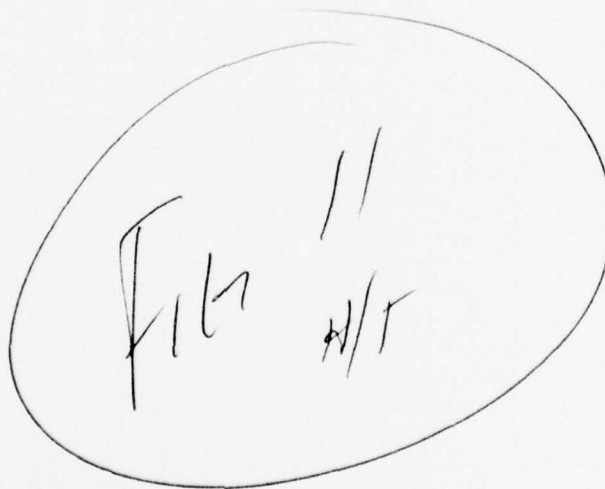


Figure 11. N73 Mechanical Housing Unit (back view)

NO. \_\_\_\_\_



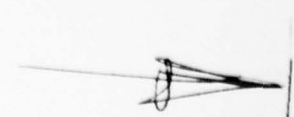
VOL. NO. \_\_\_\_\_

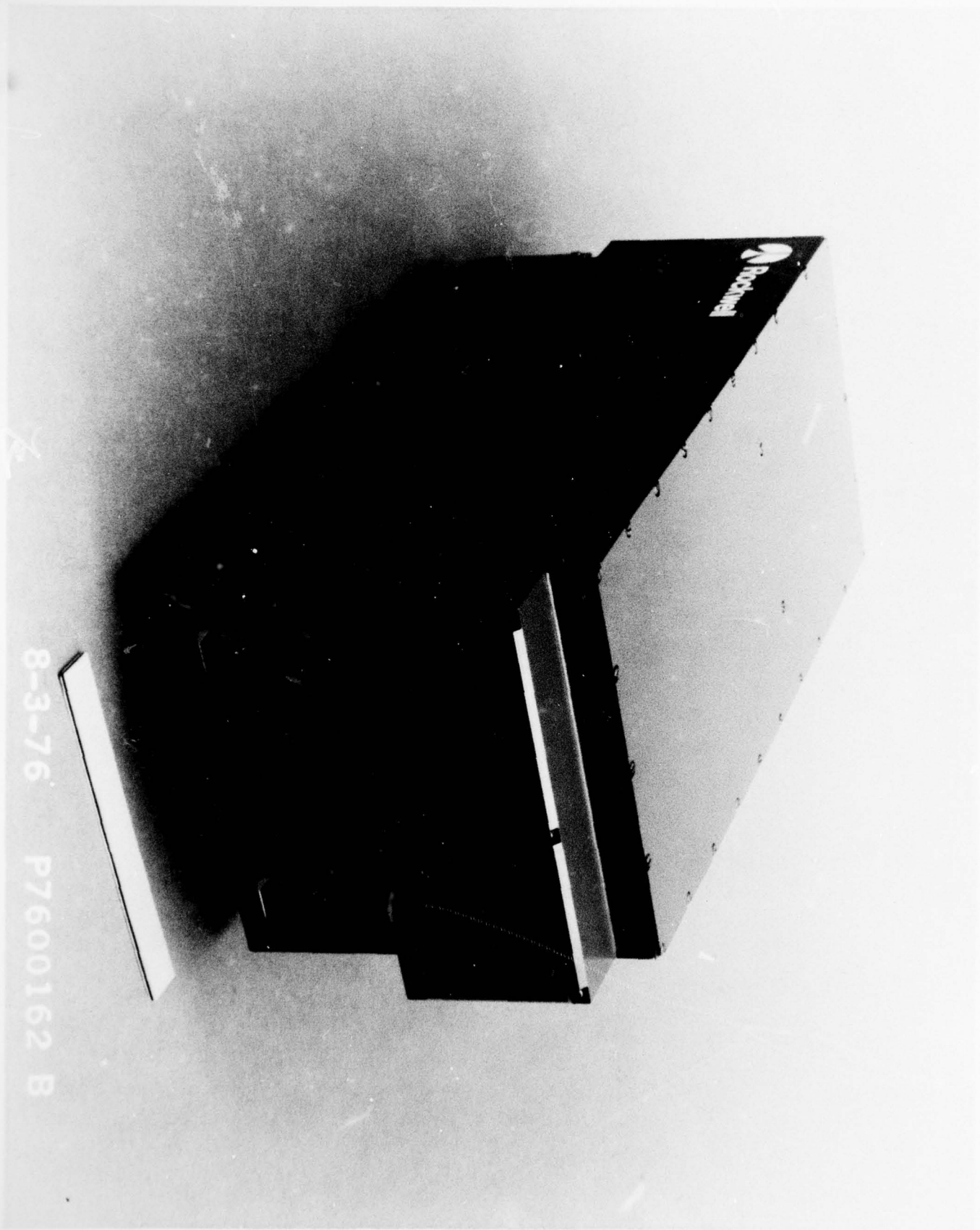
FIG. NO. 10

PAGE NO. 34



8-3-76 P7600162 F



8-3-76 P7600162 B





Figure 12. Major Components of N73 INU

PUB NO. \_\_\_\_\_

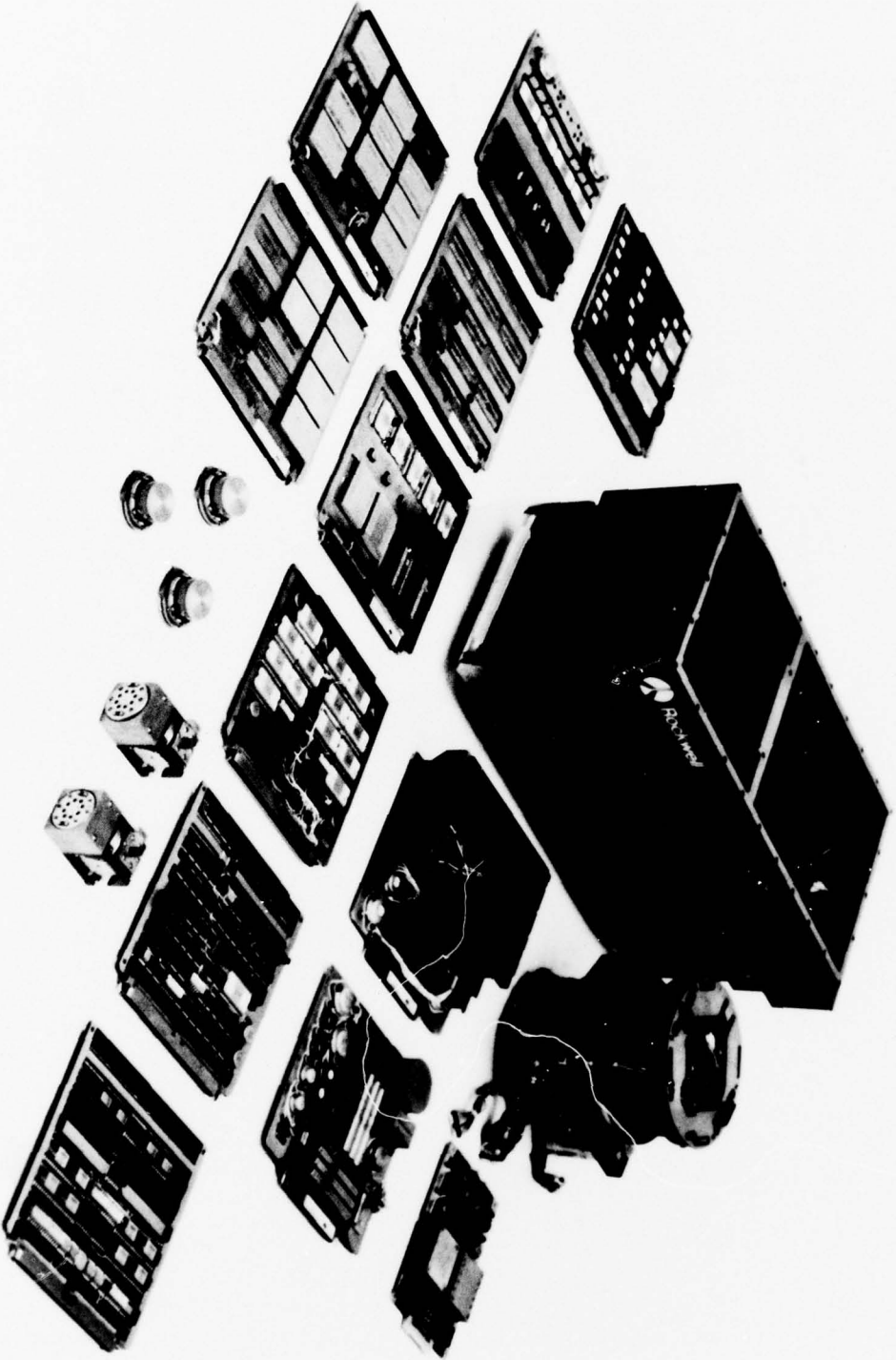
VOL NO. \_\_\_\_\_

FIG. NO. \_\_\_\_\_

PAGE NO. \_\_\_\_\_

12

35



83/4

### 2.1.5 SFU Design/Develop/Fab/Test

The System Electronics Unit (SEU) consists of the electronics contained on four multilayer boards (MLB's) designated SEU 1, 2, 3, and 4 of which SEU's 1 and 2 have identical designs.

The SEU electronics are packaged in accordance with the requirements of the contract Appendix I specification. All hybrid assemblies are hermetically sealed and thermally controlled by placing the hybrid packages on heat sink rails on the MLB. Figure 13 depicts the assembly of the MLB showing the heat sink and the heater under the heat sink (SEU 4 does not have a heater). All are bonded together with a thin adhesive film. The board, when installed in the MHU, interfaces with the MLB and is locked along the sides of the boards to the heat exchanger.

The design of the MLB was accomplished by minimizing the number of layers and number of feedthrough holes. The MLB's for SEU's 1 through 4 were four layers maximum. The hybrid container configuration was selected to standardize the form factor for design to cost and to permit plug-in installation. The engineering model MLB's have sockets installed so removal of hybrids can be accomplished with ease and without damage to the MLB. In production, the MLB could have the sockets removed and the hybrid soldered in place.

SEU 1, 2 and 3 utilize a common heater, heatsink, and bracket design. Because of the different components on SEU 4, it has a different heatsink. SEU 4 does not require thermal control so a heater is not necessary. However, the designs of the SEU MLB's were implemented to standardize parts to reduce cost.

#### 2.1.5.1 Suspension and MUM Electronics Modules (SEU 1 and 2)

There are two identical Suspension and MUM Electronics (SMUM) Modules in the FPM INU, one for each gyro. Each SMUM Module contains the following hybrid circuits:

<u>Nomenclature</u>	<u>Qty Req'd per Module</u>	<u>P/N</u>
Sample and Hold and Gap Summation	2	12520-507-1
Differential Amplifier and Notch Filter	1	12410-507-1
Servo Network	1	12405-507-1
Modulator	2	12425-507-1
MUM Demodulator	1	12415-507-1
MUM Demodulator Filter	1	12420-507-1
MUM Demodulator Sample & Hold	1	12435-507-1
Multiplexer	1	12430-507-1

A functional block diagram of the Suspension and MUM Electronics Module is shown in Figure 14. The primary functions of this module are: (1) process the signals from the Charge Amplifiers to detect rotor displacement from cavity center, and to generate signals which will result in the Charge Amplifiers applying restoring force to maintain the rotor at the cavity center; (2) extract the MUM signals and demodulate

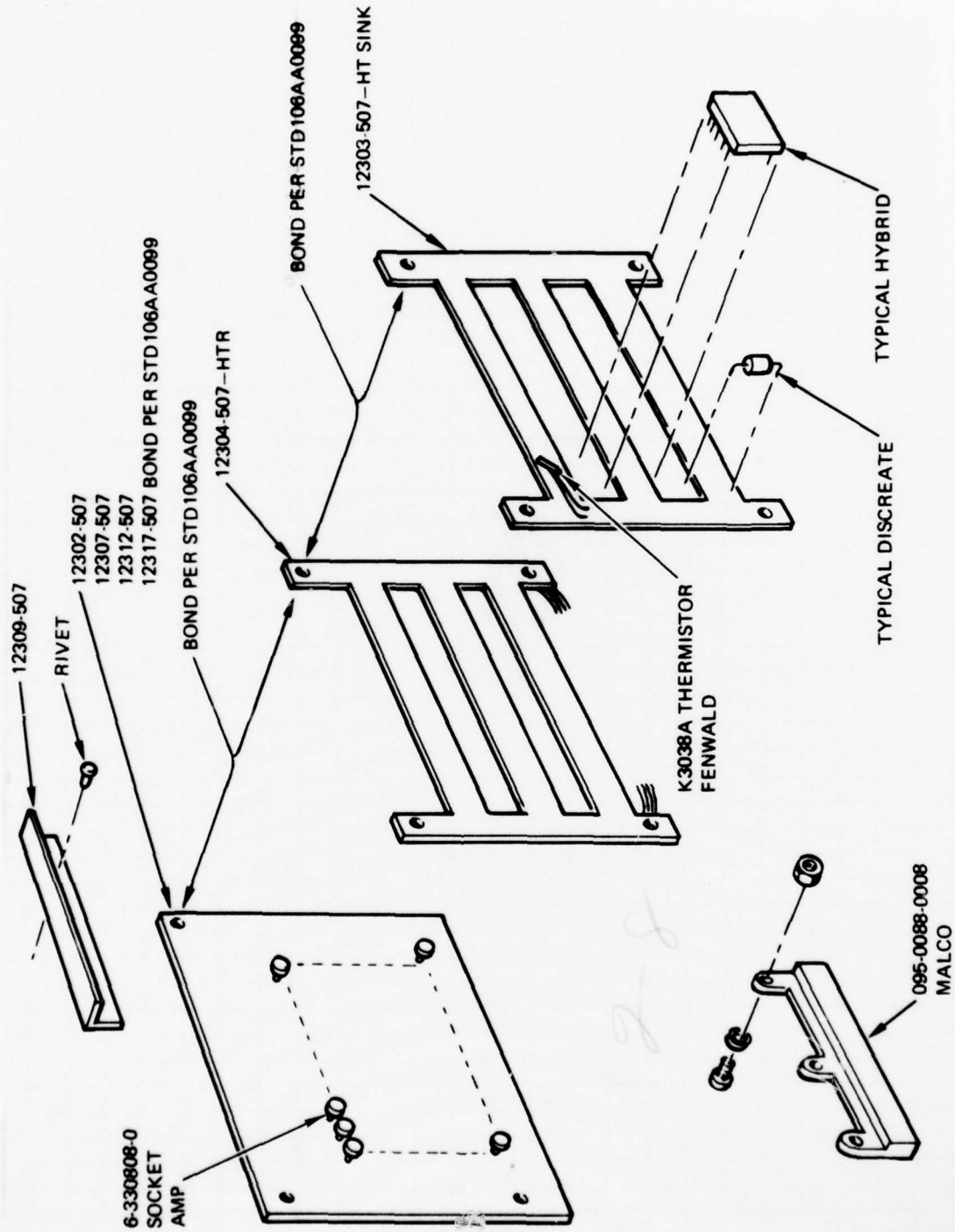


Figure 13. MLB Construction

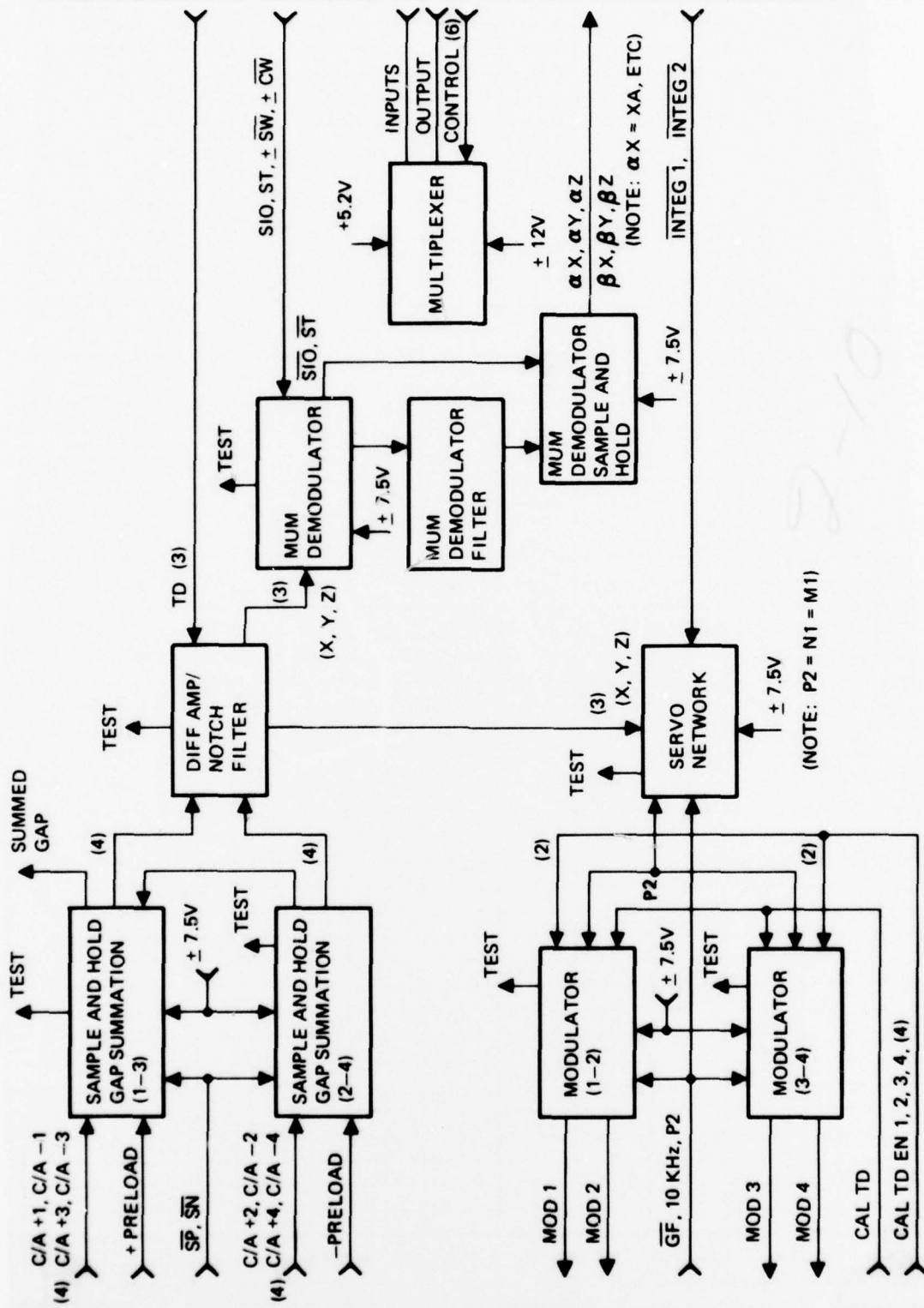


Figure 14. Suspension and MUM Electronics Functional Block Diagram (SEU 1 and 2)

and process them for conversion to digital by the analog-to-digital converter; (3) provide a multiplexing capability to time division multiplex 32 analog signals to a single output. Differences in wiring implied by the multiplexing function are accommodated in the MIB to keep the two Suspension and MUM Electronics Modules identical. The relation between the multiplexers on the two modules is shown in Figure 15.

A pulse amplitude modulation, time division multiplex scheme is mechanized to apply restoring forces to the gyro rotor and to sense rotor position. The four modulator outputs of SMUM are sent to the input transformers of the gyro Charge Amplifiers, and are as shown in Figure 16. These signals are combined with the pre-load signal as shown in Figure 16 to obtain a Charge Amplifier waveform as shown in Figure 17. The polarity of the charge applied to opposing electrode pairs is the same. The charge magnitude during forcing depends upon the sensed error from cavity center, and the plate which is further from the rotor receives the larger magnitude charge. The charge magnitude during the readout period is a constant. The polarity of the charge is reversed each half cycle of the 10 kHz timing reference.

The Charge Amplifier difference signal inputs to SMUM are in four-space. Each signal is sent to two S/H circuits (one for 10 kHz in phase polarity, the other for 10 kHz out of phase polarity). The eight S/H outputs are sent to the differential amplifiers where they are converted to three-space. The differential amplifier outputs are sent to the MUM demodulator and to the notch filter. The notch filter attenuates the MUM component (at 2500 Hz) and results in loop gain and phase characteristics which provide rotor speed control. The notch filter outputs are sent to the servo network where compensation is mechanized for the different modes (e.g., lift-off and suspend). The servo network outputs are sent to the modulator, where conversion back to four-space is accomplished and signal polarity and duration are established as indicated in Figure 16. The modulator outputs are sent to the charge amplifier input transformers.

The Sample and Hold/Gap Summation hybrid provides an output which is a measure of the average gap between rotor and cavity. This signal is used during initialization (in the heat mode), and provides BITE indication in other modes. In general, the output of each hybrid circuit is provided through a buffer resistor in the hybrid to the SMUM module connector.

A calibration disturbance signal "Cal TD" is sent to the two modulator hybrids. One of the four-space channels is selected under control of the four Cal TD select discrettes. Three disturbance signal inputs are brought out from the Differential Amplifier/Notch Filter hybrid to the SMUM module connector. These inputs will not be connected to a signal source when the module is installed in the INU. The compensation in the Servo Network hybrid is under control of the three discrete inputs (INTEG 1, INTEG 2, P2-M1-N1). The Modulator hybrids use the 10 kHz and GF logic signals to modulate the four space forcing signal, and the discrete P2-M1-N1 controls the modulator gain.

The MUM Demodulator hybrid uses the four quasi reference generator signals +SW, -SW, +CW, -CW to demodulate the MUM signals. The reference frequency is under control of the DPU. The logic signals SIO and ST are buffered in the MUM Demodulator and sent to the MUM Demodulator Sample and Hold. The demodulated MUM signals are sent to the MUM Demodulator Filter hybrid, which contains only passive elements. The outputs of this circuit are sent to the MUM Demodulator Sample and Hold hybrid, where the MUM signals are sampled and held for A/D conversion.

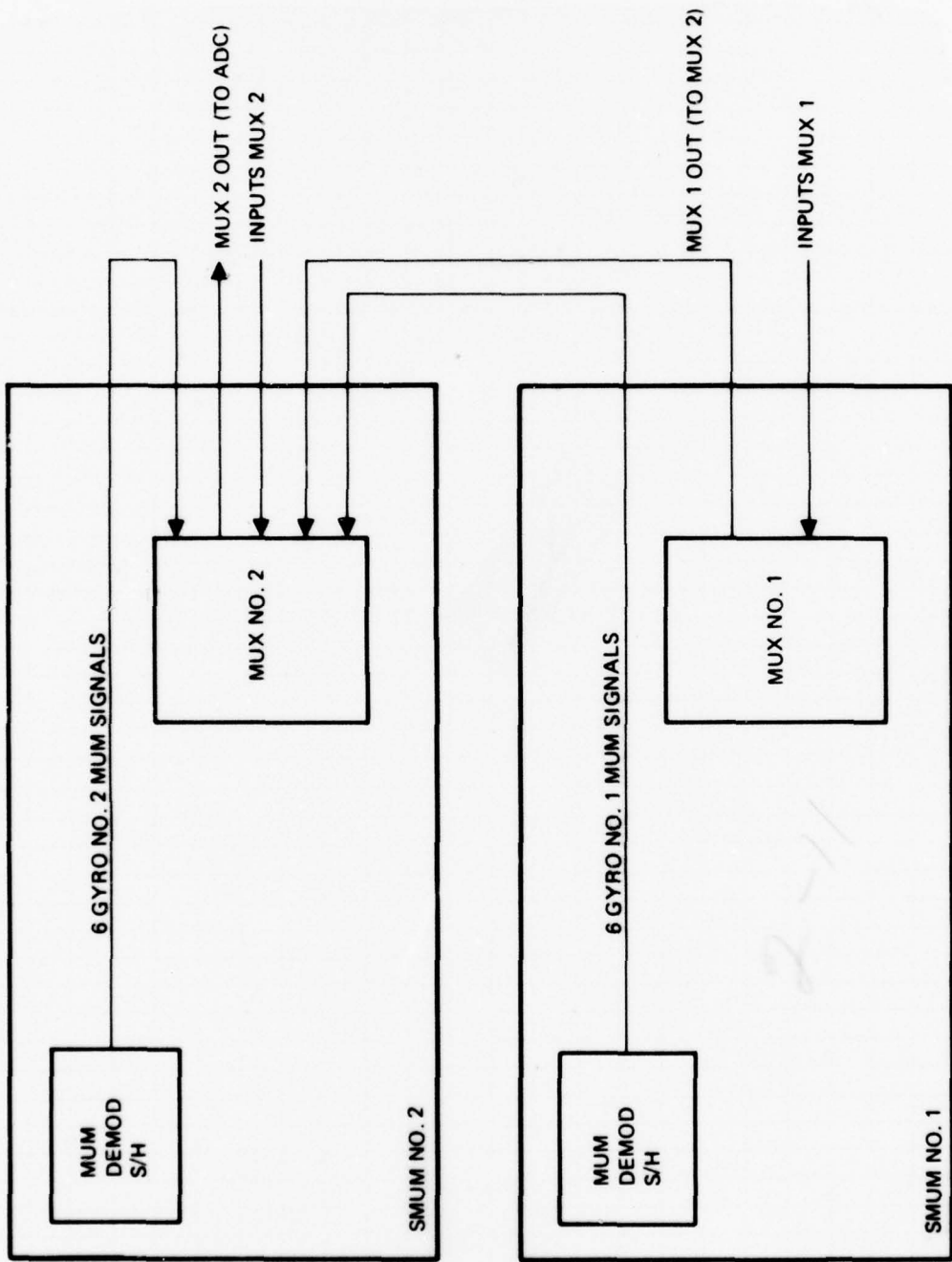


Figure 15. MUX Interconnect Diagram

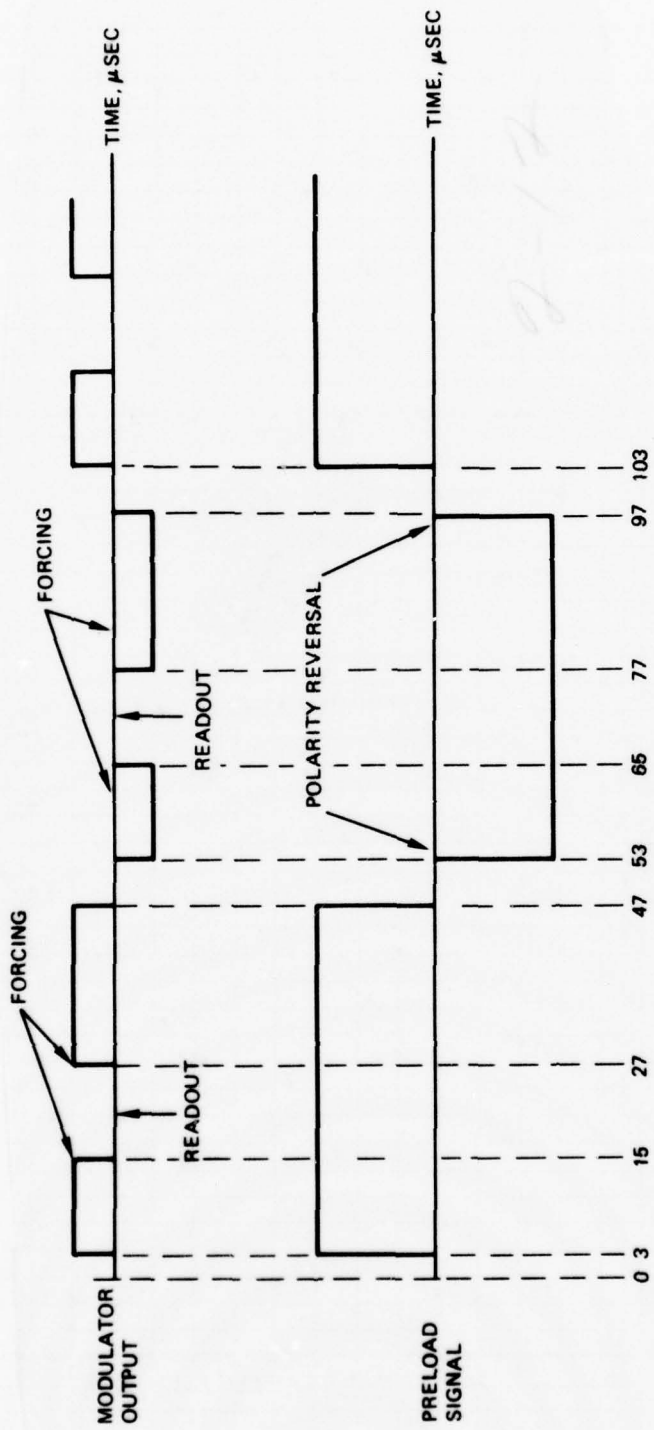


Figure 16. Modulator Output and Preload Signals

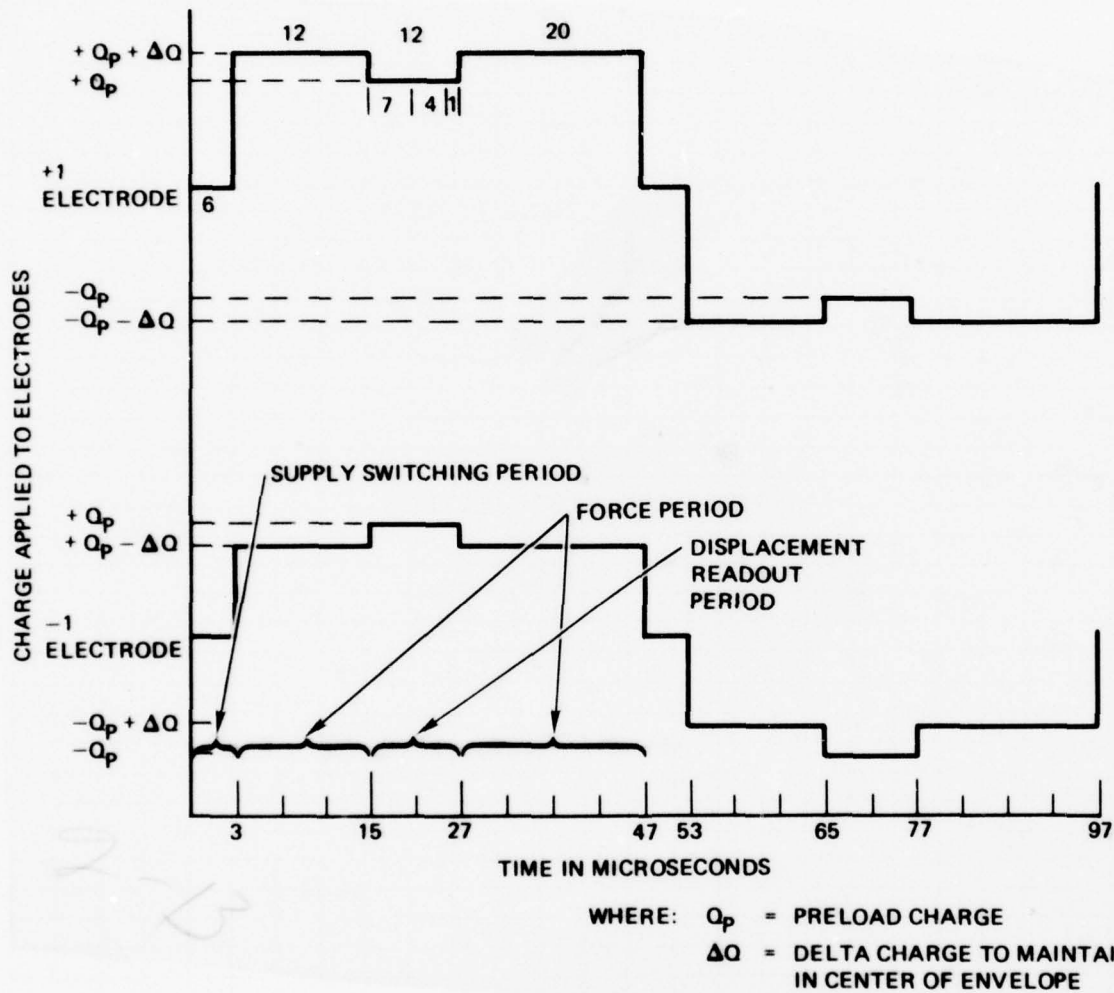


Figure 17. Suspension Servo Charge Amplifier Pulse Amplitude Waveform

The multiplexer switching functions are under control of the six logic signals A<sub>0</sub>, A<sub>1</sub>, A<sub>2</sub>, A<sub>3</sub>, ENAB 1, ENAB 2. Thirty-two inputs are accepted and sent out on one output line. The multiplexer hybrid also contains passive elements for signal conversion, to divide down some of the input signals, and to provide excitation for the temperature sensors.

The SMUM module self-test capability is under DPU control and this capability is summarized in Table 9.

TABLE 9. SMUM SELF TEST

Charge Monitor (One Time)	The ball charge shall be checked by computer monitoring of the MUM signals while a torque disturbance is applied by the computer prior to ball spin up. This means of charge monitoring is performed only during initialization
Suspension Servo Test (One Time)	The servo characteristics of the servo suspension loop shall be checked by computer monitoring of the MUM signals while a torque disturbance is applied by the computer prior to ball spin up. Performed only during initialization.
Gap No. 1 and No. 2 (Repetitive)	MESG No. 1 summed gap and MESG No. 2 summed gap shall be monitored to verify that proper gaps are maintained between the rotors and cavities.
Charge Monitor (Repetitive)	The rotor charge shall be checked once every specified time period by monitoring the MUM signals after spin-up.
MUM Data Reasonableness (Repetitive)	Demodulator bias, ADC saturation and scale factor will be checked for each gyro.
Self Calibration Test (One Time)	Too large a change in parameters from previous calibration could indicate a malfunction.
Temperature Monitor (Repetitive)	SMUM Module temperatures shall be monitored.
Multiplexer (Repetitive)	+5V, -5V and Ground Reference are routed through the MUX to ADC.

All of the substrates contained on SEU's 1 and 2 use thin film technology except for the Servo Network which utilizes thick film technology. Substrate deposited thin film resistors provide the superior performance required by the MUM Electronics in a most cost-effective manner. In particular, excellent long term stability and tight tolerances and temperature tracking coefficients are attainable with this process. A detailed description of the thick and thin hybrid technologies is given in Appendix A. Appendix A also gives an itemized listing of the activity involved in the fabrication, assembly, and testing of the hybrids. Table A-1 of Appendix A shows the total quantity of hybrids fabricated, assembled, and tested for EPM.

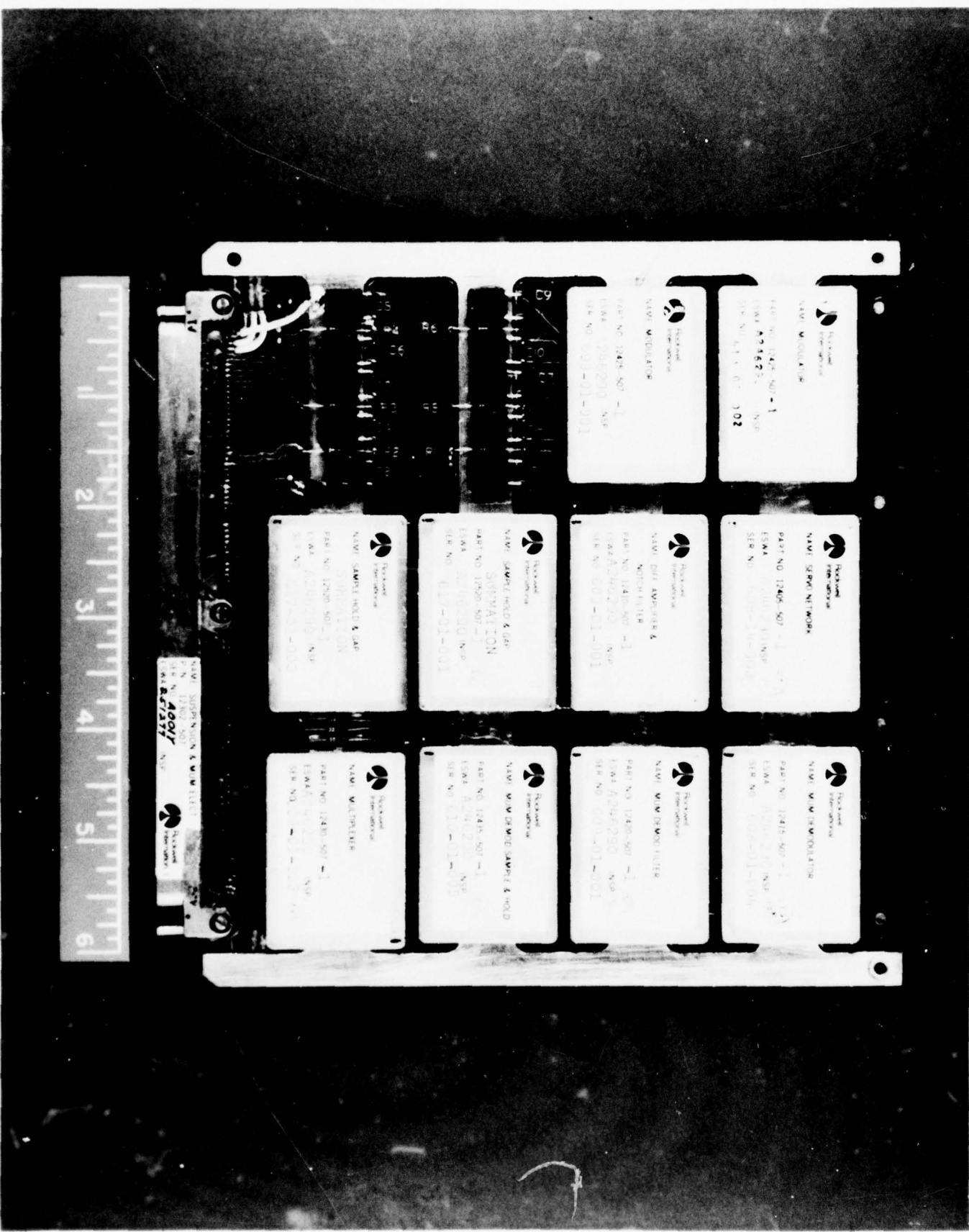
Worst case analyses were completed on all of the hybrids on SEU's 1 and 2. A thermal analysis of all of the semiconductors was also completed and this is given in Appendix B. The analyses results indicate that all the requirements in the reliability design guidelines have been met.

The functional and screen tests performed on the hybrids are listed in Appendix C of this report. Each hybrid has met or exceeded test specification requirements. Appendix D provides additional information relative to precision thin film resistor requirements and performance tests. The data shown in Appendix D indicates the resistors are exhibiting excellent stability and are meeting stability requirements also.

A total of three (including one spare) SEU 1 and 2 modules were assembled and tested. A photograph of a completed module is shown in Figure 18. Appendix E provides information relative to the tasks involved in the fabrication, assembly, and test of the modules. The functional and screen tests performed on the modules are listed in Appendix C. Each of these modules has met or exceeded detail design specification requirements.



Figure 18. Suspension and MUM Electronics Module (SEU 1 and 2)



*[Handwritten marks and scribbles at the bottom of the page]*

### 2.1.5.2 Timing and Sequencing Module (SEU 3)

The Timing and Sequencing Module contains the following hybrid circuits:

<u>Nomenclature</u>	<u>Qty Required</u>	<u>P/N</u>
Precision Crystal Oscillator & Gap Monitor	1	12470-507-1
50 kHz Buffer & EMA Power Supply	1	12475-507-1
A/D Converter	1	12440-507-1
DC Reference and Preload Modulator	1	12480-507-1
EMA Signal Filter	1	12495-507-1
Suspension Timing Generator	1	12445-507-1
Sequencer No. 1	1	12450-507-1
Sequencer No. 2	1	12455-507-1
Ladder Network	1	12565-507-1

A functional block diagram of the Timing and Sequencing Module is shown in Figure 19. The primary functions of this module are the following:

1. Provide the basic INU timing reference.
2. Convert analog signals to digital form for computer analysis.
3. Generate all timing signals required for rotor suspension.
4. Generate gyro preload signals.
5. Buffer and combine signals for the required rotor lift off sequence.
6. Provide rotor desuspension control.
7. Generate Accelerometer excitation signals.
8. Provide computer discrete input gating.
9. Provide computer discrete output latches.

An 18 MHz crystal oscillator provides the basic INU time reference. Nine MHz is sent to the Dedicated Processor Unit (DPU) Input/Output Unit (IOU), where the 4-phase clock required by MOS circuits in the INU is generated. Two MHz is utilized by the A/D Converter and Suspension Timing Generator to generate the required suspension and conversion timing intervals.

All analog signals to be digitized for computer monitoring are routed to multiplexers located external to the Timing and Sequencing module.

A single input from the multiplexers is routed to the Analog to Digital Converter where the signals are digitized and placed on a 13 line parallel bus (12 bits + sign) accessed by the INU computer.

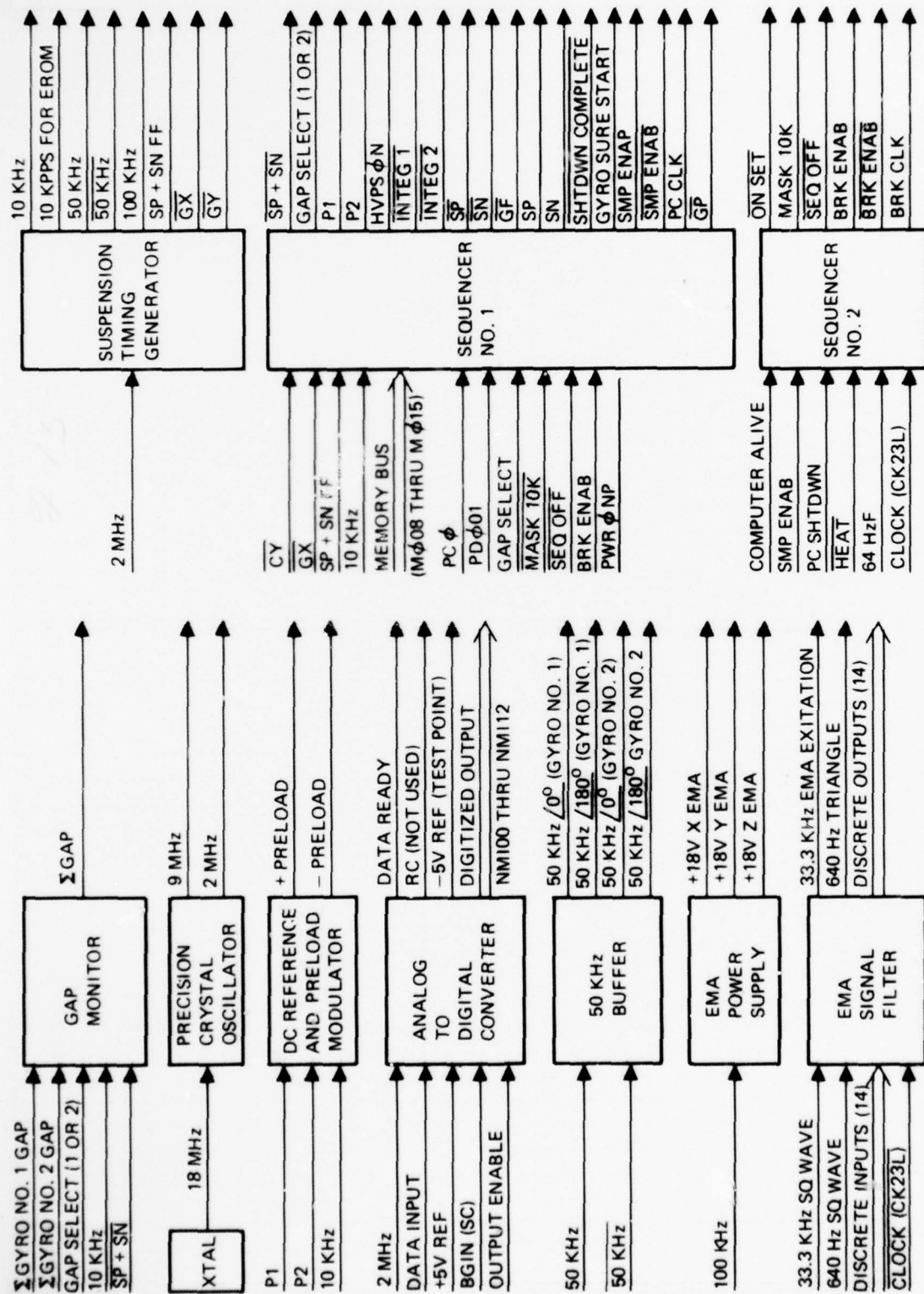


Figure 19. Timing and Sequencing Functional Block Diagram (SEU 3)

The rotor lift off sequence is controlled by the INU computer. Buffering and timing required for satisfactory lift off is generated within the Timing and Sequencing module. The quasi squarewave preload signal required for the rotor lift off sequence and to enable computer monitoring of rotor temperature prior to lift off is generated within the Timing and Sequencing Module.

Desuspension of the rotors through an orderly shutdown sequence is controlled by the Timing and Sequencing module. When commanded from an external source (ON/OFF switch or computer command) the Timing and Sequencing Module activates the rotor braking electronics and provides the necessary braking and timing signals.

The basic timing signals required by the Accelerometers (33.3 kHz and 640 Hz) are shaped and conditioned to provide the waveform characteristics required by the accelerometers. The isolated +18 VDC required by the accelerometer is also generated within the Timing and Sequencing module.

A discrete input/output interface with the INU computer is provided by the Timing and Sequencing module.

Failure of the Timing and Sequencing ON/OFF Sequencing is detected during performance of system level "one time" only testing during the initialization sequence.

A summary of the salient design features of each of the hybrids on SEU 3 is given in the following paragraphs, except for the A/D Converter which is summarized in Para 6.4.2.

#### (1) Precision Crystal Oscillator/Gap Monitor

The Precision Crystal Oscillator/Gap Monitor is a thick film hybrid consisting of two independent functional blocks of circuitry. The Precision Crystal Oscillator consists of an 18 MHz crystal oscillator which provides the basic INU time reference. (The crystal itself is external to the hybrid, being a discrete component mounted on the MLB). Also included on this hybrid are counters to divide the 18 MHz signal into a symmetrical 9 MHz signal (used by the four-phase clock generator on the IOU) and a nonsymmetrical 2 MHz signal (used by the suspension timing generator and A/D converter hybrids).

The Precision Crystal Oscillator was designed to be non-critical with respect to component tolerance, and to provide reliable operation over a wide temperature range. Laboratory test results substantiate the following performance levels:

Frequency	9 MHz symmetrical 2 MHz 5:4 Non-symmetrical
Initial Tolerance	± 10 ppm at 63°C
Long Term Stability	±5 ppm/year
Temperature Coefficient	Maximum slope 1 ppm/°C at 65°C - < 0.3 ppm/°C
Power Supply Sensitivity	Less than 1 ppm frequency change for a ±0.5 volt change in either -7.5 vdc or +5.0 vdc supplies

The Gap Monitor demodulates and samples inputs from the sample and hold/gap summation substrates to provide an analog output which is a measure of the average gap between rotor and cavity. Gap information for either gyro may be processed, under the control of a discrete digital input. Laboratory tests indicate that the following system requirements are achievable, all of which meet system performance requirements.

Scale Factor	30 mv/ $\mu$ in.
Output Range	$\pm 5$ volts dc; 0 volts = nominal gap
Accuracy	
1. Scale factor:	$\pm 6\%$
2. Scale Factor Stability over one year	$\pm 0.7\%$
3. Bias:	$\pm 0.4$ vdc
4. Bias stability over one year	$\pm 6$ mv

The thick film process was chosen for this hybrid as one of minimum cost while still meeting system requirements. An emphasis was placed on the use of non-precision resistors and low cost multiple-sourced chip components.

#### (2) 50 kHz Buffer and EMA Power Supply

The 50 kHz Buffer/EMA Power Supply hybrid houses two independent functional blocks of circuitry.

The 50 kHz Buffer outputs four 50 kHz analog square waves used to drive the Charge Amplifier output transformers on the IAU. The design approach followed has proven successful in many hours of reliable operation of previous systems.

The EMA Power Supply provides three isolated +18 vdc reference voltages to the X, Y, and Z accelerometers. The following results have been achieved in laboratory tests:

Tolerance on nominal voltage	$\pm 5\%$
Load Regulation (FL to FL + 10%)	$\pm 2\%$
Stability, repeatability of maximum deviation from nominal (including temperature and aging over one year)	$\pm 3\%$
Ripple (peak-to-peak)	< 100 mv
Maximum current (each output)	10 ma

The 50 kHz buffer/EMA Power Supply employs thick film technology coupled with loose resistor tolerances (none < 5 percent), wide substrate line specified ( $\geq 10$  mil), and conservatively derated components to achieve a producible, low-cost item.

### (3) EMA Signal Filter

The EMA Signal Filter is a thick film hybrid which outputs the analog waveforms required by the accelerometers and also provides a digital discrete input/output interface with the INU computer. The interface employs low cost low-power Schottky TTL gates and thick film pull-up resistors.

The signal processing portion of this hybrid receives digital input waveforms initially generated by the METG MOS chip and outputs a 33-1/3 kHz analog square wave and a 640 Hz analog triangular wave.

The EMA Signal Filter has been designed to meet the following goals:

#### 33 1/3 kHz Square Wave

Voltage Characteristics:	14 - 16 V ptp (Centered about 0 ±0.5 vdc)
Long Term Amplitude Stability:	±3% over one year
Rise and Fall Times:	≥ 1 μsec, ≤ 2 μsec

#### 640 Hz Triangular Wave

Voltage Characteristics:	16 ±1 V p-p (Centered about 0 ±0.1 vdc)
Long Term Amplitude Stability:	±3% over one year
Long Term Frequency Stability	≤ 6 ppm/year

### (4) Suspension Timing Generator, Sequencer No. 1, and Sequencer No. 2

The Suspension Timing Generator, Sequencer No. 1 and Sequencer No. 2 are all thick-film hybrid circuits. The semiconductors utilized to perform the logic and timing functions on these hybrids are primarily low power Schottky TTL.

The Suspension Timing Generator and the Sequencers generate all timing signals required for rotor suspension, buffers, and combine signals for the rotor liftoff sequence, and provide rotor desuspension control.

### (5) Ladder Network

The ladder network is a 13-bit 50K/100K thin-film resistor R/2R ladder network. This ladder is used in conjunction with the A/D converter hybrid circuit. The ladder networks were fabricated and tested at Hallex Inc.

### (6) DC Reference and Preload Modulator

The DC Reference and Preload Modulator provides the precision voltage reference for the A/D Converter, and for the gap monitor function. It also generates the preload signals which drive all charge amplifiers.

Appendix A to this report gives an itemized listing of the activity involved in the fabrication, assembly, and testing of the above hybrids and also provides a discussion of EPM hybrid technology

Worst case analyses were completed on all of the hybrids on SEU 3. A thermal analysis of all of the semiconductors was also completed and this is given in Appendix B. The analyses results indicate that all the requirements in the reliability design guidelines have been met.

The functional and screen tests performed on the hybrids are listed in Appendix C of this report. Each hybrid has met or exceeded test specification requirements. Appendix D provides additional information relative to precision thin film resistor requirements and performance tests. The data shown in Appendix D indicate the resistors are exhibiting excellent stability and are meeting stability requirements also.

Two SEU 3 modules, including one spare, were assembled and tested. A photograph of a completed SEU 3 module is shown in Figure 20. Appendix E provides information relative to the tasks involved in the fabrication, assembly, and test of the modules. The functional and screen tests performed on the modules are listed in Appendix C. Each of these modules has met or exceeded detail design specification requirements.



Figure 20. Timing and Sequencing Module (SEU 3)



Rockwell International  
PART: SUSPENSION TANK  
GENERATOR  
PART NO 12445-507-1  
ESNA 421402000 NSP  
SER NO 010000-1019

Rockwell International  
NAME: SOURCE NO 2  
PART NO 12445-507-1  
ESNA 421402000 NSP  
SER NO 010000-1019

Rockwell International  
NAME: SOURCE NO 1  
PART NO 12445-507-1  
ESNA 421402000 NSP  
SER NO 010000-1019

Rockwell International  
NAME: SOURCE BUFFER & EMI  
POWER SUPPLY  
PART NO 12475-507-1  
ESNA 421402000 NSP  
SER NO 010000-1019

Rockwell International  
NAME: DC 915 & PRELOAD MOD  
PART NO 12485-507-1  
ESNA 421402000 NSP  
SER NO 010000-1019

Rockwell International  
NAME: LADDER NETWORK  
PART NO 12565-507-1  
ESNA 421402000 NSP  
SER NO 010000-1019

Rockwell International  
NAME: A/D CONVERTER  
PART NO 12605-507-1  
ESNA 421402000 NSP  
SER NO 010000-1019

Rockwell International  
NAME: EM SIGNAL FILTER  
PART NO 12495-507-1  
ESNA 421402000 NSP  
SER NO 010000-1019

Rockwell International  
NAME: PRECISION DIGITAL  
OSCILLATOR FOR MONITOR  
PART NO 12470-507-1  
ESNA 421402000 NSP  
SER NO 010000-1019

### 2.1.5.3 Signal Generator and Memory Module (SEU 4)

A functional block diagram of the SEU 4 module is shown in Figure 21. The Signal Generator and Memory Module receives parallel digital data from the Processor Memory Module and combined with input timing signals provides the following signals.

1. Three-channel modulated spin motor control signals and feedback signals
2. Modulated calibration signal
3. Frequency variable timing signals for MUM Demod No. 1 and Spin Motor
4. Frequency variable timing signal for MUM Demod No. 2 and Spin Motor
5. Eighteen (18) system control discrettes
6. Eight (8) modulated heater control signals
7. Four (4) fast warm-up heater controls

MUM and EMA timing are also generated and buffered on this module. Calibration constants are stored on this module in a 1K x 16 non-volatile semiconductor memory. Access to this memory is by a parallel digital bus and associated timing signals. The module contains the following major components.

1. Modulated DAC (MOS SMC)
2. Modulated DAC (MOS TEMP CONT)
3. Spin Motor Controller
4. Temperature Controller
5. Calibration Constant Storage No. 1 (CCS 1)
6. Calibration Constant Storage No. 2 (CCS 2)
7. MUM and EMA Timing Generator (METG)
8. Quasi Reference Generator (QRFG) (MOS Gyro No. 1)
9. Quasi Reference Generator (GRFG) (MOS Gyro No. 2)

A discription of each of these major components is given in the following:

#### 1. Modulated DAC (MOS SMC)

This substrate receives parallel digital data and timing signals and outputs 12 modulated signals which are used to control the spin motor. This substrate also provides six discrettes for use on the module and external to the module.

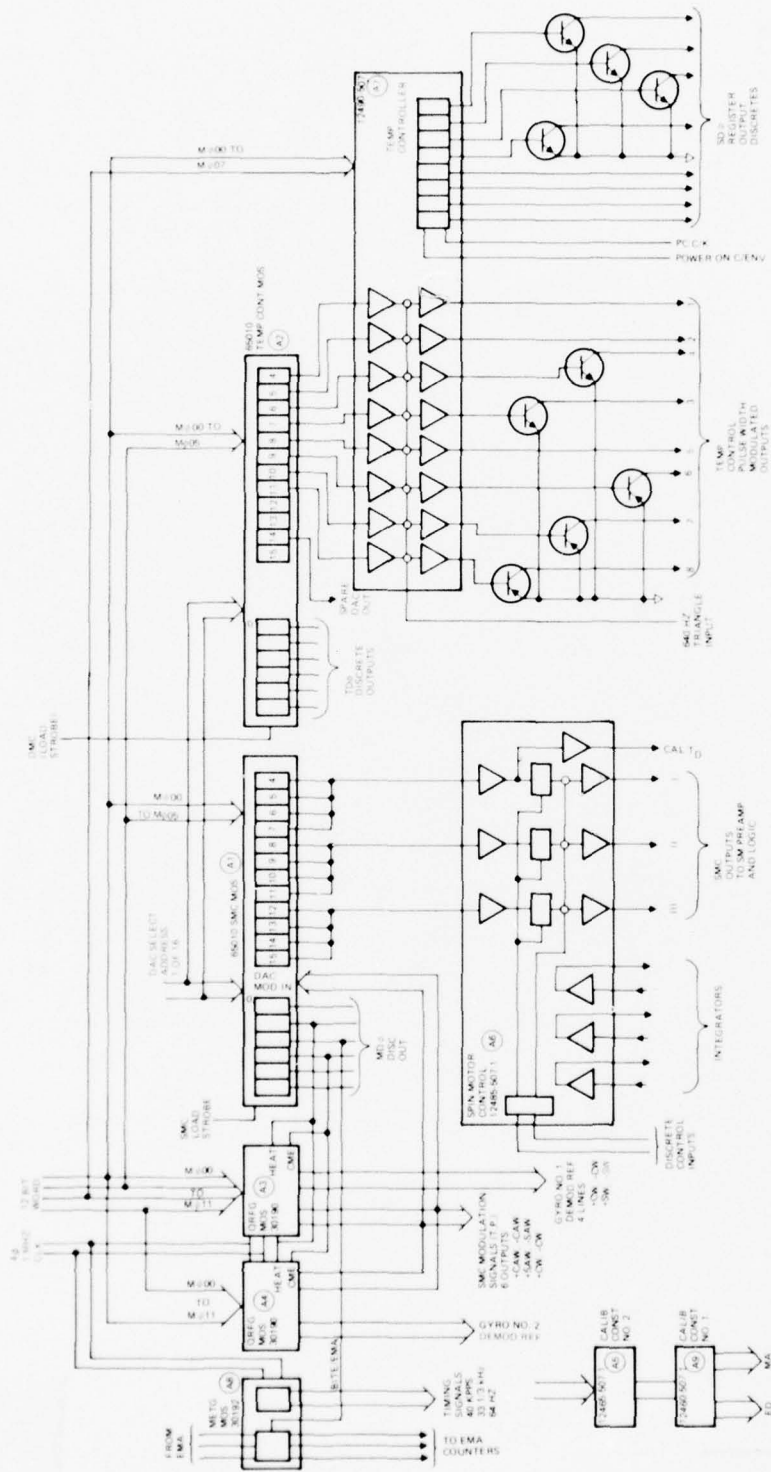


Figure 21. Signal Generator and Memory Functional Block Diagram (SEU 4)

2. Modulated DAC (MOS TEMP. CONT)

This substrate receives parallel digital data and outputs 12 d-c analog signals of which eight are used to control the temperature controllers. This substrate also provides six discretes for use on the module and external to the module.

3. Spin Motor Controller

This substrate receives from the Modulated DAC (MOS SMC) four signals summed to form  $F_x$  which is amplified and provides input signals to the IAU Spin Motor Amplifier. This output is also buffered and sent to SEU No. 1 and No. 2 Module for calibration and torque disturbance. This substrate also amplifies the summed signals of  $F_y$  and  $F_z$  to form outputs to the IAU Spin Motor Amplifier. This substrate also receives feedback signals from the Spin Motor coils for conditioning and receives discretes for filter and gain modification of the output signals.

4. Temperature Controller

This substrate receives d-c analog signals from the Modulated DAC (MOS TEMP CONT), amplifies the signals and provides a signal for heater control. The substrate also receives parallel digital data and provides a latch for eight discrete outputs for system use.

5. Calibration Constant Storage No. 1 and No. 2

These two substrates when combined provide a 1K x 16 nonvolatile memory storage for system calibration constants.

6. MUM and EMA Timing Generator (MOS)

This substrate receives signals and acceleration pulses. It outputs timing signals for the MUM Demods, Spin Motor, EMA, DMAC and conditioned EMA signals.

7. Quasi Reference Generator No. 1 and No. 2

Each substrate receives discretes, clocks and a parallel data bus to set frequency of timing signals to MUM demodulators and the Spin Motor Modulated DAC.

The Signal Generator and Memory Module provides continuous storage and readout of a calibration constant word. Additional functions will be performed as part of modes of operation which involve this module.

Self tests consists of EMA test frequency generation and readout. Output from the Spin Motor Substrate will be tested.

The Spin Motor Control MOS Circuit that is utilized on SEU 4 is described in Para 6.4.3. Both the Spin Motor Controller (12485-507) and the Temperature Controller (12490-507) are thick film hybrids. (See Appendix A.)

A worst case analysis and a thermal analysis were completed on both of these hybrids. The thermal analyses results are summarized in Appendix B. The results of these analyses show that all the reliability design guidelines have been met.

The functional and screen tests performed on the hybrids are listed in Appendix C of this report. Each hybrid has met or exceeded test specification requirements. Appendix D provides additional information relative to precision thin film resistor requirements and performance tests. The data shown in Appendix D indicate the resistors are exhibiting excellent stability and are meeting stability requirements also.

Two SEU 4 modules, including one spare, were assembled and tested. A photograph of a completed SEU 4 module, less the Cal Constant Storages No. 1 and No. 2 hybrids, is shown in Figure 22. Appendix E provides information relative to the tasks involved in the fabrication, assembly and test of the modules. The functional and screen tests performed on the modules are listed in Appendix C. Each of these modules met or exceeded detail design specification requirements.

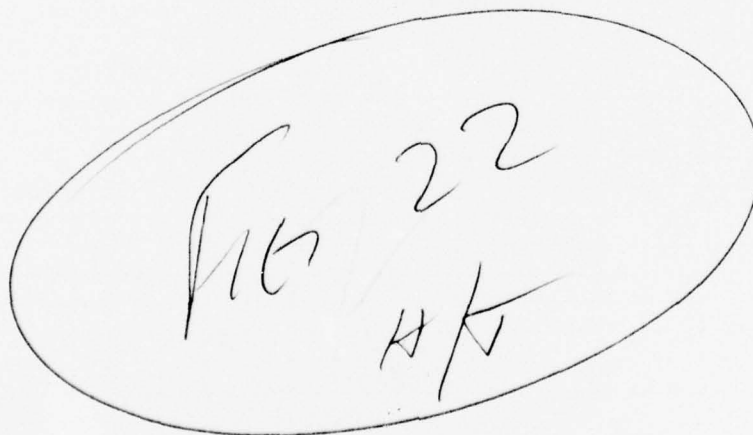
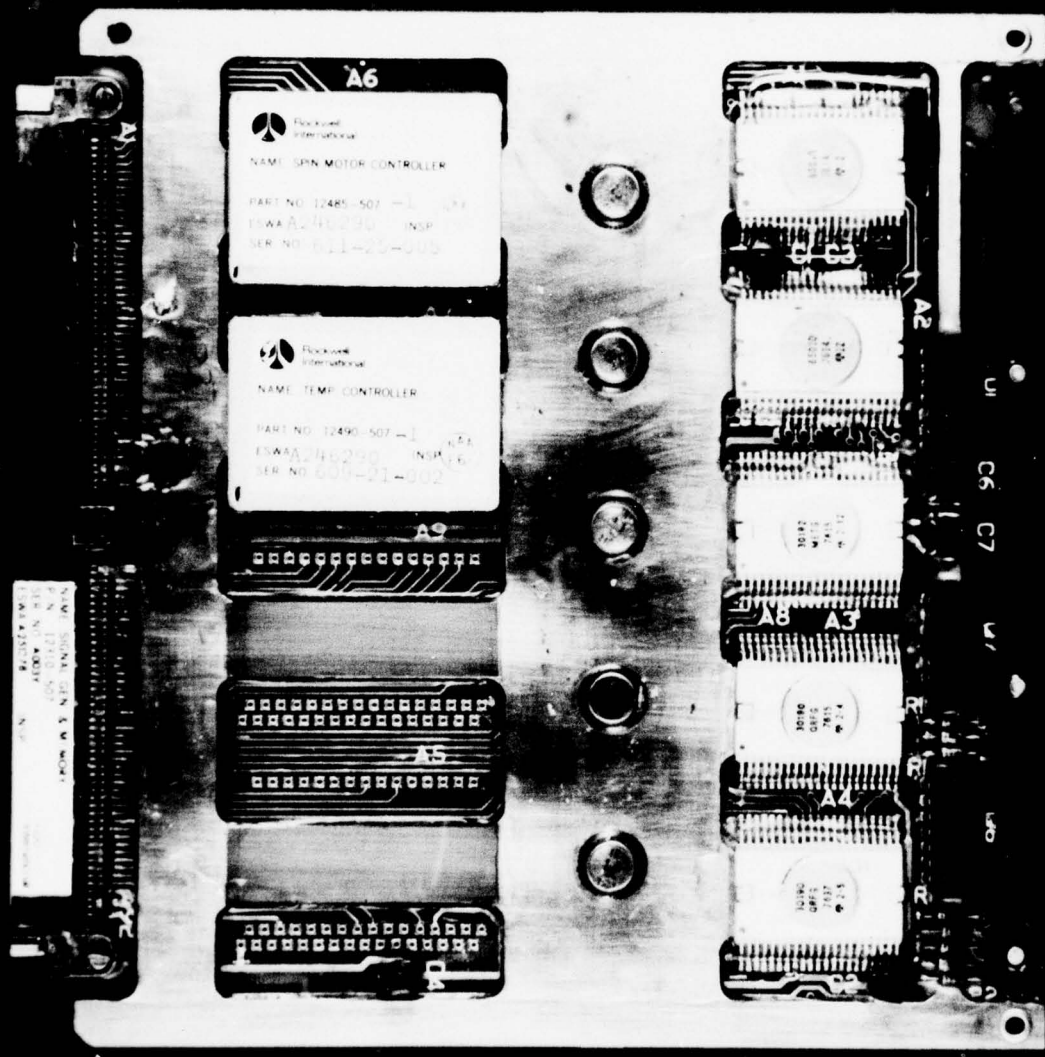


Figure 22. Signal Generator and Memory Module (SEU 4)

22

54



A

4/6 A

#### 2.1.6 IAU Design/Develop/Fab/Test

The original design of the IAU was a non-rotating, shock mounted structure. This structure was also a coldplate to provide cooling for the instruments which consisted of two ESG's, three EMA's, Spin Motor Electronics, and two Charge Amplifier Modules. This design is depicted in Figure 23.

The decision to implement a rotating IAU was made in April 1976. The rotating IAU configuration is shown in Figure 24. The unit is mounted on a shock isolated ring gear which rides on a four point contact ball radial bearing. The ring gear rotates 360 deg in 1 minute via a synchronous motor and is monitored by an encoder which communicates with the computer. A limit stop mechanism is provided to prevent overriding the reverse point in case of a failure in the system.

The rotation section which supports the ESG's, EMA's, and Charge Amplifiers required special attention. The Charge Amplifier MLB had to be redesigned into a circular configuration, (see Para 2.1.6.1.1) and the EMA mounting surfaces were changed from an orthogonal relationship to a shimed orientation slightly off of orthogonal by a few minutes of arc.

The ESG's are mounted directly below the Charge Amplifiers and are interconnected via triax cables. All IAU interconnections are via a twist capsule which interfaces with the MIB.

The functional block diagram of the IAU is shown in Figure 25 and illustrates the types of electrical interfaces made through the twist capsule to the MIB.

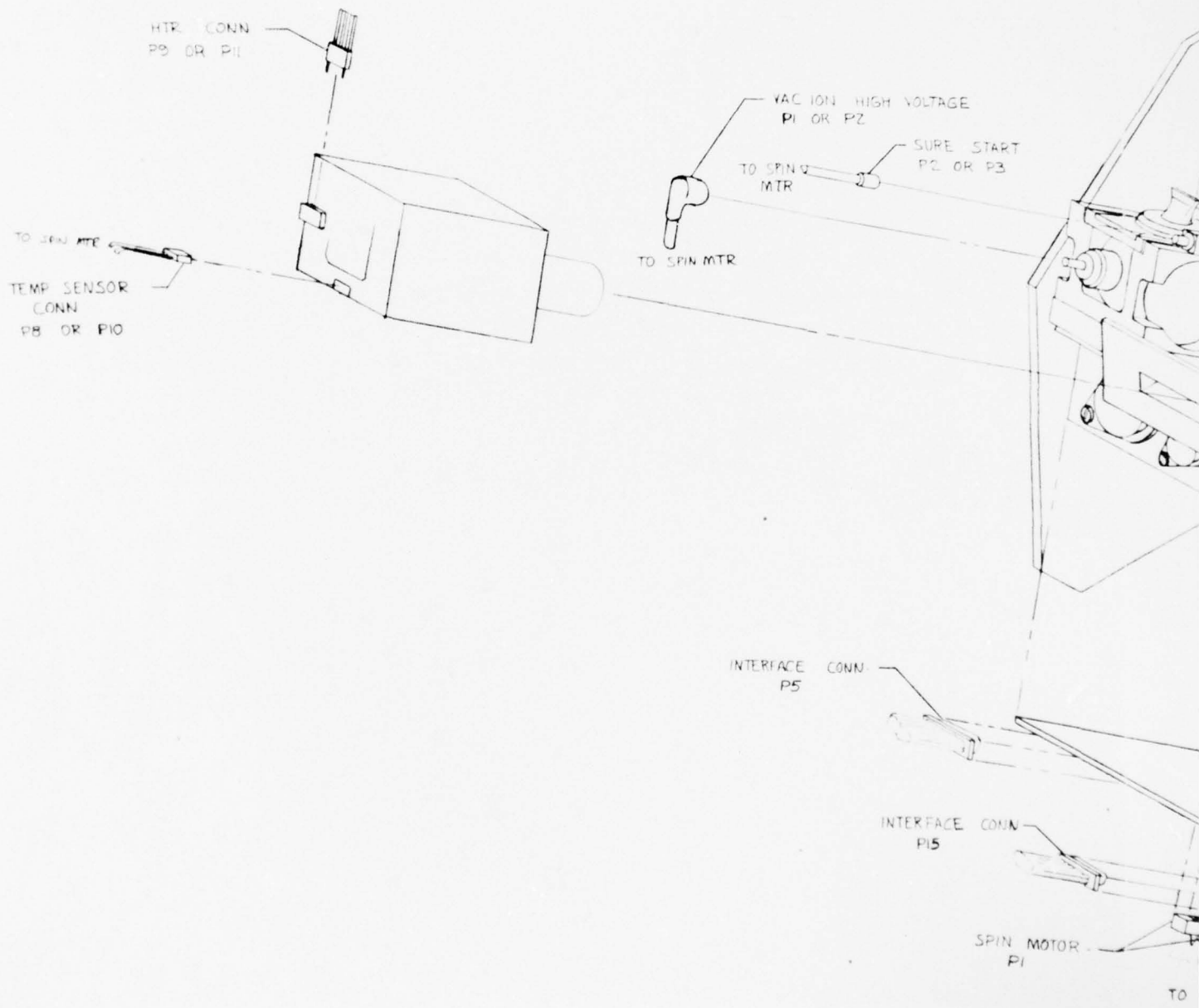
Fabrication of detail parts for the rotating IAU was started in May 1976. Assembly and wiring of the IAU started in June and was completed in July. Fit checks of the IAU into the MHU (rotating version) was also accomplished in July. In August, the IAU wiring was verified and the IAU was delivered to the integration lab. A photograph of the completed IAU is shown in Figure 26.



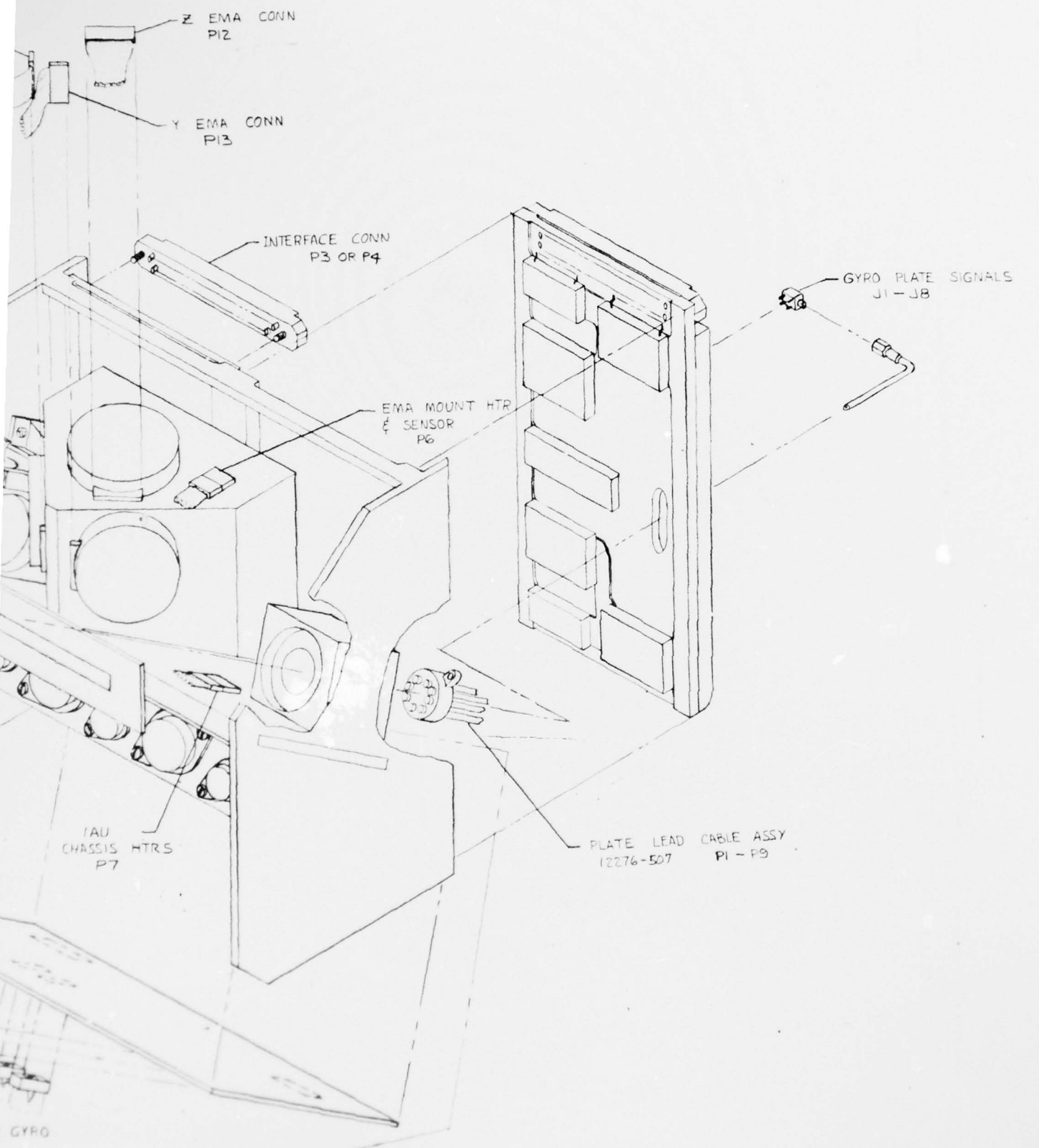
Figure 23. IAU Interface (Non-Rotating)

Figure 23. IAU Interface (Non-Rotating)

X EMA CONN  
P4



8 1/2" FIG 23 PG 50



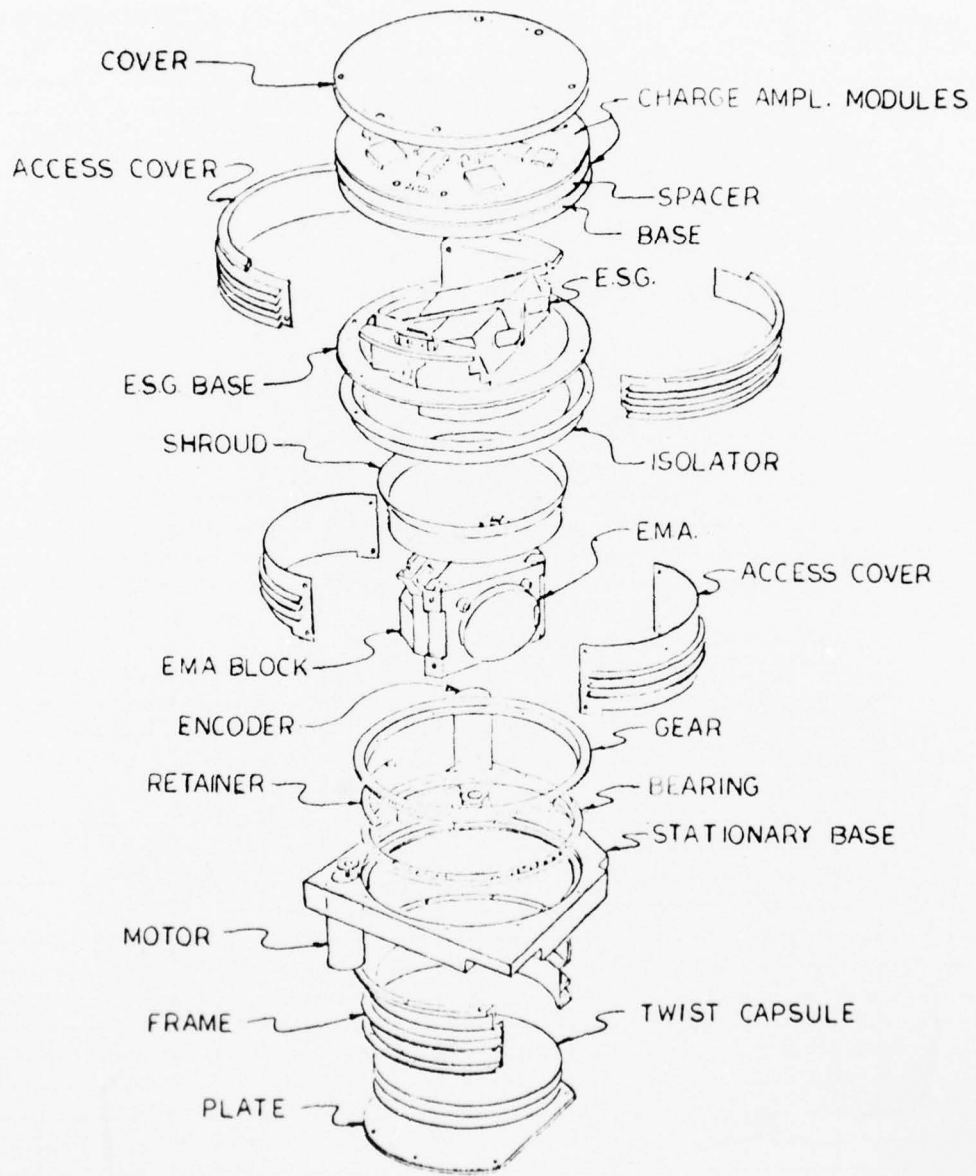


Figure 24. Rotating Instrument Assembly Unit (Exploded View)

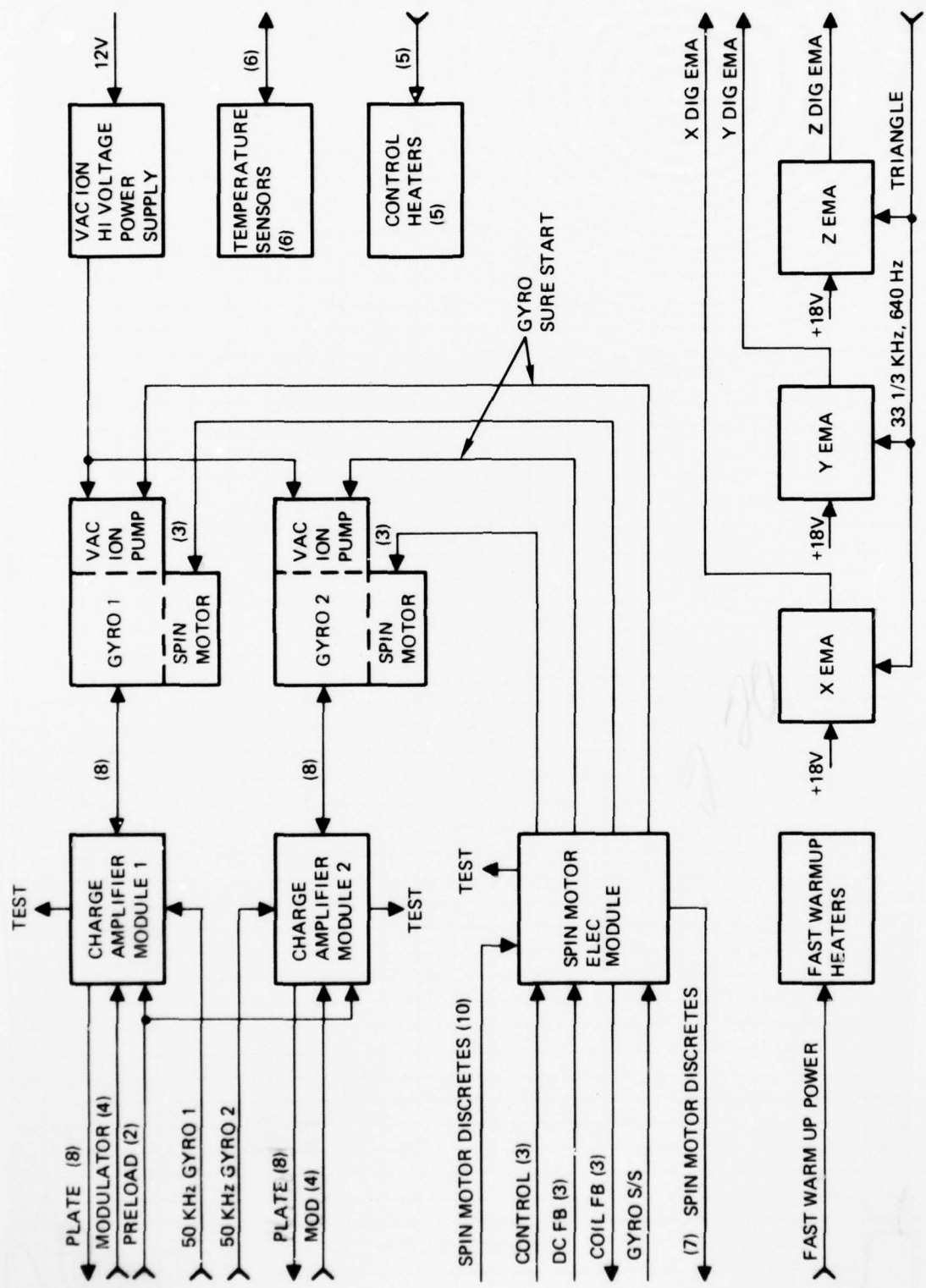


Figure 25. IAU Functional Block Diagram

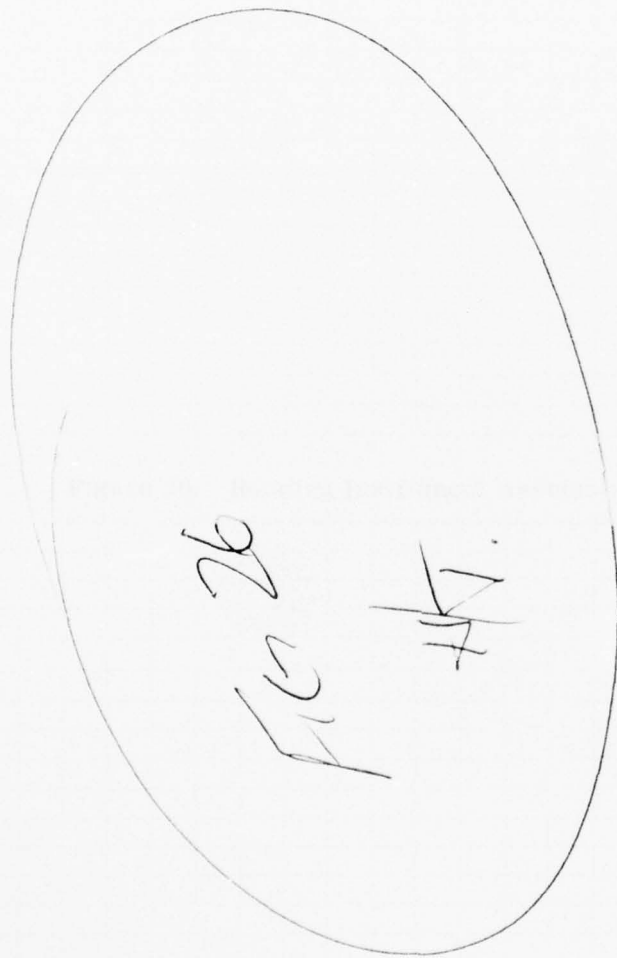


Figure 26. Rotating Instrument Assembly Unit (IAU)



*Handwritten markings at the bottom of the page, including a large 'A' on the left, a '6' in the center, and another 'A' on the right.*

#### 2.1.6.1 IAU Electronics

The IAU Electronics consist of the Charge Amplifier Electronics Assembly and the Spin Motor Electronics Assembly (see Figure 25). Each of these assemblies is discussed in the following paragraphs.

**2.1.6.1.1 Charge Amplifier Electronics Assembly.** The Charge Amplifiers provide a precision charge to the electrodes of the ESG's proportional to the signal at the Charge Amplifier input. A total of 16 Charge Amplifier hybrid circuits are required per EPM system. The Charge Amplifiers are packaged on two MLB's. The Charge Amplifiers receive the modular outputs from the Suspension and MUM Electronics Module and the preload signal from the Timing and Sequencing Module in the SEU. These signals are shown in Figure 16. These signals are combined in the charge amplifier waveform as shown in Figure 17. A pulse amplitude modulation, time division multiplex scheme is mechanized to apply restoring forces to the rotor and to sense rotor position. The four modulator outputs are zero in the readout periods, during which time a constant charge (preload level) is applied to the gyro electrodes. The plate voltage during this time therefore depends upon the distance between the plate and rotor. When the modulator outputs are nonzero, a restoring force is being applied to the rotor because the plate which is farther from the rotor receives a larger charge than its opposing plate. The polarity of the charge is reversed every 50 microseconds. A period of six microseconds is allowed for charge reversal, during which time the plates receive zero charge. Thus, each 50 microsecond interval is divided into six microseconds of zero charge, 12 microseconds for readout and 32 microseconds for forcing. A high voltage power supply is required for the Charge Amplifiers with waveforms as shown in Figure 27.

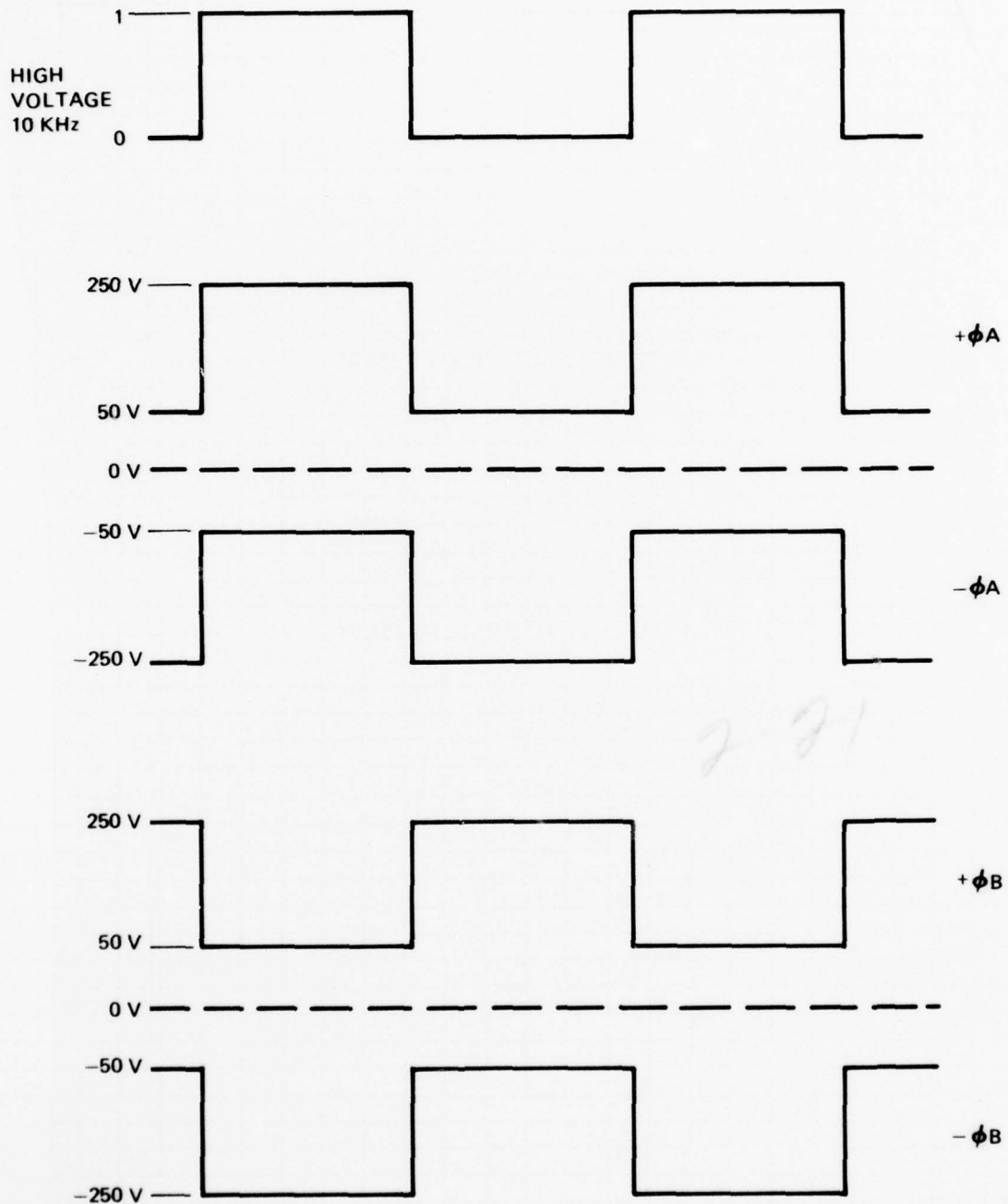
The Charge Amplifiers designed for EPM were the lowest cost configuration that could be devised which could give satisfactory operation. At one time it was thought that the floating unity gain buffer could be eliminated in the Charge Amplifier. Later tests showed that this gave excessive force-pickoff coupling.

The Charge Amplifier substrates use thin-film technology as described in Appendix A. As shown in Table A-1 of Appendix A, a total of 26 Charge Amplifier hybrids, including 10 spares, were fabricated, assembled, and tested.

A thermal analysis was conducted on all the semiconductors within the Charge Amplifier. The results of this analysis showed that junction temperatures were well below those allowed in the reliability design guidelines. The results are shown in Appendix B.

Three Charge Amplifier Electronic Assembly modules, including one spare, were assembled and tested. Appendix E provides information relative to the tasks involved in fabrication, assembly, and test of the modules.

The Charge Amplifier hybrids and modules were functionally and screen tested per the specifications listed in Appendix C. The performance of the Charge Amplifiers has been outstanding. These Charge Amplifiers have been proven to be not subject to latchup and the design is simpler and less costly than any preceding design. A photograph of a completed Charge Amplifier module is shown in Figures 28 and 29.



NOTES: TOLERANCE OF SET POINT VOLTAGES =  $\pm 5\%$

Figure 27. High Voltage Waveforms



Figure 28. Charge Amplifier Module (Front Side)

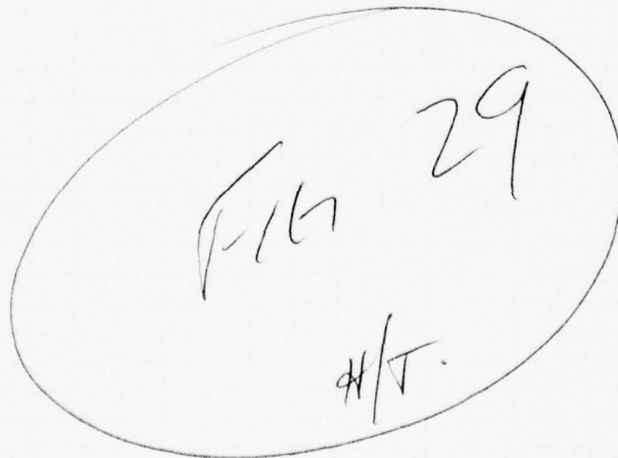
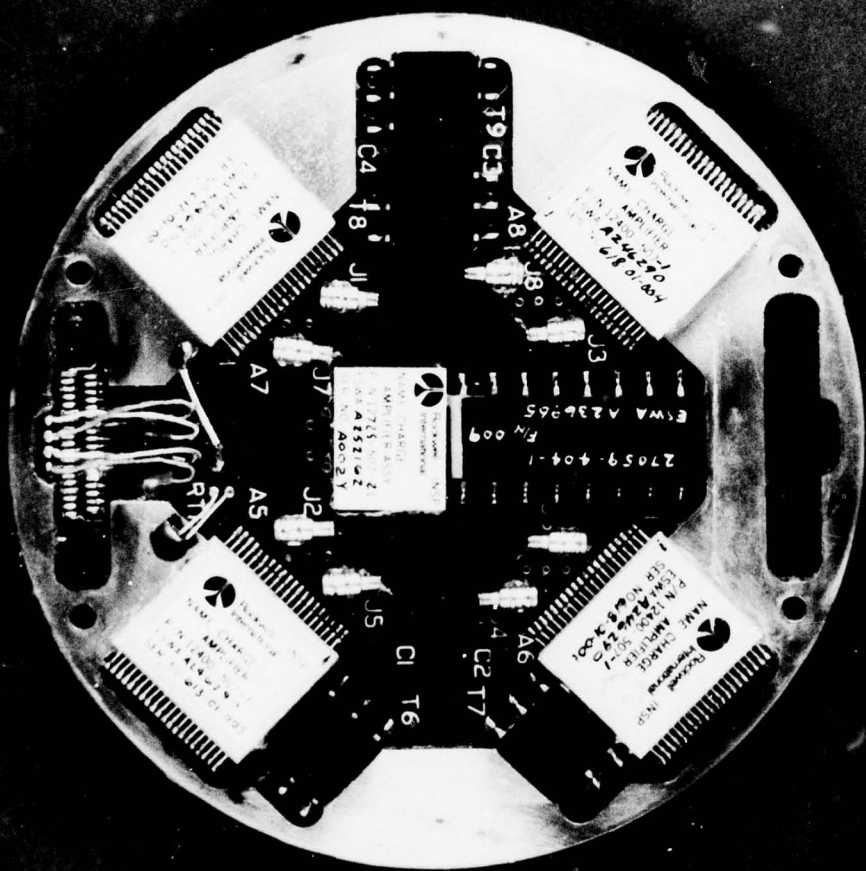


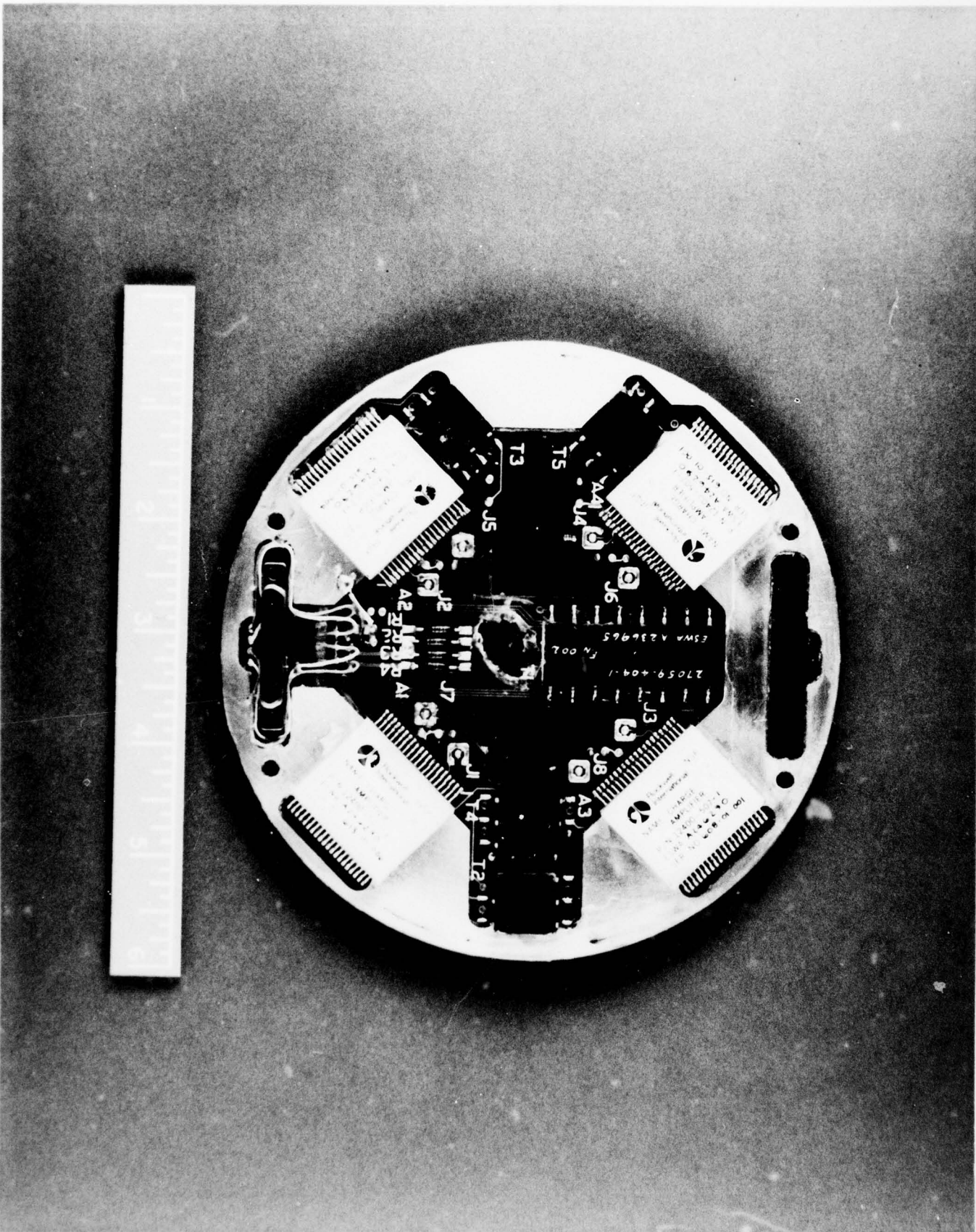
Figure 29. Charge Amplifier Module (Back Side)



*[Handwritten marks and scribbles at the bottom of the page, including a large 'A' and other illegible characters.]*

29

62



A

4

A

2.1.6.1.2 Spin Motor Electronics Assembly. The Spin Motor Electronics Assembly contains the power amplifiers, gyro motor coil select relays, and spin motor power on/off relays required to drive the gyro spin motors. The Spin Motor Electronics Assembly is contained on three printed circuit boards. There are two Spin Motor Power Amplifiers (P/N 12750-507-1 and -11) and one Spin Motor MLB Assembly (P/N 12753-507). These three Spin Motor Electronics subassemblies are shown in Figure 30.

During the design phase, tradeoff studies were conducted to determine the lowest cost and most reliable configuration for the spin motor power amplifiers. It was concluded that a bridge stage such as that used on the previous system (N77) was more complex and less efficient than a complementary power stage. The complementary power stage requires positive and negative power supplies, but this is generated simply by rectifying 400 Hz power.

The Spin Motor MLB Assembly contains one hybrid circuit (Spin Motor Power Pre-Amplifier and Logic, P/N 12525-507). This hybrid uses thick-film technology as described in Appendix A. Three Spin Motor Power Pre-Amplifier and Logic hybrids (including two spares) were fabricated, assembled, and tested.

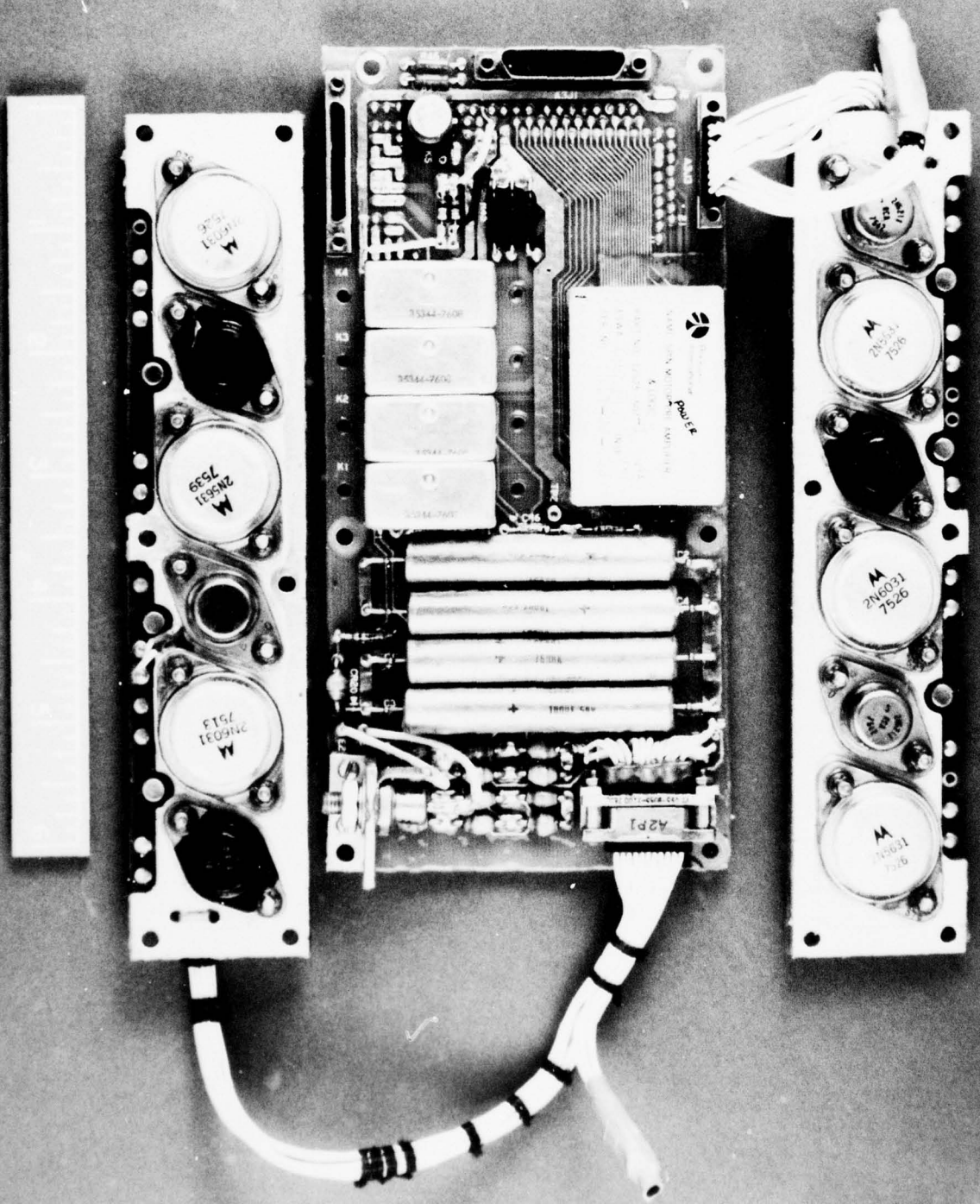
Two each of the three subassemblies which make up the Spin Motor Electronics Assembly (see Figure 30), including one spare each, were assembled and tested. Appendix E provides information relative to the tasks involved in fabrication, assembly, and test of these subassemblies.

The Spin Motor Electronics Assemblies and the Spin Motor Power Pre-Amplifier and Logic hybrids were functionally and screen tested per the specifications listed in Appendix C. All the requirements called out in the detail design specifications were met by the Spin Motor Electronics Assembly. In addition, rotor spin-up, heat, and brake tests were conducted on Test Station IV with the following results:

1. Rotor Spin-up Tests - For  $I_x = I_y = 1.9$  amps rms in the x- and y-gyro coils and  $I_z = 1.4$  amps rms in the z-coil with 2.4 amps dc from the power supply, a rotor spin-up time of 9.7 sec (to 2700 rps) was achieved. The detail design specification requires a spin-up time of 10 sec.
2. Rotor Heat Tests - With a z-coil current of 5.1 amps rms, the rotor heating rate was  $101^{\circ}\text{F}/\text{min}$ , which is well within the detail design specification requirement of  $80^{\circ}\text{F}/\text{min}$ .
3. Rotor Brake Tests - For  $I_x = I_y = 3.2$  amps rms in the x- and y-gyro coils and  $I_z = 2.3$  amps rms in the z-coil with a 1/3 duty cycle in each coil, the rotor was braked from 2550 rps to less than 2 rps within 50 sec. The detail design specification requires 64 sec. Figure 31 shows the spin down profile.

Fig 30  
AT

Figure 30. Spin Motor Electronics Subassemblies



Handwritten markings at the bottom of the page, including a large 'A' on the left, a '611' in the center, and another large 'A' on the right.

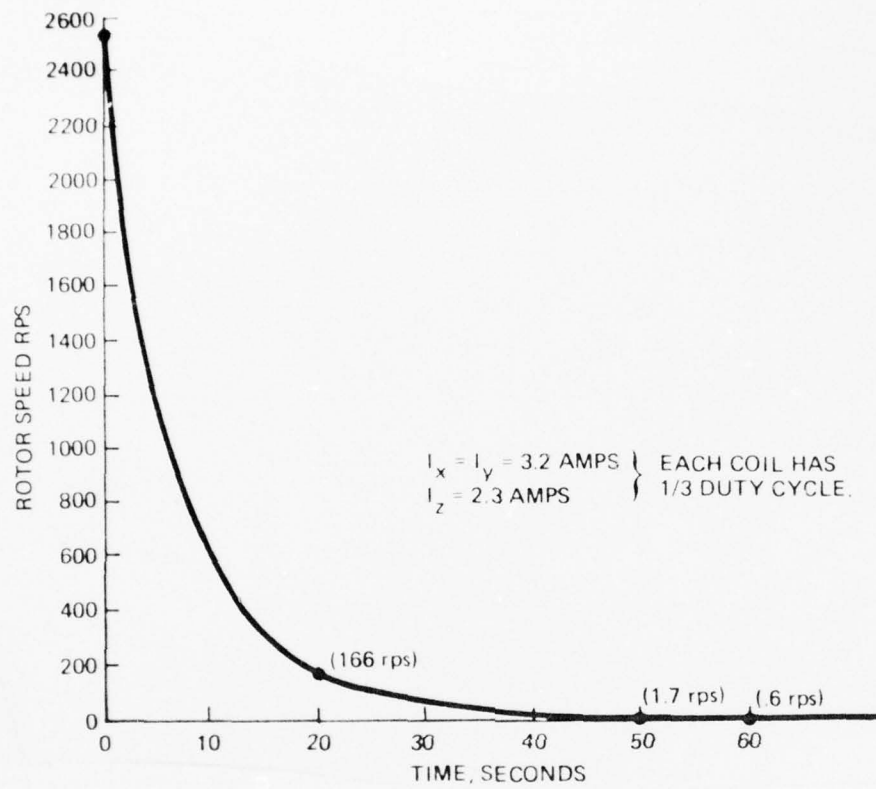


Figure 31. Rotor Speed vs Time, Rotor Brake Test

AD-A048 000

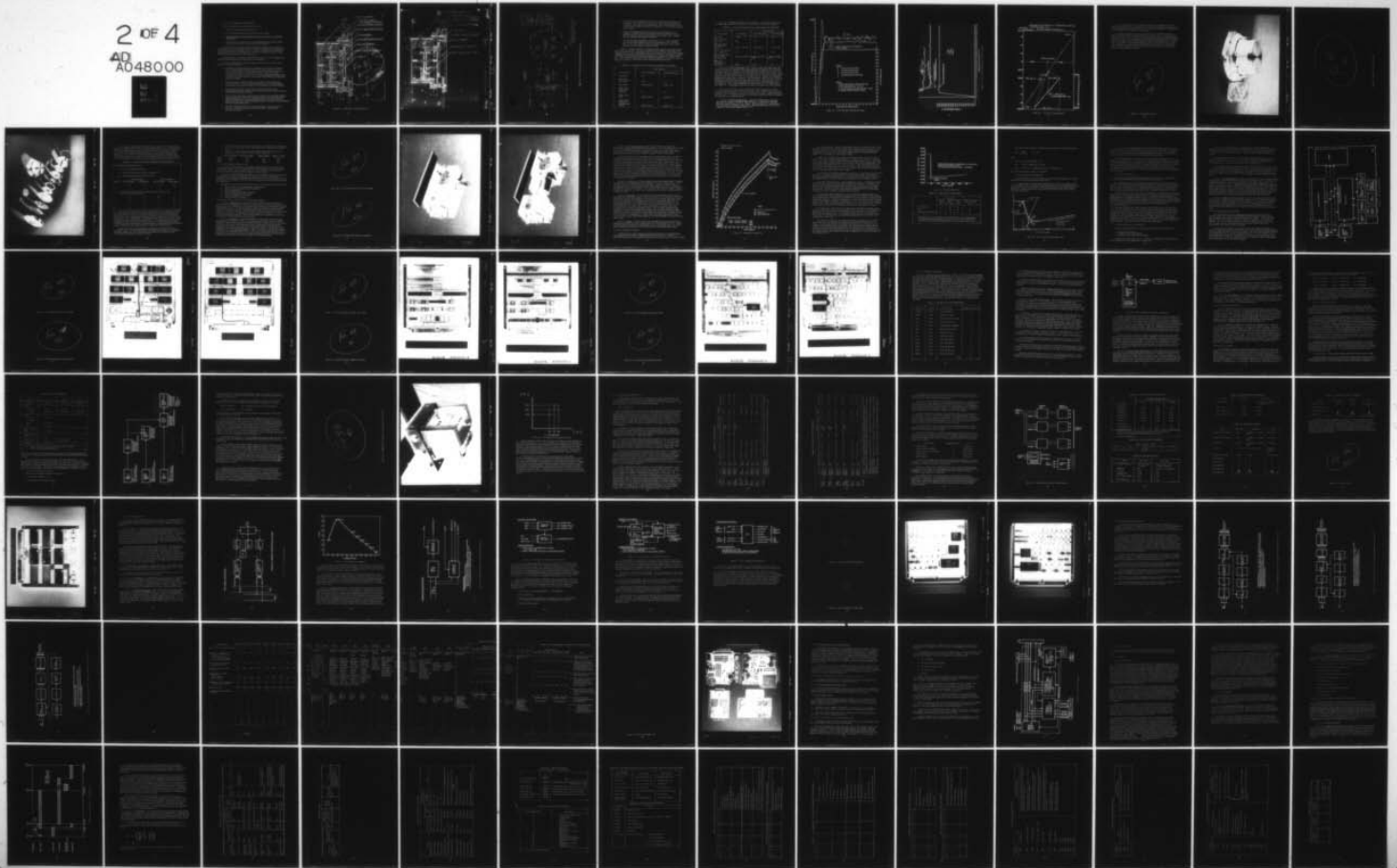
ROCKWELL INTERNATIONAL ANAHEIM CALIF AUTONETICS GROUP  
MICRO NAVIGATOR (MICRON) PHASE 2B VOLUME I. TECHNICAL REPORT.(U)  
AUG 77 J M MILLER, A P ANDREWS, T F BRASHER F33615-75-C-1301  
C75-787/201-VOL-1 AFAL-TR-77-138-VOL-1

F/G 17/7

UNCLASSIFIED

NL

2 OF 4  
AD  
A048000



#### 2.1.6.2 EMA Design/Develop/Fab/Test

The EMA design and development objectives were:

1. Reduced production and ownership costs.
2. Fast reaction performance when heated at 80<sup>0</sup>F/minute.
3. Improved stability and repeatability across the expected severe MICRON environments.
4. Fabrication and evaluation of two A77M Engineering Development Models (EDM's) and six A77M's for the MICRON EPM system.

The A77 EMA (N77 version) design was modified to address these objectives. The modified design was identified as the A77M EMA. The high-cost components and activities (processing and testing) of the A77 EMA were identified and the projected production costs for the A77M design were reduced to 44 percent of the A77. This cost is within 20 percent of the EMA target cost.

Two Engineering development models (EDM's) of the A77M were completed and functional and performance evaluation tests were conducted.

The A77M configuration is shown in Figures 32 and 33. Some of the design features and improvements are:

1. The flexure bearing and proof mass pendulum are of etched and abraded, low mechanical hysteresis fused silica. The stators and outer case are of Invar. The thermal expansion coefficients of fused silica and Invar are matched within 1 ppm/F<sup>0</sup>. Except for the forcer coils, the critical assemblies are clamped together with screws or spring loaded pressure pads. The benefits of these features are low temperature sensitivity and improved long-term stability.
2. The analog sensor and servo digitizer assembly are both hermetically sealed, separable, testable and interchangeable "plug-in" subassemblies. The benefits are long-term stability, ease of diagnosis, and cost reduction.
3. The permanent magnets are high energy product, high coercivity, unshouldered samarium-cobalt material replacing shouldered Alnico magnets. The benefit is long-term stability.
4. The total EMA scale-factor temperature sensitivity was reduced by magnetic shunt compensation of the sensor magnetic circuit. This development completely eliminated all of the costs associated with the A77 self-contained temperature controller, sensor and control heaters. Benefits are cost reduction and fast reaction performance.
5. The A77M design represents a 24 percent reduction in mass and thermal capacity. The volume has been reduced 18 percent. Benefit is fast reaction performance.

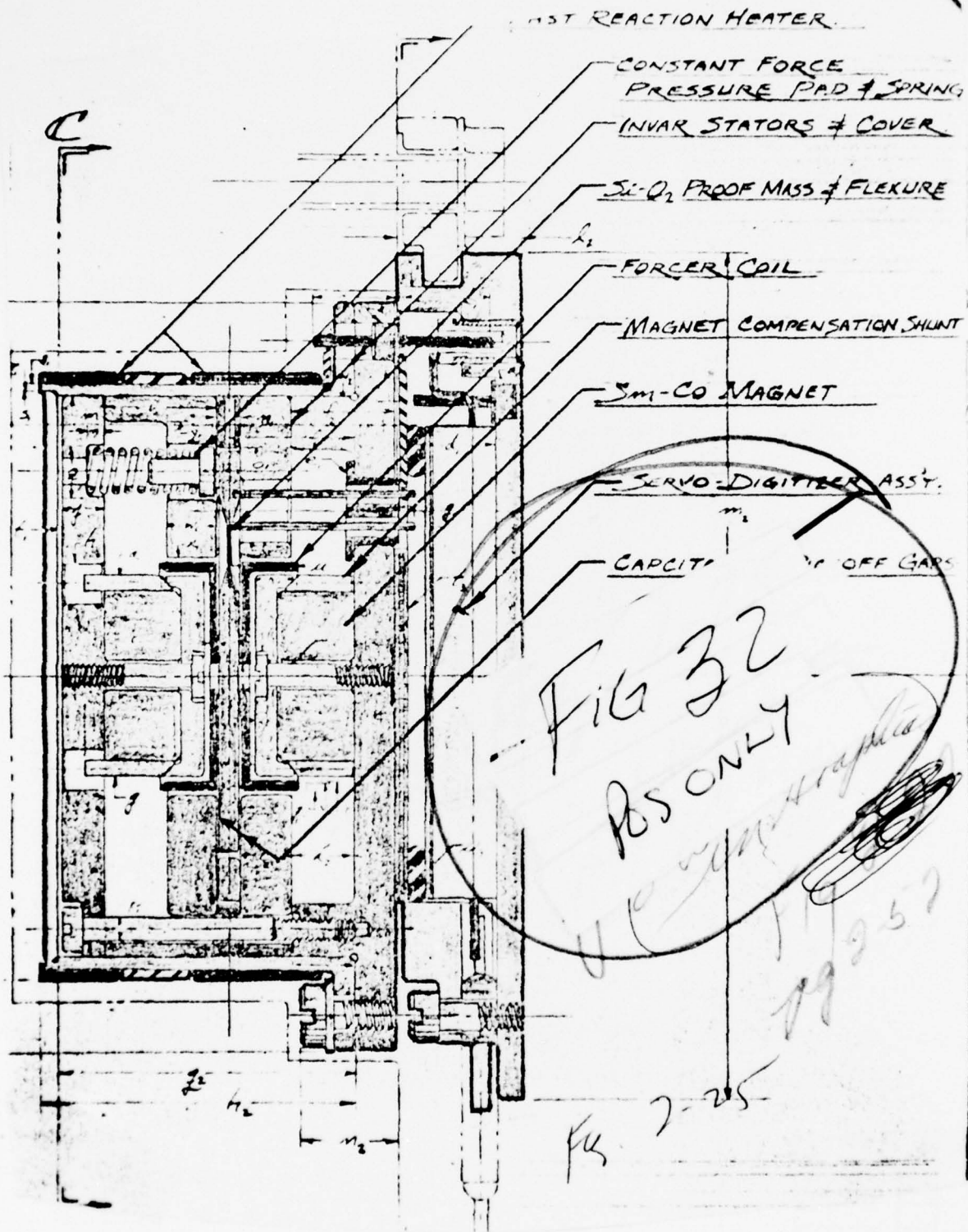
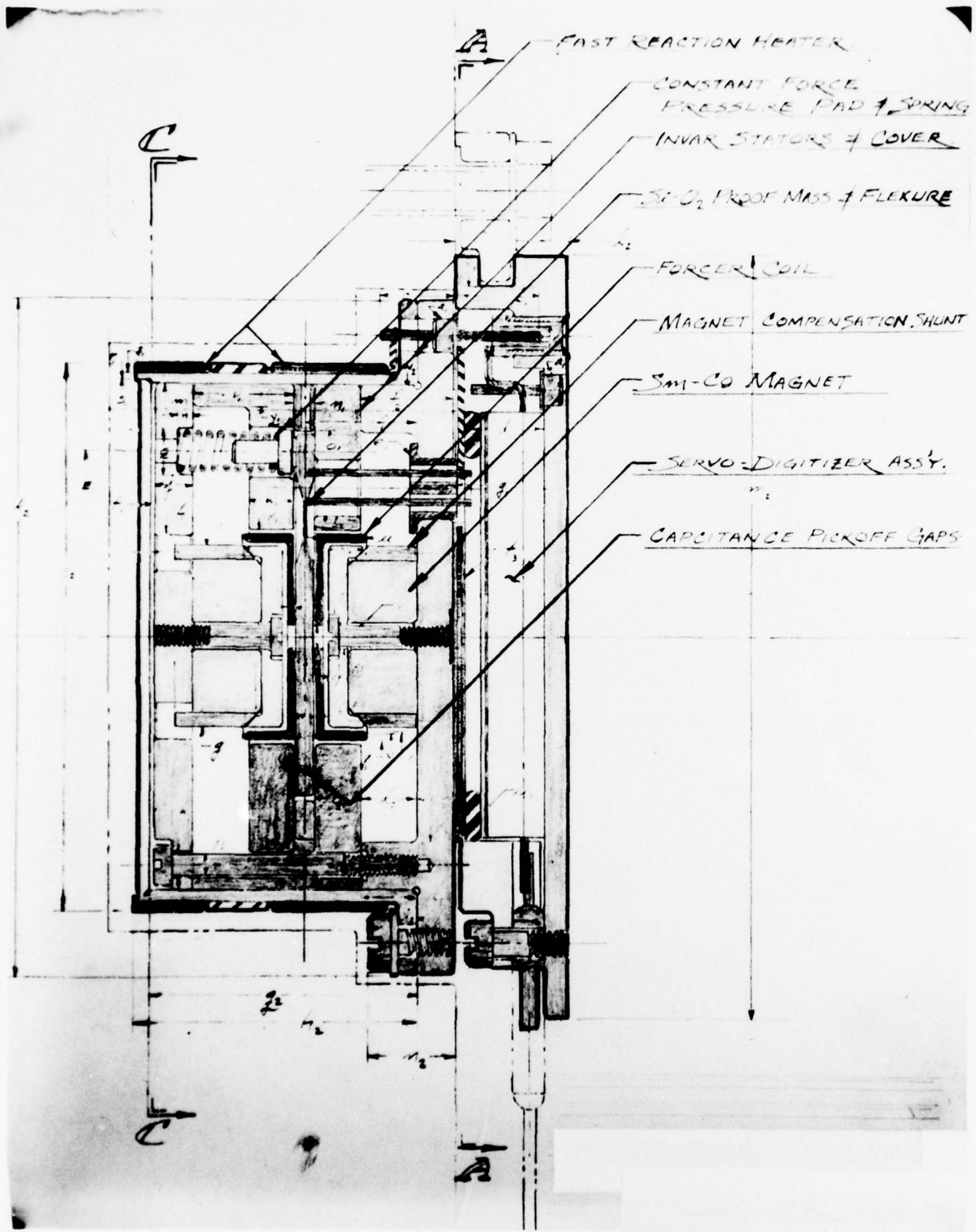


Figure 32. A77M EMA, MICRON Phase 2B

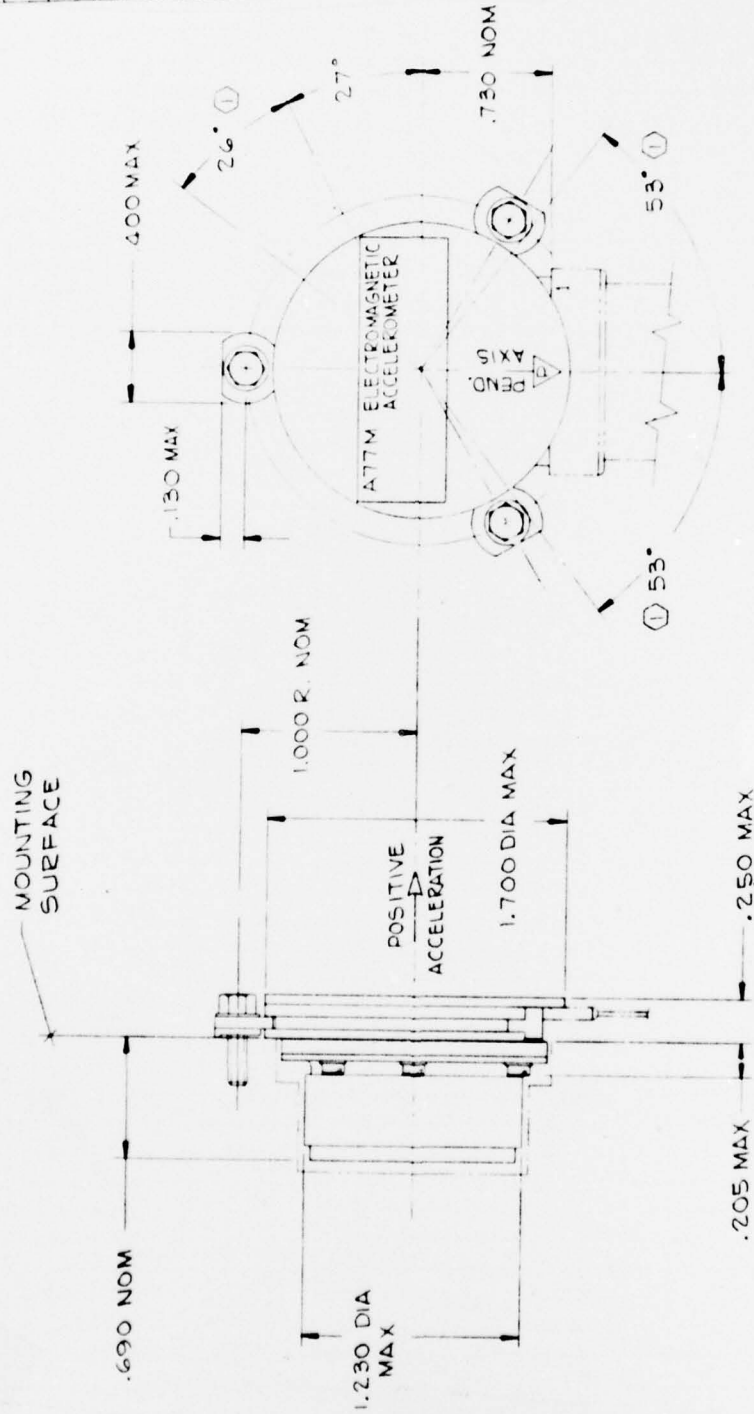


81



P3%

CONNECTOR	PIN	FUNCTION
	1	FILLED POL CAV
	2	+15V PBT
	3	+15V
	4	CHASSI GND
	5	SPARE
	6	+15V
	7	-15V
	8	GND
	9	640 Hz
	10	FILLED POL CAV
	11	FILLED POL CAV
	12	FILLED POL CAV
	13	SPARE
	14	5V
	15	DIG OUT
	16	40 KHz CLK
	17	SERVO TP
	18	33 KHz
	19	SPARE
	20	+15V
	21	+15V



NOTE:  
 (1) CENTERLINE OF EMA CLAMP  
 CANNOT BE POSITIONED  
 WITHIN THESE SECTORS

Figure 33. A77M EMA Outline and Electrical Interface

6. The sensor internal configuration is more symmetrical and requires less machining. This improves the proof-mass suspension, position pickoff symmetry, and reduces the associated bias. The assembly tooling is also simplified by the improved symmetry. Benefits are cost reduction and long-term stability.
7. Some actual and potential failure modes have been eliminated. For example, a printed circuit board and cable assembly between the servo digitizer assembly and the EMA connector are no longer used. Benefits are cost reduction and improved reliability.
8. The entire pickoff preamplifier, demodulator, servo-control amplifier and velocity output digitizer circuitry are packaged on a 0.75 in.<sup>2</sup> thin-film, hermetically sealed, substrate assembly within the A77M envelope. Benefits are cost reduction and fast reaction.

Autonetics, through cooperative development with a thin-film substrate supplier (Halex Corp. of Torrance, CA), has demonstrated the feasibility of procuring servo-digitizer substrates with exceptionally stable, and low temperature sensitivity resistors. A significant percentage of the A77M cost reduction will occur in procuring completely assembled, stabilized and hermetically packaged servo-digitizer assemblies of this type. Test results of the first two "Halex substrate" digitizers are shown in Table 10. These test results are well within the EMA specification requirements.

TABLE 10. TEST RESULTS OF "HALEX SUBSTRATE" DIGITIZER

Characteristic	Serial Number	
	A77M-7602-001D	A77M-7602-002D
Bias ( $\mu\text{g}'\text{s}$ )	-68	+59
Bias Temp Sens ( $\mu\text{g}'\text{s}/\text{F}^{\circ}$ )	-0.15	+1.1
Bias Drift	0 $\mu\text{g}'\text{s}/12$ days	0 $\mu\text{g}'\text{s}/48$ hr
Scale Factor Temp Sens ( $\text{ppm}/\text{F}^{\circ}$ )	-0.4	+0.8
Scale Factor Drift	<1 ppm/12 days	<1 ppm/48 hr
Scale Factor Short Term Stability (peak-to-peak)	4 ppm/12 days	2 ppm/48 hr

2.1.6.2.1 Functional and Short-Term EMA Tests. The results of functional and engineering evaluation tests of the two A77M EDM's are shown in Table 11.

TABLE 11. A77M FUNCTIONAL AND ENGINEERING TEST RESULTS

Characteristic	Spec Reqmt's	Serial Number	
		A77M-7602-001	A77M-7602-002
Bias ( $\mu\text{g}'\text{s}$ )	$\pm 5000$	-579	+313
Bias Temp. Sens. ( $\mu\text{g}'\text{s}/\text{F}^\circ$ )	$\pm 10$	-1.2	-3.1
Bias Short-term Stability (peak-to-peak)	10 $\mu\text{g}'\text{s}$ , rms/hr	11 $\mu\text{g}'\text{s}/16$ hrs	7 $\mu\text{g}'\text{s}/16$ hrs
Scale Factor Temp. Sens. (ppm/ $\text{F}^\circ$ )	$\pm 10$	+1.1	+2.8
Scale Factor Short-term Stability (peak-to-peak)	15 ppm, rms/hr	12 ppm, pk to pk/ 16 hr	7 ppm, pk to pk/ 16 hr
Input Axis Misalignment ( $\mu$ radians)	4363	684	582

2.1.6.2.2 A77M Fast Reaction Tests. Figure 34 shows the output pulse rate of A77M-7602-002 as a function of time and temperature during fast warm-up ramps of approximately 80  $\text{F}^\circ/\text{minute}$ . The A77M and the fast reaction heaters of both the instrument and its mounting fixture are simultaneously turned on at  $0^\circ\text{F}$  after a  $-25^\circ\text{F}$  cold soak. The three tests occur over a five-day interval. The time to output stabilization at  $160^\circ\text{F}$  after turn-on at  $0^\circ\text{F}$  is 4.5 minutes or less, which is well within the specification requirement of 6 minutes. The repeatability of the final value of the output pulse rate for the three tests is approximately 20  $\mu\text{g}'\text{s}$ . This includes any errors associated with removal and remounting of the EMA and its mounting fixture after each exposure. The average sensitivity over the full range of  $0^\circ\text{F}$  to  $160^\circ\text{F}$  is less than  $-3\mu\text{g}'\text{s}/\text{F}^\circ$ . Comparable fast reaction results were achieved on A77M-7602-001.

Two of the A77M-7604 EMAs for the MICRON EPM system were also fast reaction tested from  $0^\circ\text{F}$  after  $-25^\circ\text{F}$  cold soaks as above. Typical A77M-7604 fast reaction is shown in Figure 35 with the test results of No. 003Y. Output stabilization again occurs at  $\approx 4.5$  minutes after turn-on with output ramps better than the required 1.5  $\mu\text{g}'\text{s}/\text{min}$  in two of the three runs.

2.1.6.2.3 A77M Threshold Tests. Tests were conducted over the range  $\pm 3.5$  milli "g" to detect any offsets, discontinuities, or scale factor mismatch about the threshold zone of zero "g" inputs. Figure 36 shows the results of one such experiment. No offsets, hysteresis, or threshold dead zone were observed using 25  $\mu\text{g}$  incremental inputs around zero "g".

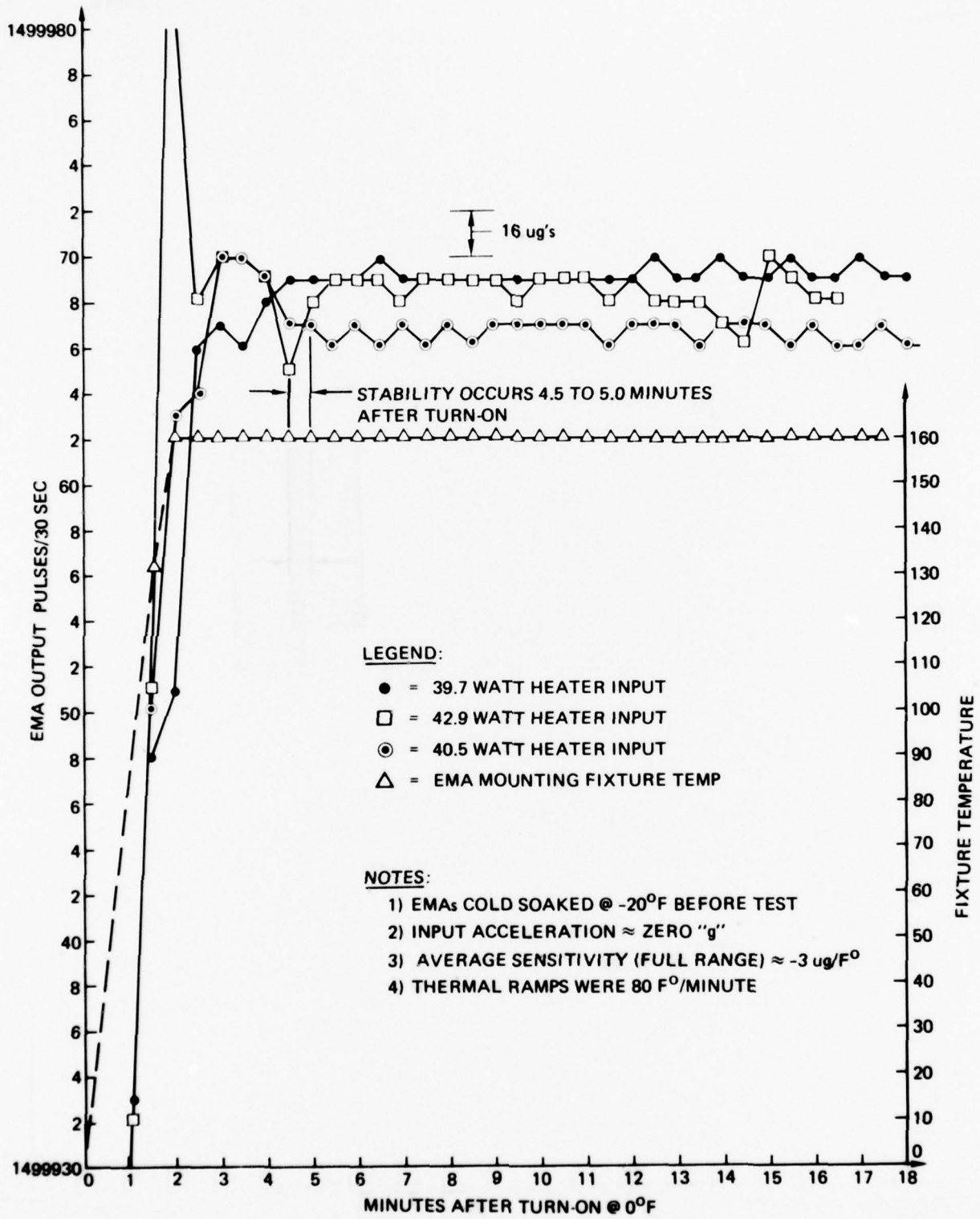


Figure 34. A77M-7602-002 Fast Reaction Tests

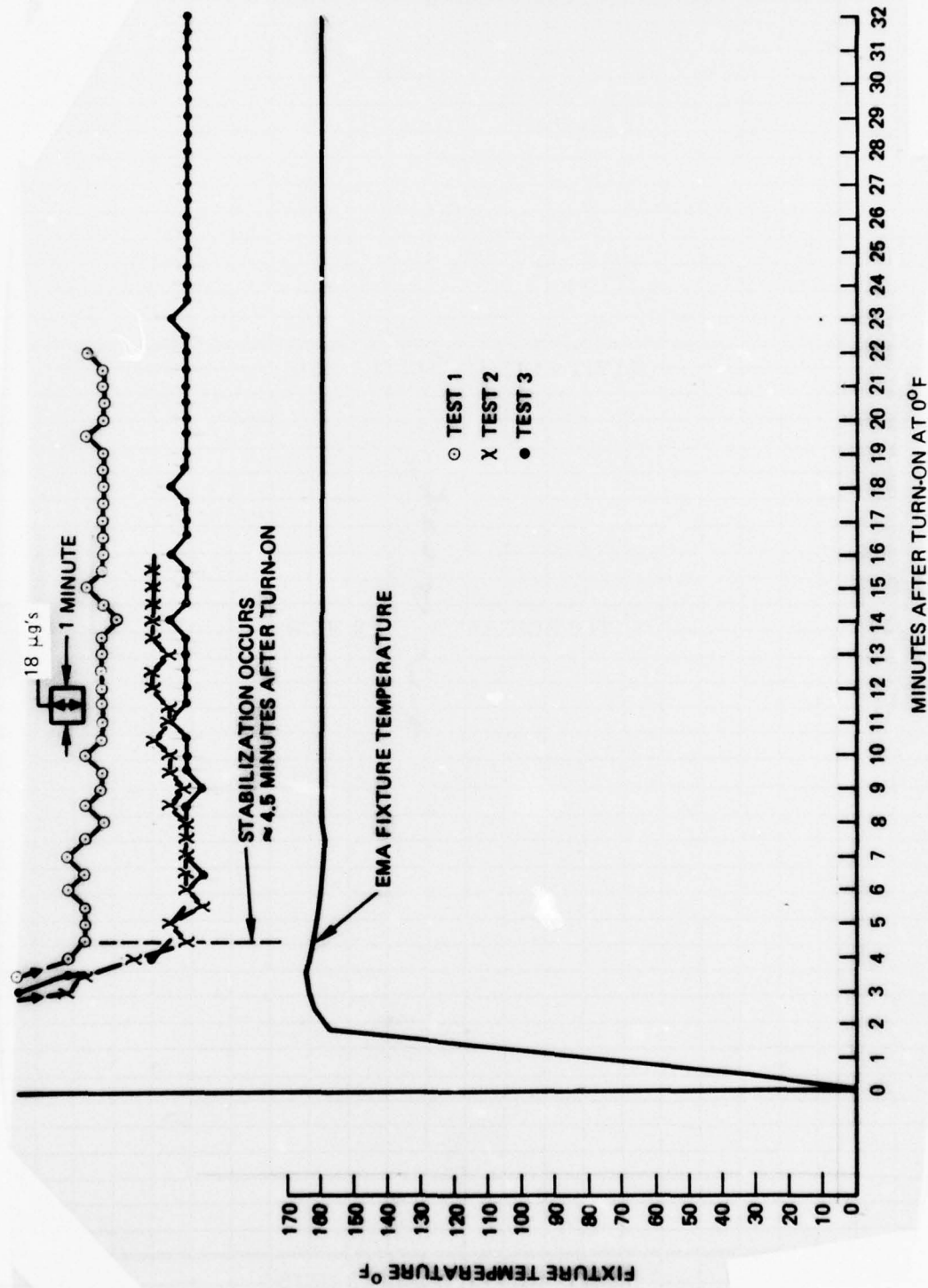


Figure 35. Fast Reaction from 0°F to 160°F at 0g Input

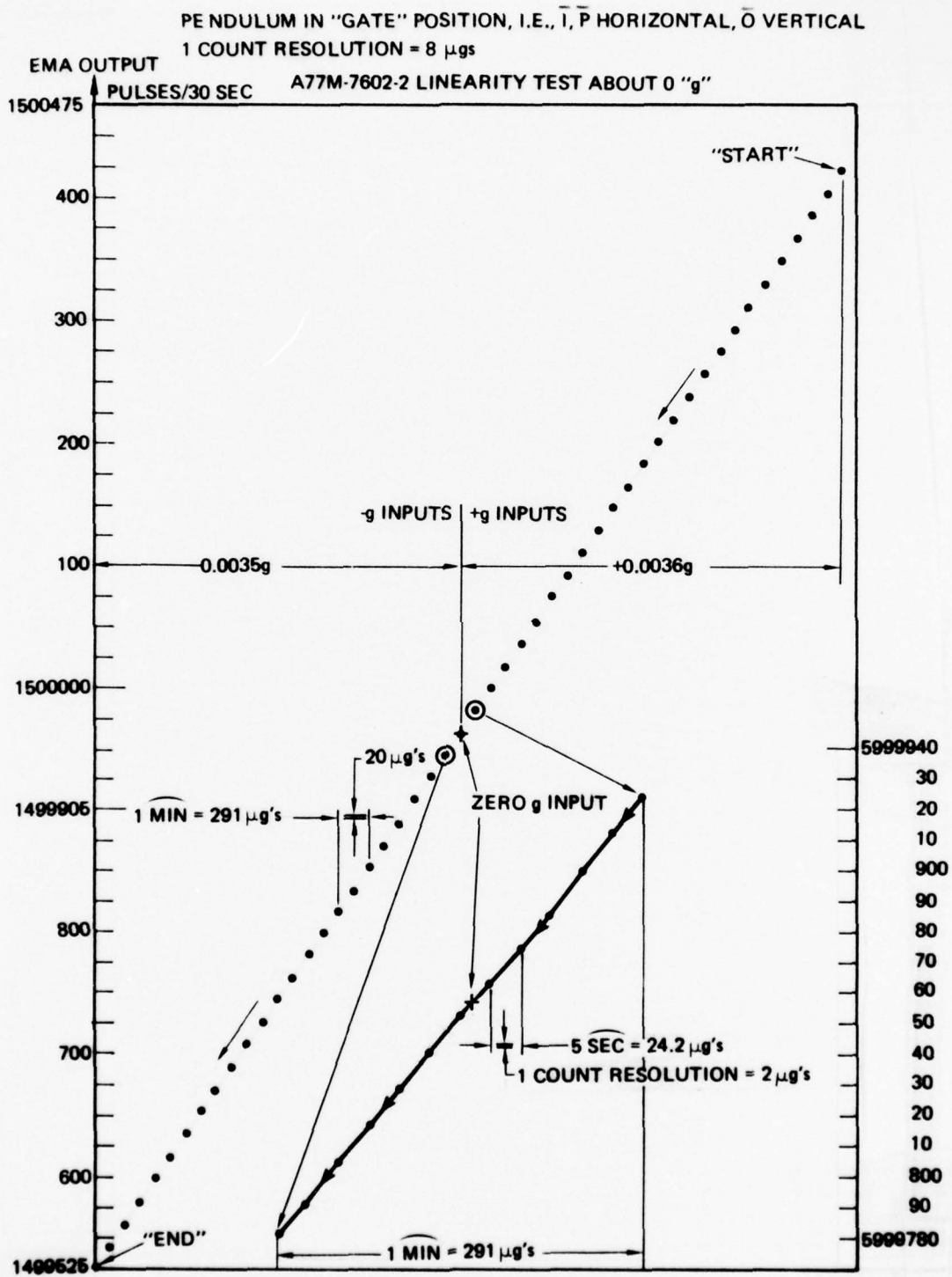


Figure 36. A77M EMA Threshold Test

The six A77M EMA's, for the MICRON EPM system (identified as A77M's 7604-001Y through 006Y) were completed and functionally tested in the period of June through September 1976. Photographs of a completed and "exploded" A77M EMA are shown as Figure 37 and Figure 38 respectively.

Evaluation of the two A77M-7602 development EMA's continued during the fabrication and functional sell-off testing of the six EPM EMA's. A 90 day stability test was conducted on A77M-7602-002. This instrument showed no unidirectional bias or input axis drift. The scale-factor drift rate decreased with time in that the initial aging was  $\approx 5$  ppm/day and the final aging at the end of the 90 day test was  $\approx 1.5$  ppm/day. A77M-7602-001 was stability tested for 60 days. This EMA showed a scale factor drift rate of  $\approx 1$  ppm/day and a bias drift rate of  $-5 \mu\text{gs/day}$ . The bias drift rate was subsequently corrected by the removal of some excess cement between a critical sensor to digitizer interface.

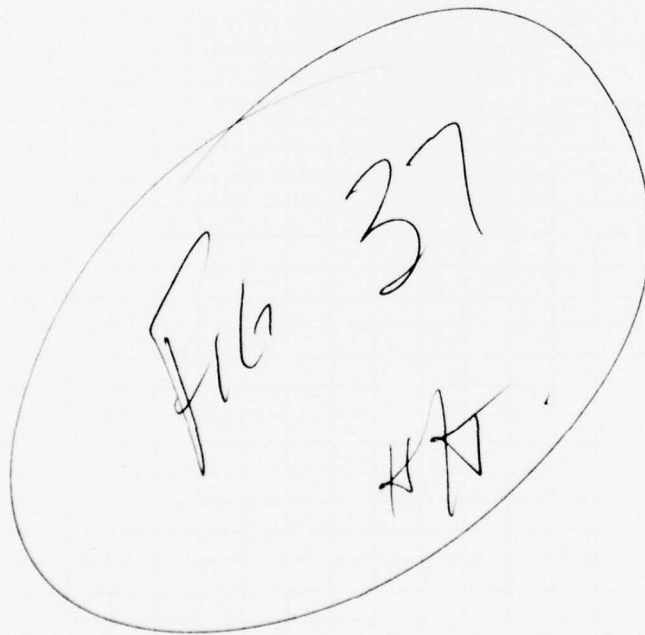


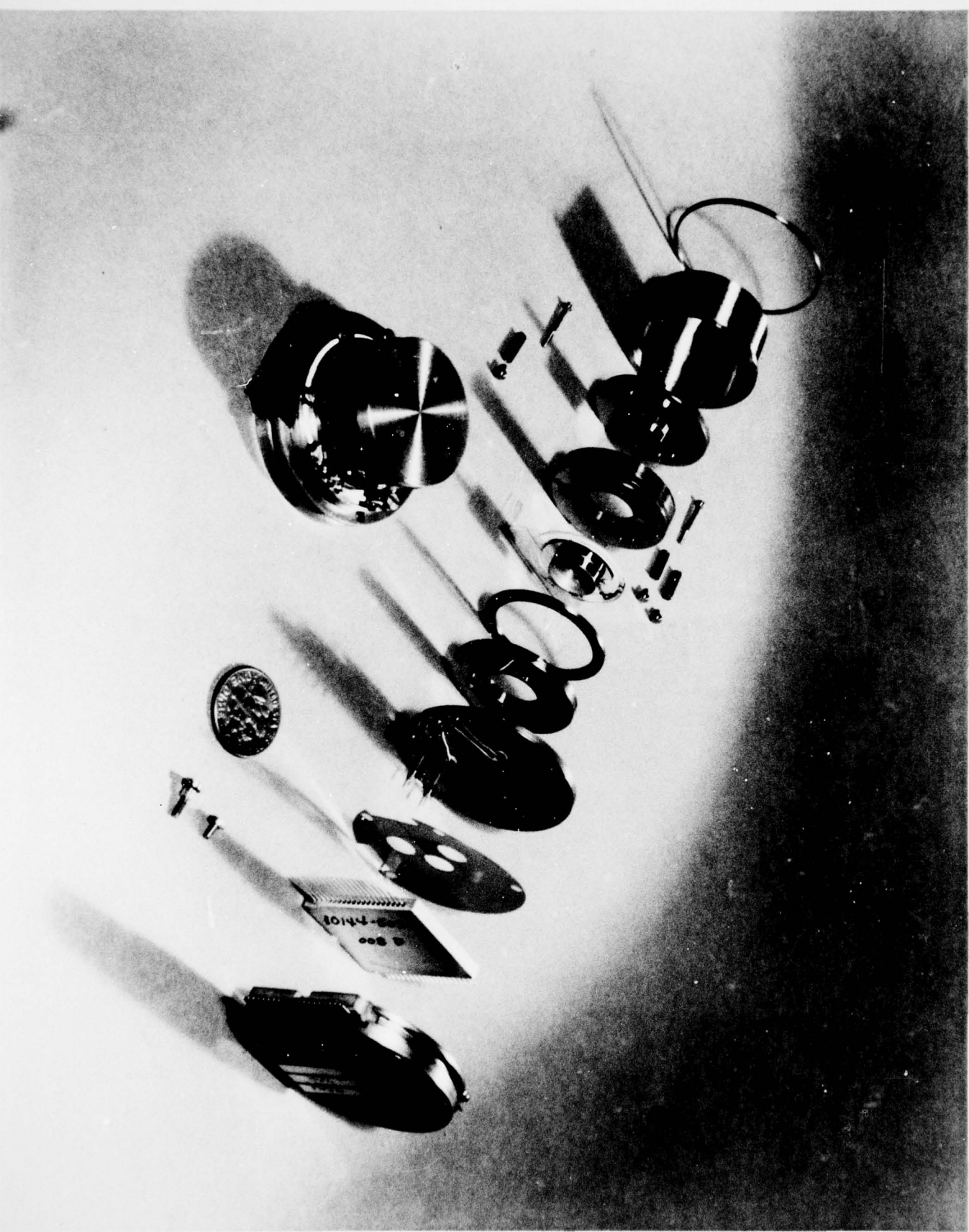
Figure 37. Assembled A77 EMA



5



Figure 38. Exploded View of A77M EMA



S/S

In the period October through November 1976, a series of EMA repeatability tests were conducted on two EPM No. 2 EMA's (non-contract). These tests simulated MICRON discontinuous operation across power-interrupt, cool-down, restart, and warm-up to normal operation temperature (160°F). Forty-eight point automatic tumble tests were conducted before and after to evaluate any scale factor or bias shifts that occurred across each power interrupt and cool-down. In addition, test No. 3 in this sequence was a series of five wide range temperature cycles (-65°F to +210°F) over one 65 hour weekend. Table 12 summarizes the results of these tests.

TABLE 12. A77M EMA, POWER INTERRUPT REPEATABILITY

EMA Stability/ Repeatability Across:				
	<ul style="list-style-type: none"> <li>• 32 days discontinuous operation</li> <li>• 5 power interruption and cool down cycles to 70°F</li> <li>*• 5 temperature cycles from -65°F to +210°F</li> </ul>			
Test No.	A77M-7608-008Y		A77M-7608-009Y	
	$\Delta$ SF/SF (PPM)	$\Delta$ Bias ( $\mu$ g's)	$\Delta$ SF/SF (PPM)	$\Delta$ Bias ( $\mu$ g's)
1	+14	-18	+5	+30
2	+ 6	- 3	+4	+ 7
3*	EMA's removed from test for 5 temp cycles (65 hr) from -65°F to +210°F and replaced on test.			
	+42	+23	-135	+17
4	-27	- 2	+1	+11
5	- 9	+ 3	+8	0
6	- 6	+ 4	-1	- 4

The total scale factor change over the 32 day period was -32 ppm and -135 ppm for A77M-7608-008Y and A77M-7608-009Y respectively. The total bias change over the 32 day period was -3  $\mu$ g and +26  $\mu$ g for A77M-7608-008Y and A77M-7608-009Y respectively. These changes include the normal drift in addition to the effect of cool-down and warm-up. Excluding the -135 ppm, which occurred in Test No. 3, the EMA's have stability which meets system requirements. The exceptionally large change of 135 ppm, from later evidence, could have been due to a feed-through leak caused by stresses from temperature cycling. Improvements have subsequently been made (under separate funding) in processing techniques to control any leakage problem.

Three A77M's have been operating on the MICRON EPM system test since 9 December 1976. EMA's are periodically calibrated on system test by a 41 position "all angle" tumble test. The results of 13 EMA calibrations during the period 9 December 1976 through 10 January 1977 show:

1. None of the EMA scale factors or bias changes are monotonic or "running away".
2. Some of the scale factor and bias shifts appear to be systematic while others do not.
3. The data as a whole appears somewhat noisy with the following mean and standard deviations calculated from the initial calibration.

	$\Delta SF/SF, \bar{X}$ (ppm)	$\Delta SF/SF, \sigma$ (ppm)	$\Delta Bias, \bar{X}$ ( $\mu g's$ )	$\Delta Bias, \sigma$ ( $\mu g's$ )
A001Y	-18.6	71.7	-6	23.6
A004Y	-27.1	44.1	16.5	37.4
A005Y	35	53	-61.4	39.6

#### 2.1.6.3 ESG Design/Develop/Fab/Test

The purposes of this task were to design, develop, fabricate, and test the MESH instrument to meet the form, fit, and functional requirements of the Engineering Prototype MICRON system. Also included under the task was the fabrication of hardware assets in sufficient quantity to assure continuous system support.

A total of six ESG's (including four spares) were assembled and tested for the EPM. In addition, Phase 2A ESG instruments were upgraded to the EPM configuration. A photograph of the completed instrument is shown in Figure 39. Figure 40 shows the ESG with the spin motor detached. (The ESG can be removed from the EPM without removing the spin motor.)

During Phase 2B, the primary activities relative to development of the MESH were:

1. Narrow Groove Cavity Development and Fabrication
2. Small Gap Gyro Development and Fabrication
3. Heater Incorporation
4. Sure Start Development and Fabrication
5. Motor Development and Fabrication
6. Fast Reaction Rotor Development
7. Magnetic Sensitivity Studies

Each of these efforts is discussed in the following paragraphs.

**2.1.6.3.1 Narrow Groove.** The narrow groove configuration cavity members were fabricated with nominal 5 mil grooves as compared to the formerly standard 10 mil grooves (Phase 2A configuration). The purpose of the change was primarily for improved modeling and accuracy. The decreased groove width does provide an additional benefit in that electrode area is increased approximately four percent which enhances the g capability. Phase 2A MESH units were retrofitted with the narrow groove cavity members as repair was required. The units which were evaluated on Test Station IV (T/S IV) showed good functional integrity. Phase 2B instruments were evaluated on T/S IV and in the system environment with very good results.

**2.1.6.3.2 Small Gap.** All MESH instruments were fabricated to the small gap configuration ( $225\mu$ -inches at  $160^{\circ}F$ ) vs the formerly standard  $300\mu$ -inches at  $160^{\circ}F$ . The purpose of the change was for cost reduction purposes. While there is no cost delta ramification with regard to the instrument, there is significant cost reduction with regard to the electronics associated with the instrument. Phase 2A MESH units were retrofitted to the small gap configuration as repair was required. The units were then evaluated on T/S IV for functional integrity. There was some concern that some degradation could occur in modeling since the gap was decreased considerably but rotor/cavity roundness was not improved. However, testing of the updated phase 2A instruments and verification testing of the Phase 2B instruments showed no degradation.

Fig 39  
H/V

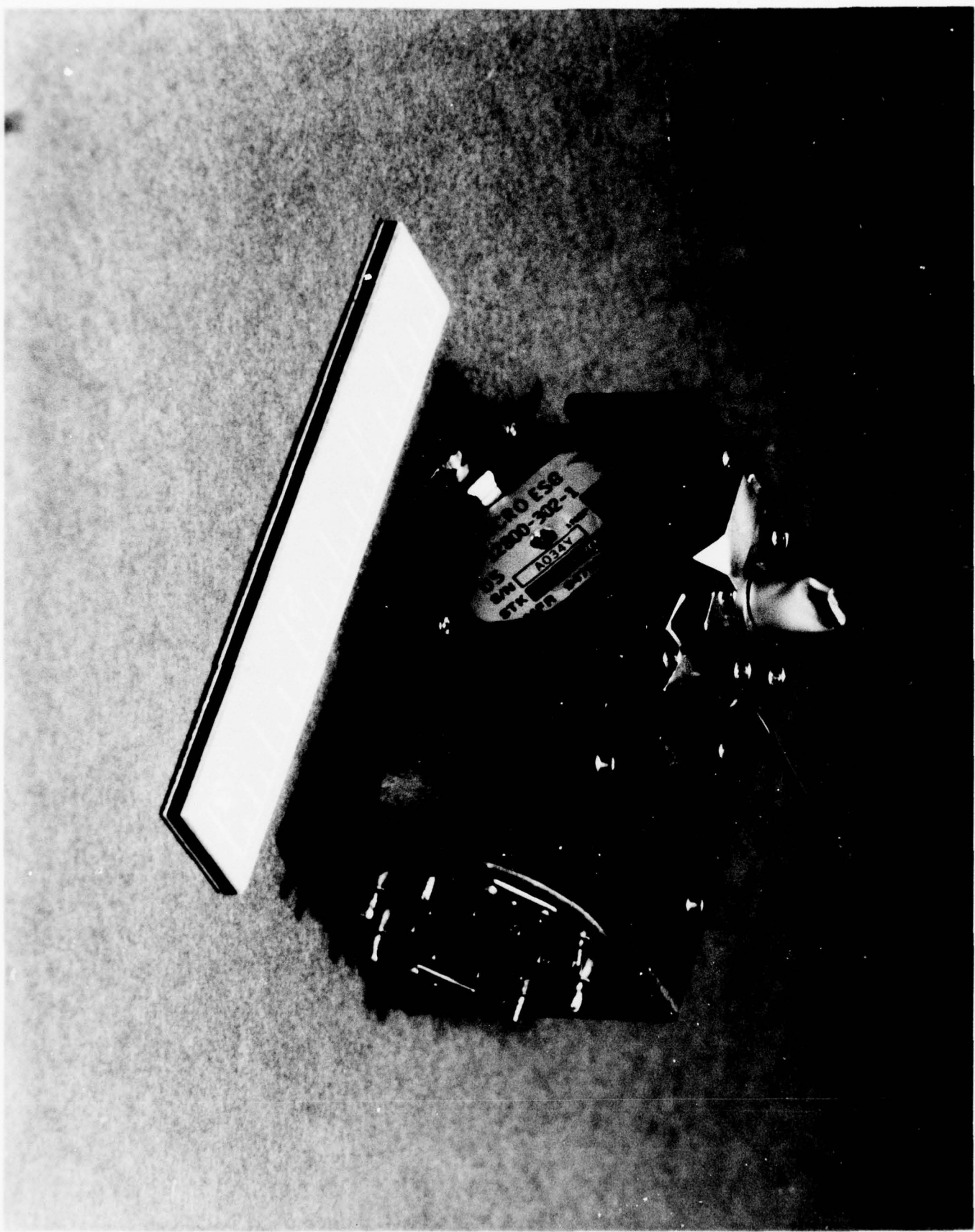
Figure 39. EPM Electrostatic Gyro (ESG) Assembly

Fig 40  
H/V.

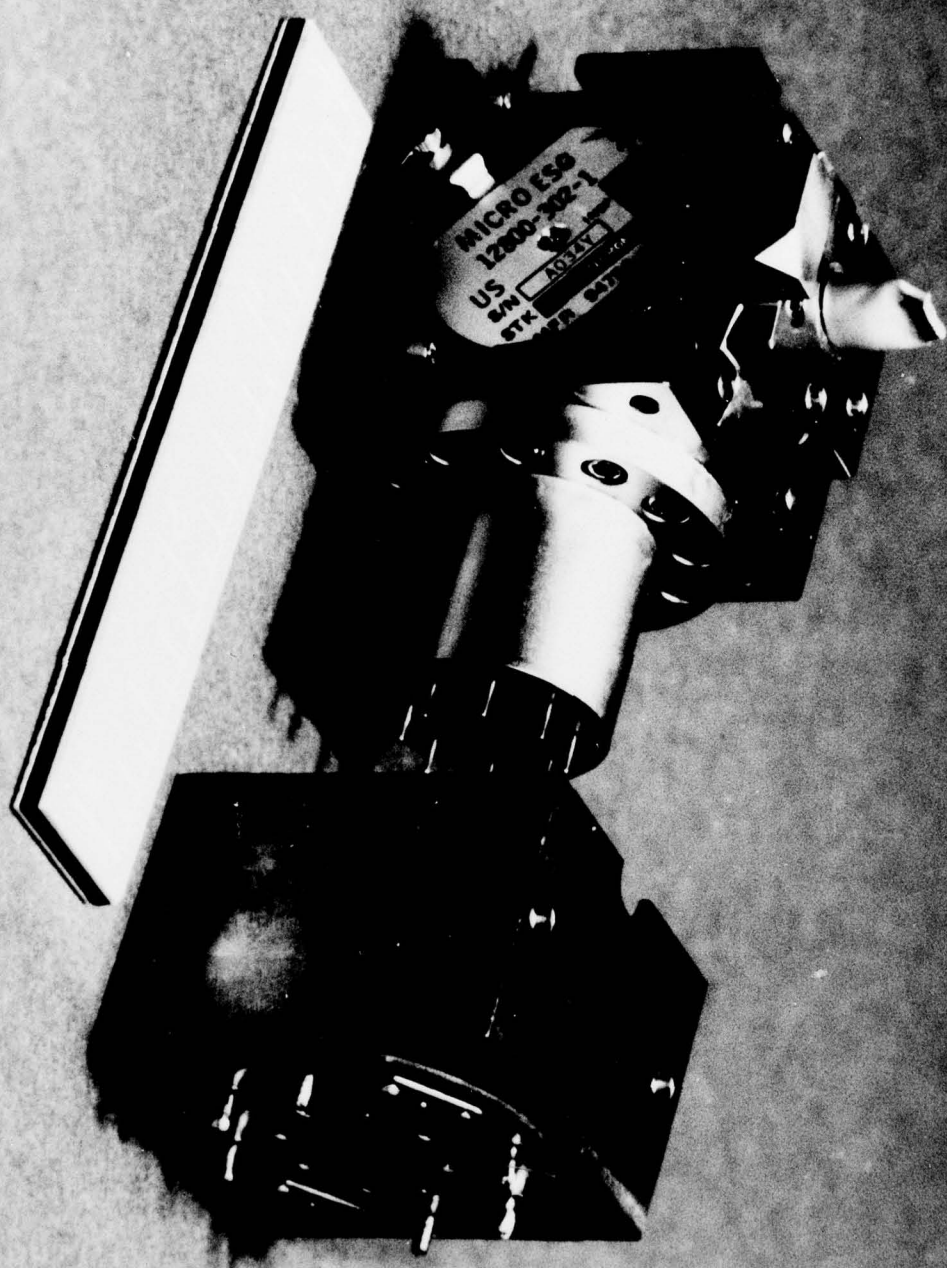
Figure 40. EPM ESG With Spin Motor Detached

39

78



T A  
 4"  
 T



4"  $\nabla$

2.1.6.3.3 Heater Incorporation. In the January 1976 time period it was determined by N77 testing and more detailed analyses of thermal paths that there would be a need to install heaters directly on the MESH bases. The requirements to drive the cavity at a rate of 80°F/minute could not be accomplished readily using heaters mounted on the system because of the high resistance of those thermal paths.

An initial method of heater incorporation was designed and heaters were placed on order in the latter part of January 1976. Tooling was designed, fabricated and developed to install the heater on the MESH base. Cementing techniques were developed to assure good bonding and intimate contact between the heater and the MESH base. A heater was then applied to a test piece to verify bond integrity and the unit was then exposed to -65°F cold soaks and, while in the cold soak chamber, (at -65°F controlled environment) the heater power was applied. Heating rates in excess of 200°F/minute were achieved. The test was repeated approximately ten times and the test piece was inspected for integrity. No sign of bond or heater degradation was observed. The tests were repeated again and there was still no evidence of degradation. A heater was then applied to the base of a beryllium base Phase 2A MESH instrument and the tests were begun which would permit design of the final heater which would drive the MESH unit at a nominal 80°F/minute.

Tests were conducted on a Phase 2B full-up instrument configuration by wrapping the total unit in an insulation blanket and allowing the unit to thermally soak to -65°F until the temperature stabilized at that temperature. System level power was then applied to the heaters and, with the chamber still maintained at -65°F, the instrument was allowed to heat up to about 200°F. The results of these tests are shown in Figure 41. As shown in Figure 41, an average rate of warmup for a two minute period was approximately 81°F/min.

2.1.6.3.4 Sure Start. The beryllium base units as designed in Phase 2A were not capable of meeting fast reaction requirements because vac ion pumps are inherently hard starters and are not predictable as far as time for starting is concerned. Three of the Phase 2A gyros were modified to include a sure start configuration and were evaluated for integrity. The design did prove to be a workable arrangement. The installation however was very cumbersome in that it was necessary to take the gyro apart completely, cut a hole in the vac ion pump and then E-Beam the sure start cartridge in place and then reassemble the gyro. The processing jeopardized the integrity of the base/pump configuration because of the necessary handling by many individuals. During the initial part of Phase 2B, another design was completed which incorporated the sure start unit in the pinch off flange configuration. Installation of the sure start unit was accomplished by removing the original pinch off flange (remove 8 screws and the gold o-ring) and installing the new pinch off flange (8 screws and a new gold o-ring).

2.1.6.3.5 Motor. The MESH motor was redesigned for purposes of functional compatibility with the new power supplies which were developed for the EPM. Another goal of the motor redesign was to significantly reduce cost of fabrication. The efforts and accomplishments in both areas are summarized in the following paragraphs.

(a) Motor Function Development

Redesign of motor power supply electronics (for purposes of compatibility with aircraft power) also caused the redesign of the EPM MESH motor. A number of analytical redesigns were accomplished and motors were fabricated for test and evaluation.

B<sub>e</sub> BASE GYRO AO31Y (8-10-76)  
 HTR. P/N 114229

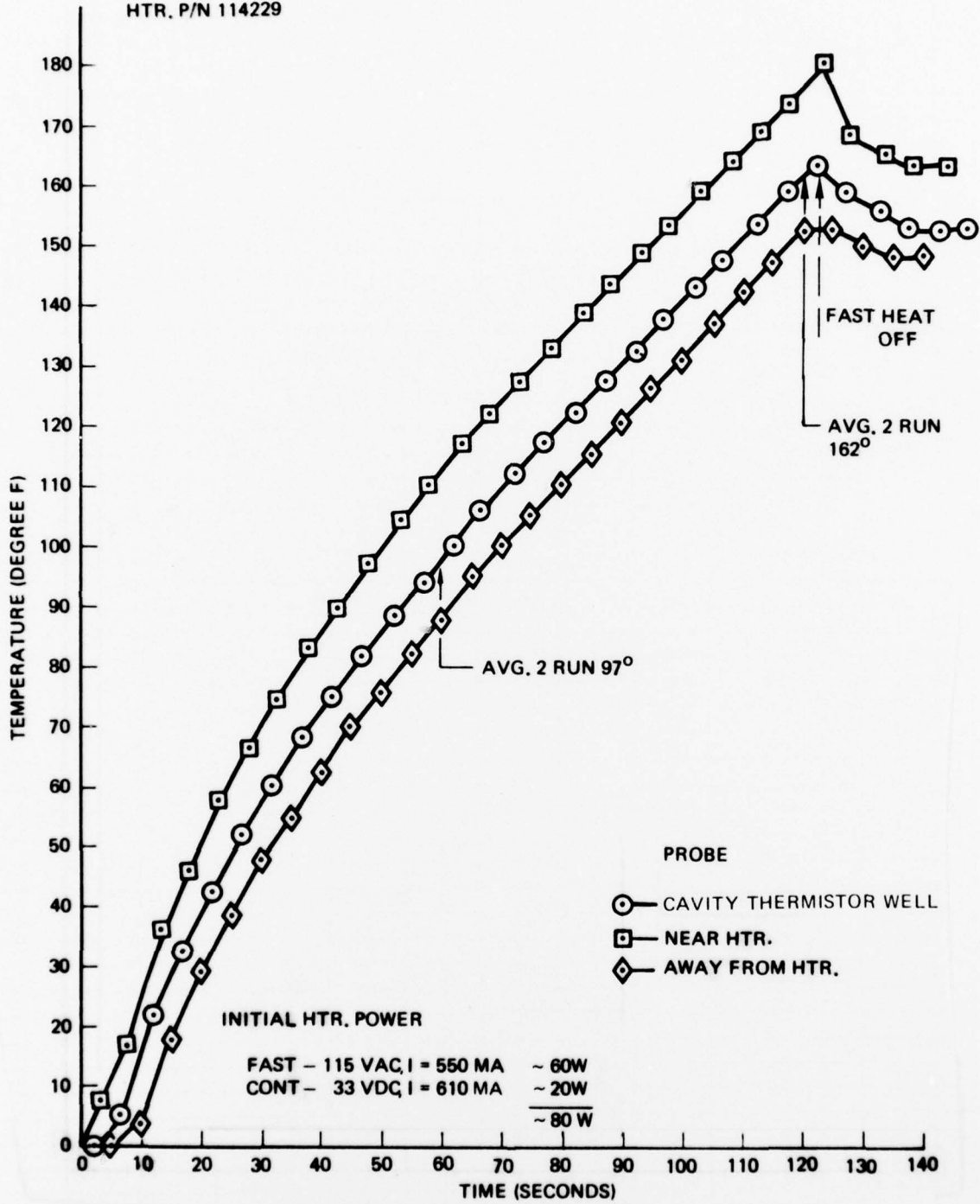


Figure 41. Temperature Ramp Test

Three coil designs were made with maximum voltage requirements of 33.1, 40.0 and 45.0 volts (rms). The coils were designed for equal flux per unit current. The Z coil copper volume was increased to further reduce losses in copper winding during rapid warmup. The motor cover (Mumetal) inside diameter was increased about 0.020 in. to accommodate the added copper volume.

A motor coil combination was designed which optimized the dc source requirements. The design employed unequal flux in the z coil per unit current as compared to the x and y coils. A motor of this design was assembled (Motor No. 5). The motor was designed and fabricated in support of total Motor/Power Supply optimization. The "Z" coil had 72 turns of No. 26 wire. The "X" and "Y" coils each had 84 turns/coil of No. 30 wire (two coils/axis). In this design, equal torques are produced when the "Z" current is 59.5 percent of the "X" or "Y" currents. All previous coil designs were such that equal currents produced equal torques.

A test was then devised and conducted to evaluate X, Y, and Z motor coils relative efficiencies. The desired end result of the test and evaluation was to permit final design of a motor which would provide rotor heating rates of 80°F/minute while using the maximum voltage available from the system (and therefore minimum current).

Tests were conducted using a 4-slot Beryllium Base gyro. A standard high power MICRON prototype motor (with a fiberglass bobbin) was evaluated. In summary, the motor met the requirements of the motor power supply, 80°F/minute z coil heating warm up rate (actually over 100°F/min) and spinup/polhode damping and spin down requirements. The motor was tested in conjunction with EPM type electronics which used power as will be supplied eventually from the aircraft.

In July of 1976 alumina bobbins were received and were assembled into the final design MICRON Phase 2B motors in support of the EPM system. Motor verification testing was then performed on Test Station IV (T/S IV) in conjunction with the EPM motor power supplies. All motor functions were evaluated with the exception of polhode damping which cannot be computer controlled on T/S IV. The results of these tests are summarized in Table 13 along with results obtained at the EPM system level. Specification requirements for these functions are also given for comparative purposes.

A beryllium-base gyro was used to evaluate the z-coil heating capability of an EPM type motor power supply integrated with an EPM type motor. The z-coil heating applied was 4.2 amps rms at a 5 kHz excitation frequency for 30 sec elapsed time. The results are shown in Figure 42 and summarized in Table 13. The observed gap change was 67  $\mu$ -in. which is an equivalent rotor heating rate of 101.5°F/min. The required rate is 80°F/min.

The method of evaluating rotor heating is illustrated in Figure 43. The solid line in Figure 43 represents the gap change as a function of rotor and cavity size change. The rotor size increase is separated from the cavity size increase by projecting the "rotor change only" section of the curve (Section D) back to that point in time when the motor was turned off (Point 2). The actual rotor size change rate is the slope of the line connecting Points (1) and (2). All of the above is possible because of the short thermal time constant of the cavity compared to the long time constant of the suspended rotor.

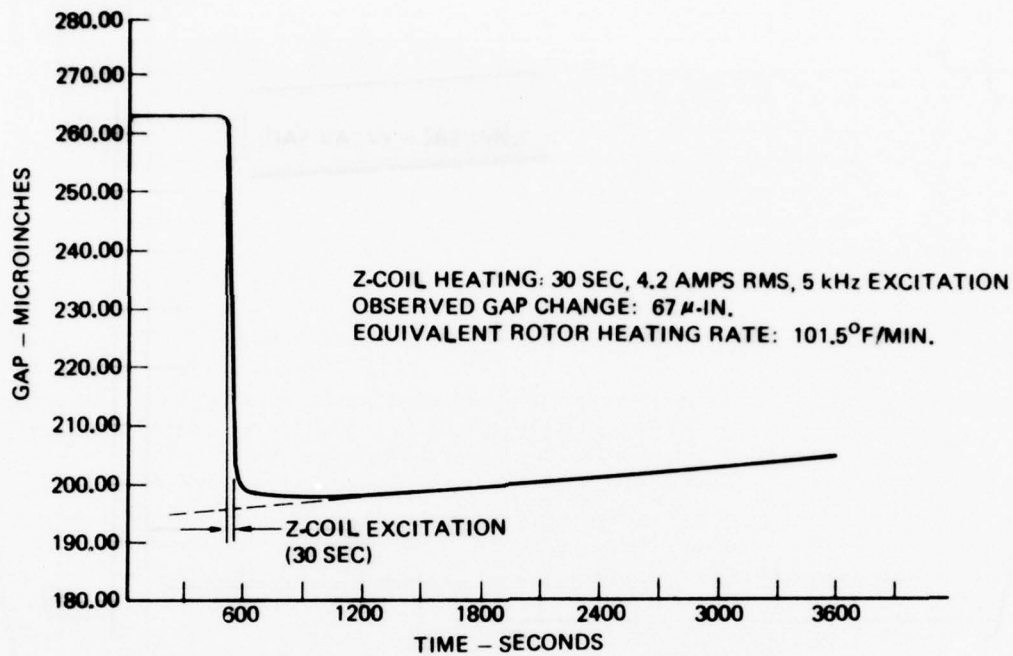


Figure 42. Z-Coil Heating Tests

TABLE 13. RESULTS OF MOTOR TESTS

	Spin-up Time (sec)	Z-coil Heating Rate (°F/min)	Braking* Time (sec)	Polhode Damping Time per Gyro (sec)
Test Station IV	9.7	101	30	-
EPM	7	114	≈ 60	30
EPM Spec Requirement	10	80	64	30

\*Braking time may be controlled by the amount of DC current programmed sequentially through the motor X, Y and Z coils. Tests have shown that the rotor can be spun down reliably in 30 sec with adequate battery reserve.

The actual rotor heating rate (HR) can be determined by the following equation:

$$HR = \frac{\Delta G}{\Delta t \cdot K_R} \quad (^\circ F/\text{min})$$

where

$\Delta G$  = observed gap change,  $\mu$ -in.

$\Delta t$  = z-coil excitation time, minutes

$K_R$  = 1.32  $\mu\text{in.}/^\circ\text{F}$  - expansion factor for beryllium rotor

(b) Motor Fabrication Technique Development

(1) Encapsulation of the Motor Coil

The intent of this task was to improve the heat transfer characteristics from the motor coils to the extremities of the MESH Motor.

An encapsulating tool was designed and built to be used on the molding machine in the Transducer Lab. A coil form was designed and parts were machined which were suitable for pressure encapsulation. These coil forms were made from fiberglass (which were replaced later by the  $\text{Al}_2\text{O}_3$  coil form described in the cost reduction effort discussed later).

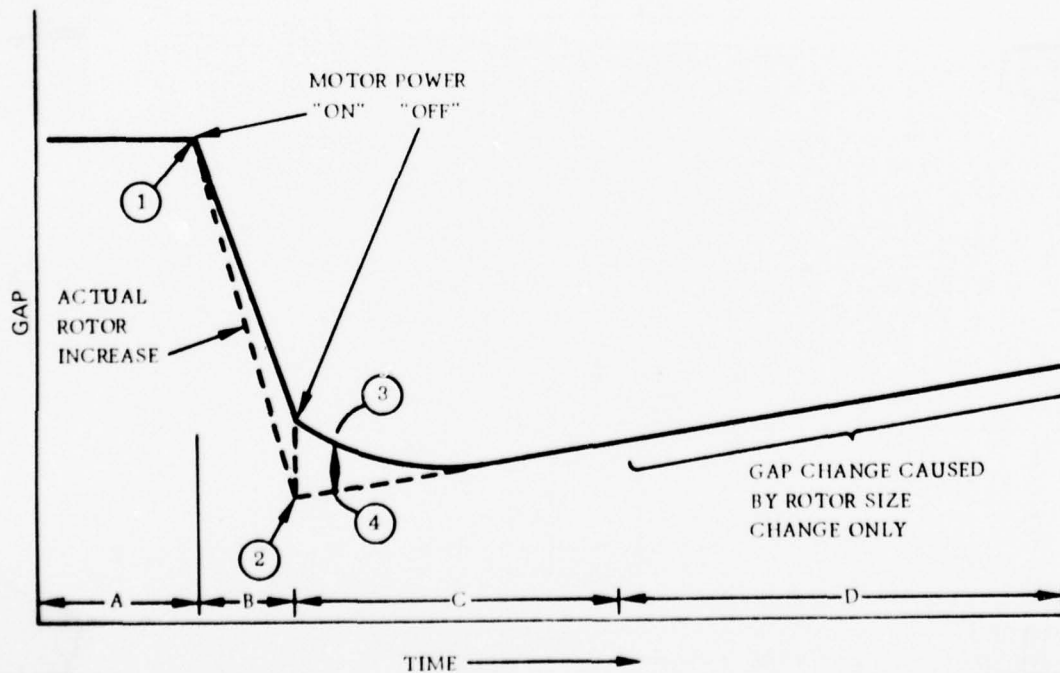


Figure 43. Gap vs Time, Rotor Heating Tests

The first try for encapsulating the wound coil assembly in the motor cover used Stycast 2850 KT, with a thermal conductivity of  $.01 \text{ cal-cm/cm}^2\text{-sec}^{\circ}\text{C}$ . This material was chosen because it had the highest thermal conductivity of the available moldable epoxies. The encapsulation was not successful because the particles were too large to penetrate the space between the coil assembly and the motor cover.

The next material tried was Stycast 2850 FT with a thermal conductivity of  $0.0034 \text{ cal-cm/cm}^2\text{-sec}^{\circ}\text{C}$ . This material was found to be successful. Five assemblies with different windings were encapsulated. The molding pressure of about 800 psi and a temperature of about 175 F (77 C) were sufficient to get good penetration. The encapsulated assembly was held in the machine for curing for 16 hours. The fifth of these assemblies was postcured at 300 F (149 C) to prevent failure of the motor in case of accidental overheating in operation. All EPM motors were fabricated (potted) using this latter technique.

## (2) Low-Cost Coil Form

Iterations of design and fabrication techniques were pursued to establish a low-cost coil form which would satisfy all motor function requirements.

The initial effort consisted of designing tooling to mold a coil form with Stycast 2850 FT. The coil form was simple and had only one flange with holes for the terminals. The 0.031 in. wall thickness was re-enforced by four ribs which also separated the "X" and "Y" coils. Several vendors were contacted for fabrication of the coil form but no one had had enough experience with Stycast 2850 FT to respond to Autonetics' request.

Parallel to the above effort, a search was continued to establish a low-cost source for the motor coil form which would provide a greater thermal conductivity path from the copper motor coils through the motor coil form. Parmatech Development Corp. in Huntington Beach was contacted and discussions were held as to how a coil form could be generated to fit our geometry and to be suitable for their Wiech process. (The Wiech process is described in Business Week, September 15, 1975, pages 36D and 36F.) The ceramic selected was 99.8 percent  $\text{Al}_2\text{O}_3$  which had a thermal conductivity of  $.01 \text{ cal-cm/cm}^2\text{-sec}^{\circ}\text{C}$ .

The tool for the coil form and a sample batch of 25 pieces were ordered from Parmatech Development Corp. These low-cost alumina coil forms for the spin motors were received in July 1976. The receipt of these coil forms culminated a nine month coordination effort between Autonetics and the supplier (Parmatech Development Corporation) with respect to tooling, fabrication, and final delivery of the part. The coil form represents a significant cost reduction item and yet enhances the operational capability of the motor. The coils were wound, installed on the coil form, and injection molded with the Stycast material at Autonetics. The units were assembled and tested without problems. The motors functioned properly in all respects.

## (3) Low-Cost Motor Cover and Shield

Three possible approaches were pursued for fabrication of the motor covers:

1. Drawn from NiFe sheet.
2. Casting the part from Mumetal.
3. Forging the part from a Mumetal billet.

Vendors for all three processes were contacted. Forging and casting required a large amount of finish machining and were dismissed.

Vendors were approached for the first procedure. Arnold Engineering was willing to draw the parts but would not finish machine and etch the parts. The Magnetic Shield Division, Perfection Mica Co., sent in a quote for the deep drawn part from .050 NiFe sheet per AB0170-061, Type II. The quote included finish machining and etching.

Twenty motor covers were received from the Magnetic Shield Division. The measured retentivity of 6 of the motor covers was 0.5 lines of flux peak-to-peak and these six parts were sent to the heat-treat shop for reannealing. All EPM motors were made from the above hardware and have worked satisfactorily.

Twenty motor shields were received from the Magnetic Shield Division. The parts were dimensionally acceptable, but the retentivity of two lines of flux peak-to-peak was excessive. The parts were returned and the vendor contacted about the problem. They annealed the parts again and sent them back. This time the measured retentivity was 0.08 lines of flux peak-to-peak, and these motor shields were successfully used in the EPM.

**2.1.6.3.6 Fast Reaction Rotor.** MESH rotors must have certain specific characteristics in order to be useable in the EPM system. Development and test activities were continued during Phase 2B to verify the latest three wire rotor configuration to be adequate for EPM use. The requirements of MUM amplitude, polhode family signature, limits on axial mass unbalance, polhode period, and consistency of the family characteristics continued to be verified. The test and evaluation of approximately 15 rotors indicated that all of the rotor characteristics are acceptable and consistent. One MESH instrument was disassembled for a rotor replacement because of excessive MUM. The actual MUM magnitude was 98 percent of the A/D Converter capacity but a small amount of noise with the signal caused slight saturation of the A/D Converter.

**2.6.6.3.7 Magnetic Sensitivity Studies.** Tests were conducted at the instrument and system levels to determine sensitivity to magnetic fields. A detailed discussion of the magnetic sensitivity testing is given in Appendix F. This effort was performed under a separate IR&D task using the N57A system. Although this activity was not performed under the contract, the results of the tests are included in this report because they provide information on the sensitivity of system performance to magnetic fields.

#### **2.1.7 DPU Design/Develop/Fab/Test**

The purpose of the MICRON Dedicated Processor Unit (DPU) is to accept MICRON sensor data, provide compensation for drift and attitude readout sources, solve navigation equations, and provide backup data bus control. A functional block diagram of the DPU is shown in Figure 44. The DPU consists of three multilayer modules. They are the Central Processor Unit (CPU) shown in Figures 45 and 46, the Processor Memory (PM) shown in Figures 47 and 48, and the Processor Input/Output (PIO) shown in Figures 49 and 50.

The three DPU modules are of the same size as other MICRON Modules. The boards are high density multilayer printed circuit boards, developed to standard ground rules compatible with MIL-P-55640 requirements. The CPU MLB consists of 12 layers, the PM MLB has 6 layers, and the PIO MLB has 9 layers. The CPU module design was subcontracted to Algorex Corporation for the computerized component placement and board layout. The memory and PIO modules were designed in-house using manual layout and computerized verification techniques.

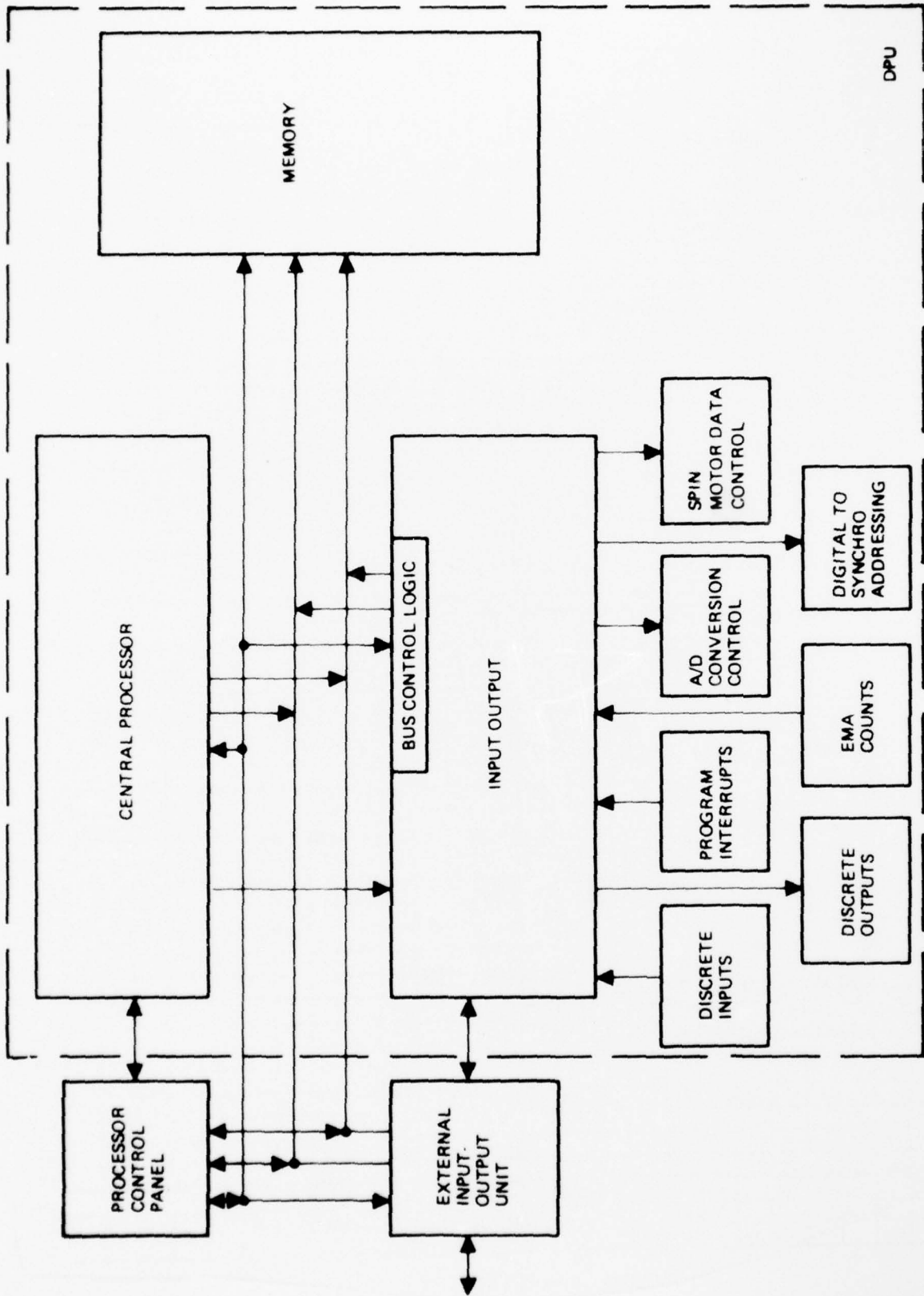


Figure 44. DPU Functional Diagram

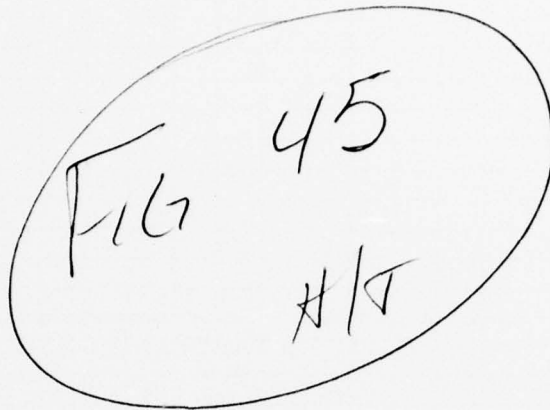
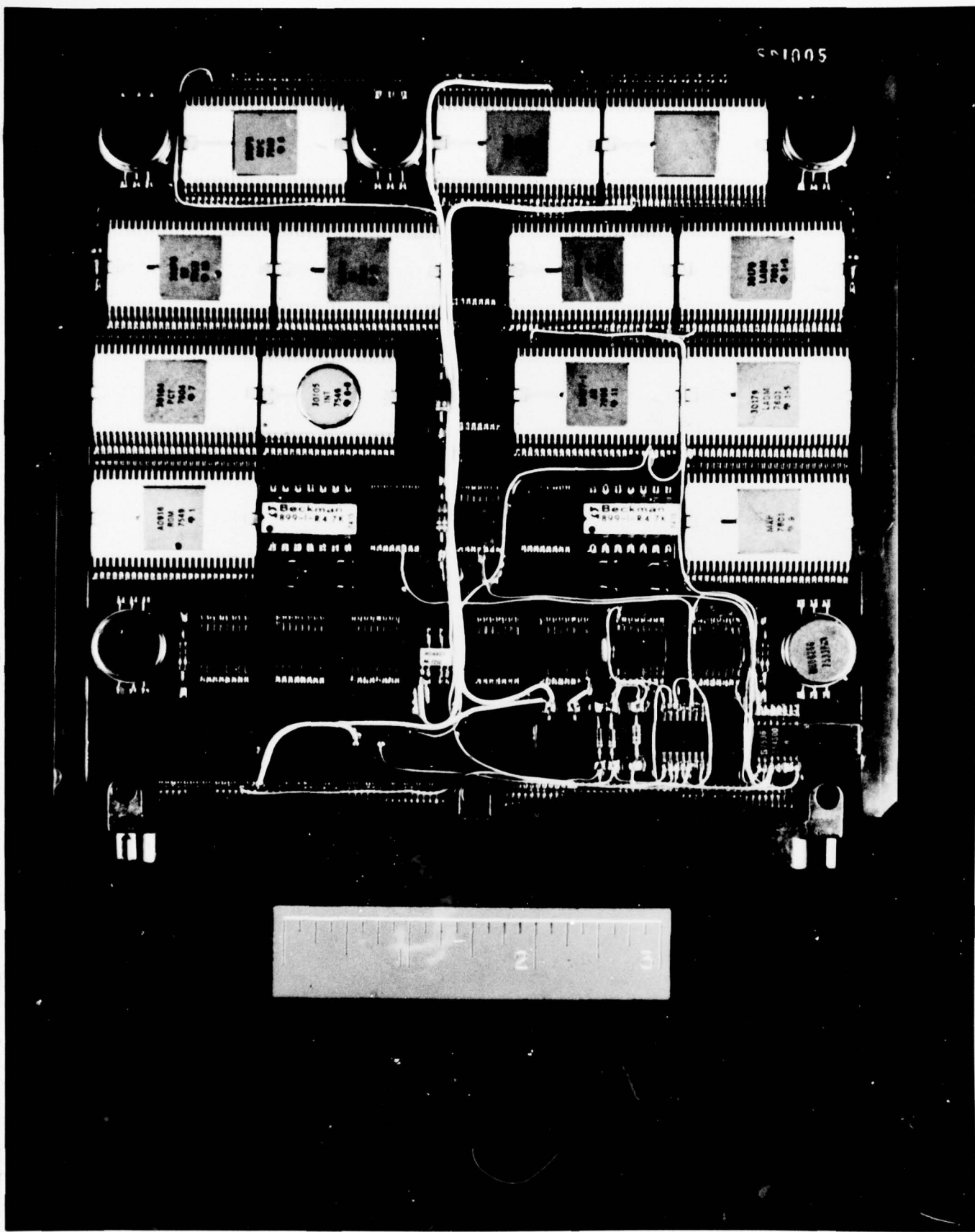


Figure 45. Central Processor Unit (Front Side)



Figure 46. Central Processor Unit (Back Side)



S. NO. \_\_\_\_\_ VOL. NO. \_\_\_\_\_ FIG. NO. \_\_\_\_\_ PAGE NO. \_\_\_\_\_



4"

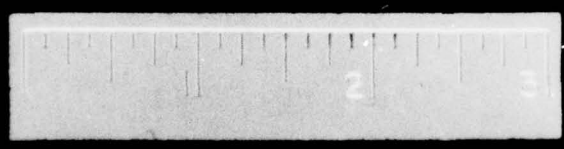
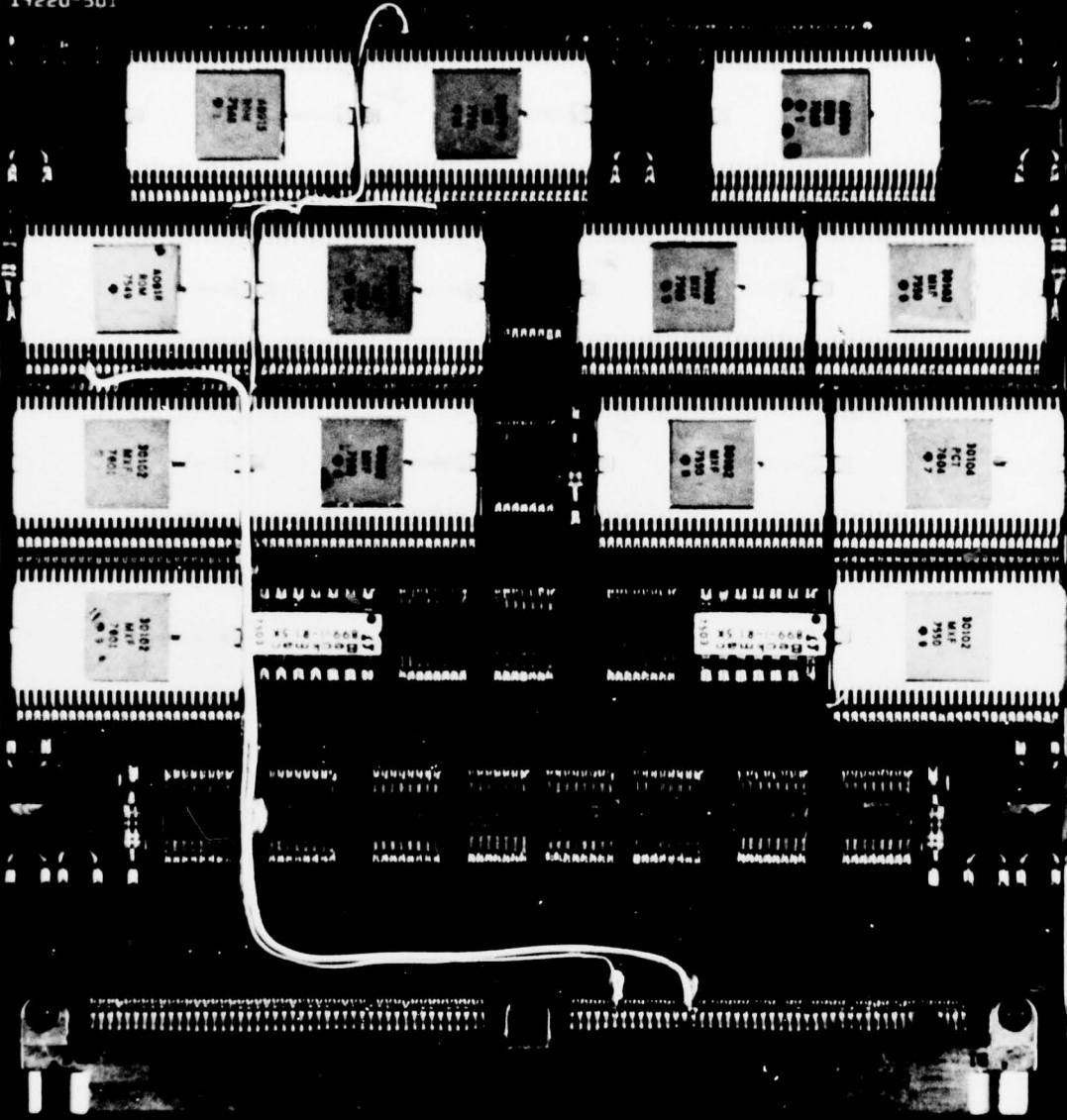
45



87

SUB ASSY  
14220-501

PWB 14221-501



4"



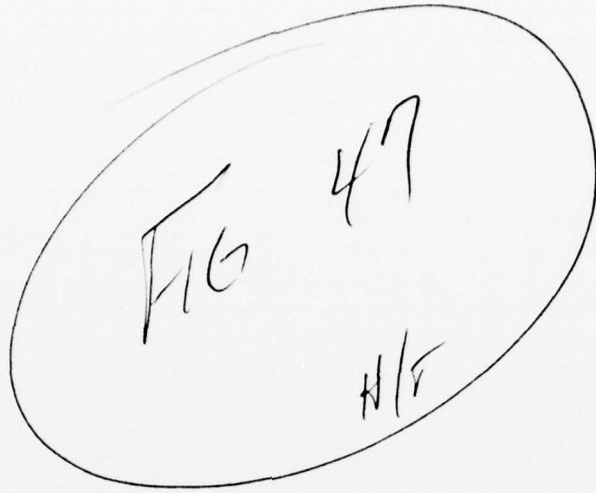


Figure 47. Processor Memory Module (Front Side)

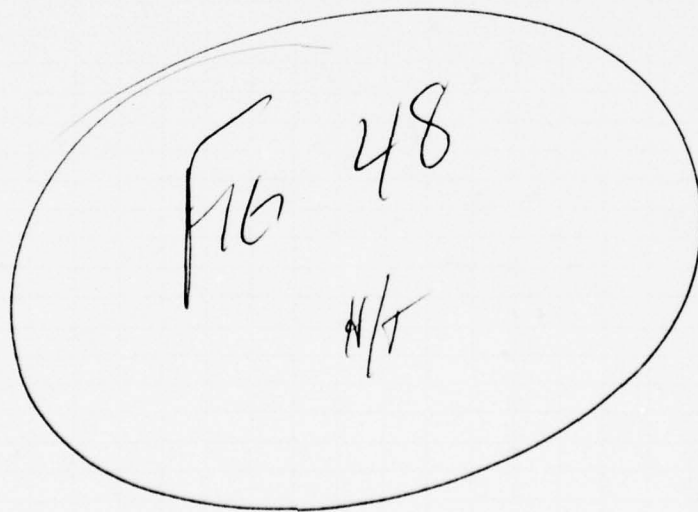
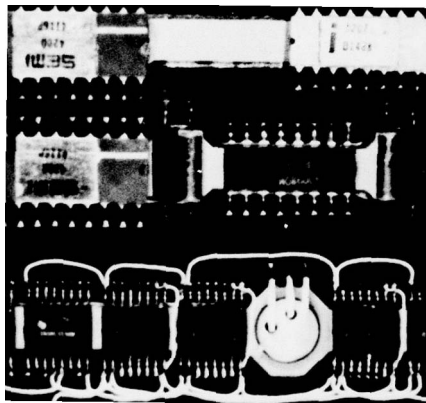
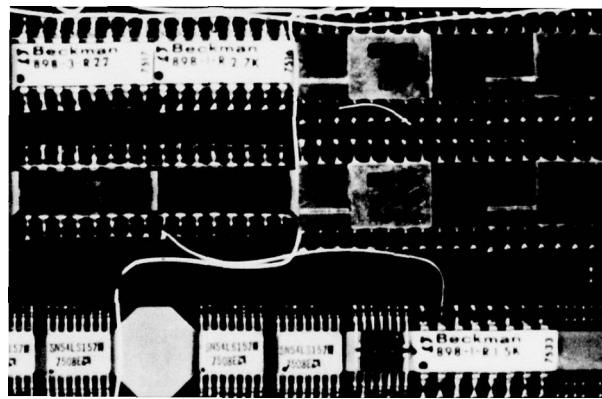


Figure 48. Processor Memory Module (Back Side)





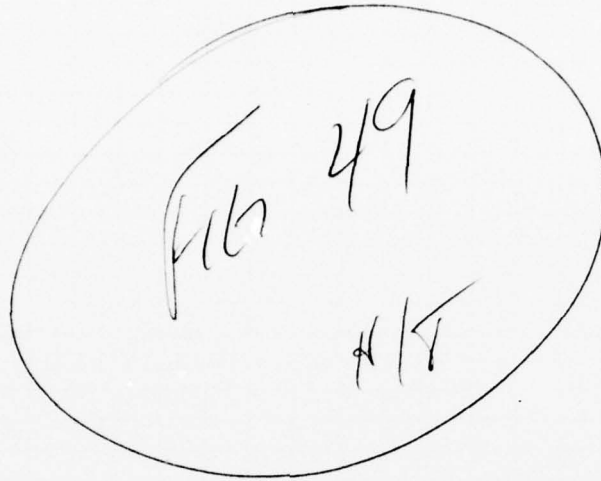
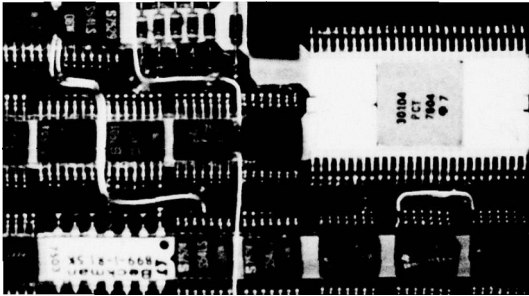
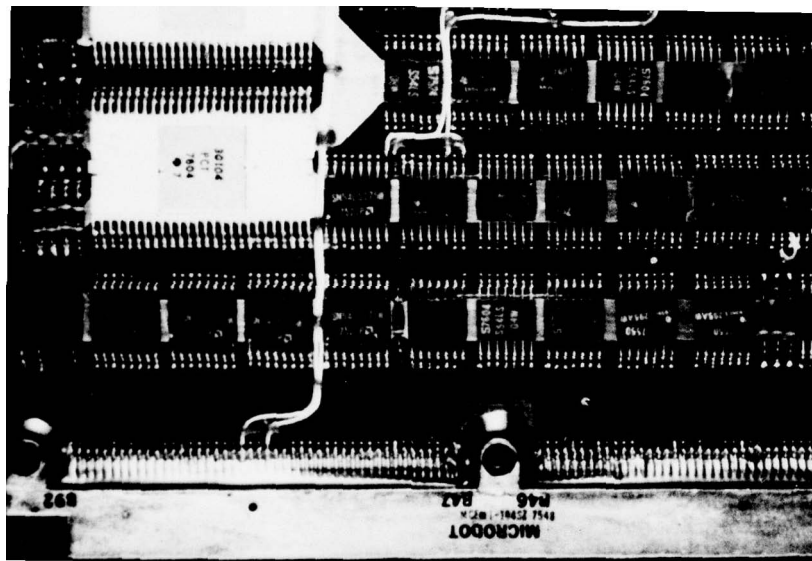


Figure 49. Processor Input/Output (Front Side)



Figure 50. Processor input/Output (Back Side)





### 2.1.7.1 Functional Description

2.1.7.1.1 Central Processor Unit (CPU). The CPU is a 16-bit microprogrammed processor with architecture and instruction repertoire designed to accommodate the high speed arithmetic of the MICRON navigation system. Seven general registers are provided and double precision instructions, including double precision multiply, have been incorporated to offer the high precision required while maintaining the efficiency of a 16-bit processor. The CPU functions are implemented with only 26 MOS/LSI components. These components can be separated into two categories: standardized logic building blocks and read-only memory (ROM) devices used to implement the instruction set in the microprogram control section. Table 14 summarizes the usage of these components. The standard building blocks had been developed earlier under a company funded program and their applicability to the MICRON DPU was demonstrated under AF contract F33615-72-C-1674. Therefore, no redesign of the MOS building blocks was necessary with the exception of the LADM device. The redesign of this device was initiated to allow the deletion of two MXF devices in the CPU, lowering the cost and improving reliability.

TABLE 14. MICRON CPU MOS COMPONENTS

MOS Type	Part No.	Name/Function	Quantity Per CPU
LADM	30179	Logic and Adder	2
MXF	30102	Multiplexer Four	8
PCT	30104	Program Counter Timer	2
INT	30105	Program Interrupt	1
AB	30077	Accumulator and Buffer	4
MPC	30075	Micoprogram Control	1
PS	30076	Register Storage	2
AC	30074	Algorithm Control	1
ROM	A0914	Read Only Memory	1
ROM	A0915	Read Only Memory	1
ROM	A0916	Read Only Memory	1
ROM	A0917	Read Only Memory	1
ROM	A0918	Read Only Memory	1
Total			26

New microprogram ROM codes were developed to permit block transfer of data between the RAM and the nonvolatile EAROM. The five microprogram ROM devices contain storage for 512 eight bit microinstructions; 496 locations are currently used, allowing some additional features to be added at a later time.

Extensive simulation effort was performed to validate the new microprogram codes and the logic of the CPU with the improved LADM. The simulation was performed on IBM 370 using a program called SIMSTRAN (System Simulation with Signal Tracing Analysis).

SIMSTRAN simulates operation of digital systems that are described in terms of their logical and functional attributes. The system element can be of a wide range of types, including analog elements, which may be described as digital elements with discrete time delays. Any combination of synchronous or asynchronous elements may be simulated directly.

**2.1.7.1.2 Processor Memory (PM).** The DPU can operate with either core or semiconductor memories. A core memory was used in the integration phase because of the need to maintain software flexibility. A semiconductor memory with electrically programmable PROMs and mask programmable ROMs was designed for the production configuration. The memory modules were fabricated and tested to ensure that cost, performance and packaging constraints of the production configuration could be attained.

Tradeoffs were made for the memory to determine the best possible mix of memory types considering cost, area of the standard MICRON board, storage requirements, and power. These trades were based upon available state-of-the-art military components. Devices under consideration were 8K EPROM's, 4K PROM's, 8K ROM's, 16K ROM's, and both static and dynamic 4K RAM's. The final configuration for the Engineering Prototype MICRON was established as follows: 4096 words of volatile Read/Write memory, 4096 words of Programmable Read-Only Memory (PROM), and 8192 words of mask programmable Read Only Memory (ROM), as shown in Figure 51. Provisions to expand the memory to 32K are included in the design.

The Read/Write memory is implemented with 16 SEMI 4200 devices. These are 4K N-channel devices organized into 4K x 1 memory. The devices feature TTL compatibility and static operation, eliminating the need for complex refresh circuitry.

The Programmable Read-Only memory is implemented with sixteen MMI 5350 devices. These are bipolar fusible link devices with a 1K x 4 organization and have open collector outputs.

The Read-Only Memory is mechanized with eight MMI 5275 bipolar 2K x 8 devices. Features of these devices include an access time of 120 ns over the full military temperature range, open collector outputs, and low current inputs which minimize address line loading.

Both ROM and PROM memories have their VCC terminals connected to +5 volts through power switches, so that the devices are in standby condition when no memory cycles are requested, thus minimizing the power requirements.

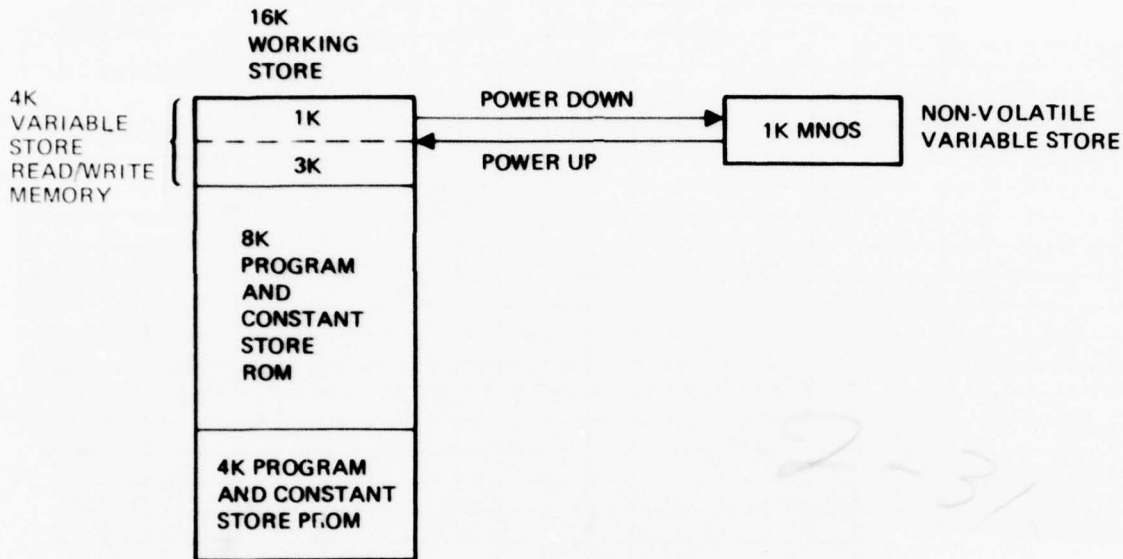


Figure 51. DPU Semiconductor Memory Organization

Because performance data on RAM's over full military temperature range was not available at the time of the memory design, sample quantities of the RAM devices were ordered and their characteristics were measured over full military temperature range (-55 C to +125 C). The characteristics tested at each temperature included the access time of the device, its ability to write into and read from eight address locations: an all 1's pattern, alternate 1's and 0's, and all 0's. Also tested was the current used by the device at different modes: standby, read, write, and alternate read and write. Testing was also performed to determine minimum chip select time necessary to both read and write. The tests indicated that adequate design margins exist in the memory design.

In order to provide nonvolatile storage for critical data and constants, a 1024 word electrically alterable read only memory (EAROM), implemented with MNOS technology, is provided in two hybrid packages (Calibration Constant Storage 1 and 2) physically located on SEU No. 4 module (see Para 2.1.5). This memory is used only in power-up and power-down sequences. At power-on, the contents of the MNOS memory is mapped into a portion of the volatile RAM. At power-down, the process is reversed, and a portion (1024 words) of the volatile RAM is safely preserved in the nonvolatile EAROM.

**2.1.7.1.3 Processor Input/Output (PIO).** The PIO module contains three major sections: The CPU related input/output, the DMAC input/output which transfers data between the Processor Memory and SEU, and the DPU - External I/O interface. The DMAC logic controls the transfer of a fixed amount of data in a fixed sequence by use of direct memory access. This sequence is initiated by the occurrence of the fast cycle interrupt. During the Phase 2A cost reduction study, it was determined that this logic could be implemented by a single MOS/LSI device, lowering the cost of the DPU. At

the outset of the Phase 2B contract, it was found that it would be desirable to be able to modify the sequence or amount of data transferred during the system integration. With the DMAC MOS implementation, these changes are very difficult and costly to implement. Therefore, in order to reduce the schedule and cost risk during systems integration, the DMAC function was mechanized with bipolar devices.

Subsequent to the initial logic apportionment, it was determined that some of the MIL-STD-1553 terminal interface logic should be mechanized on the PIO module. The addition of this logic presented a significant design challenge in order to stay within the constraints of the board size and connector pin limitations. The effort was successfully completed, the final product being a nine layer multilayer board with components mounted on both sides.

**2.1.7.1.4 DPU Software.** A set of support software was prepared for the MICRON DPU. A symbolic assembler, macro preprocessor, and functional test programs are among these tools. Users manuals, including a Programmers Reference Manual, an Assembler Users Manual, and a Macro Processor Users Manual were completed. The DPU Software is described in the following paragraphs.

#### General Assembler Program (GAP)

The GAP/MICRON system provides basic assembly language programming capability that increases efficiency in coding, debugging, and documenting the MICRON programs. The program is written in FORTRAN IV and can be executed on a variety of general purpose (host) computer systems which support the usage of the FORTRAN IV compiler language. The assembler accepts inputs in assembler source language and translates them into machine code programs and listings. The assembler and macro preprocessor are available through both Time Sharing Option (TSO) and batch processing on the Corporate System 370's located in Downey, CA.

The GAP/MICRON assembler is a symbolic two-pass system that assembles the object processor programs in either relocatable or absolute format. All object machine instructions and data formats are supported as well as assembler directives for assembler control, storage allocation, data declaration, output listing formatting, and assembler output options. Error detection and reporting includes syntax and machine restrictions for common errors. Warnings are generated to indicate possible violations of CPU hardware restrictions. Errors are flagged on the generated listing where they occur and are also summarized in an error table printout. The printed output includes a listing of all symbols used, including a complete cross-referencing. The assembler output is a punched paper (mylar) tape that is compatible with the MICRON Test Equipment.

#### Functional Test Program

The functional test program is designed to provide an extensive checkout of the MICRON CPU, PIO, and Memory Modules. Included in the program are segments which may be characterized as instrument decoder tests, memory read/write tests, shift and cycle tests, logical and mask operation tests, arithmetic and double precision arithmetic tests, timer tests, and I/O tests. Each of the segments consists of subtests which exercise the various possible instruction variations. The structure of the program is modular, i. e., the subtests or subroutines are controlled by a test table which may be manipulated by a test operator. Thus, the user can execute all or any

selected portions of the program. The Functional Test Program is comprised of three test tapes which test the various combinations of DPU modules:

Self Test Program	CPU, P/N 14219-501-1	No. 2T012-0004
Self Test Program	PM, P/N 14225-501-1	No. 2T012-0005
Self Test Program	PIO, P/N 15390-501-1	No. 2T012-0006

Module level tests are conducted on Digital Automatic Test Equipment (DATE). Object programs for the DATE tester were prepared for each of the three DPU modules. Three support software programs were used to generate the module test tapes. Documentation of the test software is, therefore, in the form of output listings of the three programs. The three programs used are the MICRON Assembler, the SIMSTRAN logic simulator, and a DATE compiler. The MICRON Assembler is used only for generating test programs for the CPU.

#### 2.1.7.2 Fabrication and Test

Two sets of DPU modules (one flight set and one spare set) were fabricated, assembled and tested. It should be noted that the memory modules were partially populated since the final code for ROM's and PROM's were not available. The partially populated memory includes the full complement of RAM, 2K of ROM with a test pattern, and 1K of PROM with a self-test program.

All DPU components were procured from outside vendors with the exception of the MOS logic devices and microprogram ROM's, which were fabricated in-house. Test specifications were established for the MOS devices to assure proper operation in the MICRON system environment. Table 15 shows the test conditions the MOS devices are subjected to at both wafer probe and packaged device levels. It should be noted that at device level testing, the voltages were varied over twice the system specification range to assure adequate design margins. The equipment used for these tests was a Rockwell build MOS/LSI tester. The tester provides clocks, voltages and input stimuli and monitors the device outputs. Test patterns for each individual device type were developed from the logic equations using the SIMSTRAN simulator. In cases where test results indicated potential problems or marginal operations, additional test plots were made showing the curve of clock voltage as a function of  $V_{DD}$  that defines the border between operating and non-operating zones.

A test plan for DPU subassembly level integration was written. The test plan specifies functional testing at module and subassembly level as shown in Figure 52. The final test in the flow consists of testing at both high and low temperature extremes, under worst case voltage conditions. Each of the two sets of DPU modules successfully passed these DPU level tests. However, several problems were discovered and corrected during these tests.

At CPU system level testing, two problems with MOS/LSI devices were found.

A problem with the AB-1 devices produced an erroneous output on one pin under certain input conditions, causing the loss of eight CPU instructions. The source of the problem was traced to a metal connection which shorted out a speed-up capacitor. A

TABLE 15. TEST CONDITIONS

Test No.	*1a	**1b	**1c
VDD (VDC)	$-20.0 \pm 0.5$	$-18.0 \pm 0.2$	$-22.0 \pm 0.2$
Clocks			
"0" (VDC)	$-1.0 \pm 0.5$	$-1.0 \pm 0.5$	$-1.0 \pm 0.5$
"1" (VDC)	$-20.0 \pm 0.5$	$-18.0 \pm 0.2$	$-22.0 \pm 0.2$
Inputs			
"0" (VDC)	$-1.0 \pm 0.5$		
"1" (VDC)			
High	$-18.0 \pm 2.0$		
Low	$-5.0 \pm 0.5$		
Clock Frequency (MHz)	$1.0 \pm 0.02$		
Clock Separation (nsec)	$52 \pm 5$		
Temperature	25°C	25°C, 125°C	
VR (VDC)	$-5.0 \pm 0.1$		
Note: *Test 1a performed at wafer probe and at pre-seal only. **Performed after sealing of devices.			

cost effective solution to this problem was implemented by reworking existing wafers. The metal line causing the short was etched out using a special mask prepared for this purpose.

The second problem required recycling of a MOS ROM A0915 device. This problem was caused by a microprogram coding error, affecting the double precision add and subtract instructions during cycle steal. Recycling of the device was completed in two weeks. Meanwhile, double precision add and subtract instructions were replaced by macros in the assembler. In this way, the assembler generated double precision macro routines which did not contain the instructions affected by the micro code error.

#### 2.1.7.3 DPU Temperature Testing

Temperature testing was conducted in two phases:

1. Preliminary confidence tests
2. Comprehensive temperature testing

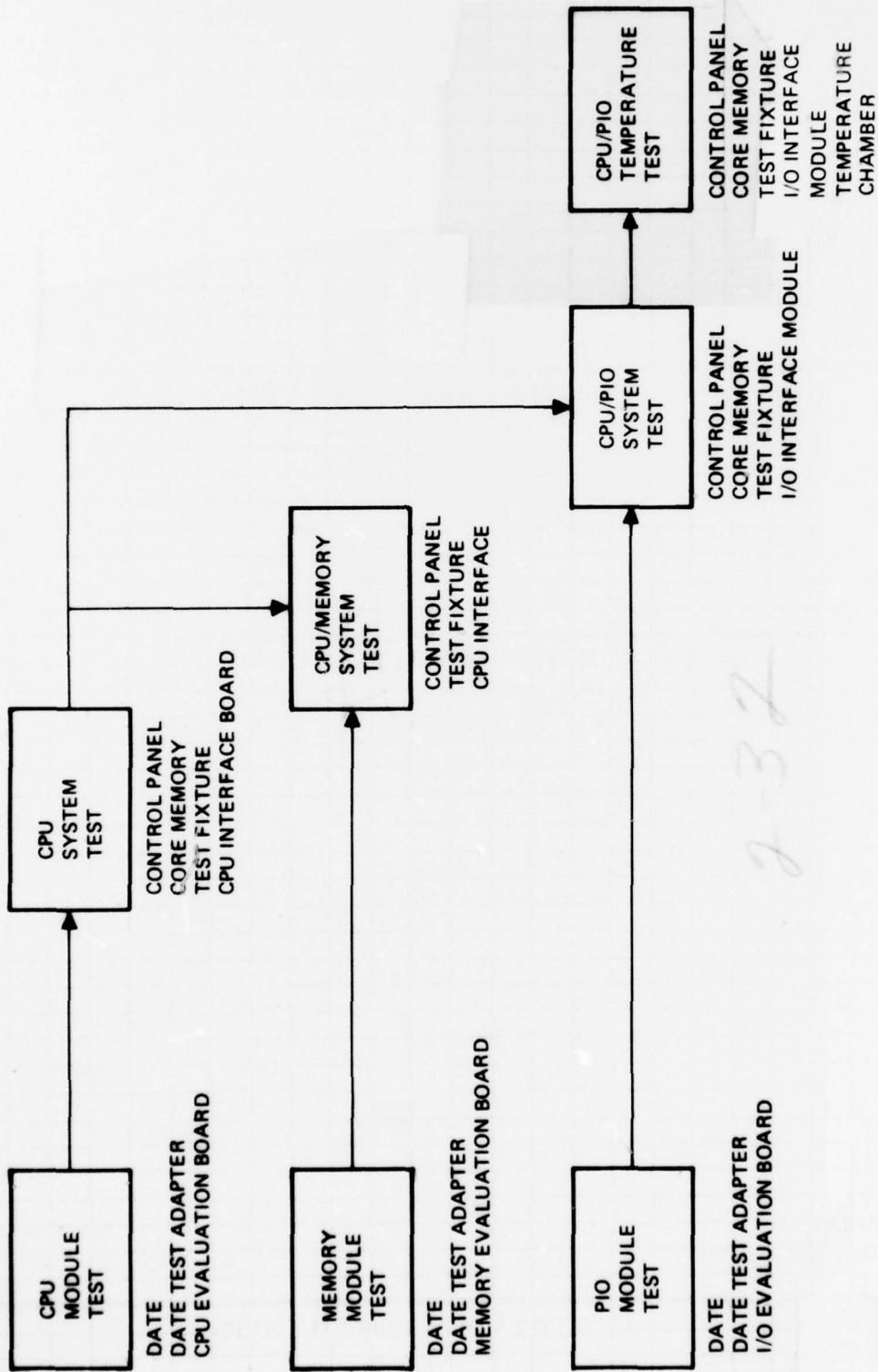


Figure 52. MICRON DPU Test Flow

The purpose of the preliminary tests was to check out the test fixture at temperature extremes, identify any potential design problems, and verify the adequacy of the test procedures and equipment.

Preliminary tests were conducted by inserting the test fixture with the DPU modules into the temperature chamber and adjusting the temperature as follows:

High Temperature: 75 C at hottest heat rail with MOS components

Low Temperature: -54 C cold soak

These limits were based on MICRON EPM specification requirements and detailed thermal analysis of the system.

The preliminary high temperature test was completed successfully. It was observed that the thermal profile of the CPU differed from the profile predicted for the module when mounted in the EPM chassis. The test set-up showed approximately 3C Thermal gradient across the module, against 19C worst case temperature rise in the chassis. For comprehensive temperature tests, the test fixture was modified by adding two heat sinks with module clamps and appropriate covers to simulate the actual thermal conditions that exist in the EPM chassis. The modified test fixture is shown in Figure 53. The heat sink is maintained at 50 C for high temperature tests and at -54 C for low temperature tests. Temperature tests were conducted at nominal and worst case voltage conditions as shown in Figure 54.

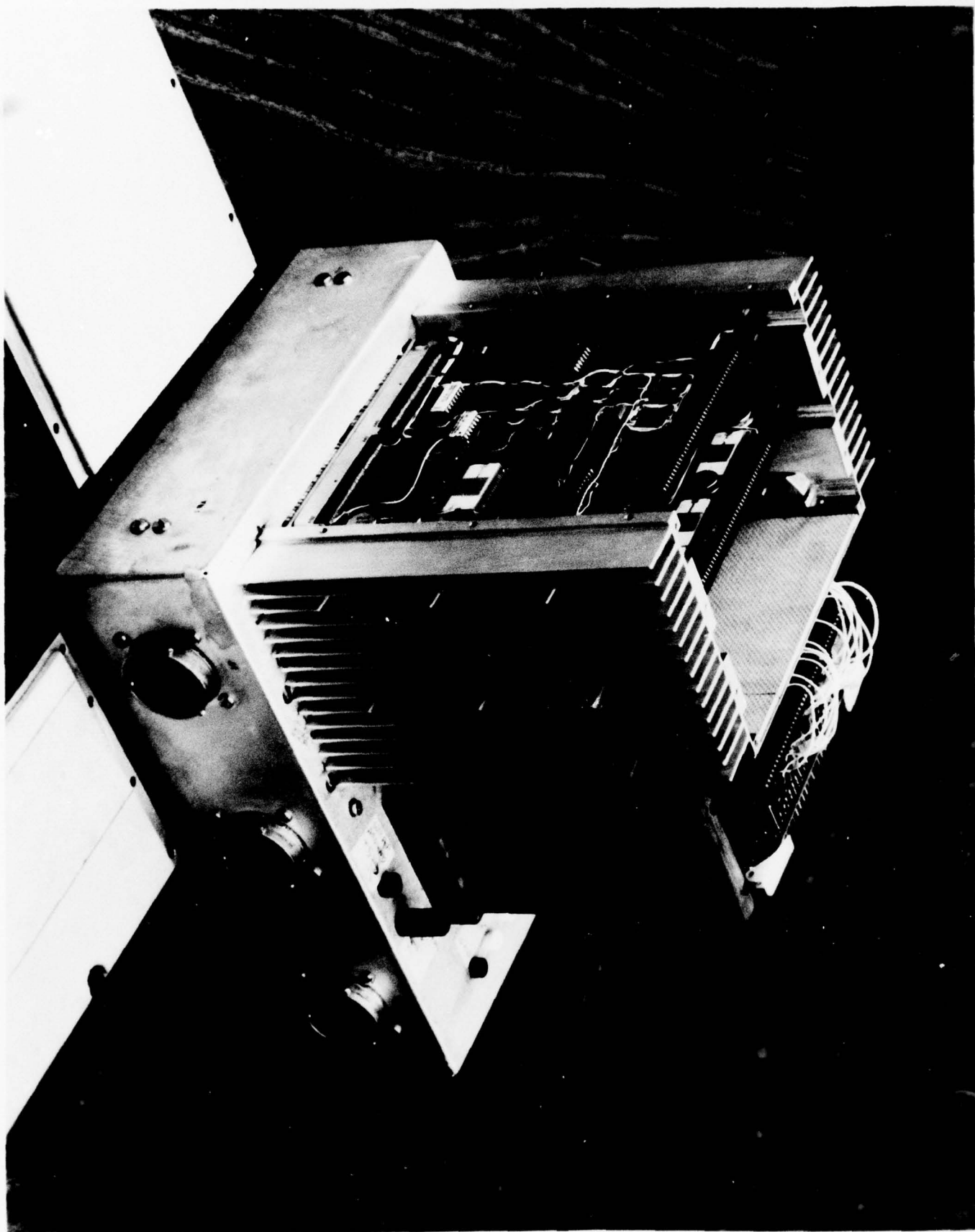
Several MOS/LSI problem areas were identified and corrected while the DPU was in temperature test. The following is a description of the problems and the corrective actions taken.

During preliminary temperature testing, it was noted that the AB devices were sensitive to noise at high power supply voltage and low temperature (-7 C and below) conditions. Further analysis and testing indicated that the problem could be eliminated by adding some capacitance to the circuit node susceptible to noise. This required minor redesign of the AB device. Test results with new devices indicated that the problem was corrected by the redesign. However, a new problem was observed with the redesigned devices, which affected DBO output under low clock voltage and low temperature conditions. An analysis of wafer processing data showed that the affected parts came from a low threshold ( $V_{GST} = 1.9$ ) lot. To overcome the problem, high threshold ( $V_{GST} = 2.4$  v) devices were fabricated that yielded acceptable parts after low temperature screening.

A design iteration of the RS (Register Storage) device was required because of its marginal operation at high  $V_{DD}$ . The problem was caused by noise within the decoding structure to the internal read/write memory. Cross clamping techniques in the decode signals were incorporated to correct the problem. In redesigning the device, a short to  $V_{DD}$  was inadvertently placed on the circuitry related to one of the outputs, requiring a second iteration to make the device 100 percent operational. The effort was completed successfully in record schedule and the new RS devices have been incorporated on CPU modules.

FIG 53  
A/T

Figure 53. Modified Test Fixture for DPU Temperature Testing



Handwritten text at the bottom of the page: Δ 9

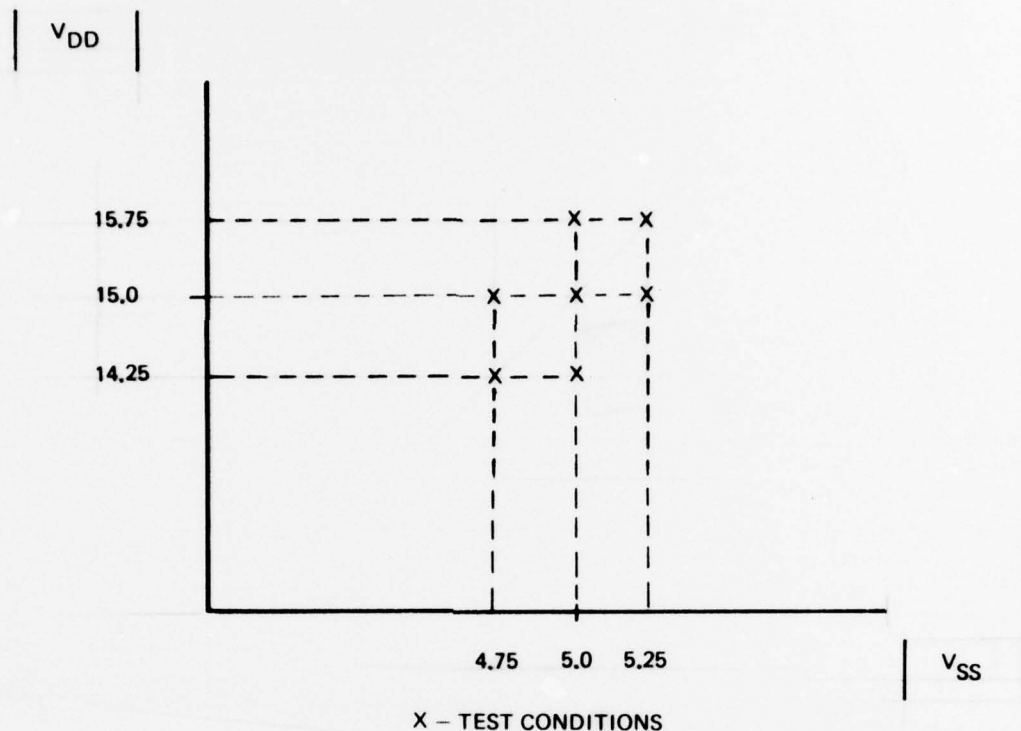


Figure 54. Test Conditions for Voltage Extremes

Another problem related to MOS/LSI devices was uncovered while testing the DPU at low temperature (-54 C). It was identified as a potential race condition between LADM device float B control and the AB device outputs feeding the LADM B input port. The problem could be corrected by either (1) LADM device redesign, or (2) the addition of bipolar logic gates between the AB and LADM devices. The latter approach was selected due to cost and schedule constraints. The additional logic was first breadboarded and tested over full temperature range and later was permanently incorporated into all CPU's.

A failure caused by a MOS device was observed in low temperature testing. The failure was traced to one of the microprogram memory devices, ROM 918. The remaining ROM 918s in inventory were tested off-line and most devices were found to be marginal at low temperature. Other ROM devices (ROM 915 through 917) were also tested at low temperature to determine whether the failure was due to the design or processing problems. All other ROMs were performing well within specifications. Further analysis confirmed that the problem was process oriented and limited to ROM 918s only. A new ROM 918 wafer lot was fabricated which yielded an adequate number of devices with satisfactory performance over the full temperature range.

### 2.1.8 IOU Design/Develop/Fab/Test

The EPM Input/Output Unit (IOU) contains those functions required for the INU to electrically interface with other systems within the overall avionic system. The IOU consists of two modules, the Converter Module and the Data Terminal Unit. Each of these modules is discussed in the following paragraphs.

#### 2.1.8.1 Converter

The Converter Module receives parallel digital data from the Processor Memory Module. This digital data is used to convert a 400 Hz input reference signal into five synchro output channels and two DC channels. In addition, this digital data is used to control four discrete outputs for rotation control, select discrete inputs or encoder inputs, and provide control for one spare discrete output. This module also receives six discrete inputs and provides optical isolation for four of the six discrettes. Five output discrettes, one interrupt, and a 28VPS failure discrete are also provided. BITE feedback is provided from seven synchro outputs, two DC outputs and three of the discrete inputs.

This module has space available and wiring provided (no active components, however) for four additional dependent synchro output channels and two independent synchro output channels. Provisions for a synchro input channel, conditioning, and output have also been provided. Space and wiring have also been provided for optical isolation between four discrete inputs and outputs.

The Converter Module has provisions for BITE and Self Tests. Self tests are those tests that are performed during the initialization phase of the align mode while BITE is a continuous dynamic test performed during all modes. The analog outputs are summed and fed back as Roll BITE, Pitch BITE, Hdg BITE, DC No. 1 FB, and DC No. 2 FB for computer monitoring of outputs. The discrete outputs PRG, DISC, FB, HDG DISC FB, and 26 V DISC FB are fed back for computer monitoring.

Tables 16 and 17 summarize the analog output requirements for communication between the digital channel and the synchros in the aircraft avionics. The initial mechanization of the digital/synchro circuit required separate holding registers and off-the-shelf digital-to-synchro converters. In an effort to reduce space, required power, and cost, an alternate scheme was considered which used  $\sin \theta$  and  $\cos \theta$  digital data from the computer to drive multiplying Digital-to-Analog converters (DAC's). This configuration used separate discrete devices for the registers, switches, ladder network, and output amplifiers.

A third configuration was also evaluated. This mechanism incorporates most of the separate components of the previous scheme into a single DAC device. This scheme requires less space and is a less complex and lower cost design. Three DAC devices having a self-contained input holding register were evaluated. (1) The Rockwell DAC, P/N 65008, is a MOS device developed for use as an ADC. Several of these devices were tested in a breadboard circuit and passed the minimum accuracy requirements. However, this device requires an external ladder network and additional circuitry for level shifting and synchronizing to the MOS 4-phase clock. (2) The Beckman DAC, P/N 877-69, has an internal ladder network and output amplifier. The sample tested passed the minimum accuracy requirements. However, this device is only available in a large (0.99 x 1.49 in.) dual-in-line package. (3) The Analog Devices DAC, P/N AD7522, has an internal ladder but requires an output amplifier circuit. The samples tested passed the minimum accuracy requirements.

TABLE 16. ANALOG OUTPUTS

Signal	Type	Range	Resolution	Accuracy	Index Ref	Positive Direction	Scale Factor	External Load	Phase Shift
Roll No. 1	Buffered Synchro	0° to 360°	0.1° rms	0.1° rms	0° = Horiz	Right Bank	1° = 1°	Note 1	+14 ±4° Lead
Pitch No. 1	Buffered Synchro	0° to 90°	0.1° rms	0.1° rms	0° = Horiz	Nose up	1° = 1°	Note 1	+14 ±4° Lead
True Heading No. 1	Buffered Synchro	0° to 360°	0.5° rms	0.5° rms	0° = North	CW wrt North	1° = 1°	Note 2	+14 ±4° Lead
Spare DC No. 1	DC Analog	0 to 15 vdc	0.15 vdc	±0.15 vdc				500 ohms	
Spare DC No. 2	DC Analog	0 to 15 vdc	0.15 vdc	±0.15 vdc				500 ohms	
Spare No. 1	Buffered Synchro	0° to 360°	0.5° rms	0.5° rms			1° = 1°	Note 2	+14 ±4° Lead
Spare No. 2	Buffered Synchro	0° to 360°	0.5° rms	0.5° rms			1° = 1°	Note 2	+14 ±4° Lead

NOTES: 1. Minimum impedance = Two parallel AY500-5 (222 + j470 Z<sub>SO</sub>) with a maximum of 0.01 μf capacitance to ground, each leg.  
 2. Minimum impedance = CRC-8-A-1(10+j45Z<sub>SO</sub>) with a maximum of 0.01 μf capacitance to ground, each leg.

TABLE 17. ANALOG OUTPUT PROVISIONS

	Type	Range	Resolution	Accuracy	Index Ref	Positive Direction	Scale Factor	External Load	Phase Shift
Spare (Roll No. 2)	(Note 1) Buffered Synchro	0° to 360°	0.1° rms	0.1° rms	0° = Horiz	Right Bank	1° = 1°	Note 4	+14 ±4° Lead
Spare (Roll No. 3)	(Note 1) Buffered Synchro	0° to 360°	0.1° rms	0.1° rms	0° = Horiz	Right Bank	1° = 1°	Note 6	+14 ±4° Lead
Spare (Pitch No. 2)	(Note 2) Buffered Synchro	0° to 90°	0.1° rms	0.1° rms	0° = Horiz	Nose Up	1° = 1°	Note 6	+14 ±4° Lead
Spare (True Heading No. 2)	(Note 3) Buffered Synchro	0° to 360°	0.5° rms	0.5° rms	0° = North	CW wrt North	1° = 1°	Note 5	+14 ±4° Lead
Spare No. 3	Buffered Synchro	0° to 360°	0.5° rms	0.5° rms			1° = 1°	Note 5	+14 ±4° Lead
Spare No. 4	Buffered Synchro	0° to 360°	0.5° rms	0.5° rms			1° = 1°	Note 4	+14 ±4° Lead

- NOTES:
1. Roll No. 2 and Roll No. 3 are buffered outputs of the same digital to synchro converter as Roll No. 1.
  2. Pitch No. 2 is a buffered output of the same digital to synchro converter as Pitch No. 1.
  3. True Heading No. 2 is a buffered output of the same digital to synchro converter as True Heading No. 1.
  4. Minimum impedance = Two parallel AY500-5 (22 + j470Z<sub>SO</sub>) with a maximum of 0.01 μf capacitance to ground, each leg.
  5. Minimum impedance = CRC-8-A-1 (10 + j45 Z<sub>SO</sub>) with a maximum of 0.01 μf capacitance to ground, each leg.
  6. Minimum impedance = 5K Ω balance with a maximum of 0.01 μf capacitance to ground, each leg.

The Analog Devices DAC was selected as best of the three DAC's for use in the Digital/Synchro Converter design. This decision was based upon the device cost, space required, circuit complexity, and accuracy.

Figure 55 is a block diagram of the Digital/Synchro Converter. Computer data are strobed into the DAC holding registers (Synchro DAC) from the parallel lines. The decoded address lines (Reference Generator) then enable the corresponding DAC to convert this digital data to analog signals. The analog signals are then amplified (Buffer Amplifier) before going to the Synchros. The critical signals are monitored (Synchro Bite) and corresponding test signals are sent to the computer.

The most stringent requirement is for the Roll and Pitch synchro signals where  $\geq 10$  DAC bits are needed. Three DAC candidates for the Digital/Synchro circuit were lab tested at three temperature environments. The DAC accuracy is calculated from a computer program using the lab test data. Accuracy test results are shown in Table 18 (The Beckman and Rockwell DAC's were tested using 13-bits before the minimum number of bits requirement, 10-bits, was known).

Tables 19 through 23 give a summary of the analog input provisions, discrete input provisions, discrete output provisions, discrete inputs and discrete outputs which are also mechanized on this module.

The Converter Module has components and hybrids mounted on both sides of a 6-layer printed circuit board. For this reason the flatpack package was used for the hybrids rather than the plug-in type of package. Heatsinks are bonded to the MLB like the SEU design (see Para 2.1.5). The hybrid types required for the Converter Module are as follows:

Nomenclature	Quantity Required	P/N
Synchro Bite	1	12505-507-1
Synchro Buffer Amplifier	3	12510-507-1
Synchro Reference Generator	1	12515-507-1
Synchro DAC	2	12545-507-1
DAC Amplifier	1	12560-507-1

A detailed description of the hybrid thick and thin film technologies is given in Appendix A. Appendix A also gives an itemized listing of the activity involved in the fabrication, assembly, and testing of the hybrids.

Worst case analyses were completed on all of the Converter Module hybrids. A thermal analysis of all of the semiconductors was also completed and this is given in Appendix B. The analyses results indicate that all the requirements in the reliability design guidelines are being met.

The functional and screen tests performed on the hybrids are listed in Appendix C of this report. Each hybrid has met or exceeded test specification requirements. Appendix D provides additional information relative to precision thin film resistor requirements and performance tests. The data shown in Appendix D indicate the resistors are exhibiting excellent stability and are meeting stability requirements also.

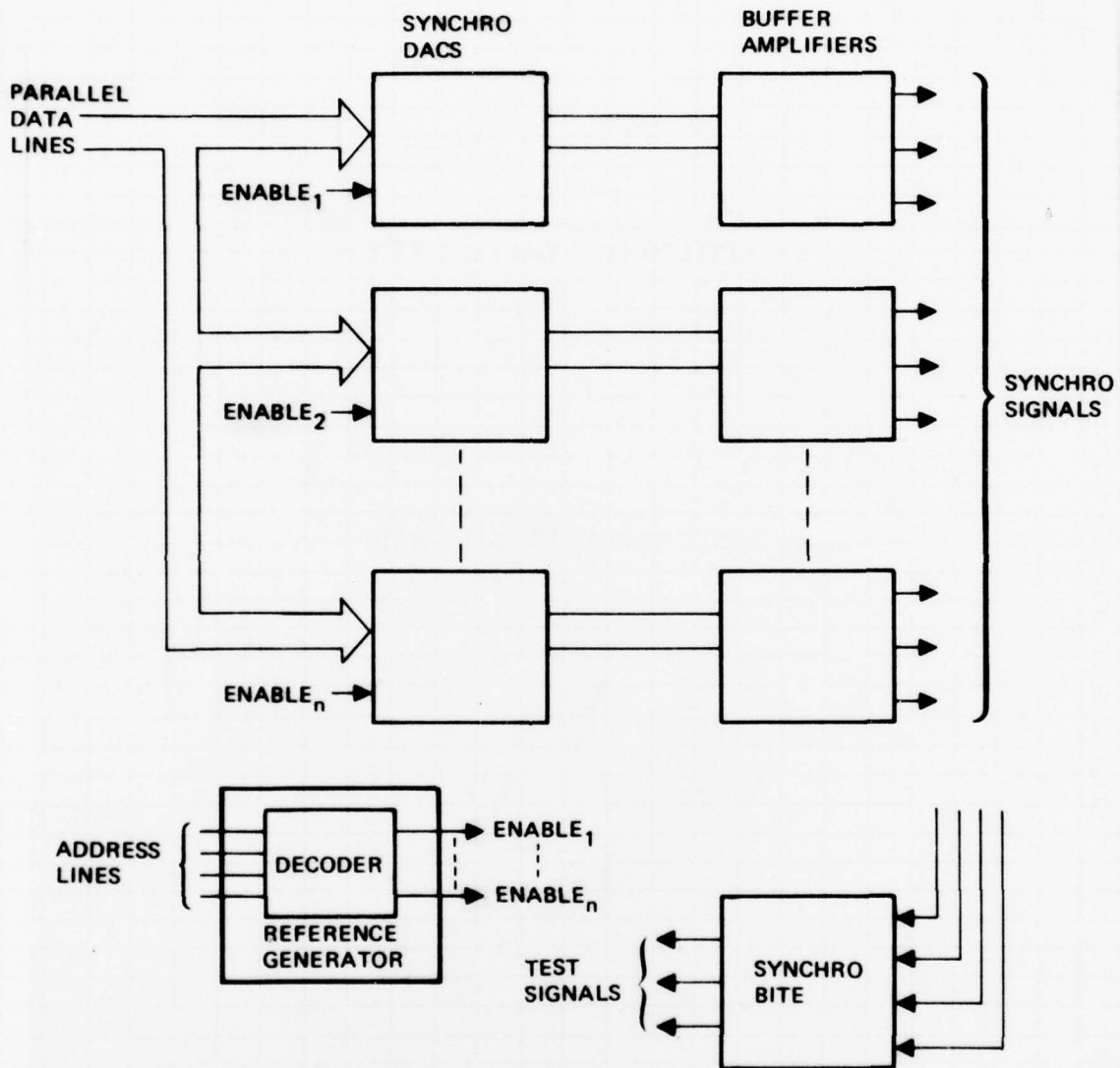


Figure 55. Digital/Synchro Converter Block Diagram

TABLE 18. DAC ACCURACY TEST RESULTS

DAC	*Standard Deviation (in mv)		
	@ -55 C	@ 25 C	@ 100 C
Using 13 bits:			
Beckman #1	0.393	0.246	0.882
Rockwell #1	0.998	1.068	n/a
Rockwell #2	0.928	1.198	0.678
Rockwell #3	1.259	1.290	0.938
Rockwell #4	0.955	1.161	0.642
Rockwell #5	0.832	1.089	0.689
Using 10 bits:			
Analog Devices #1	7.73	7.71	8.24
Analog Devices #2	5.77	5.65	5.71
*for 13-bits, standard deviation should be less than 1.22 mv and for 10-bits, standard deviation should be less than 19.53 mv. n/a = data not available			

TABLE 19. ANALOG INPUT PROVISIONS

Signal	Type	Range	Index Ref	Positive Direction	Scale Factor	Accuracy	Phase Shift
Spare	Synchro	0° to 360°	0°	CW wrt North	1° = 1°	±0.5°	+14 ± 4° Lead

TABLE 20. DISCRETE INPUTS

Signal	False State	True State
FCC Bus Control	-0.4 to 0.5 VDC or Open	2.4 to 5.5V DC = FCC is Bus Controller
Designate	Open	+28V DC A/C = Designate
To/From	0 VDC	5 VDC
Heading Good	0 VDC	5 VDC
26 Vac Ref. Enable	0 VDC	5 VDC
Pitch/Roll Good	5 VDC	0 VDC

TABLE 21. DISCRETE INPUT PROVISIONS

Signal	False State	True State
Attitude Mode	Open	+28 VDC A/C = Attitude Mode Selected
Spare +28V	0 VDC	28 VDC
Spare Number 1 5V	0 VDC	5 VDC
Spare Number 2 5V	0 VDC	5 VDC

TABLE 22. DISCRETE OUTPUTS

Signal	False State	True State	Load
Attitude Good Number 1	Open	28VDC A/C = Attitude Good	720 $\Omega$ Min.
Attitude Good Number 2	Open	28 VDC A/C = Attitude Good	720 $\Omega$ Min.
Heading Bad	Open	28 VDC A/C = Heading Bad	720 $\Omega$ Min.
To/From	0 $\pm$ 5 $\mu$ A	+325 $\pm$ 100 $\mu$ A = TO	200 $\Omega$ $\pm$ 15% or 100 $\Omega$ $\pm$ 15%
Designate Interrupt	0 VDC	+5 VDC	TTL Gate (LS)
FCC Bus Cont.	↓	↓	↓
28 VPS Fail			
PRG DISC FB			
HOG DISC FB			
26V DISC FB			
	0 VDC	+5 VDC	TTL Gate (LS)

TABLE 23. DISCRETE OUTPUT PROVISIONS

Signal	False State	True State	Load
Attitude, Mode	0 VDC	+5 VDC	TTL Gate (LS)
Spare Number 1 5V	↓	↓	↓
Spare Number 2 5V	↓	↓	↓
Spare 28V	0 VDC	+5 VDC	TTL Gate (LS)

Two Converter Modules (including one spare) were assembled and tested. A photograph of the Converter Module is shown in Figure 56. The module is not completely filled out because the provisional electronics discussed above are not required for the EPM system. (Only those functions listed in Table 16 need to be performed.) Appendix E provides information relative to the tasks involved in the fabrication, assembly, and test of the modules. The functional and screen tests performed on the modules are listed in Appendix C. Each of these modules has met or exceeded detail design specification requirements.

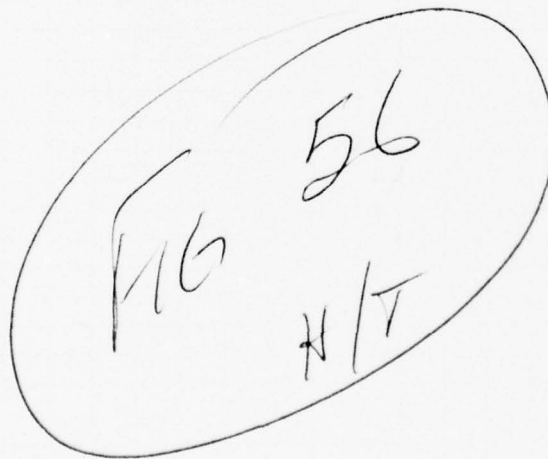
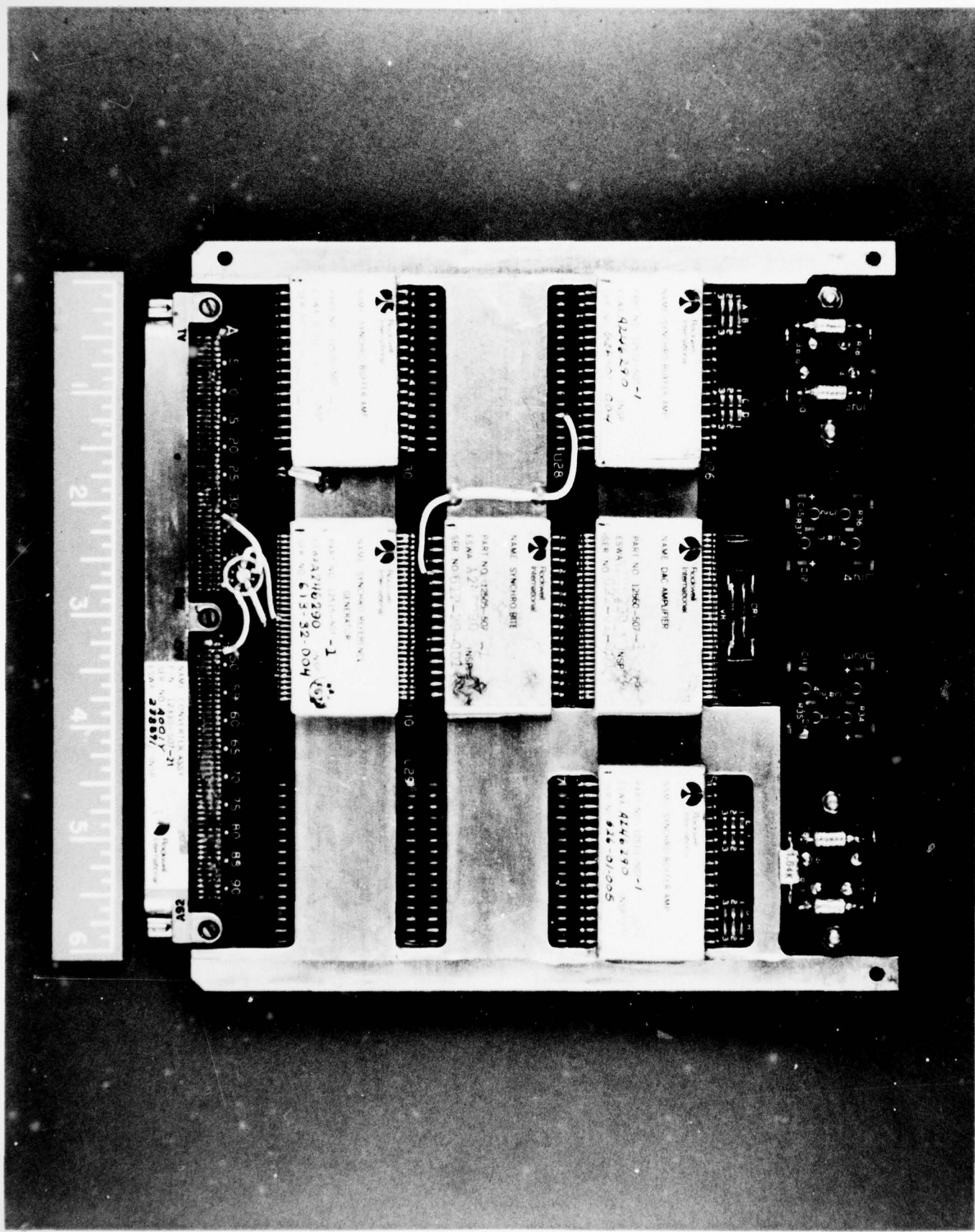


Figure 56. Converter Module



4/6

△

#### 2.1.8.2 Data Terminal Unit

The Data Terminal Unit (DTU) function is to provide a port through which data can be transferred bilaterally between the Flight Control Computer and MICRON, or between MICRON and any other station which has a port on a MIL STD 1553A type data bus.

The DTU evolution can be broken down into three functional activities. The first activity involved (1) definition and development of the transmitter/receiver (T/R) circuitry and associated encoding (EL) and decoding (DL) logic, (2) breadboard development and test, including integration with an operational data bus system, and (3) hybridization of these devices to reduce the real estate requirements and to assure a relatively constant electrical environment. The second activity involved definition, development and breadboard test of the Subsystem Interface Unit (SSIU), and integration with the T/R, EL and DL circuitry. The third activity involved design and development of the multi-layered DTU module.

The organization of the DTU is illustrated in Figure 57. The illustration shows a long stub configuration. The T/R accepts or outputs 1 MHz bi-phase Manchester on the bus end and accepts or outputs NRZ data on the other. The EL assimilates the command or data word and outputs it along with the appropriate timing signals to the T/R during the transmit mode. Since only one channel is active at a time, one set of EL logic is shared between the two channels. Each channel has its own dedicated DL logic set to decode incoming data. Although only one channel is active at a given time, the other channel must monitor its bus and cause the DTU to respond to any valid commands it detects, aborting whatever activity was currently in progress on the 'active' channel.

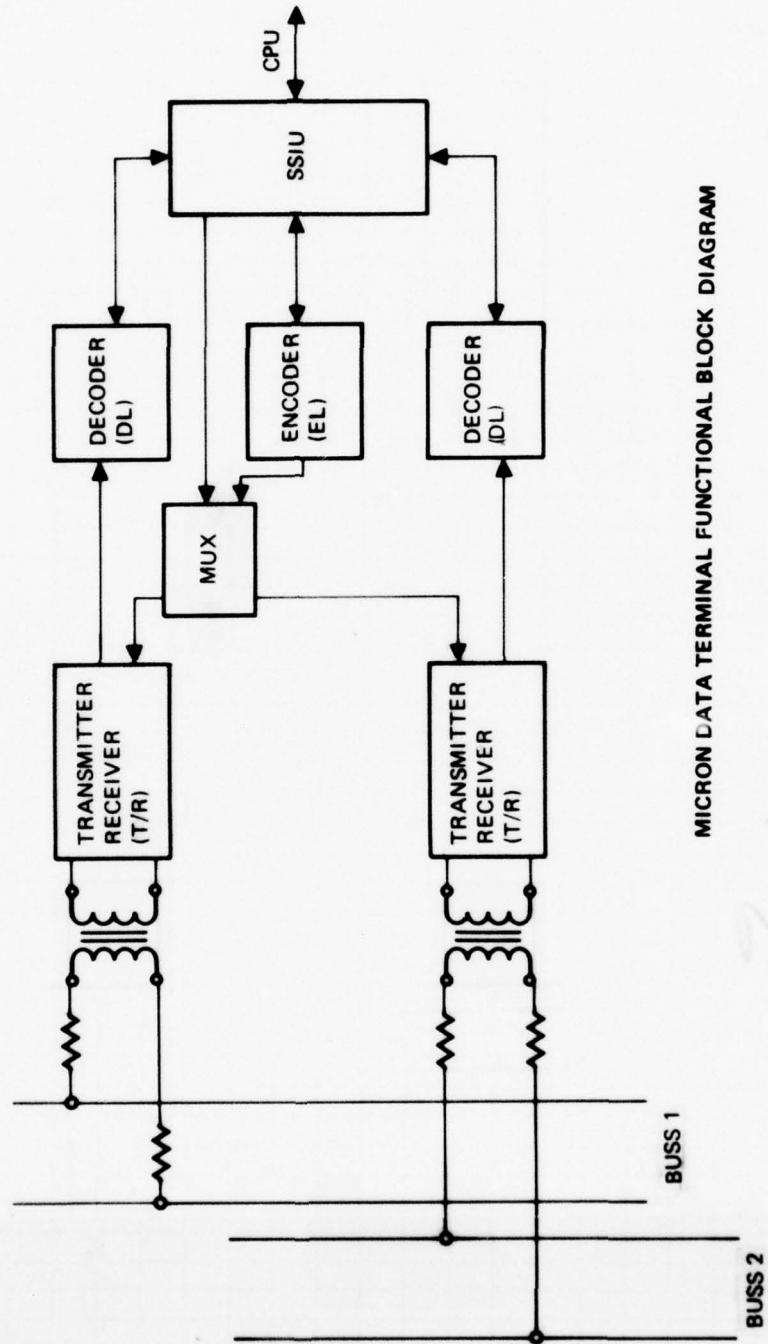
The SSIU contains the redundancy management logic, status register, direct memory access (DMA) initiation logic, indirect CPU address logic and the control and timing logic required to make the overall system coherent.

Each functional block defined in the DTU organization diagram (Figure 57) is an entity and is discussed in the following paragraphs.

**2.1.8.2.1 Transformer.** The transformer provides the means to couple the DTU to the data bus. The bi-phase Manchester output amplitude was designed to be 8.8V (peak-to-peak, normal) with a worst case of 7.3V (peak-to-peak) into a properly terminated data bus. The input impedance presented to the bus was designed to be  $2K\Omega$ (min) over the frequency range of 100 kHz to 1.0 MHz. Figure 58 is a plot of these parameters as measured on the assembled, functional DTU module.

**2.1.8.2.2 Transmitter/Receiver.** The T/R functional organization is shown in Figure 59. The receiver channel consists of a six pole Bessel active filter which couples into a dual comparator, the outputs of which are compatible with T<sup>2</sup>L logic. The output of the receiver is logical manchester (i.e., 0 to +5 VDC) data. The receiver is designed not to saturate during continuous operation (i.e., no restriction on duty cycle). The comparator thresholds are set at  $\pm 0.6V = '1'$  out. There is a deadband of  $0 \pm 0.4V$  and the output is indeterminate at +0.4 to +0.6 and -0.4 to -0.6 V.

DATA TERMINAL ORGANIZATION



MICRON DATA TERMINAL FUNCTIONAL BLOCK DIAGRAM

Figure 57. Data Terminal Organization

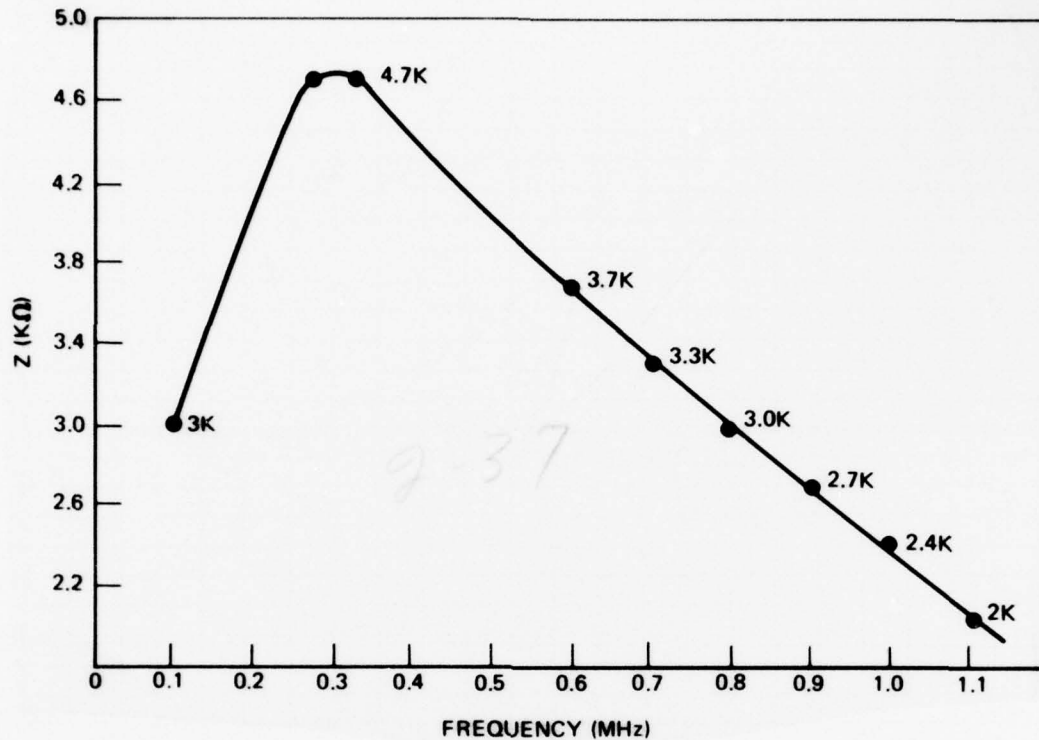
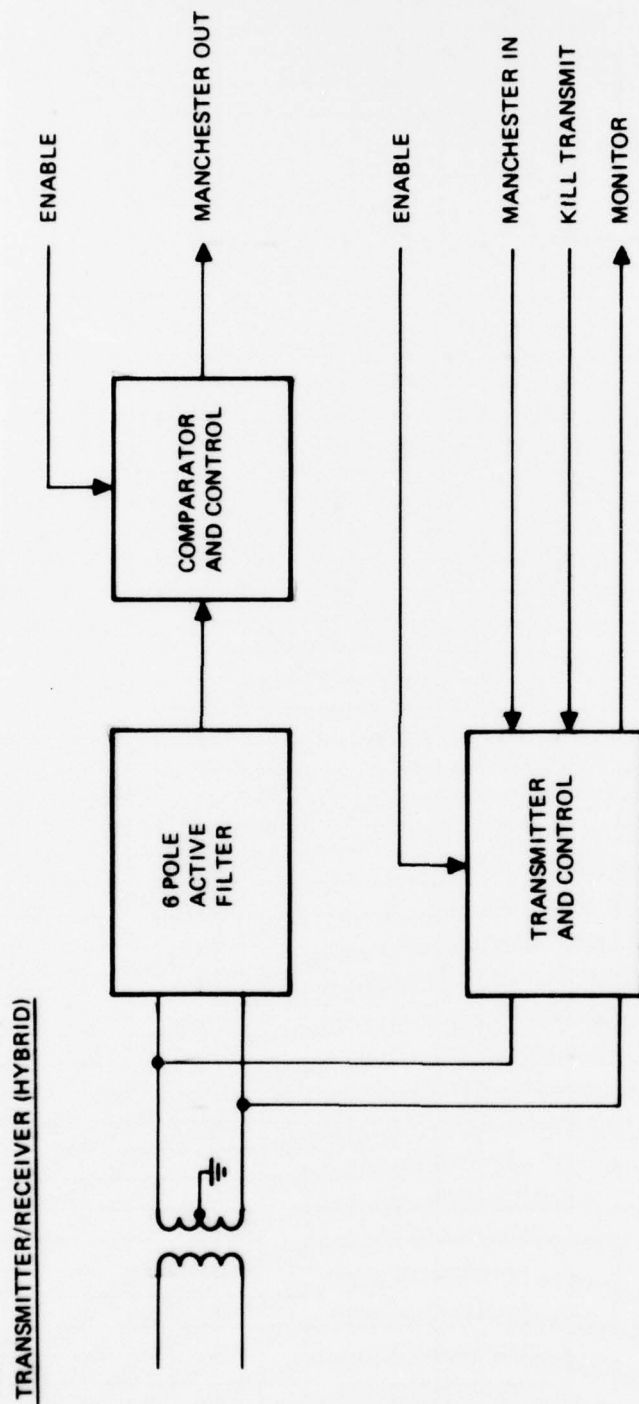


Figure 58. DTU Input Z vs Frequency

The transmitter was designed to run in a non-saturated mode to allow control of the output rise time which is set at 150 ns (nominal). The transmitter can be operated continuously and outputs about two watts at a minimum voltage of 24V p-p at the transformer. The T/R is not sensitive to power sequence.

The T/R hybrid consists of two substrates: (1) A thick film substrate which carries the high power devices (output transistors) and devices which are required to track in temperature, and (2) a thin film substrate which contains the filter, receiver and transmitter control stages. A thermal analysis of the device predicted a worst case junction temperature rise of 48°C on the transmitter output stages. Measurements made while the device was operating in an ambient environment of 25°C showed a 25°C rise to 50°C.

2.1.8.2.3 Encoding Logic (EL). The Encoding Logic performs the function of providing logical Manchester data to the T/R for output. A functional block diagram of the EL is shown in Figure 60. A "ready" signal from the SSIU activates the logic. When synchronized, the EL responds with an acknowledge to the SSIU. It then assimilates the output word into the correct format by multiplexing first the command or data sync (3-bits-invalid Manchester), then 16-bits of data derived from the Computer through the SSIU, and finally the parity bit which it creates. At the start of the transmit sequence, the transmitter is activated by setting the 'Transmit Enable' discrete high. The 'Transmit Clock' is used to shift data out of the SSIU. Mechanization of the EL was done with low power Schottky devices in order to minimize power and heat.

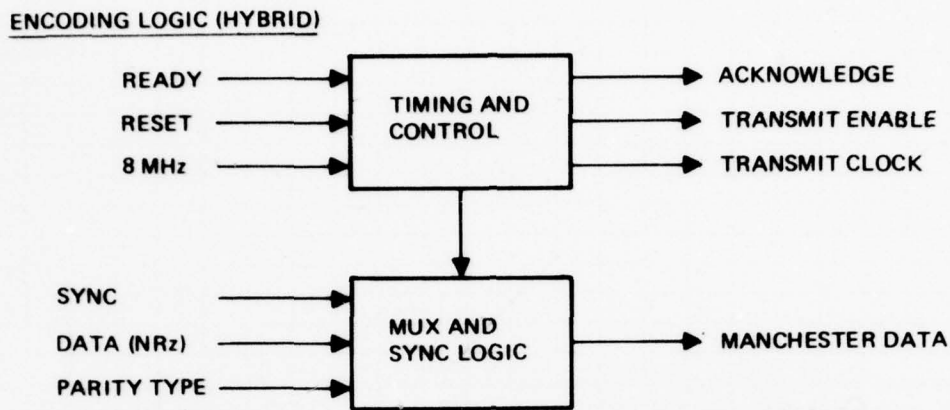


HYBRID DESCRIPTION

1. 0.75 X 1.8 IN. COMPOSITE SUBSTRATE  
0.75 X 1.5 IN. THIN FILM (1 DIODE QUAD, 15 TRANS, 3 IC, 14 CAPS, 46R)
2. 1 X 2 IN. CAN. 38 BUTTERFLY LEADS, 100 MIL CENTERS

9-38

Figure 59. Transmitter/Receiver Functional Block Diagram



**HYBRID DESCRIPTION**

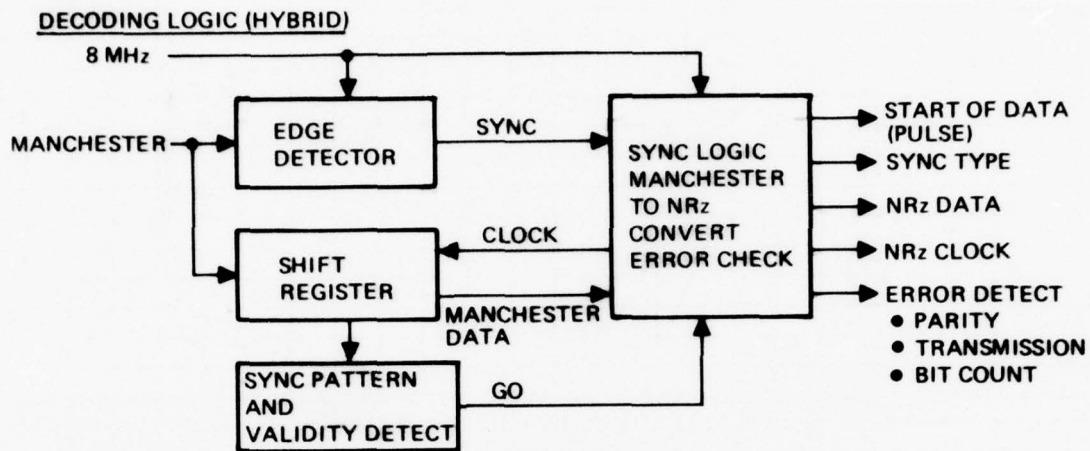
1. 0.8 X 1 IN. THICK FILM SUBSTRATE (2 LAYERS)  
18 IC, 1 RES, 1 CAP
2. 0.945 X 1.130 IN. CASE, 44 BUTTERFLY LEADS, 50 MIL CENTERS

Figure 60. Encoding Logic Functional Block Diagram

2.1.8.2.4 Decoding Logic (DL). The purpose of the DL is to synchronize the incoming Manchester data with the DTU Clock, and to initiate a receive cycle upon detection of 10 valid data samples. The sample rate on incoming data is 8 MHz. The DL continuously monitors incoming data for non-valid Manchester (transmission error), correct bit count and parity. The DL output is NRZ data and the associated one MHz Clock. A functional block diagram of the DL is shown in Figure 61. Mechanization of the DL was done primarily with low power Schottky devices. Where timing was critical, e.g., in the Manchester sampling, Schottky devices were used.

2.1.8.2.5 Subsystem Interface Unit (SSIU). The primary purpose of the SSIU is to initiate and control data transfers between the MICRON DPU and the data bus or to respond to a valid command detected on the data bus. As such, it must assimilate and transfer data in the format and timing levied by MIL STD 1553A and by the MICRON Computer I/O Circuitry. The SSIU can be divided into the following functional blocks:

1. Data Transfer Control (SSIU  $\leftrightarrow$  DPU, EL/DL  $\leftrightarrow$  SSIU)
2. Status Monitoring
3. Message Formatting and timing as a function of whether or not MICRON is the controller, and whether data are being inputted or outputted.
4. Redundancy Management.



**HYBRID DESCRIPTION**

1. 0.8 IN. X 1 IN. THICK FILM SUBSTRATE (2 LAYERS)  
21 IC, 5 RESISTORS, 1 CAPACITOR
2. 0.745 X 1.130 IN. CASE, 44 BUTTERFLY LEADS, 50 MIL CENTERS

Figure 61. Decoding Logic Functional Block Diagram

The only problem area encountered was due to lack of definition of terminal address and subaddress assignments and combinations which must be supplied by the user (system or aircraft). The problem was worked around by going to a two-tier PROM system for address decoding and indirect DPU address selection. This system will accommodate any combination of Address/Subaddress assignments simply by the reprogramming and replacement of two flat pack PROMs.

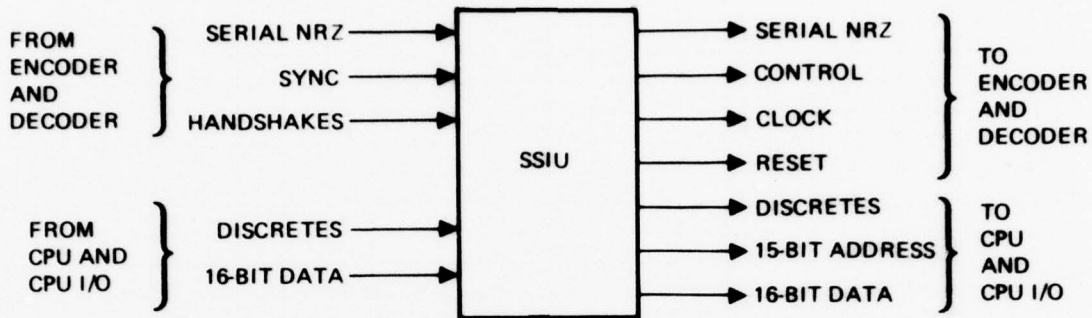
The SSIU was mechanized with T<sup>2</sup>L logic. Low Power Schottky was used whenever practical to minimize power consumption. A summary of the SSIU is presented in Figure 62.

2.1.8.2.6 DTU Assembly. The DTU circuitry is packaged on a 10-layer MLB. Photographs of the front and back sides of the module are shown in Figures 63 and 64. Two DTU modules, including one spare, were assembled and tested.

Appendix A provides information relative to the fabrication, assembly, and testing of the hybrids. Appendix E provides information relative to the tasks involved in fabrication, assembly, and test of the modules. The functional tests performed on the hybrids and modules are listed in Appendix C.

A thermal analysis was performed on the DTU which resulted in the adoption of 30 mil heat sinks. Measurements in the lab indicated a 36°C temperature rise of the T/R case without circulating cooling air and without providing a sink for the heat rails. This was done as part of an empirical thermal evaluation outside of the MICRON system.

### SUBSYSTEM INTERFACE UNIT



### HARDWARE DESCRIPTION

114 IC (MSI, SSI) FLAT PACKS  
26 RESISTORS (21 PULL-UPS, 4 TRIM, 1 PULSE SHAPING)  
45 CAPACITORS (44 DECOUPLING, 1 PULSE SHAPING)

Figure 62. SSIU Functional Block Diagram

The two Data Terminal modules were both functionally tested with special engineering test equipment to ensure compliance with MIL-STD-1553A requirements.

As a remote terminal, the module was tested for its ability to accept and properly execute command words on either channel. Also checked was its ability to reject command words with terminal addresses other than its own. As a Bus Controller, the module was tested to verify its ability to transmit command words and properly transmit and receive data words. Also verified was the DTU's ability to initiate a Terminal to Terminal transfer. This is a message in which the Data Terminal will transmit two command words, and then verify receipt of two status words. In all modes of operation the Data Terminal module performed to the specifications of MIL-STD-1553A.

Fig 63  
HIT

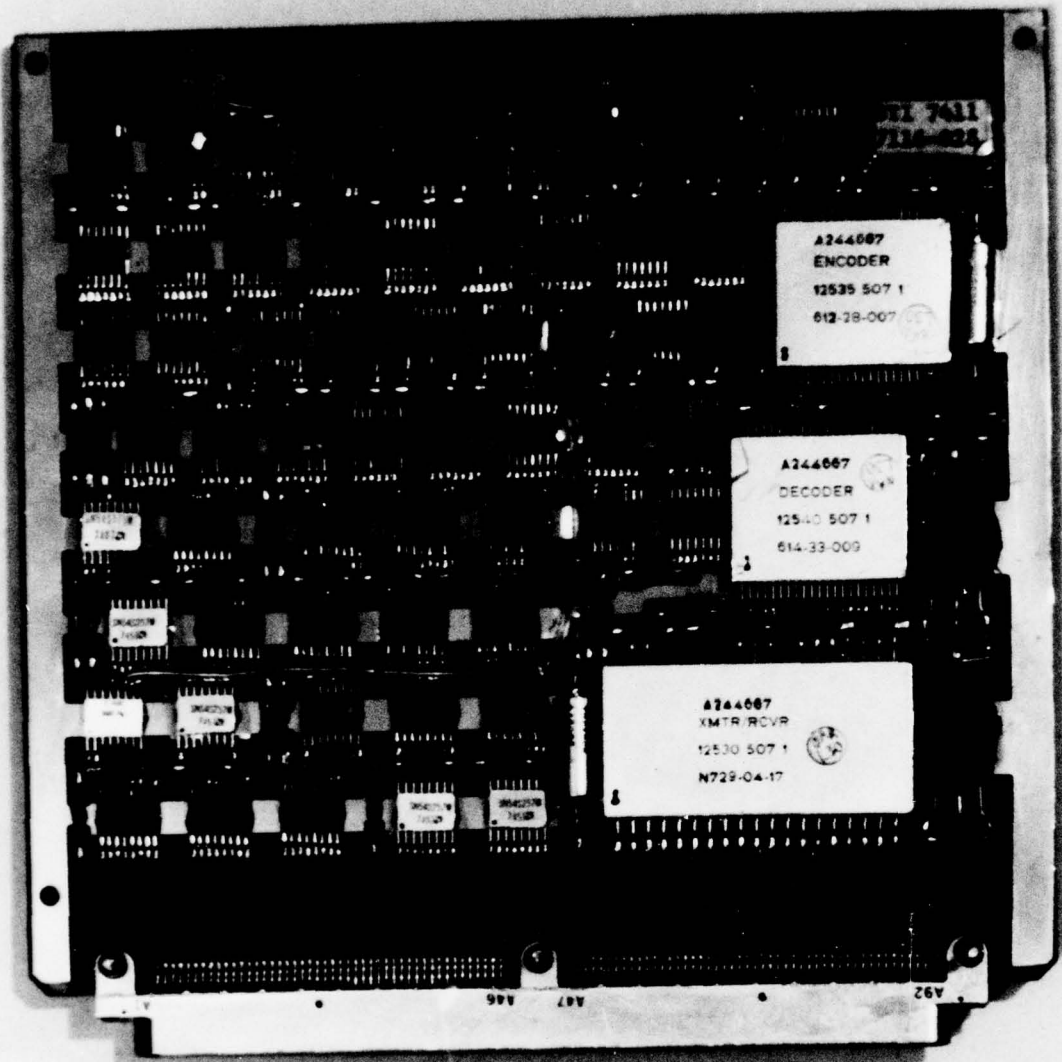
Figure 63. Data Terminal Unit (Front Side)

Figure 64. Data Terminal Unit (Back Side)

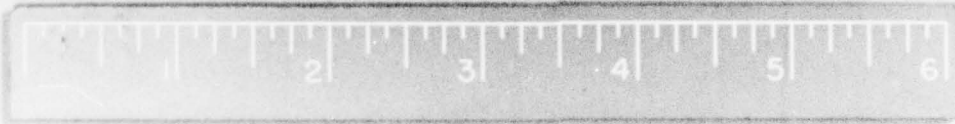
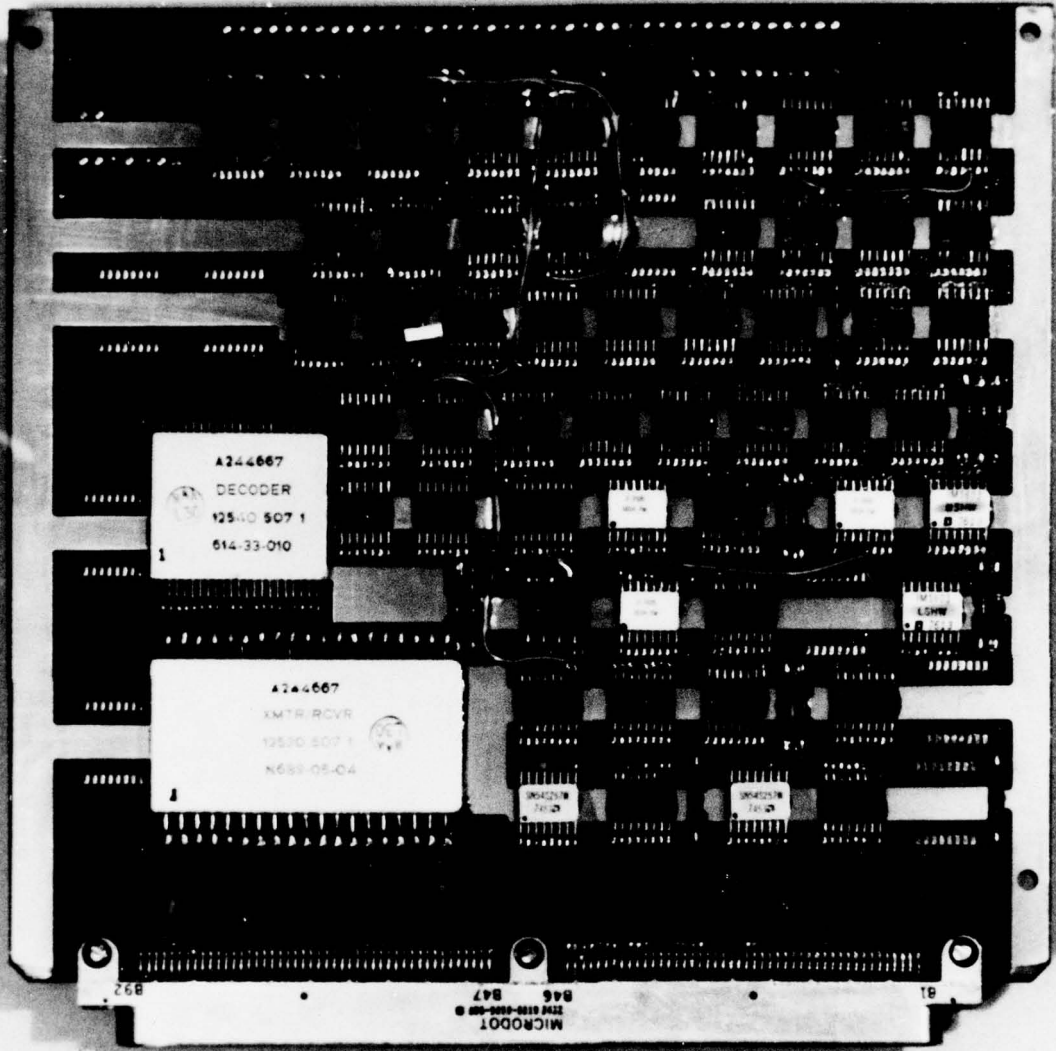
Fig 64  
HIT

Figure 64. Data Terminal Unit (Back Side)

CLASSIFICATION



NO. \_\_\_\_\_ VOL. NO. \_\_\_\_\_ FIG. NO. 63 PAGE NO. 115



4"

67

115

### 2.1.9 PSU Design/Develop/Fab/Test

During the design phase, many different power supply configurations were evaluated. Tradeoffs were conducted which included cost, size, weight, reliability and efficiency considerations. Figures 65, 66, and 67 show some of the configurations evaluated. The configuration of Figure 65 is the mechanization that was chosen for the EPM system.

The EPM Power Supply Unit (PSU) is designed to operate from 3 $\phi$ , 400 Hz, 115 volt aircraft power, as specified in MIL-STD-704A, equipment category B, or +28V battery power. Aircraft 28 VDC is also utilized for battery charging. The 3 $\phi$ , 400 Hz power input to the power supply is 310 watts nominal and 336 watts peak. The PSU also contains battery charge and test capability with automatic battery power backup in the event of a power failure. All power supply outputs are protected against a continuous short circuit on any required output. Table 24 gives a summary of all the power outputs. (The nominal power listed in Table 24 is slightly higher than the actual measured power on the system which was 310 watts. This is due to the fact that Table 24 was derived from calculations.)

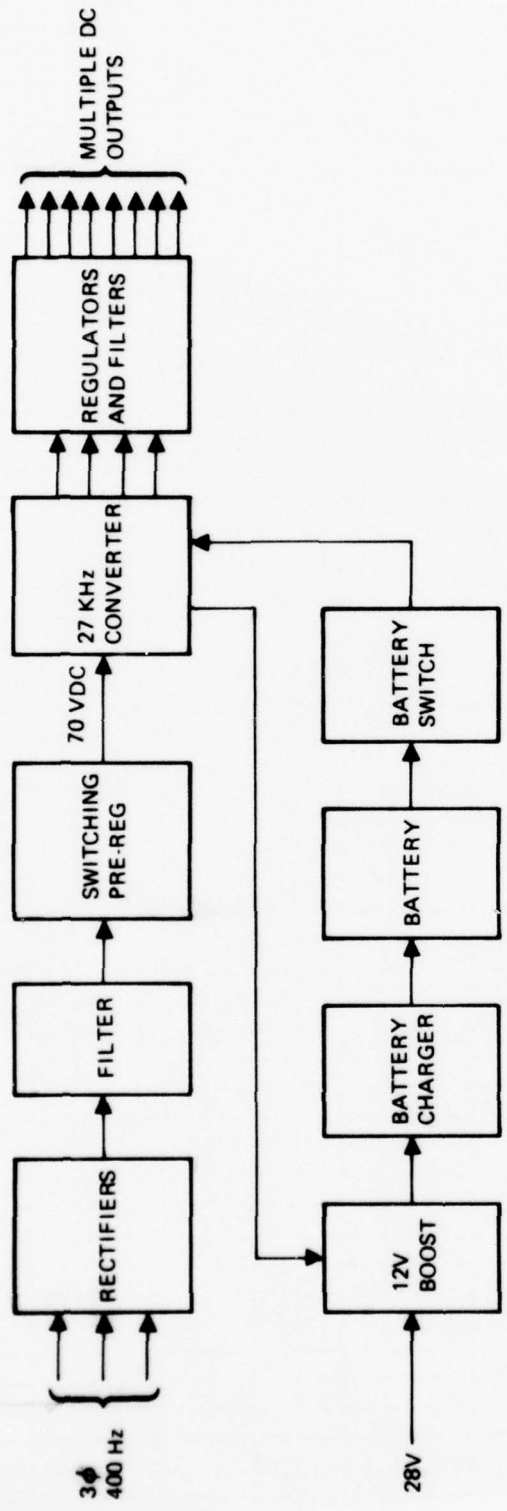
A worst case analysis was performed on all of the PSU circuits. The analysis revealed that a total of 10 components were overstressed. The design was modified to correct this condition. A subsequent analysis with the new components indicated that all of the components are now within derating requirements.

A thermal analysis was also performed on the components within the PSU. This analysis revealed that the temperature of all components was low enough to project an MTBF of 22874 hr which is in excess of the allocation for the PSU.

The PSU is packaged on four printed circuit boards; namely, Board Assembly No. 1, Board Assembly No. 2, Board Assembly No. 3, and the High Voltage Switch. All discrete components (no hybrids) are used in the PSU.

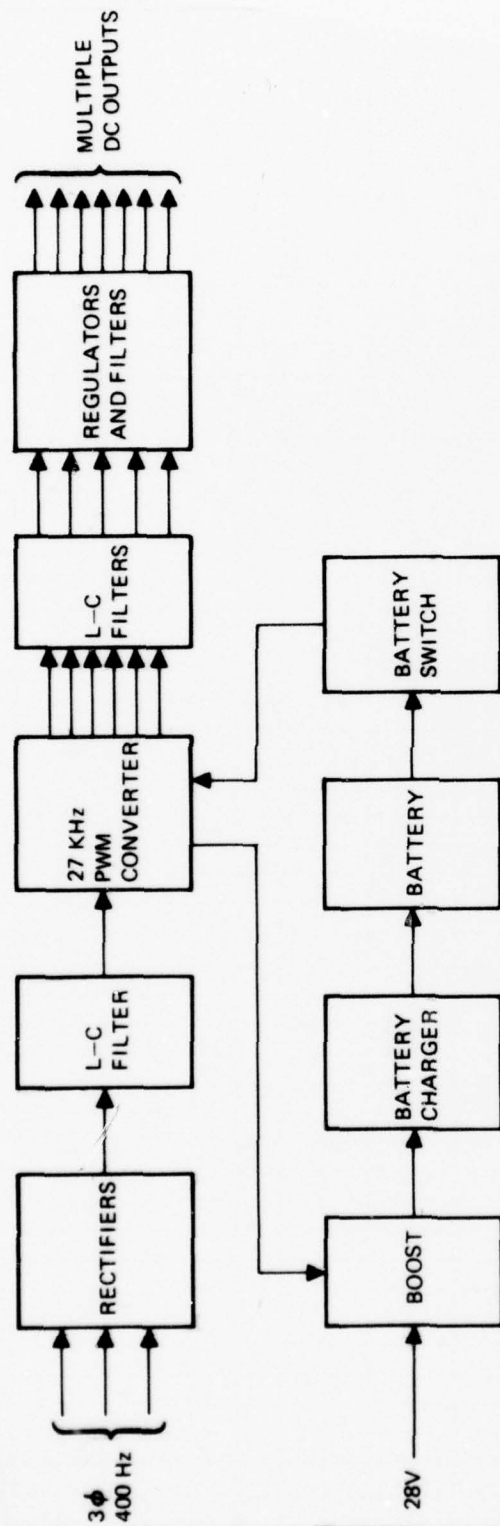
Two sets of PSU modules, including one spare set, were fabricated, assembled, and tested. A photograph of these modules is shown in Figure 68.

The functional tests performed on these modules are listed in Appendix C. The PSU met or exceeded the detail design specification requirements.



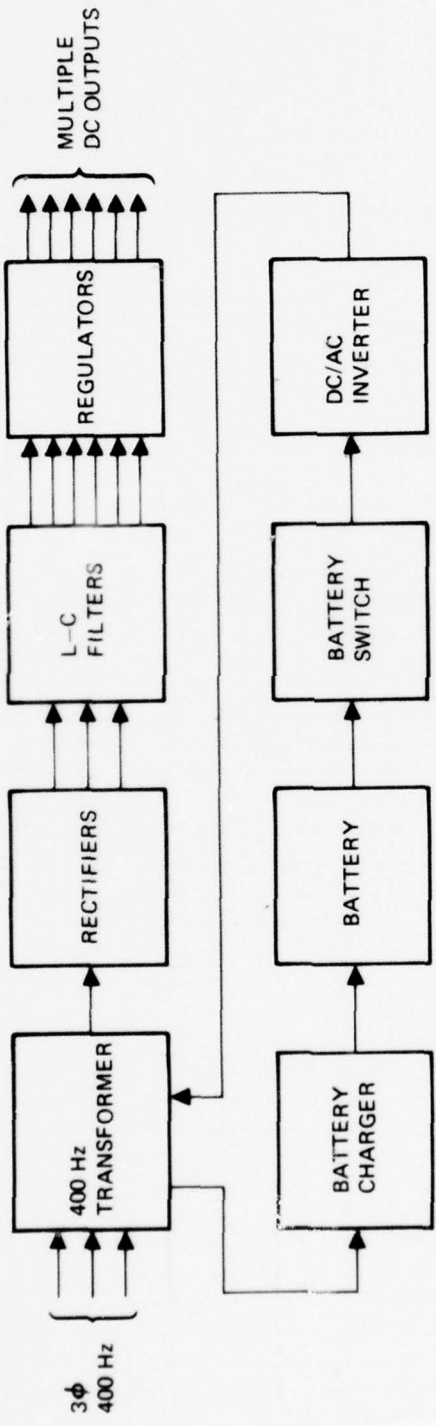
- SWITCHING PRE-REG ELIMINATES BULKY, HEAVY AND EXPENSIVE L-C FILTER
- CONVERTER VERY SIMPLE AND LOW COST. REQUIRES NO L-C FILTER FOR EACH OUTPUT SINCE EACH OUTPUT HAS VERY LITTLE RIPPLE
- TRANSFER-TO-BATTERY MECHANISM VERY SIMPLE
- CONVERTER NOISE MINIMAL

Figure 65. Functional Diagram of Power Supply Configuration Selected for EPM



- REQUIRES BULKY, HEAVY AND EXPENSIVE L-C INPUT FILTERS
- PWM REGULATED CONVERTER HAS BIG OUTPUT RIPPLE
- TRANSFER-TO-BATTERY MECHANISM COMPLEX
- CONVERTER IS NOISY DUE TO HIGH CURRENT SPIKES

Figure 66. Functional Diagram of Power Supply Configuration Evaluated for EPM



- REQUIRES FACTOR OF 2.7 WEIGHT AND 2 VOLUME INCREASE OVER OTHER CONFIGURATIONS
- L-C FILTERS MUST ALSO BE HEAVY AND VOLUMINOUS
- ADDITIONAL DC/AC CONVERTER REQUIRED TO CARRY FULL POWER FOR A LIMITED PERIOD

Figure 67. Functional Diagram of Power Supply Configuration Evaluated for EPM

Blank

Nominal Voltage	+5.2 VDC(1)	+5.2 VDC(2)	+7.5 VDC(1)	-7.5 VDC(1)	+12 VDC(1)	-12 VDC(1)	-15 VDC(2)	-15 VDC(2)	-15 VDC(1)
● Tolerance on nominal voltage	±5%	±5%	±5%	±5%	±5%	±5%	±3%	±3%	±5%
● Stability, repeatability or maximum deviation from nominal (over -40°C to +71°C temperature range, and one year time period)	±2%	±2%	±2%	±2%	±2%	±2%	±2%	±2%	±2%
● Line and load regulation (nominal load ±25%)	±2%	±2%	±2%	±2%	±2%	±2%	±2%	±2%	±2%
● Maximum ripple & noise (MV P-P)	200	200	200	200	500	500	500	500	500
● Maximum AC ripple (MV P-P)									
1200 to 2800 Hz	10	10	10	10	20	20	20	20	20
7kHz to 13kHz	20	20	20	20	50	50	50	50	50
● Maximum source impedance 14 ohms (DC to 20kHz)	0.1	0.1	0.1	0.1	0.2	0.2	0.3	0.3	0.3
● Response time	10μs	10μs	10μs	10μs	10μs	10μs	10μs	10μs	10μs
● Nominal power required (watts)	20	28	4	5	19	6	21	15	2

15 VDC(2)	-15 VDC(1)	-15 VDC(1)	-24 VDC(1)	+24 VDC(1)	-24 VDC(1)	+24 VDC(1)	-24 VDC(1)	26 VAC 400 Hz(3)	+28 VDC(3)
3%	±5%	Unregulated Output	±5%	Unregulated Output	Unregulated Output	Unregulated Floating Output	Unregulated Floating Output	26 VAC 400 Hz Aircraft	Aircraft 28 volt Bus
2%	±2%	(This output shall provide 97 watts for rotor break- ing purposes in the emer- gency shut down mode i.e., 30, 400 Hz input power failure. The duration 128 sec.)	±2%	Current design con- figuration requires 17W peak. Provisions exist to add addi- tional circuitry. If all of that circuitry is added to max of 28 watts will be required	Current design con- figuration requires 11 watts. Provisions exist to add addi- tional circuitry. If all of that circuitry is added to max of 22 watts will be required	Current design con- figuration requires zero watts. Provisions exist to add addi- tional circuitry. If all of that circuitry is added to max of 7.2 watts will be required	Current design con- figuration requires zero watts. Provisions exist to add addi- tional circuitry. If all of that circuitry is added to max of 7.2 watts	Bus power for EPM con- verter module synchro reference generator	Power for EPM power control relay operation, connector module generator of "ATT good" & "HDG bad" discretes and fast/trickle change of the EPM battery
2%	±2%		±2%						
500	500		500						
20	20		25						
50	50		50						
0.3	0.3		0.3						
10μs	10μs		10μs						
15	2	3 (Once per turn on pulse time dura- tion 2 sec.)	6	22 [18] [14.4] *(11) (17 watts peak) 28w peak	22 [18] [14.4] *(11)	0 [3.6] [7.2] *(0)	0 [3.6] [7.2] *(0)	0.5	18 (68 watts peak for ≤ 30 min.)

TABLE 24. POWER

-24 VDC(1)	26 VAC 400 Hz(3)	+28 VDC(3)	+35 VDC(4)	-35 VDC(4)	115 VAC, 3 Phase 400 Hz (3)	High Voltage (5)					
						ØA1	ØA1	ØB1	ØB1	ØA2	ØA2
Unregulated loading	26 VAC 400 Hz Aircraft	Aircraft 28 volt Bus	Unregulated Output	Unregulated Output	Aircraft 3Ø 400 Hz Bus Power:	±5%	±5%	±5%	±5%	±5%	±5%
Output	Bus power for EPM con- verter module synchro reference generator	Power for EPM power control relay operation, connector module generator of "ATT good" & "HDG bad" discreet and fast/trickle change of the EPM battery	Provides power for spin motors & control heaters	Provides power for spin motors & control heaters		±2%	±2%	±2%	±2%	±2%	±2%
Current design con- figuration requires provisions exist to add addi- tional circuitry. all of that circuitry is added to max of 7.2 amps						5V	5V	5V	5V	5V	5V
						(6)	(6)	(6)	(6)	(6)	(6)
						(6)	(6)	(6)	(6)	(6)	(6)
	0.5	18 (68 watts peak for ≤ 30 min.)	35 (200w peak for 2 min max.)	35 (210w peak for 21 min max.)	382 watts (2462 watts peak for 2 minute maximum *(342 watts current config)	<div style="border-top: 1px solid black; width: 100%; margin-bottom: 5px;"></div> (10 watts peak)					(10)

13

TABLE 24. POWER CHARACTERISTICS AND CONSUMPTIONS

35 V(4)	-35 VDC(4)	115 VAC, 3 Phase 400 Hz (3)	High Voltage (5)								Notes
			$\overline{\phi A1}$	$\overline{\phi A1}$	$\overline{\phi B1}$	$\overline{\phi B1}$	$\overline{\phi A2}$	$\overline{\phi A2}$	$\overline{\phi B2}$	$\overline{\phi B2}$	
Unregulated Output	Provides power for spin motors & control heaters	Aircraft 3 $\phi$ 400 Hz Bus Power:	$\pm 5\%$	$\pm 5\%$	$\pm 5\%$	$\pm 5\%$	$\pm 5\%$	$\pm 5\%$	$\pm 5\%$	$\pm 5\%$	(1) Output is always present when EPM is "on".
			$\pm 2\%$	$\pm 2\%$	$\pm 2\%$	$\pm 2\%$	$\pm 2\%$	$\pm 2\%$	$\pm 2\%$	$\pm 2\%$	(2) Output turned off under computer control during shutdown sequence when aircraft 3 $\phi$ power is not available and EPM is on the battery power source.
			$\pm 2\%$	$\pm 2\%$	$\pm 2\%$	$\pm 2\%$	$\pm 2\%$	$\pm 2\%$	$\pm 2\%$	$\pm 2\%$	(3) MIL-STD-704A, category E aircraft bus power
			5V	5V	5V	5V	5V	5V	5V	5V	(4) This output derived from a transformer/rectifier located external to the EPM PSU but internal to the EPM MHU.
			(6)	(6)	(6)	(6)	(6)	(6)	(6)	(6)	(5) These outputs "on" under computer control and "off" under computer or sequenc control
			(6)	(6)	(6)	(6)	(6)	(6)	(6)	(6)	(6) Reference figures & for voltage and waveform characteristics.
35 (210w peak for 21 min max.)		382 watts (2462 watts peak for 2 minute maximum *(342 watts current config)	6 (10 watts peak)				6 (10 watts peak)				[ ] = Power requirements of possible design configurations. *( ) = Current configuration power requirement.

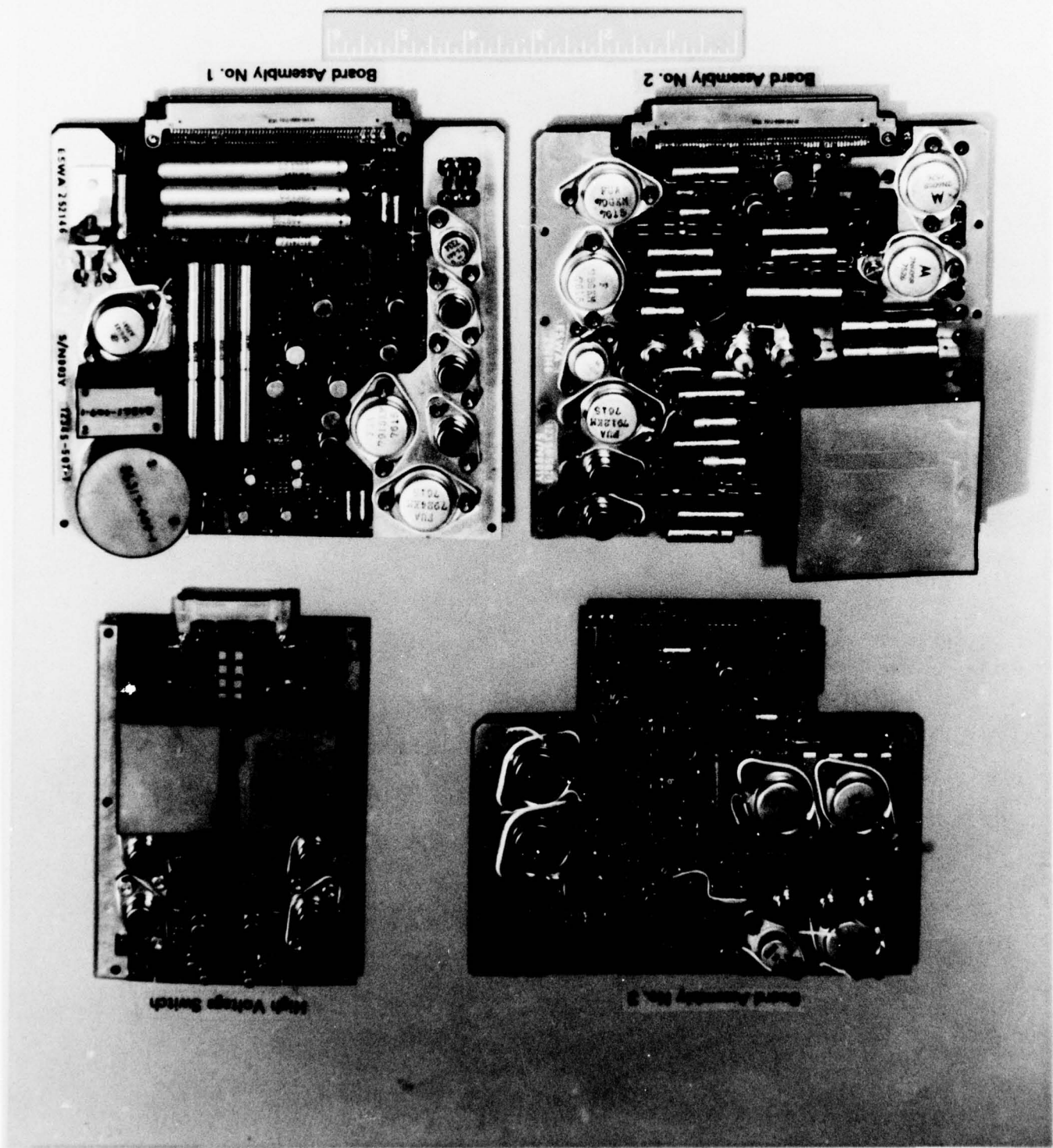
4

HIT

Figure 68. EPM Power Supply Unit

CLASSIFICATION

36



21

62

#### 2.1.10 Fabrication of MESSAGES for Second Source

The purposes of this task were to (1) fabricate four MESSAGES (without rotors or cavities) to support the second source and non-destructible gyro efforts, (2) fabricate eight cavity sets with the following characteristics; ground to final size, unplated, suitable for plating, lapping, and finishing by CSDL (small cracks were allowable so long as they would not interfere with CSDL's lapping and plating procedures), and (3) fabricate 12 rotors and six cavity sets. The last set of 12 were finished, inertial grade and had the proper radial mass unbalance. The six cavity sets were inertial grade (no cracks), ground to final size, unplated, suitable for plating, lapping, and finishing by CSDL.

All of the above activity was completed on schedule. Activity related to the use of the four MESSAGES in the testing of second source assets and non-destructible rotors and cavities is discussed under Task 2.2, Developmental Test, Section 3.2. Additional second-source and non-destructible gyro activities are discussed in Section 6.2, (Task 5.2, Associate Contractors Support).

#### 2.2 TASK 1.2, INERTIAL NAVIGATION BATTERY UNIT (INBU)

The purposes of this task were to develop a detail design specification for the INU mount and to fabricate/procure the mount and spares.

##### 2.2.1 Detail Design Specification for Mount

The detail design specification for the INBU mount (AJ00092) was completed and issued 18 November 1975. This specification established the functional, performance, design configuration, and development requirements for the INBU Mount.

##### 2.2.2 Fab/Procure Mount

The Inertial Navigation Battery Unit (INBU) design was an evolution based on iterative inputs from the Standard Navigator's Appendix V. Fabrication of the INBU began in April 1976 and was completed in May. Assembly of the INBU began in May and was completed in June 1976.

The battery unit is supplied with the INBU. The battery is a 22-cell design of 1.8 amp/hours for lab testing. The battery unit was completed in May 1976.

The INBU, along with the battery unit, was delivered to the integration lab in June 1976. This activity completed Task 1.2.

#### 2.3 TASK 1.3, CONTROL/NAVIGATION PANEL (CNP)

The purposes of this task were to design/modify the N57A CDU to interface with the EPM and fabricate/procure spares as necessary.

The CNP is composed of a N57A CDU and a CDU/Memory Adapter (Figure 69). The CDU initiates power on/off and provides data display, data insertion and mode switching for the INU. The CDU/Memory Adapter provides the interface from the MICRON computer to the CDU. It also provides for interfacing data to/from the Test Station calibration computer (HP2100S) and to a strip printer. A 16 K word core

memory is contained within the Adapter which served as the EPM's main memory during software development for the ROMs on the semiconductor memory part of the DPU.

No modifications to the N57A CDU were required for it to meet its function. All interfacing and buffering was accomplished within the Adapter. Figure 69 is a block diagram of the Adapter. The unit is composed of the following items:

1. One I/O Module
2. One CNP/EPM Support Module
3. One SEMS-9P core memory
4. One Power Supply
5. Housing

The I/O module was designed/developed on the N77 INS program. It is a five layer printed circuit board (PCB) containing various types of integrated circuits. One I/O module was fabricated, assembled, and tested.

The CNP/EPM Support Module is multi-purpose, but its main function is to buffer the Memory output lines from the core memory, buffer the status discretes from the adapter to the EPM, and synchronize the power on/off of the Adapter with the EPM. It is a three layer PCB. Two CNP/EPM Support Modules (one spare) were fabricated, assembled, and tested.

The SEMS-9P is a 16 bit x 16,384 (16K) word core memory purchased from Electronic Memories. It has a one microsecond cycle time, and allows operating the EPM with similar timing requirements as the final Semiconductor memory. One memory was purchased.

The Power Supply generates all the secondary voltages required for the Adapter and the CDU. It also contains the relays to control power for the Adapter, CDU, and EPM. One Power Supply with spare parts was fabricated.

The Housing is the chassis that physically supports the modules, memory, and power supply. A fan is mounted at one end for cooling the electronics. One housing was designed and fabricated, wired and continuity tested.

Complete checkout of the CDU/Memory Adapter was accomplished in May 1976 and the unit was delivered to the integration lab. This activity completed Task 1.3.

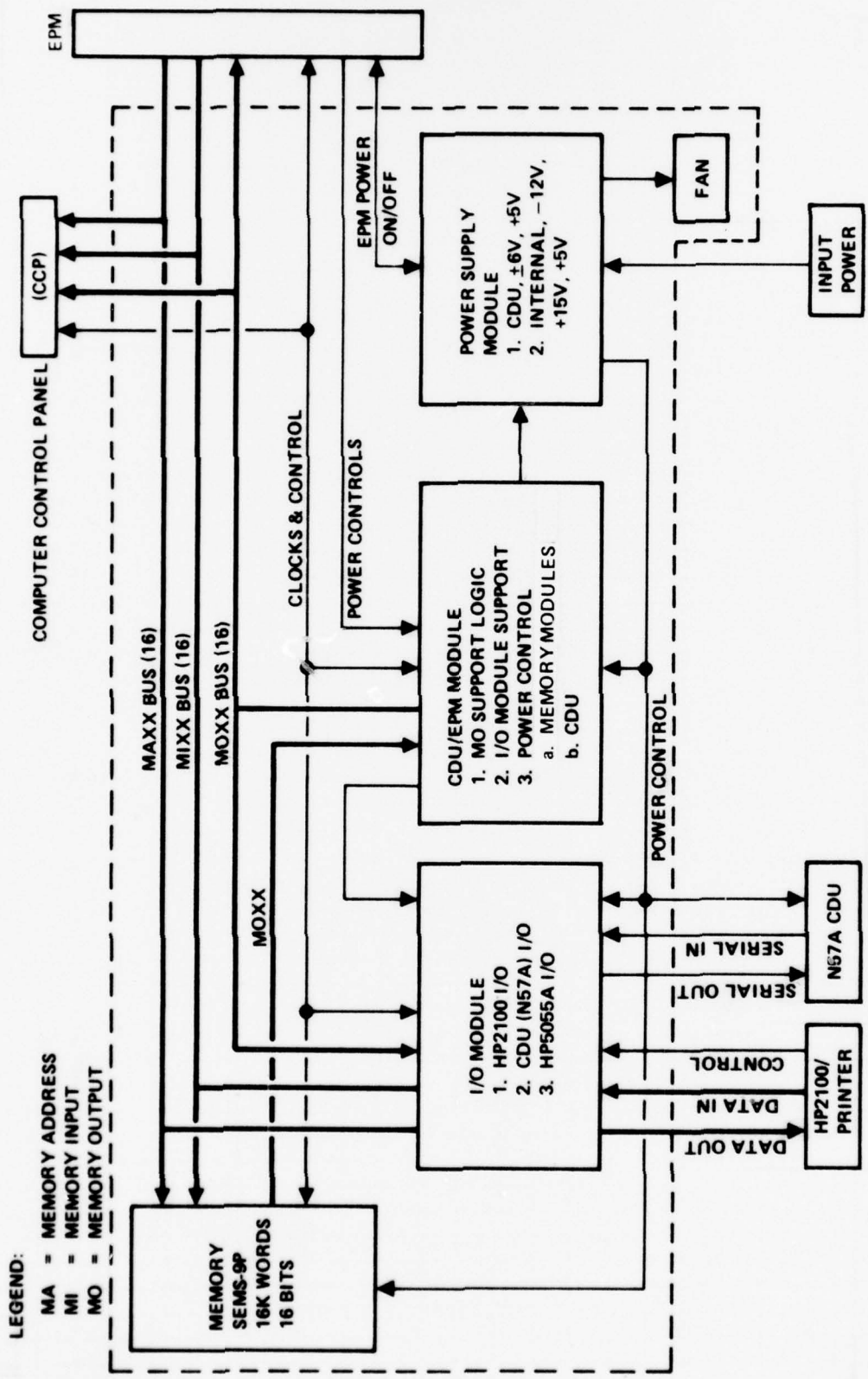


Figure 69. CDU/Memory Adapter

## 2.4 TASK 1.4, SOFTWARE

The purposes of this task were to develop INU and test station software. The task to conduct data analysis on the EPM system was deleted from the contract per Ref 5.

### 2.4.1 INU Software

#### 2.4.1.1 Background

The software for autonomous operation of the INU is implemented in the MICRON DPU. The DPU is an integral part of the INU. It is a low-weight, low-power, low-cost dedicated processor with 372 basic machine instructions, including fast double-precision instructions that were specifically designed for MICRON requirements. The operational memory for the DPU is designed to be mostly read-only memory (for fixed program) to minimize system life-cycle costs. However, an auxiliary external core memory was used for program development and verification. The program structure has been defined such that when it has been verified in the field, it can then be converted into fixed read-only memory. For the meantime, the core memory allocation has been partitioned so that the variable part of memory has the identical address range of the read/write section of memory in the eventual DPU memory, and only fixed information occupies the address range of the read-only memory.

The Phase 2B program benefitted from the development of programs for the N77 system with a MICRON DPU which preceded the development INU software. By imposing the same memory constraints on the N77 software, it was possible to structure these programs in such a way that they were similar to the corresponding EPM programs, and made the software development task somewhat easier. The interface hardware and functional requirements were sufficiently different between N77 and the INU that the programs could not be made identical. However, the fundamental modes of operation and the assembly language were identical, and this was beneficial to INU software development.

During the first part of Phase 2B (through May 1976), the definition of INU program requirements was finalized. From April through August of 1976, the Fast Cycle, Start, and Cal Data Collect program segments were coded and partially checked out. Coding was done in the GAP/MICRON assembler language, and the software previously developed for the N77 system was used as a baseline in order to minimize effort. Checkout was accomplished primarily by using the DEBUG and Simulator programs as real-time software checkout tools.

In parallel with the effort described above, a new assembler and associated support software were developed and verified. The new assembler (the MICRON Macro Assembler) improves coding efficiency by reducing the number of OP code mnemonics by a factor of four, and provides the capability of assembling the program as a series of relocatable object segments which can be link-loaded to form the executable program. Coding of the Align and Nav program segments was done in the MICRON Macro Assembler language beginning in July 1976. Due to the complexity of the Align and Nav computations, the first stage of checkout was performed by using several independently-coded HP2100 check problem programs for comparison of step-by-step results. Then simulator runs were used for dynamic checkout and evaluations of mechanization design improvements. This checkout procedure was quite successful as few software problems were encountered during subsequent software integration and alignment and navigational runs with the integrated system.

The support software developed with the new assembler includes a translator program which converts a source program from the old assembler language to the new assembler language. This program is used to translate that portion of the INU software coded in the old assembler language into the MICRON Macro Assembler language.

INU software development was aided considerably through the development and use of several support programs which make use of the HP2100/MICRON interface. Notably, these programs include DEBUG, LOADM, and SAVEM. A version of DEBUG has been developed in which control is exercised through the HP2100 CRT console to display and change MICRON memory locations, set program traps, and start the program counter at any selected location while the MICRON DPU is in the run mode. The LOADM program provides the capability of loading an object program module from an HP2100 disc data file into the DPU memory. With the SAVEM program, the entire 16K MICRON memory can be stored in an HP2100 disc data file. Together, LOADM and SAVEM provide the capability of rapidly overlaying program object segments and then creating and saving a single program load module from which a tape can be punched, if desired. All software which makes use of the HP2100/MICRON interface incorporates a checksum feature to verify accurate data transmission.

The INU software has been designed according to the requirements in the INU CI specification. All software functional requirements have been checked out and verified in system integration testing with the exceptions of synchro analog outputs, digital data bus outputs at fast cycle rate, position update via data bus, and data bus control. The integration testing of these functions was deleted from the integration test plan at the request of the customer. All INU software necessary to support the current testing has been checked out.

#### 2.4.1.2 Description

The EPM computer program, which controls the INU during all modes, is described in this section. The description includes program mode control, program structure (executive and I/O), background, major subroutines, simulator, and utility subroutines. Detailed flow charts and tables of program constants and variables are included in Appendices G through L.

2.4.1.2.1 Program Mode Control. The program is controlled through the Control/Navigation Panel, which currently consists of a modified N57A CDU. There are three basic program modes: "Start," "Align and Navigate," and "Calibration Data Collect." The latter mode is used only in a test station environment with an HP2100 Data Acquisition System interface.

If automatic sequencing is selected by the operator (the "normal" operational case), the program sequences through the various sub-modes of the START program, through the selected alignment mode, and into the navigate mode. The operator is given indications of progress and BITE status, according to the selected display mode, via the CDU. The NAV READY indicator is illuminated when the sequence is completed.

The program also has the capability of manual mode sequencing in any order commanded by the operator. Manual mode control is provided primarily for test purposes. The computer also has an interface to a line printer for test data collection. Tables 25 through 38 define program mode control, program commands, printer control, CDU displays, discrete assignments, and interrupt assignments.

2.4.1.2.2 Program Structure. Program executive control is contained in the fast cycle routine, which is interrupt-driven at a 64 Hz rate. The fast cycle is structured around the SEU I/O by means of three interrupts: 64 Hz, ENDMUC, and CMPLTC. A timing diagram depicting this structure is shown in Figure 70.

Major functions performed by the fast cycle routine are listed below:

1. Program Controlled I/O, including discrettes
2. Accelerometer compensation
3. Velocity accumulation, spin axis coordinates
4. Partial angle compensation
5. Certain BITE tests
6. Demod frequency control
7. Spin motor commands (damp mode only)
8. Normalize spin vectors
9. Thermal control

Fast cycle detailed flow charts are presented in Appendix G.

The program controlled I/O includes the CDU, printer and HP2100. The HP output and printer output share a common channel. Only one of the devices can be connected and operated at one time. The fast cycle time shares HP input, HP output, printer output, and CDU input/output so only one function is performed each 1/64 sec. HP input, HP output and printer output are only performed when requested by another program module. Printer output can only be executed at a maximum of 8 times/sec. HP input or output is executed whenever data block length words HPIN or HPOUT are nonzero. If the input or output is successful word HPIN or HPOUT is set zero. If it is not successful (probably due to insufficient time) the word HPIN or HPOUT will be left nonzero and the transmission will be initiated from the beginning on the next cycle. A BITE flag is set whenever an I/O function is not completed.

#### 2.4.1.2.3 Background Program

2.4.1.2.3.1 Organization. Background is initially entered from the computer reset. It performs a first time initialization followed by common initialization and then enters the normal background loop. The background loop is executed once per second. After common initialization is completed the interrupts are enabled which allows the 64 Hz interrupt to initiate the fast cycle. Common initialization is re-entered when transferring to either the navigation or cal data collection program modules.

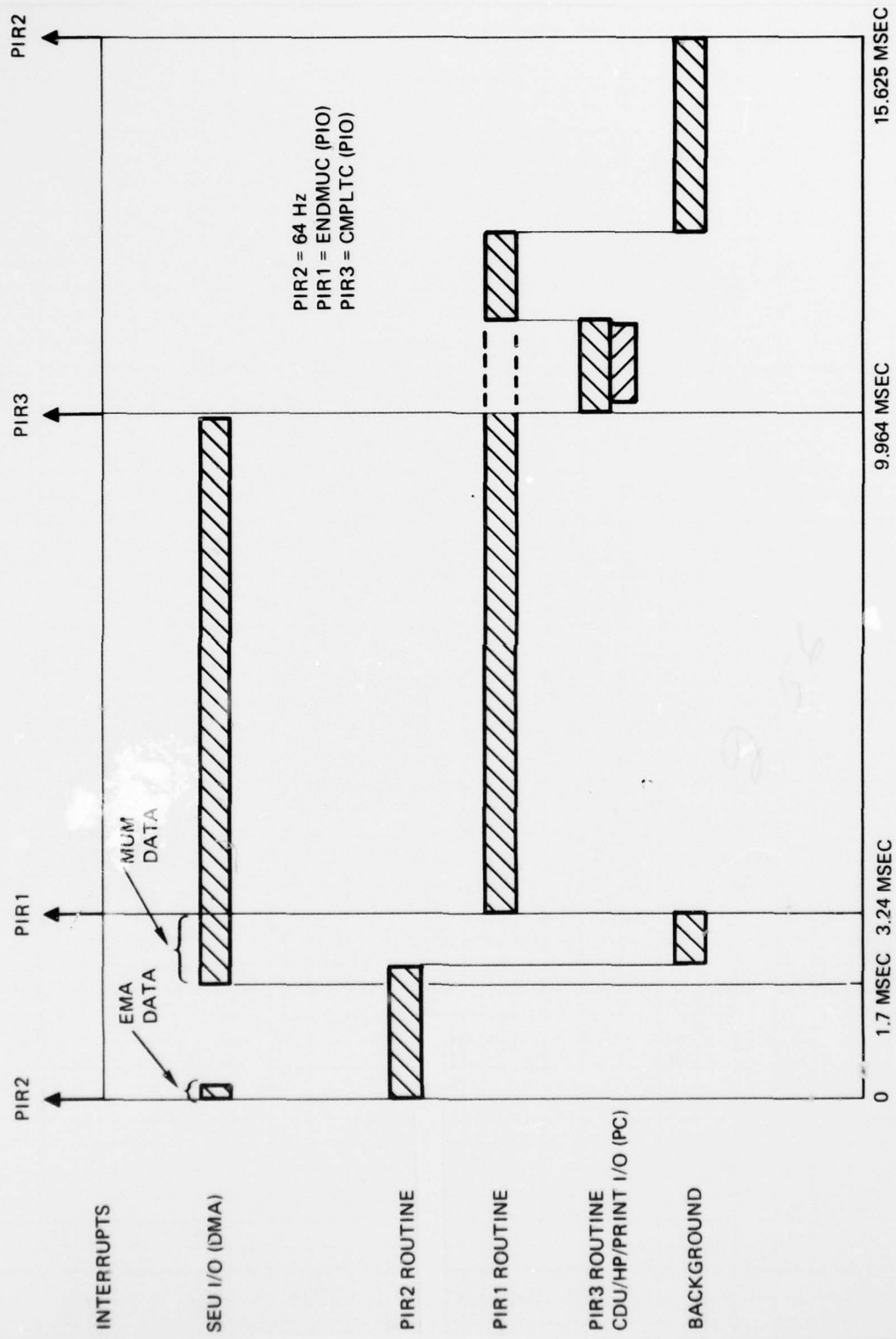


Figure 70. EPM Fast Cycle - Normal Structure

The major functions performed in background include data processing for control/display panel, scheduling of printer lists, BITE testing, and background computations for nav, start, and cal data collection program modules. Background also schedules the Simulator program when in the simulation mode (no external interrupts).

The CDU display provides the data specified by the data select switch when in align or navigate modes. In all other modes temperature, gap, and rotor speed is output on the display. Table 29 gives the correspondence between data displayed and data select position. When "press to test" is on all lights on the CDU are lit. If "press to test" is on while the hold switch is on, all BITE's are cleared. Eight words are output on the BITE display. The BITE display is sequenced by pressing the "press to test switch." If any BITE is set, the BITE flag is latched on. If all BITE's are zero the BITE flag is latched off. Keyboard inputs are determined by position of the data select switch and the first BCD character of the input word. Latitude, longitude, heading, and altitude are input. Also program commands are entered when the data select switch is in MODE STATUS position.

The program commands are given in Tables 25 and 26. Start mode commands are prefixed by S, Nav mode commands are prefixed by N, and printer commands are prefixed by E. Start mode commands initialize the mode word, TCI. TCI values are given in Table 28. The mode status display is a compacted word defining program mode. The display code is defined in Table 30. Discrete and interrupt assignments are defined in Tables 31-38. Background performs those BITE tests not performed elsewhere in the program. Background detailed flow charts and definition of all BITE tests are presented in Appendix H.

2.4.1.2.3.2 Computations. The navigation background computes velocity change magnitude over 1 sec intervals. The value of gravity is computed based on altitude and earth ellipticity. ALPHA, the clockwise angle from the "platform" axis (defined by software only) to the true north, is computed in background during alignment only. This is used to provide an azimuth response display during alignment and has no impact on the navigation function.

In the calibrate data collection mode, the demod control routine cannot use  $Y_1 \times Y_2$  as the phase reference vector because  $Y_1$  and  $Y_2$  may be colinear. A quasi inertial reference set ( $R_i, RQ_i, Y_i$ ) is computed to provide the phase reference where

$$RQ_i = Y_i \times \begin{pmatrix} 0 \\ 0 \\ 1 \end{pmatrix} \Big/ \left| Y_i \times \begin{pmatrix} 0 \\ 0 \\ 1 \end{pmatrix} \right|$$

$$R_i = RQ_i \times Y_i$$

if  $Y_i$  is not very close to the z axis. If  $Y_i$  is very close to the z axis an alternate equation is used

TABLE 25. PROGRAM MODE CONTROL

Function	CDU SYSTEM Mode Switch	CDU Keyboard Input	CDU DATA SELECT Switch (During Keyboard in)	MODE STATUS Display	Mode Light	Notes
Reset	CAL	None	Any	N00000 or S00000	STBY	
Auto Start	ALIGN or NAV	None	Any	SXX0KK (KK = 01 - 15)	STBY	Gyros initially desuspended
Manual Start Mode No. KK	STBY	S0000KK	MODE STATUS	SXX0KK	STBY	
Auto Start from Mode No. KK	STBY	S1000KK	MODE STATUS	SXX0LL (LL = KK - 15)	STBY	
Abort any Start Mode	STBY	S000000 or S100000	MODE STATUS	S00000	STBY	
Stored Heading Align	1. STBY 2. ALIGN	N000002 None	MODE STATUS None	N00000 N00001	STBY CAL/ ALIGN flash	Key-in is latched until G/C is commanded
Gyrocompass Align	1. STBY 2. ALIGN	N000003 None	MODE STATUS None	N00000 N00002	STBY ALIGN/ ALIGN flash	Pgm load initializes to G/C. No key-in required unless stored heading is commanded
Nav	NAV	None	Any	N00003	NAV	
Cal Data Collect mode	STBY	N000000	MODE STATUS	+/- (NGP + NEP)	CAL	Key-in is latched until Nav mode is commanded.

TABLE 25. (Cont)

Function	CDU SYSTEM MODE Switch	CDU Keyboard Input	CDU DATA SELECT Switch (During Keyboard in)	MODE STATUS Display	Mode Light	Notes
Nav mode (Exit Cal Data Collect)	STBY	N000001	MODE STATUS	N00000	STBY	Pgm load initializes to nav mode. No key in required unless Cal is commanded.

TABLE 26. PROGRAM COMMANDS

Command	Program Mode	CDU Keyboard Input	CDU DATA SELECT Switch (during keyboard in)	Notes
Initialize latitude	Start or Nav Stby	(N/S)xxx°xx.x'	LAT, LONG	
Initialize longitude	Start or Nav Stby	(E/W)xxx°xx.x'	LAT, LONG	
Initialize heading	Start or Nav Stby	(+)xxx°xx.x'	GS, HDG	
Initialize altimeter	Start or Nav Stby	(+)xxxxx.x	V. VEL, ALT	
Manual charge monitor	Start	S000016	MODE STATUS	For nonspinning rotors only!
Unscheduled charge monitor	Nav mode	N000004	MODE STATUS	For spinning rotors only
Low gain offset filter	Nav mode	N000005	MODE STATUS	Initialized low gain at start of align
High gain offset filter	Nav mode	N000006	MODE STATUS	Use in STBY only
No gyros operating	Any	N000007	MODE STATUS	
Gyro 1 operating	Any	N000008	MODE STATUS	
Gyro 2 operating	Any	N000009	MODE STATUS	
Both gyros operating	Any	N000010	MODE STATUS	Initialized at pgm load

TABLE 27. PRINTER CONTROL  
(CDU DATA SELECT = MODE STATUS)

Printer Command	CDU Keyboard Input	Notes
Print Gap list	E000001	Automatically printed in START every 30 sec in STBY every 10 min
Print Align list	E000002	Automatically printed in ALIGN every 2 min
Print Nav list	E000003	Automatically printed in NAV every 5 min
Print BITE list	E000004	Automatically printed after BITE failure
Print Rotor charge list	E000005	Automatically printed after charge monitor
Temperature list	E000006	

TABLE 28. START MODE COMMANDS

Mode Number (TCI)	Description
0	Abort current START mode
1	System checks
2	Z coil heat
3	Suspend
4	Charge monitor
5	Suspended Z coil heat
6	Low frequency degauss
7	Spin gyro 1
8	Damp gyro 1
9	Final spin gyro 1 (NA*)
10	Spin gyro 2
11	Damp gyro 2
12	Final spin gyro 2 (NA)
13	Temperature stabilization
14	High frequency degauss
15	Standby
16	Manual charge monitor
17	Desuspend
18	Manual de-spin (NA)

\*NA = Not currently available

TABLE 29. CDU DISPLAY DURING START, NAV STANDBY, AND CAL DATA COLLECTION

CDU DATA SELECT Switch	Left Display	Right Display
LAT, LONG	Latitude (deg, min)	Longitude (deg, min)
GS, HDG	Gyro 1 case temp (°F)	Heading (deg, min)
V. VEL, ALT	Gyro 2 case temp (°F)	Altitude (ft)
N/S VEL, E/W VEL	Gyro 1 gap (μin)	Gyro 2 gap (μin)
PITCH, ROLL	Gyro 1 demod freq (Hz)	Gyro 2 demod freq (Hz)
MODE STATUS	Mode	BITE/SSTAT
PITCH, ROLL (NAV MODE)	Checkpoint latitude	Checkpoint longitude

TABLE 30. CDU MODE STATUS DISPLAY

Display	Mode
S00000	Start idle mode
S000KK	Start mode no. KK
SYZ0KK	Start damp mode (If KK = 08, 11: Y = IFAM, Z = NMIN)
N00000	Nav standby
N00001	Stored heading align
N00002	Gyro compass align
N00003	Navigation
(+/-) xxoyy	Cal Data Collection
	+ = cal data collection
	- = raw data collection
	xx = No. gyro points to be taken
	yy = No. EMA points to be taken

TABLE 31. PDO DISCRETE OUTPUT (OM COMMANDS)

0	1	2	3	4	5	6	7	8	9	10	11	12	13	14	15
1															
1															
	1														
		1													
			1												
				1											
					1										
						1									
							1								
								1							
									1						
										1					
											1				
												1			
													1		
														1	
															1

TABLE 32. RDO DISCRETE OUTPUT (WDO COMMAND WITH PDO ENABLE)

0	1	2	3	4	5	6	7	8	9	10	11	12	13	14	15
1															
	1														
		1													
			1												

TABLE 33. SDO DISCRETE OUTPUT (WDO COMMAND WITH PDO ENABLE)

0	1	2	3	4	5	6	7	8	9	10	11	12	13	14	15
1															
1															
	1														
		1													
			1												
				1											
					1										
						1									
							1								
								1							
									1						
										1					
											1				
												1			
													1		
														1	
															1

TABLE 34. MDO DISCRETE OUTPUT (I/O WORD 114)

0	1	2	3	4	5	6	7	8	9	10	11	12	13	14	15
1															
	1														
		1													
			1												
				1											
					1										
						1									
							1								
								1							
									1						
										1					
											1				
												1			
													1		
														1	
															1

TABLE 35. TDO DISCRETE OUTPUT (I/O WORD 17)

0	1	2	3	4	5	6	7	8	9	10	11	12	13	14	15
1															
	1														
		1													
			1												
				1											
					1										
						1									
							1								
								1							
									1						
										1					
											1				
												1			
													1		
														1	
															1

TABLE 36. DISCRETE INPUTS

Discrete Number	Title	Logic Definition (Referenced to Software)
DI00	PC Shutdown	Logic 1 indicates INU shutdown has been commanded with the CDU mode control switch and the INU sequencer has initiated the shutdown sequence.
DI01	Heading Good Monitor	The Heading Good output discrete (PD005) is monitored with this discrete for bite purposes.
DI02	P&R Good Monitor	The Pitch and Roll Good output discrete (PD006) is monitored with this discrete for bite purposes.
DI03	26 vac Ref. Enable Monitor	The 26 VAC Reference Enable output discrete PD012 is monitored with this discrete for bite purposes.
DI04	Battery Status	This discrete is valid following initiation of an INU battery test by discrete PD011. A logic 1 indicates the INU battery is good.
DI05	Rotor Suspend	Logic 1 indicates rotors suspended. Logic 0 indicates rotors desuspended.
DI06	SD009 Monitor	Logic 1 indicates preload charge ON. Logic 0 indicates preload charge OFF.
DI07	Spare	
DI08	Spare	
DI09	Spare	
DI10	Spare	
DI11	Spare	
DI12	Spare	

TABLE 36. DISCRETE INPUTS (Cont)

Discrete Number	Title	Logic Definition (Referenced to Software)
DI113	FCC Bus Control	Logic 1 indicates the INU is the Bus Controller.
DI114	28 vdc Aircraft Power Loss	Logic 1 indicates loss of +28 vdc.
DI115	System On Battery	Logic 0 indicates system on battery.

TABLE 37. STATUS INPUT DISCRETES

Status Discrete Number	Destination and Title	Logic Definition (Referenced to Software)
ST00	Data Terminal Active	Logic 1 indicates Data Terminal Busy
ST01	SYC0MPC (System I/O Command Completed)	Logic 1 indicates System I/O Busy
ST02	SYL0SC (System I/O Command Lost)	Logic 0 indicates I/O Command Lost
ST03	HPRTSD (HP 2100 Ready to Send Data)	Logic 1 indicates HP 2100 Ready to Send Data
ST04	CDU Status Discrete No. 1	} See Table Below
ST05	CDU Status Discrete No. 2	
ST06	CDU Status Discrete No. 3	
ST07	Power status, external memory	Logic 1 indicates memory power supply out-of-tolerance
ST08	HP 2100 Interface Status	Logic 1 indicates HP 2100 is connected to MICRON
ST09	} Spares	
ST10		
ST11		
ST12	} CPU Internal	
ST13		
ST14		
ST15		

TABLE 37. (Cont)

CDU Status Discrete No.1 (ST04)	CDU Status Discrete No. 2 (ST05)	CDU Status Discrete No.3 (ST06)	CDU Status
1	1	1	Off
1	1	0	System Mode Word
1	0	1	Keyboard MSR
1	0	0	Keyboard LSR

AD-A048 000

ROCKWELL INTERNATIONAL ANAHEIM CALIF AUTONETICS GROUP  
MICRO NAVIGATOR (MICRON) PHASE 2B VOLUME I. TECHNICAL REPORT.(U)  
AUG 77 J M MILLER, A P ANDREWS, T F BRASHER F33615-75-C-1301  
C75-787/201-VOL-1 AFAL-TR-77-138-VOL-1 NL

F/6 17/7

UNCLASSIFIED

3 OF 4  
AD  
A048000

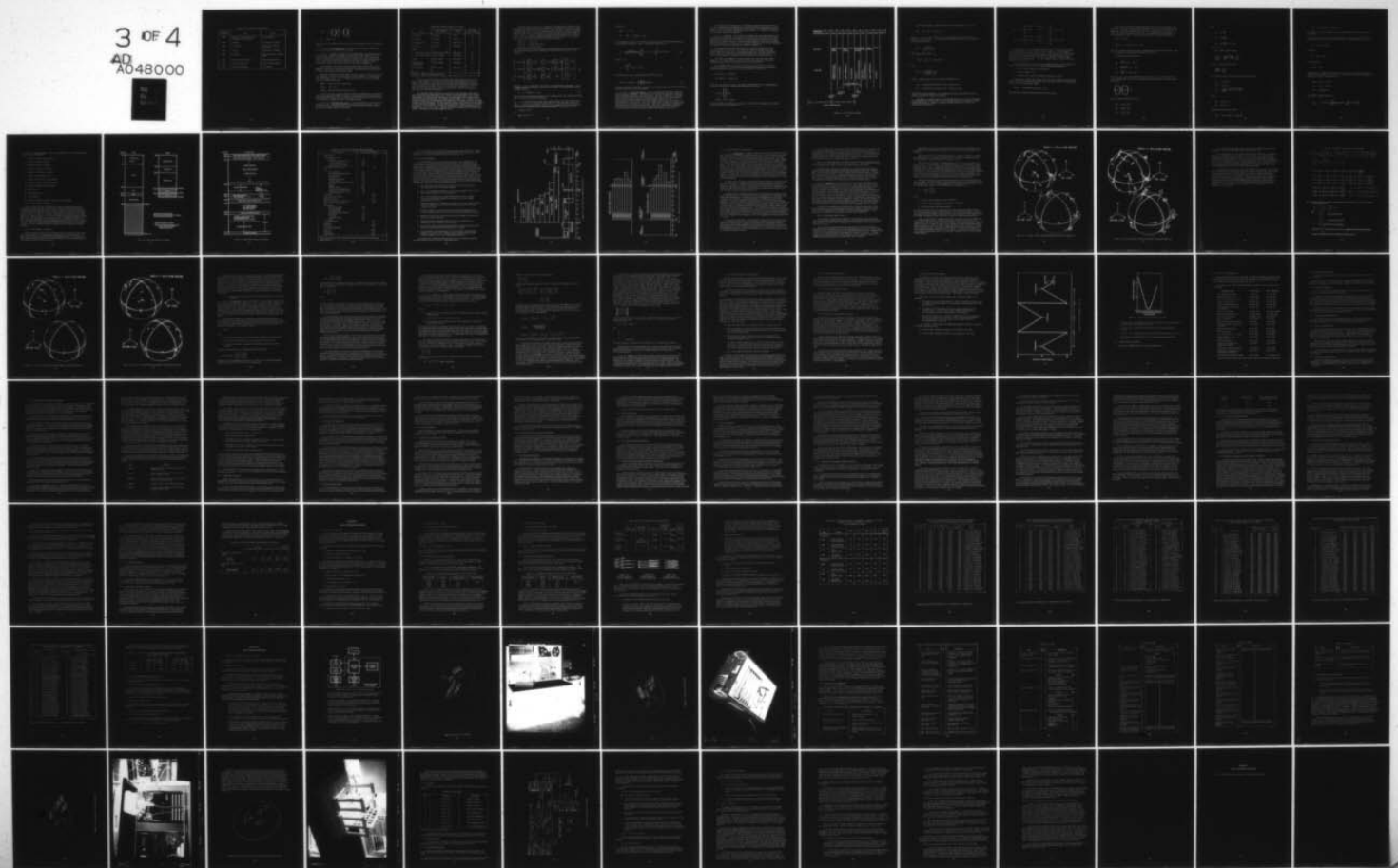


TABLE 38. INTERRUPT ASSIGNMENTS

Interrupt Designation	Title	Source
PIR0	Biomotion Trigger (immediate shutdown if not spinning)	Test Equipment
PIR1	Endmuc	Processor I/O Module
PIR2	64 Hz Clock	MUM & EMA Timing Generator
PIR3	Cmpltc	Processor I/O Module
PIR4	Designate	Converter Module (Throttle Grip)
PIR5	Transmission Complete	Data Terminal Module
PIR6	Input Message Error	Data Terminal Module
PIR7	CPU Interval Timer	CPU Internal

$$RQ_i = Y_i \times \left( \begin{array}{c} 0 \\ 1 \\ 0 \end{array} \right) \Bigg/ \left| Y_i \times \left( \begin{array}{c} 0 \\ 1 \\ 0 \end{array} \right) \right|$$

$$R_i = RQ_i \times Y_i$$

The reference set is updated in the cal data collection program whenever the table is turned.

2.4.1.2.4 Major Subroutines. The three major subroutines called by the fast cycle executive are START, CAL, and NAV.

2.4.1.2.4.1 START. During first-time initialization, background sets up for the start mode. When the interrupts are enabled, the START routine is entered. The sub-mode of START is determined by the variable TCI. Table 28 lists these modes. If automatic sequencing is selected, START will sequence through modes 1 to 15. In the manual mode, TCI is entered on the CDU, according to Table 25. Detailed flow charts of all START routines are presented in Appendix I.

Fast warmup heater control is operated continuously in all START modes, in subroutine WRMUP. Phase locked demod frequency control routines NOSPN and DESIR are scheduled as required in each mode. Table 39 lists the uses for demod frequency and its source for all START modes.

Spin Motor Control electronics (SMC) are used to generate both motor currents and TD signals. The modes are controlled by discrete outputs. It is important to have SMC outputs zero (A = B = S = 0) before and at least 1/64 sec after changing states on the following discrettes.

- SD015 Spin motor power amp on/off
- MD002 Heat mode
- TD000 Spin motor power amp gyro select.

It is also necessary to set the heat mode discrete (MD002) prior to setting spin motor power amp enable (SD015) in order to avoid latching the long shutdown mode. These sequencing requirements are implemented in the "front end" or driver section of START prior to jumping to a mode-servicing subroutine.

2.4.1.2.4.2 Calibration Data Collect. Cal data collection is entered from the navigate mode by a command through the control/display panel keyboard. Once in the calibrate mode, the program will remain in that mode until commanded out by another control display panel keyboard entry.

TABLE 39. DEMOD FREQUENCY USAGE

Mode	Demod Frequency Control Source	SMC Frequency Source	Initialize PLDC* Routine
Z coil heat	Constant	Gyro 1	No
Z degauss	Constant	Gyro 1	No
Charge Monitor	Constant	Other gyro	No
Servo Test	Constant	Same gyro	No
Spin			
Speed Detect Mode	Speed detect routine	Other gyro	No
Speed Adjust Mode	PLDC* routine	Same gyro	Yes
Damp	PLDC routine	Same gyro	No
Temperature Stabilization	PLDC routine	Same gyro	Yes
Final Degauss	PLDC routine	Same gyro	No
*PLDC = Phase Locked Demod Control			

The data collection program is in an idle mode until instructions are received from the HP computer. The requested data is collected and output to the HP computer. The program then returns to idle waiting for another instruction. The data collection program can collect either raw data from gyros and EMAs or calibration data from gyros and/or EMAs. Raw data is sampled and transmitted 64/sec. Both gyro and EMA data may be collected simultaneously. Detailed CAL program flow charts are presented in Appendix J.

The calibration data collection may consist of several calibration "data points" (NGP = number of gyro data points, NEP = number of EMA data points, NES = number of seconds of EMA data per EMA data point). Each data point is the result of a least squares fit to a specified number of instantaneous data samples (NGS = number of 64 Hz gyro data samples per gyro data point, the product  $NES \cdot 64$  = number of 64 Hz EMA data samples per EMA data point). The data collection program only performs the summations for the least squares solution. The final solution involving a matrix inverse is left to the HP computer. Data collection is completely specified by 4 numbers input from the HP computer; NGP, NEP, NGS, NES. Raw data collection is specified by NGP negative and NEP=0. The number of raw data samples is -NGP.

Each data point is output as it is completed. The output data is buffered so that the program may immediately begin collecting more data before the old data is output. The output data blocks are raw, gyro1, gyro2, EMA, and BITE. Only one data block is output during 1/64 sec interval. Output of the entire data block must be completed within 1/64 sec. If it is not completed, the entire data block will be retransmitted on the next 1/64 sec. Failure to complete data block transmission will cause a BITE to be set. The BITE data block will be transmitted whenever a BITE is set. The first three words of every data block output to the HP will contain:

Word No. 1 - Check sum;

Word No. 2 - length of data block;

Word No. 3 - data block name.

Gyro calibration data collection consists of a least squares analysis to determine sin and cos of slip frequency and DC amplitudes of the MUM data  $\alpha$ ,  $\beta$  vectors. The solution is

$$\begin{bmatrix} \text{cos amplitude} \\ \text{sin amplitude} \\ \text{DC amplitude} \end{bmatrix} = \begin{bmatrix} \left( \sum_{i=1}^{\text{NGS}} \cos^2 \theta_i \right) & \left( \sum_{i=1}^{\text{NGS}} \cos \theta_i \sin \theta_i \right) & \left( \sum_{i=1}^{\text{NGS}} \cos \theta_i \right) \\ \left( \sum_{i=1}^{\text{NGS}} \cos \theta_i \sin \theta_i \right) & \left( \sum_{i=1}^{\text{NGS}} \sin^2 \theta_i \right) & \left( \sum_{i=1}^{\text{NGS}} \sin \theta_i \right) \\ \left( \sum_{i=1}^{\text{NGS}} \cos \theta_i \right) & \left( \sum_{i=1}^{\text{NGS}} \sin \theta_i \right) & (\text{NGS}) \end{bmatrix}^{-1} \begin{bmatrix} \sum_{i=1}^{\text{NGS}} D_i \cos \theta_i \\ \sum_{i=1}^{\text{NGS}} D_i \sin \theta_i \\ \sum_{i=1}^{\text{NGS}} D_i \end{bmatrix} \quad (1)$$

where  $D_i = \alpha$  or  $\beta$  from gyro 1 or 2 and  $\theta_i$  is the demod phase slip angle.  $\theta_i$  is computed from demod frequency control reference phase, SL, and frequency control residual, DMRO,

$$\theta = \text{SL} + (\text{DMRO}) (1/64 \text{ sec}). \quad (2)$$

Only the eight summations in Equation (1) are computed in the data collection program. Equation (1) is solved in the HP computer.

Between data collection intervals the table may be turned. The demod control reference vector,  $R_i$ , is case fixed during data collection. When the table is turned  $R_i$  and  $Y_i$  may become nonorthogonal. Therefore,  $R_i$  is updated between data collection intervals if the magnitudes of the following dot products exceed the given limits:

$$\begin{aligned} & |R_i \cdot Y_i| > \sin 5^\circ \\ \text{or} & \\ & |RQ_i \cdot Y_i| > \sin 5^\circ \end{aligned}$$

The update is

$$RQ_i = Y_i \times R_i$$

$$R_i = RQ_i \times Y_i / |RQ_i \times Y_i|$$

EMA calibration consists of a 64 point least squares analysis to determine the slope of the accumulated EMA pulse counts. The solution in pulses/sec is

$$R = \frac{6(64/\text{sec})}{(\text{NES}) N (N+1) (N-1)} \left[ \sum_{n=1}^N (2n - N - 1) P_n \right] + \text{DVO} (64/\text{sec}) \quad (3)$$

where  $N = 64$

$$P_n = \sum_{i=1}^{(n)(\text{NES})} (\text{DVP}(i) - \text{DVO}) \quad (4)$$

and  $\text{DVP}(i)$  is the pulse count measured on the  $i^{\text{th}}$  fast cycle

$$\text{DVO} = 312 \text{ pulses} = \left[ \frac{20000}{64} \right] \text{ truncated} \quad (5)$$

Only the summations of Equations (3) and (4) are computed in the data collection program. Equation (3) is solved in the HP computer.

**2.4.1.2.4.3 Align and Navigate.** The NAV program has three basic submodes: Standby, Align, and Navigate. The Align mode can be either gyrocompass (normal) or stored heading (optional by manual command). The NAV standby mode is normally entered automatically when the one-second background loop has detected completion of the automatic startup sequence through the START standby mode ( $\text{TCI}' = 15$ ). Background then transfers control to a mode initialization section, where the primary mode flag STNV is set negative. After five seconds in NAV standby, the program will automatically enter the selected align mode. Then, after completing the alignment, the program will sequence into the free inertial navigate mode. The operator can exercise control over mode switching according to the information in Table 25.

One complete cycle through the NAV calculations requires eight fast cycles or 1/8 sec. The functions to be performed are divided among eight subroutines or "slow cycles", which are executed sequentially and then repeat. The assignment of functions to slow cycles and the relative timing are shown in Figure 71. Detailed NAV program flow charts are presented in Appendix K.

2.4.1.2.5 Simulator. The simulator is scheduled by Background whenever the flag SIMUL is set non-zero. It generates simulated data for gyro angle readout, EMA, gaps and temperatures, and IAU rotation. It accepts spin motor commands to damp, spin, process, or heat the rotor. It accepts demod frequency commands and simulates the MUM demodulators. It also accepts temperature control and IAU rotation commands. Detailed flow charts of the simulator are included in Appendix L.

The simulator is initialized in background. There are two primary modes - navigation mode and start mode. The start mode simulates polhode motion and accepts spin motor commands. The navigation mode moves the spin vector on the case at earth rate. Start mode is commanded by flag STNV = positive number (non-zero). Charge monitor is simulated for both a spinning and non-spinning gyro.

The EMAs are simulated as a constant pulse rate. The output pulse count is truncated to an integer number of pulses and the fractional pulse is accumulated. During precounter BITE test a fixed pulse rate is put out (40 KHz).

The simulator holds an inertial, non-rotating  $\alpha$  and  $\beta$  vector for each gyro (ALSIM<sub>i</sub> and BTSIM<sub>i</sub>). The vectors are expressed in earth-fixed (body) coordinates. During navigation the inertial  $\alpha$ ,  $\beta$  vectors are updated at earth rate.

$$d/dt \text{ ALSIM}_i = \text{ALSIM}_i \times \Omega$$

$$d/dt \text{ BTSIM}_i = \text{BTSIM}_i \times \Omega$$

where  $\Omega$  is the earth rate vector. The update is performed 16/sec. During start the inertial  $\alpha$ ,  $\beta$  vectors are computed from the spin vector,  $WS_i$ ,

$$\text{ALSIM}_i = \begin{bmatrix} 0 \\ 0 \\ 1 \end{bmatrix} \times WS_i$$

$$\text{BTSIM}_i = WS_i \times \text{ALSIM}_i$$

and both ALSIM<sub>i</sub> and BTSIM<sub>i</sub> are normalized. This precludes spinning up the simulator on the Z axis due to the singularity.

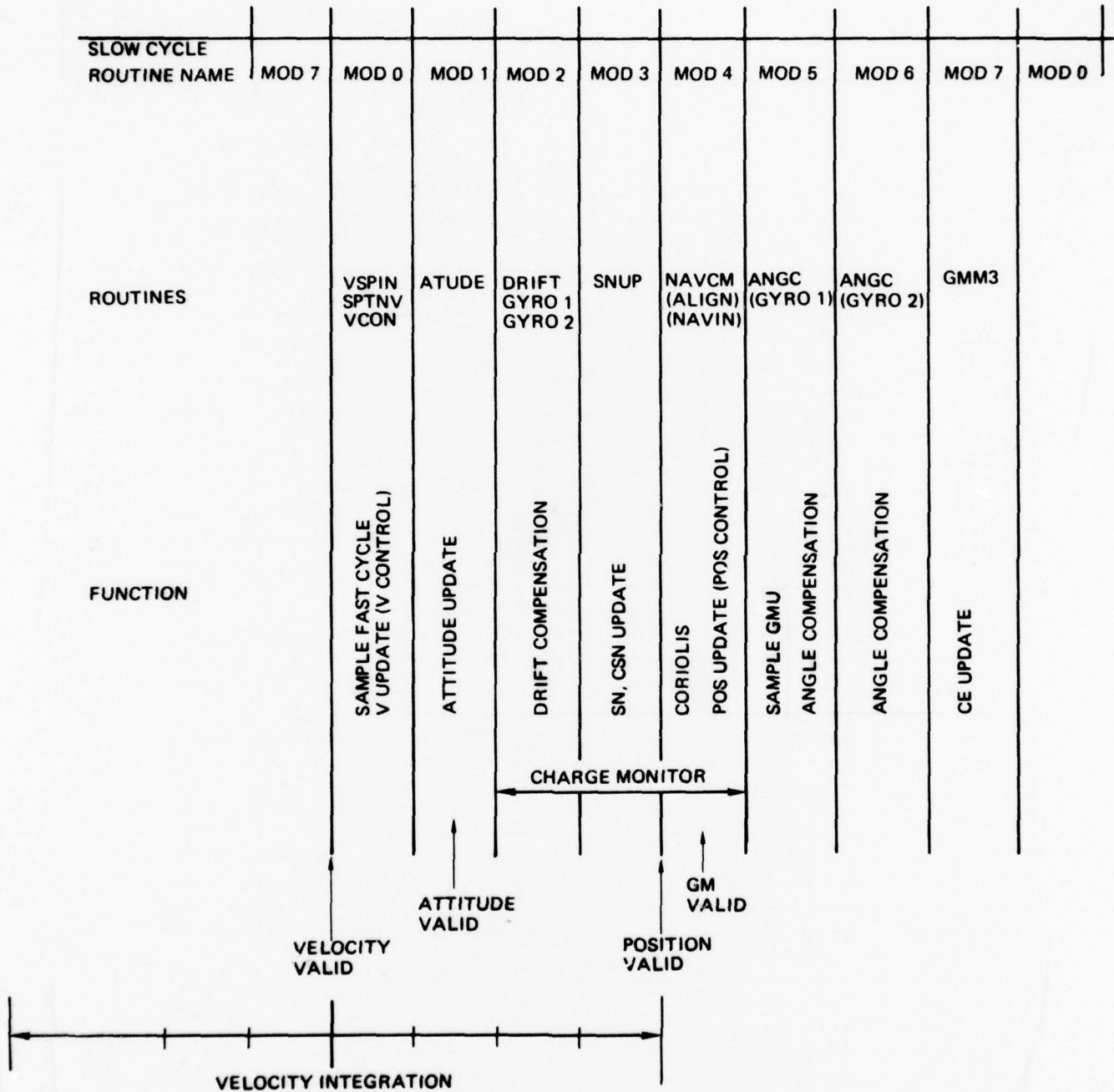


Figure 71. NAV Program Timing

The MUM demodulator simulator updates the demod slip angle,  $PH_i$ , 64/sec

$$PH_i^+ = PH_i^- + (SP_i - DMOD_{i \text{ old}}) \Delta t$$

where  $\Delta t = 1/64$  sec,  $SP_i = i^{\text{th}}$  gyro speed, and  $DMOD_{i \text{ old}}$  is commanded demod frequency 1/64 sec before. The frequency characteristics of the demod are simulated by the amplitude function

$$\text{Gain} = \frac{(32 \text{ Hz})^2}{(32 \text{ Hz})^2 + W_S^2}$$

where  $W_S$  is slip frequency. If

$$(32 \text{ Hz})^2 + W_S^2 > 2^{-7} (2604.16 \text{ Hz})^2$$

then

$$\text{Gain} = \frac{(32 \text{ Hz})^2}{2^{-7} (2604.16 \text{ Hz})^2}$$

The  $\alpha$ ,  $\beta$  vectors ( $AL'_i$ ,  $BT'_i$ ) in earth fixed coordinates are

$$AL'_i = (\text{Gain}_i)(\text{MUM}_i)(\text{ALSIM}_i \cos PH_i + \text{BTSIM}_i \sin PH_i)$$

$$BT'_i = (\text{Gain}_i)(\text{MUM}_i)(-\text{ALSIM}_i \sin PH_i + \text{BTSIM}_i \cos PH_i)$$

where  $\text{MUM}_i$  is MUM amplitude. MUM amplitude will vary when polhode motion is simulated and will be constant in navigation.

The output  $\alpha$ ,  $\beta$  vectors ( $AL_i$ ,  $BT_i$ ) are obtained from ( $AL'_i$ ,  $BT'_i$ ) by transforming first through the IAU rotation angle EN, then through a constant IAU platform-to-gyro transformation [CEG]. Finally, a simulated DC-offset term DCB is added to the vectors in gyro coordinates.

$$\begin{aligned}
 AL_i &= [CEG] \begin{bmatrix} \cos(EN) & \sin(EN) & 0 \\ -\sin(EN) & \cos(EN) & 0 \\ 0 & 0 & 1 \end{bmatrix} AL_i' + DCB \\
 BT_i &= [CEG] \begin{bmatrix} \cos(EN) & \sin(EN) & 0 \\ -\sin(EN) & \cos(EN) & 0 \\ 0 & 0 & 1 \end{bmatrix} BT_i' + DCB
 \end{aligned}$$

Charge monitor may be simulated with a TD input by setting the appropriate discrete output bits. Only plate center 1 TD is simulated. The TD signal is generated from the other gyro demod frequency. The charge monitor "MUM signal" is generated with the MUM demodulator simulator using the other gyro demod frequency in place of rotor speed. Therefore, the difference in the two demod frequencies is the slip frequency. The "MUM signal" output is scaled by the simulated charge on the rotor.

Charge monitor may be simulated with a spinning rotor by not commanding TD input. The normal MUM signal is used with the following modifications:

1. X and Y channel signals are interchanged;
2. Z channel signal is zero;
3. All signals are scaled by the simulated charge on the rotor.

Temperatures and gaps are output. These are both corrupted by ground voltage, GND. Gap is computed using case coefficient of expansion, TXPS, case temperature  $TEMP_i$ , and rotor temperature  $TROT_i$ :

$$SMGAP = (TXPS)(TEMP_i) - TROT_i + GND$$

The output gap reading is time shared between the two gyros.

In the start mode the gyro simulation parameters are rotor spin vector in case coordinates,  $WS_i$ , and rotor spin vector direction cosines, in rotor coordinates,  $WA_i$ ,  $WB_i$ ,  $WC_i$ . The length of  $WS_i$  is rotor speed,  $SP_i$ . Vector  $(WA_i, WB_i, WC_i)$  has unit length with components along the rotor A, B, and C principle axes, respectively. Axis A has maximum moment of inertia and C has minimum moment of inertia. For a non-spinning rotor  $WS_i = 0$ , however,  $WA_i$ ,  $WB_i$ ,  $WC_i$  are already initialized.

In the spin mode

$$\frac{d}{dt} WS_i = (81.5 \text{ Hz/sec}) (AS \times BS)$$

where the maximum length of spin motor command vectors AS and BS are unity. However, maximum current input is half amplitude AS and BS.

The polhode motion equations are

$$\dot{W}_A = \frac{B-C}{A} W_B W_C + Q_A/A$$

$$\dot{W}_B = -\left(\frac{A-C}{B}\right) W_C W_A + Q_B/B$$

$$\dot{W}_C = \frac{A-B}{C} W_A W_B + Q_C/C$$

where  $(Q_A, Q_B, Q_C)$  is the applied torque vector,  $(W_A, W_B, W_C)$  is the spin vector in rotor coordinates and A, B, C are principle moments of inertia. Normalizing the spin vector:

$$\begin{pmatrix} W_A \\ W_B \\ W_C \end{pmatrix} = \begin{pmatrix} W_A \\ W_B \\ W_C \end{pmatrix} / SP$$

gives an unforced equation of motion

$$\dot{W}_A = K_A W_C W_B$$

$$\dot{W}_B = K_B W_C W_A$$

$$\dot{W}_C = K_C W_A W_B$$

where

$$K_A = SP \frac{B-C}{A}$$

$$K_C = SP \frac{A-B}{C}$$

$$K_B = -SP \frac{A-C}{B} \approx -K_A - K_C$$

since  $A \approx B \approx C$ ,

For C family polhode motion

$$\left| \frac{W_A}{W_C} \right| < \sqrt{\frac{B-C}{A} / \frac{A-B}{C}} = \sqrt{\frac{K_A}{K_C}}$$

and for A family polhode motion

$$\left| \frac{W_A}{W_C} \right| > \sqrt{\frac{K_A}{K_C}}$$

For C family polhode motion the equation can be linearized

$$\dot{W}_A = S_A W_B / \Delta t$$

$$\dot{W}_B = S_B W_A / \Delta t$$

$$W_C = \left( \frac{W_C}{|W_C|} \right) \sqrt{1 - W_A^2 - W_B^2}$$

where

$$S_A = K_A W_C \Delta t$$

$$S_B = K_B W_C \Delta t$$

which has a second order solution

$$W_A = W_A + S_A (W_B + 1/2 \dot{W}_B \Delta t)$$

$$\dot{W}_B = W_B + S_B (W_A + 1/2 \dot{W}_A \Delta t)$$

The solution for A family polhode motion is identical with the roles of A and C axes interchanged:

MUM vector is the component of pendulosity vector,  $P_{ABC} = (P_A, P_B, P_C)$  that is orthogonal to spin vector,  $W_{ABC} = (W_A, W_B, W_C)$ . MUM quadrature vector is

$$M_Q = P_{ABC} \times W_{ABC}$$

and MUM is

$$M = M_Q \times W_{ABC}$$

MUM magnitude is

$$MUM_i = |M|$$

Damping torque is applied with amplitude proportional to the square of the current command vector amplitudes AS, BS, SS. Torque direction is in the M,  $M_Q$  plane with angle from the MUM vector computed as

$$\sin \theta = (AL_i \cdot AS) / NTQ$$

$$\cos \theta = (AL_i \cdot BS) / NTQ$$

$$NTQ = W_S / |W_S| \cdot SS$$

The polhode torquing equations are

$$\dot{W}_{ABC} = (2^{-2} \text{ rad/sec}) \left[ \frac{MQ}{|M|} \sin \theta NTQ^2 + \frac{M}{|M|} \cos \theta NTQ^2 \right]$$

2.4.1.2.6 Utility Routines. Utility routines which have been developed for the EPM DPU are listed below:

1. Double precision fractional divide
2. Single precision arctangent
3. Double precision arctangent
4. Single precision sine and cosine
5. Double precision sine and cosine
6. Double precision square root
7. Single precision vector cross product
8. Double precision vector cross product
9. Double precision dot (inner) product
10. Unit vector
11. Root Sum Squares
12. Print formatter
13. Single precision 3 x 3 matrix times 3 x 1 vector multiply

#### 2.4.1.3 DPU Memory Allocation

The DPU memory has been allocated according to the planned operational configuration of 12K read-only, 4K read/write. Memory allocation maps are presented for read-only memory in Figure 72 and for read/write memory in Figure 73. A detailed listing of read-only memory requirements for the present version of the program is given in Table 40. As shown, approximately 250 locations of read-only memory are unused. However, the present version of the program includes the simulator routine, the Biomation trigger interrupt routine, and HP2100 and printer I/O logic. These functions will be deleted from the operational flight program. After these functions are deleted, approximately 2000 locations of read-only memory will be available. (Still to be added is the 1553A Data Bus control function.) About half of read/write memory and about half of the EAROM memory is available for growth functions.

#### 2.4.1.4 INU Software Timing Data

The INU software architecture is based on a 64 Hz interrupt-driven fast cycle routine which operates in the foreground, and contains the executive control. All time-critical functions are implemented in foreground routines. It is necessary that all foreground routines complete execution and control revert to background prior to the occurrence of the next 64 Hz interrupt.

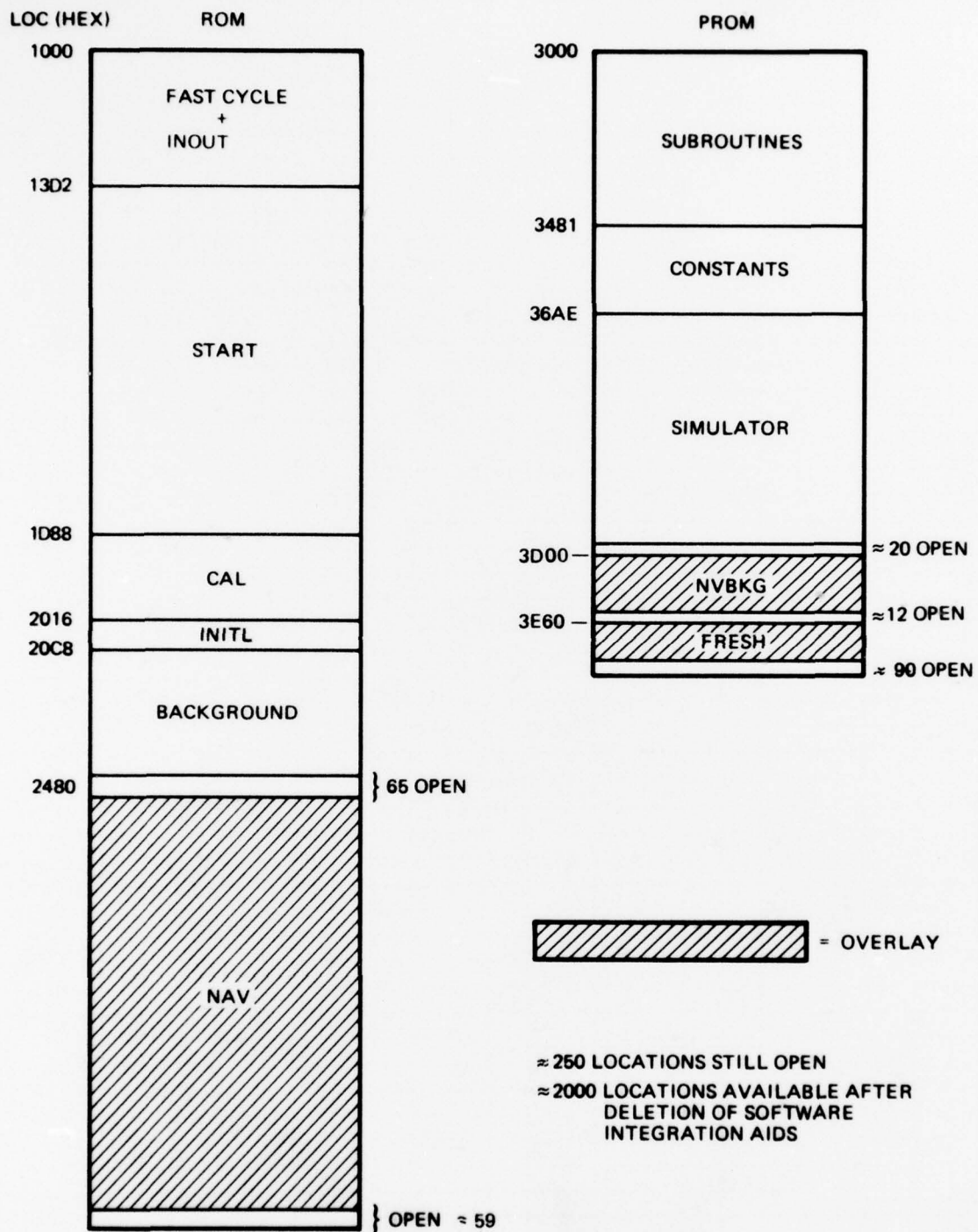


Figure 72. Read-Only Memory Utilization



TABLE 40. READ-ONLY MEMORY REQUIREMENTS

FUNCTION	NO. OF LOCATIONS
Initialization	178
Interrupt Processing	
Linkage	44
Biomation Trigger & Abort*	56
64 Hz & Discrete I/O	101
Fast Cycle Calculations	567
HP2100, Printer, CDU I/O*	208
Total Interrupt Processing	976
Start	
Driver Section	218
Fast Warmup & Sure-Start	47
System Checks	171
Z-Coil Heat	211
Suspend, Desuspend	72
Charge Monitor	229
Spin Motor Command Offset Cal	61
De-Gauss	91
Spinup	194
Polhode Damp	1126
Temperature Stabilization	118
Standby & Nav Initialization	10
Start Subroutines	251
Total Start	2799
Calibration Data Collect*	654
Align & Navigate	2885
Digital Output Data Fast Refresh	320
Math and Utility Subroutines	900
Background	
Start Background	104
Nav Background	347
Cal Background	3
Simulator/Debug Linkage*	43
Check Sum	25
I/O Logic	483
Thermal Control	52
BITE	106
Total Background	1163
Constants	556
Simulator*	1599
Zero Memory Routine*	14
Total Used	12044
Still Open	244
Total Memory	12288

\*The major portions of these functions will not be required in an operational flight program

The execution time required for foreground depends on the mode of the program. Estimates were obtained for foreground execution time as a function of mode. These estimates are presented graphically in Figure 74 and Figure 75.

#### 2.4.2 Test Station Software

Test Station Software is used in integration, calibration, and diagnosis of the EPM sensors, and for aiding DPU software development. In calibration, the test station software controls the automatic tilt table, sequences the collection of data, monitors data reasonableness, stores and identifies the data on magnetic disk files, estimates the calibration constants, formats the constants for EPM scaling, and sends the calibration constants back through the data link for storage in EPM memory. All of the operations in this "standard" sequence of system calibration are controlled by a special interactive program called the Strapdown System Monitor (SSM). The SSM program is designed to interface with the test station operator in plain English, so that the operator does not have to know how the Test Station Computer operates. The test station operator can perform the entire system calibration with several commands in English. The SSM program for ESG calibration had been developed under IR&D funding. The following tasks were completed under this contract:

1. The EPM Calibration Mode mechanization for the DPU was developed and checked out on the Test Station computer.
2. The error compensation models for the ESG were changed to the "γ-level" angle readout model and "K-73" drift model.
3. The "Fast Triangular Square-Root Mechanization" of N. A. Carlson (Ref 6) was successfully applied to estimation of ESG angle readout compensation parameters.
4. Calibration software was modified to account for the unique sensor mounting attitudes in EPM, and to use the new interface between the test station computer and EPM.
5. Calibration software was developed for formatting and scaling all calibration constants and generating the punched tape for loading EPM memory.
6. Diagnostic software was developed for using the HP2100 to interface with EPM via the 1553A Data Bus.
7. Diagnostic software for analysis of ESG noise was modified for the configuration of the HP2100-to-EPM interface.
8. Special data collection and plotting programs for diagnosis real-time EPM data were developed and used in support of EPM testing.
9. A new assembler and linking loader were developed for supporting INS software development, and a program which translates from the "old" assembly language to the "new" language was developed.

The backgrounds, approaches and results of each of the numbered tasks are presented separately in the respective subsections below.

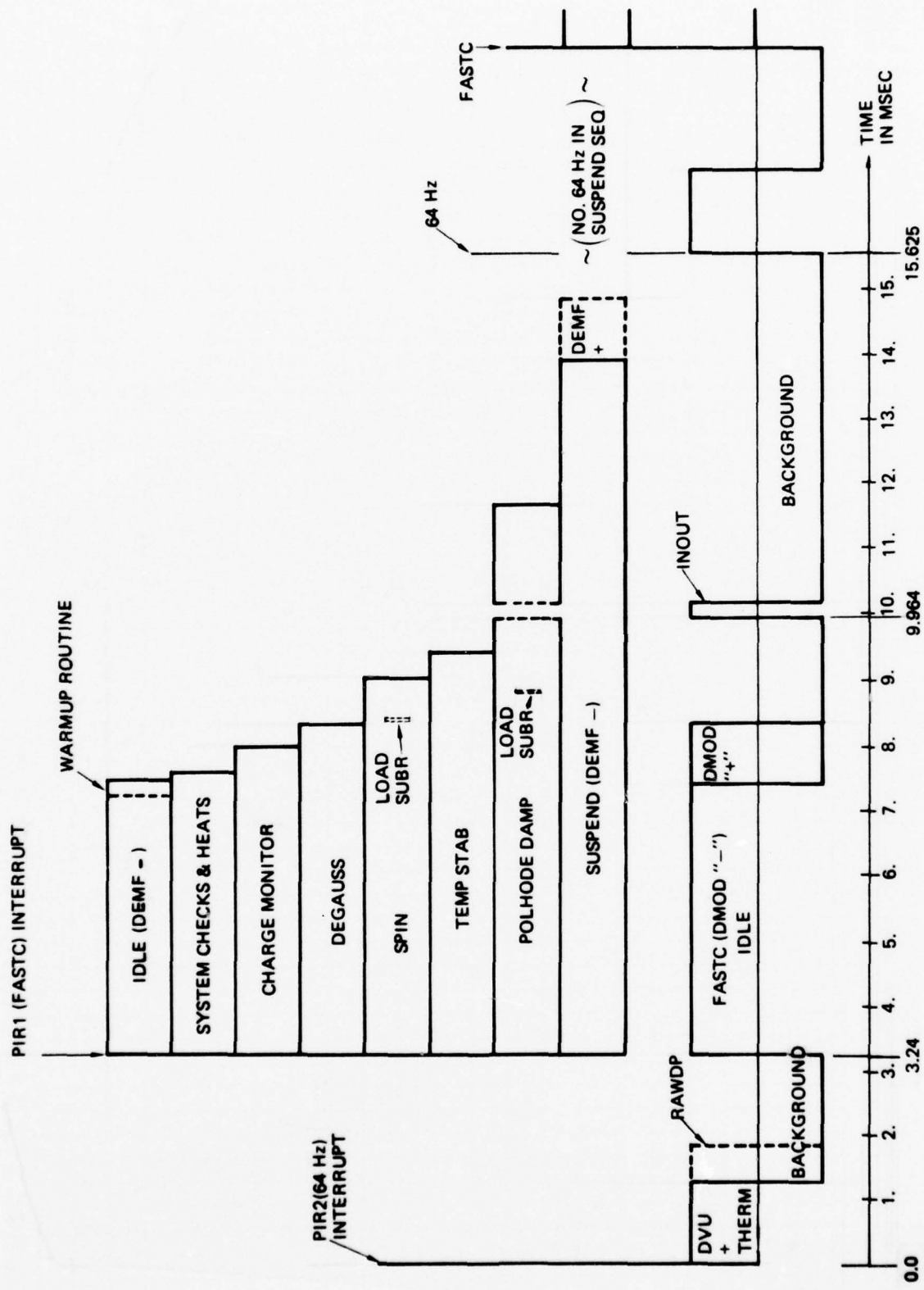


Figure 74. Start Mode Foreground Execution Times

FAST CYCLE TIMING - NAVIGATE

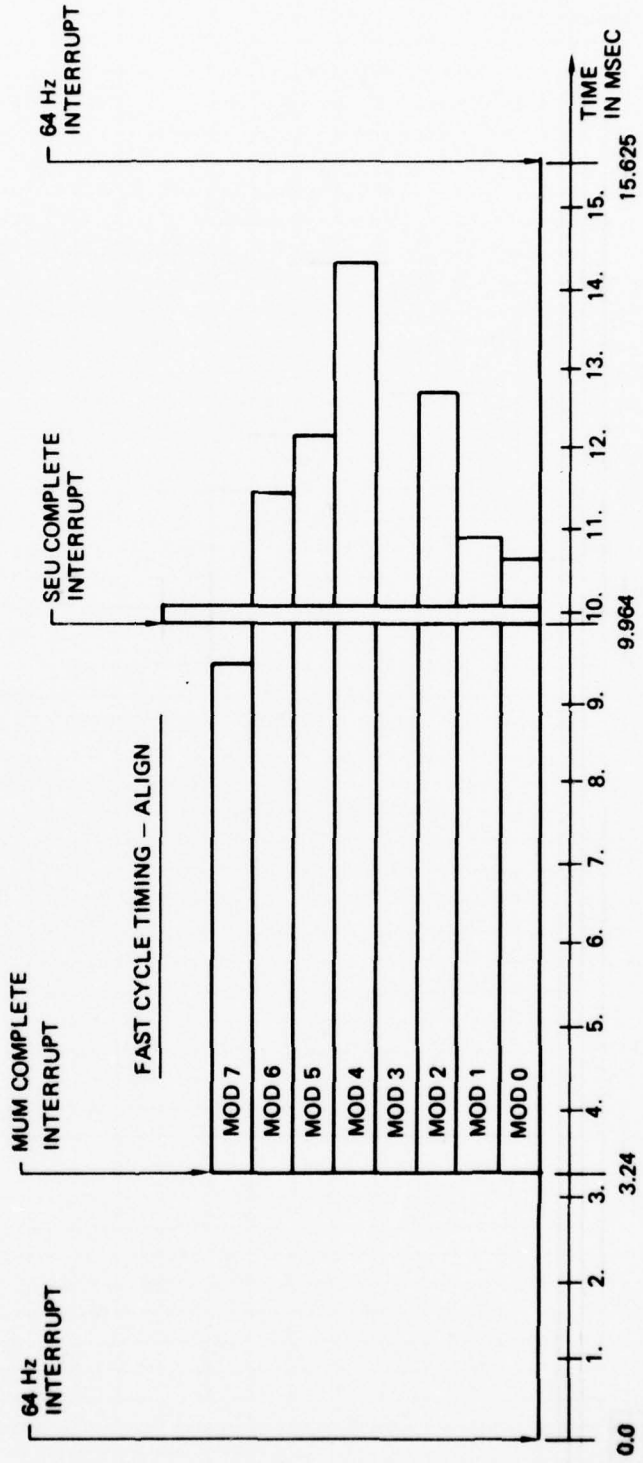
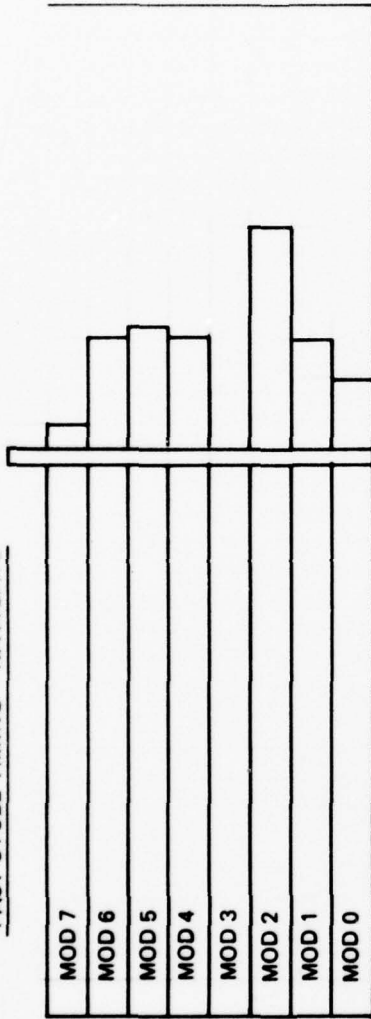


Figure 75. Align and Navigate Mode Foreground Execution Times

#### 2.4.2.1 EPM Calibration Mechanization

2.4.2.1.1 Background. The angle readout information for the MESH is derived from the deliberate radial mass unbalance of the rotor. This information is present in the suspension servo error signals as fundamental harmonics of the rotor spin frequency, and it is extracted by demodulation of the suspension servo error signals. In order to "average out" certain errors in this information, the demodulator reference signal frequencies are purposely displaced 5.086 Hz from the rotor spin frequency. The output information is then varying sufficiently slowly (at 5.086 Hz) that it can be converted to digital information and used in navigation mechanization as though it were "dc" information. Error mechanisms which cause small, zero-mean errors at the first and second harmonics of "slip frequency" (5.086 Hz) are "averaged out" in the navigation mechanization (which behaves like a low-pass filter with an 84-minute period). This is the reason for using the slip frequency in the demodulator outputs. It is important to keep this slip frequency constant to within about 0.01 Hz, however, because there are other error mechanisms which are sensitive to the value of the slip frequency.

It is important to sample the data which will be used for angle calibration under the same slip frequency conditions that will exist during alignment and navigation. However, it is necessary that the zero-mean noise level in this generic data be reduced by smoothing. (In order to reduce the level of bias errors significantly below the level of the zero-mean noise, it is necessary to reduce the level of noise in the data that will be used in estimating the biases.)

Smoothing of this "slipping frequency" data is accomplished by doing real-time fourier fitting of the data to "cosine" and "sine" components of the fundamental phase of the output information. The fidelity of this filtering algorithm is extremely sensitive to errors in the assumed slip frequency. In order to overcome this sensitivity, a real-time estimator of the output phase is included in the smoothing algorithm. This phase estimation algorithm uses the zero-crossings of the output data as a measurement of phase (by interpolating between samples before and after a zero-crossing), and uses a simple kalman filter mechanization for simultaneously estimating slip frequency and instantaneous phase. The slip frequency estimate can then be used to apply control (by changing the demodulator reference frequency) to maintain the slip frequency within the required bounds. On the N57A system, the quantization level for demodulator frequency control was sufficiently fine that this control loop could be made very "sluggish" (rotor frequency is also very sluggish) and be iterated only every 15 seconds.

In the EPM system design, it was possible to reduce the life cycle cost per system by relaxing the tolerance on the demodulator output filters (which tightened the tolerance on slip frequency), using fewer bits input to the demodulator reference frequency generator (which tightened the requirements on the frequency control loop) and making up for it in the software mechanization. It was then necessary to move the demodulator frequency control mechanization into the "fast cycle", where it could be iterated 64 times per second.

A new mechanization was developed for demodulator frequency control under the N77 program. Rather than use zero-crossings to estimate phase, it generates a fictional "MUM" vector that is rotating at precisely 5.086 Hz. The dot product of the sampled MUM vector "alpha" with the fictional vector is used as an error signal in a control loop that slaves the sampled MUM vector "alpha" to be perpendicular to the fictional MUM vector and, consequently, phase-locked to it.

The zero-crossing algorithm can still be used for the data smoothing algorithm, except that it no longer applies control to the demodulators. This algorithm was used for N77 calibrations, and gave results comparable to N57A performance.

The EPM system software is designed so that all real-time functions which require precise timing with respect to the instrument outputs will be done within the DPU. This convention simplifies the test station software requirements, and makes the test station software more versatile and adaptable to different computer systems. It also means that the real-time smoothing for calibration must be done within the DPU. If the N77 smoothing algorithms were used for this purpose, there would be two independent algorithms estimating the same thing (demodulator phase).

2.4.2.1.2 Approach. A version of the N77 "fast cycle" foreground program was modified so that the demodulator control phase error signal was added to the whole-value phase of the fictitious MUM vector, and this phase angle for each of the two gyros was passed through common for use in calibration data smoothing. A separate program was developed for calibration data smoothing. This program uses the Instrument Status Word (ISWD) convention of the EPM mechanization to be able to use only one gyro. (The N77 mechanization would "hang up" waiting for a zero-crossing from the output of a missing gyro.) It picks up the appropriate demodulator phases, computes the associated sines and cosines, accumulates the appropriate sums of products of these quantities with the demodulator outputs, and does the timing control to achieve the required level of smoothing. It also preserves the sums of data needed for determination of demodulator output dc biases. This program simulates the real-time function of the EPM "Calibration Mode" program on the N77 system.

A separate set of programs was developed for forming the appropriate matrix inversions and products for determining the smoothed "Fourier coefficients" for the data, and for formatting and storing this data in the calibration data files. These programs were used for EPM test station software during calibration.

#### 2.4.2.2 Calibration Model Changes

These software modifications included the implementation in the calibration programs of the drift compensation model which was designated "Model K-73" and the angle readout error model which compensates for servo sensing axis misalignments, etc at the "Y-level."

The new drift compensation model was designated "Model K-73" because it includes three new parameters, the need for which was first observed on N-73 (EPM). The cause for the associated drift rate has subsequently been traced to a coupling among the three servo channels on one hybrid module (the Notch Filter hybrid). A design change has been developed and tested for elimination of the coupling. However, the software change compensates the resulting drift rates adequately.

Model modifications were implemented in the INU and Test Station Software as a result of analysis and modelling of drift rate errors observed during calibration and navigation.

The residual drift rates of both EPM gyros, after removal of calibrated effects, were unusually large. The rms magnitude of these residuals was 0.024 deg/hr per axis on Gyro No. 1 and 0.033 deg/hr per axis on Gyro No. 2.

The patterns of residuals are shown in Figure 76 for Gyro No. 1 and Figure 77 for Gyro No. 2. In these figures, the residual drift rates are represented by arrows drawn on a sphere. The arrows represent the direction in which the rotor spin axis would move as a result of residual drift rates (the ESG rotor is not torqued), and the magnitude of the arrow is related to the magnitude of the drift rate by the scale shown on the figures. The octants on the spherical surfaces represent the suspension electrode surfaces of the ESG, with the ESG X-Y-Z axes oriented as shown on the figure. The tail of each arrow (representing a drift rate) is at the location of the spin axis (with respect to the ESG electrodes) at the time that the drift rate was observed.

The observed pattern of residuals was analyzed to determine its functional form and, if possible, its physical cause. In general, the pattern of arrows is away from the -Y axis toward the +Y axis, and has maximum value halfway between the two (i. e., near the X-Z plane of the figure). The functional form of this pattern is

$$\dot{Y} = Y \times \left( Y \times \begin{bmatrix} 0 \\ P \\ 0 \end{bmatrix} \right)$$

where

$Y$  is a unit vector parallel to the rotor spin axis

$\dot{Y}$  is its time-rate-of-change (= the arrows in the figures)

$P$  is the associated calibration parameter

This functional form had been identified in earlier drift modelling studies as being due to causes which exchange energy between the rotor and its environment, such as non-uniform magnetic fields or suspension servo characteristics at rotor spin frequency. Previously, no significant drift rates had been observed with this functional form.

Some experiments were conducted to measure the ambient magnetic fields in the vicinity of the ESG's and to see whether the observed drift rates were affected by rotation of the IAU with respect to the EPM housing. It was concluded that the magnetic fields in the IAU were close to natural levels, and that the observed drift rates were, indeed, fixed with respect to the IAU. This means that the drift rates observed during calibration (when the IAU is not being rotated) will be the same as those experienced in navigation and alignment (when the IAU is rotated). Consequently, the drift rates can be calibrated and compensated, by appropriate changes in the test station software and INS software.

SCALE: 1 IN. = 0.05 DEG/HR

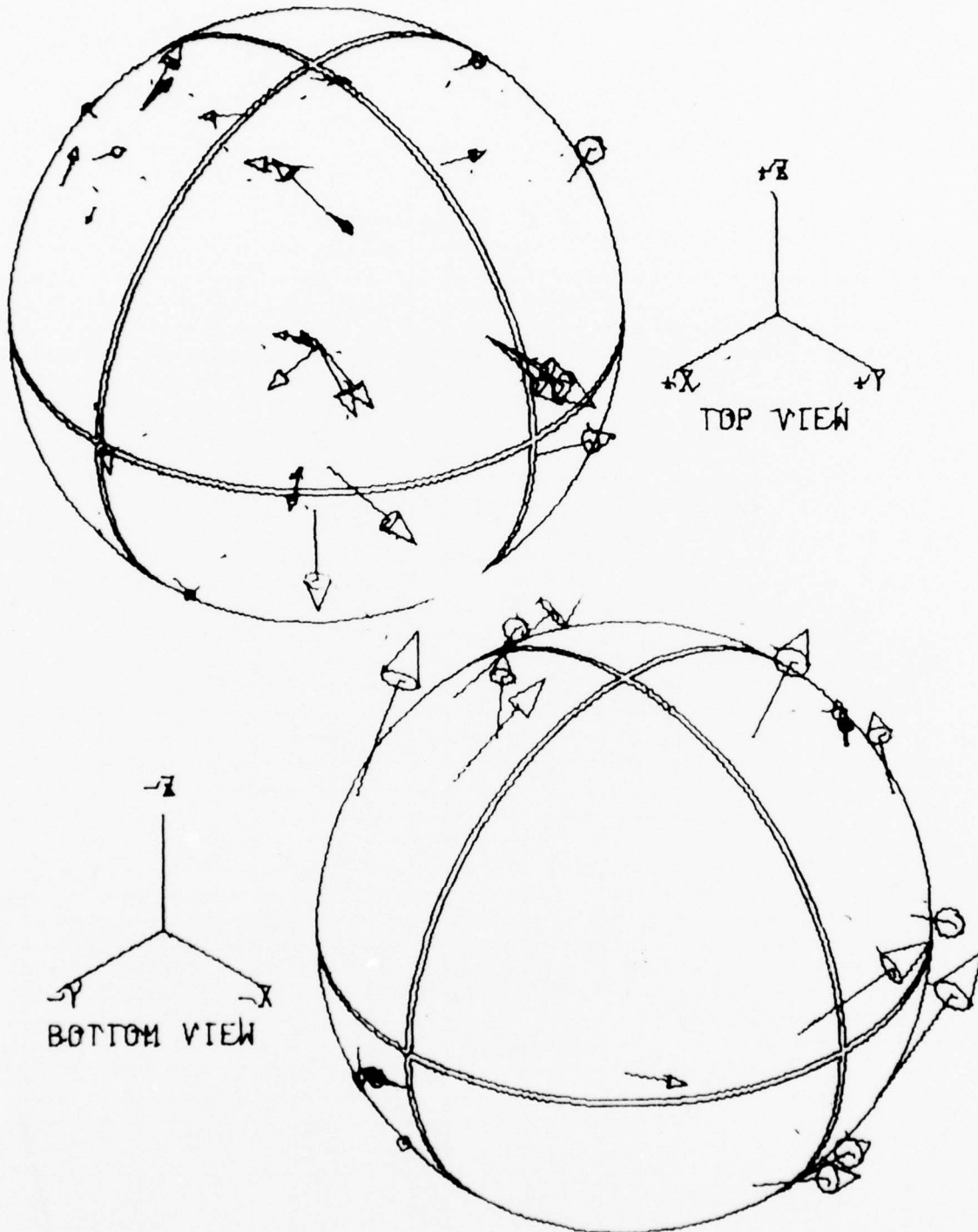


Figure 76. Gyro No. 1 Drift Calibration Residuals Using Drift Model K46

SCALE: 1 IN = 0.05 DEG/HR

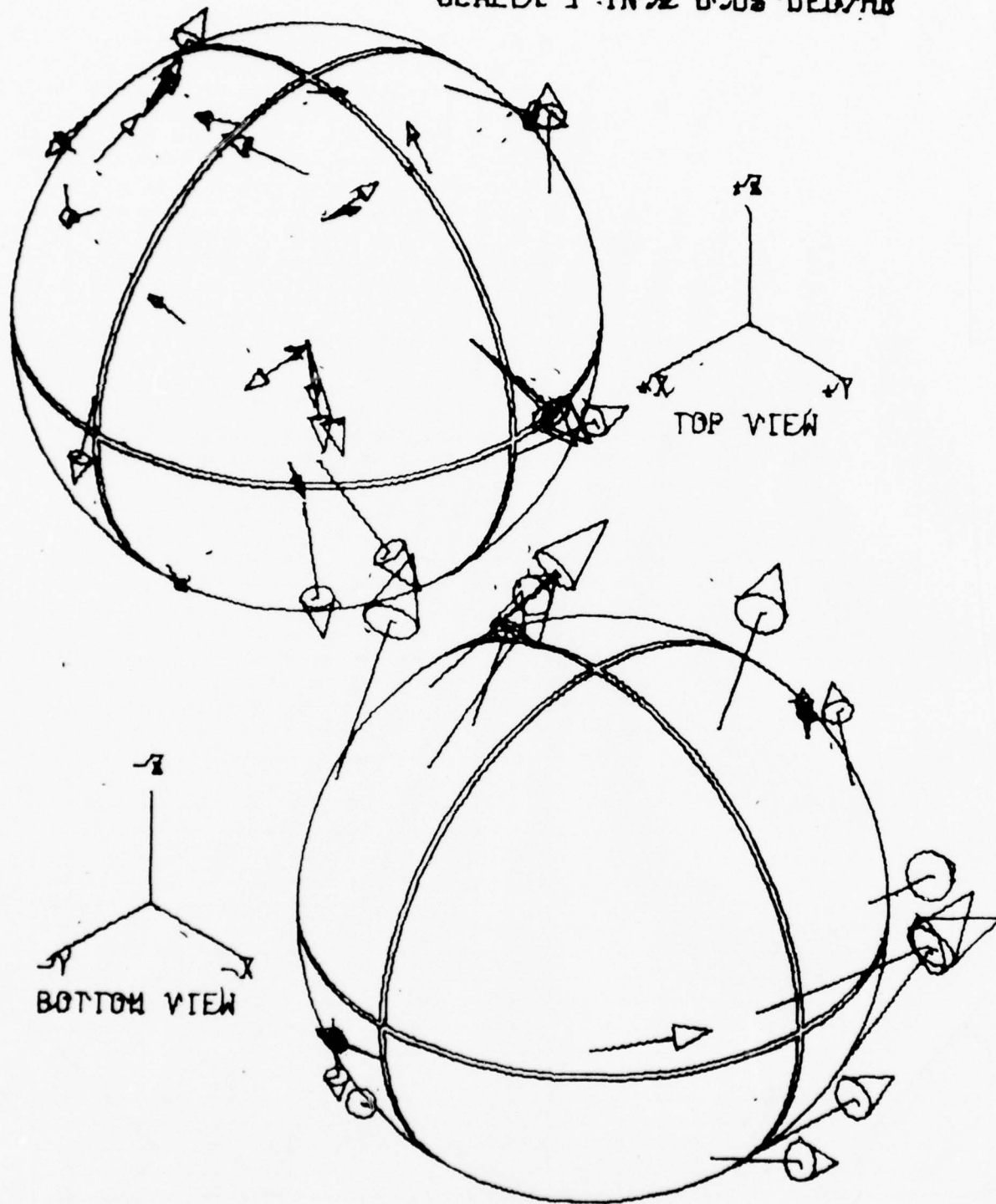


Figure 77. Gyro No. 2 Drift Calibration Residuals Using Drift Model K46

Three calibration coefficients ( $P_{36}$ ,  $P_{37}$  and  $P_{38}$ ) were added to the drift rate model. The new model (Drift Model K73) is shown in Table 41.

The residual drift rates, after calibration with Drift Model K73, are shown in Figures 78 and 79 for Gyro No. 1 and No. 2, respectively. The respective rms magnitudes are 0.008 and 0.011 deg/hr per axis. The drift compensation software in the INS was then modified to use the K73 Drift Model with the derived parameters. As a result, the drift rates observed during navigation were then reduced to the levels observed in the calibration residuals. It was observed that the values of the three "new" drift parameters obtained by calibration were identical in sign and of almost the same magnitude on all gyros that were calibrated in EPM.

The physical cause for the new drift error models has been found. Investigation of the suspension servo electronics revealed that about 8 percent of the input "X-axis" servo input signal (called the "MUM" signal, for "Mass Unbalance Modulation") is coupled into the "Y-axis" servo, and that 8 percent of the "Y-axis" servo input signal is coupled into the "Z-axis" servo. The functional form of the resulting drift rates (as a function of spin axis direction) contains a term proportional to MUM-magnitude-squared and of the functional form associated with the new parameters  $P_{36}$  and  $P_{38}$ . The fact that the term is proportional to MUM-magnitude-squared explains the observed variation in  $P_{36}$  and  $P_{38}$  with the magnitude of the MUM signal of the relevant gyros.

Table 41. Functional Formulas for Drift Model K73

$$\begin{aligned}
 F(\gamma, a) = & \begin{bmatrix} P_1 \\ P_2 \\ P_3 \end{bmatrix} + P_4 \begin{bmatrix} 0 & a_1 a_2 & a_1 a_3 \\ a_1 a_2 & 0 & a_2 a_3 \\ a_1 a_3 & a_2 a_3 & 0 \end{bmatrix} \begin{bmatrix} \gamma_1 \\ \gamma_2 \\ \gamma_3 \end{bmatrix} + \begin{bmatrix} P_5 + P_6 & P_9 & P_8 \\ P_9 & P_5 - P_6 & P_7 \\ P_8 & P_7 & 0 \end{bmatrix} \begin{bmatrix} \gamma_1 \\ \gamma_2 \\ \gamma_3 \end{bmatrix} + \begin{bmatrix} 0 & -\gamma_3 & \gamma_2 \\ \gamma_3 & 0 & -\gamma_1 \\ -\gamma_2 & \gamma_1 & 0 \end{bmatrix} \begin{bmatrix} P_{14} + P_{15} & P_{18} & P_{17} \\ P_{18} & P_{14} - P_{15} & P_{16} \\ P_{17} & P_{16} & 0 \end{bmatrix} \begin{bmatrix} \gamma_1 \\ \gamma_2 \\ \gamma_3 \end{bmatrix} \\
 & + P_{13} \begin{bmatrix} a_1 \\ a_2 \\ a_3 \end{bmatrix} + P_{21} \begin{bmatrix} \gamma_1 (2\gamma_1^2 - 1) \\ -\gamma_2 (2\gamma_2^2 - 1) \\ 0 \end{bmatrix} + P_{11} (a_1 \gamma_1 + a_2 \gamma_2 + a_3 \gamma_3) \begin{bmatrix} a_1 \\ a_2 \\ a_3 \end{bmatrix} \\
 & + \left[ \begin{array}{l} 0 \\ 0 \\ \gamma_3 (2\gamma_3^2 - 1) \left\{ P_{20} + (2\gamma_3^2 - 1) \left\{ P_{19} + (2\gamma_3^2 - 1) \left\{ P_{22} + (2\gamma_3^2 - 1) \left\{ P_{23} + (2\gamma_3^2 - 1) \left\{ P_{10} + (2\gamma_3^2 - 1) P_{12} \right\} \right\} \right\} \right\} \right\} \right\} \right\} \right\} \\
 & + \left[ \begin{array}{l} \gamma_1 (2\gamma_1^2 - 1) \left\{ P_{25} + (2\gamma_1^2 - 1) \left\{ P_{26} + 2\gamma_1^2 - 1 \right\} \left\{ P_{27} + (2\gamma_1^2 - 1) \left\{ P_{28} + (2\gamma_1^2 - 1) \left\{ P_{29} + (2\gamma_1^2 - 1) \left\{ P_{30} + (2\gamma_1^2 - 1) P_{31} \right\} \right\} \right\} \right\} \right\} \right\} \right\} \\
 & + \left[ \begin{array}{l} \gamma_2 (2\gamma_2^2 - 1) \left\{ P_{25} + (2\gamma_2^2 - 1) \left\{ P_{26} + 2\gamma_2^2 - 1 \right\} \left\{ P_{27} + (2\gamma_2^2 - 1) \left\{ P_{28} + (2\gamma_2^2 - 1) \left\{ P_{29} + (2\gamma_2^2 - 1) \left\{ P_{30} + (2\gamma_2^2 - 1) P_{31} \right\} \right\} \right\} \right\} \right\} \right\} \\
 & + \left[ \begin{array}{l} \gamma_3 (2\gamma_3^2 - 1) \left\{ P_{25} + (2\gamma_3^2 - 1) \left\{ P_{26} + 2\gamma_3^2 - 1 \right\} \left\{ P_{27} + (2\gamma_3^2 - 1) \left\{ P_{28} + (2\gamma_3^2 - 1) \left\{ P_{29} + (2\gamma_3^2 - 1) \left\{ P_{30} + (2\gamma_3^2 - 1) P_{31} \right\} \right\} \right\} \right\} \right\} \right\} \\
 & + \begin{bmatrix} a_1 \left\{ P_{24} + (2\gamma_1^2 - 1) \left\{ P_{33} + (2\gamma_1^2 - 1) \left\{ P_{34} + (2\gamma_1^2 - 1) P_{35} \right\} \right\} \right\} \\ a_2 \left\{ P_{24} + (2\gamma_2^2 - 1) \left\{ P_{33} + (2\gamma_2^2 - 1) \left\{ P_{34} + (2\gamma_2^2 - 1) P_{35} \right\} \right\} \right\} \\ a_3 \left\{ P_{24} + (2\gamma_3^2 - 1) \left\{ P_{33} + (2\gamma_3^2 - 1) \left\{ P_{34} + (2\gamma_3^2 - 1) P_{35} \right\} \right\} \right\} \end{bmatrix} + P_{32} \begin{bmatrix} 0 & a_3 & a_2 \\ a_3 & 0 & a_1 \\ a_2 & a_1 & 0 \end{bmatrix} \begin{bmatrix} \gamma_1 \\ \gamma_2 \\ \gamma_3 \end{bmatrix} + \begin{bmatrix} 0 & P_{38} & -P_{37} \\ -P_{38} & 0 & P_{36} \\ P_{37} & -P_{36} & 0 \end{bmatrix} \begin{bmatrix} \gamma_1 \\ \gamma_2 \\ \gamma_3 \end{bmatrix}
 \end{aligned}$$

NOTES: DRIFT MODEL FOR TIME RATE OF CHANGE OF DIRECTION COSINES OF ROTOR SPIN AXIS WITH RESPECT TO GYRO-FIXED COORDINATES, DUE TO DETERMINISTIC DRIFTS IS

$$\frac{d\gamma}{dt} = \begin{bmatrix} 0 & -\gamma_3 & \gamma_2 \\ \gamma_3 & 0 & -\gamma_1 \\ -\gamma_2 & \gamma_1 & 0 \end{bmatrix} \sum_{N=1}^{35} P_N F_N(\gamma, a)$$

WHERE  $\gamma = \begin{bmatrix} \gamma_1 \\ \gamma_2 \\ \gamma_3 \end{bmatrix}$  = VECTOR OF DIRECTION COSINES

$a = \begin{bmatrix} a_1 \\ a_2 \\ a_3 \end{bmatrix}$  = VECTOR OF SENSED ACCELERATION

$F_n = \frac{\partial F}{\partial P_n}$ , WHERE THE VECTOR F IS AS DEFINED ABOVE

THE UNIT VECTOR  $\begin{bmatrix} e_1 \\ e_2 \\ e_3 \end{bmatrix}$  IN THE DIRECTION OF LOCAL "EAST" IS FOR COMPENSATING CALIBRATION STAND MISALIGNMENTS.

THEREFORE, THE 13TH MODEL TERM IS NOT USED IN COMPENSATION DURING NAVIGATION, ETC.

SCALE: 1 IN = 0.05 DEG/HR

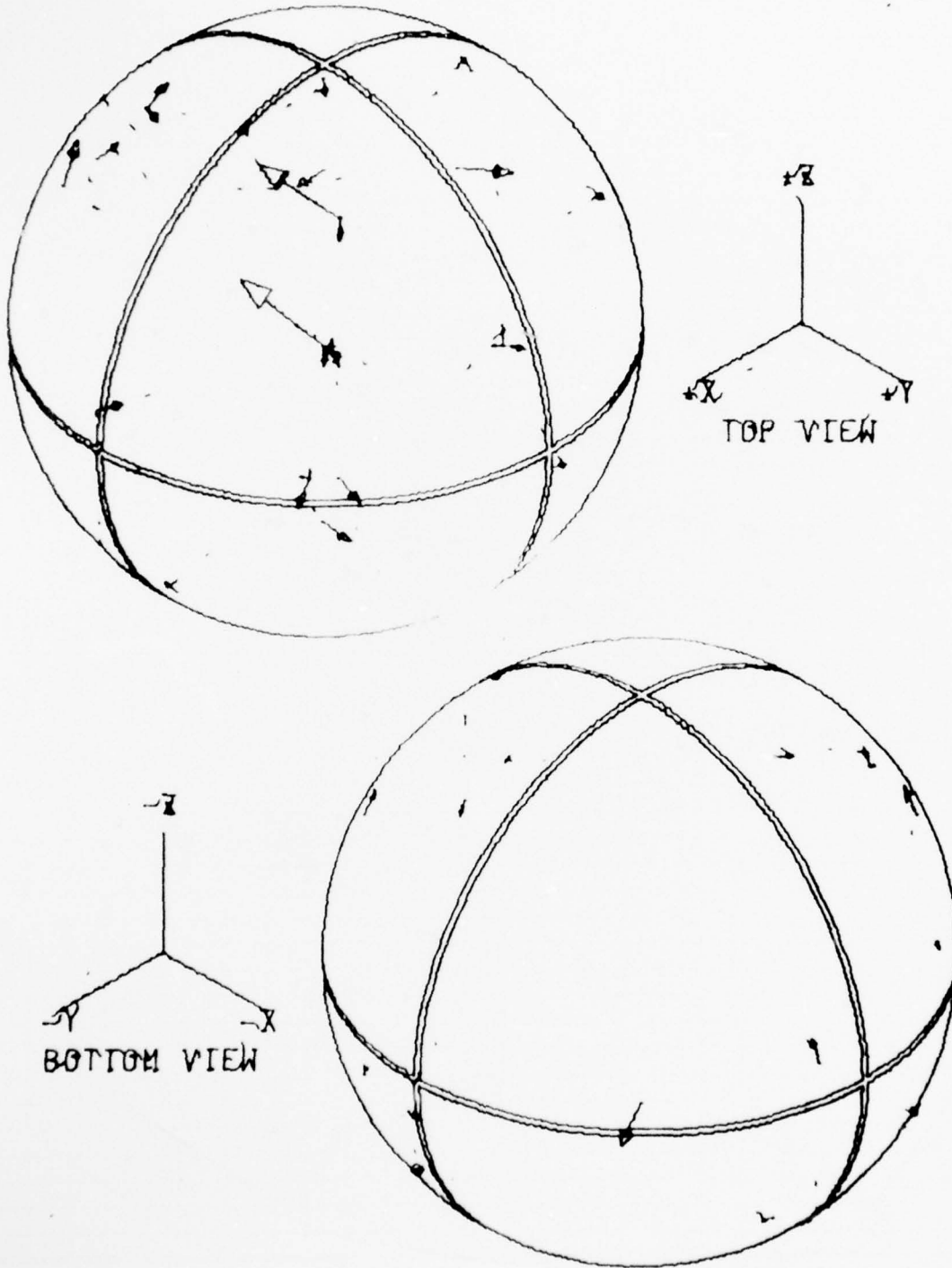


Figure 78. Gyro No. 1 Drift Calibration Residuals Using Drift Model K73

SCALE: 1 IN. = 0.05 DEG/HR

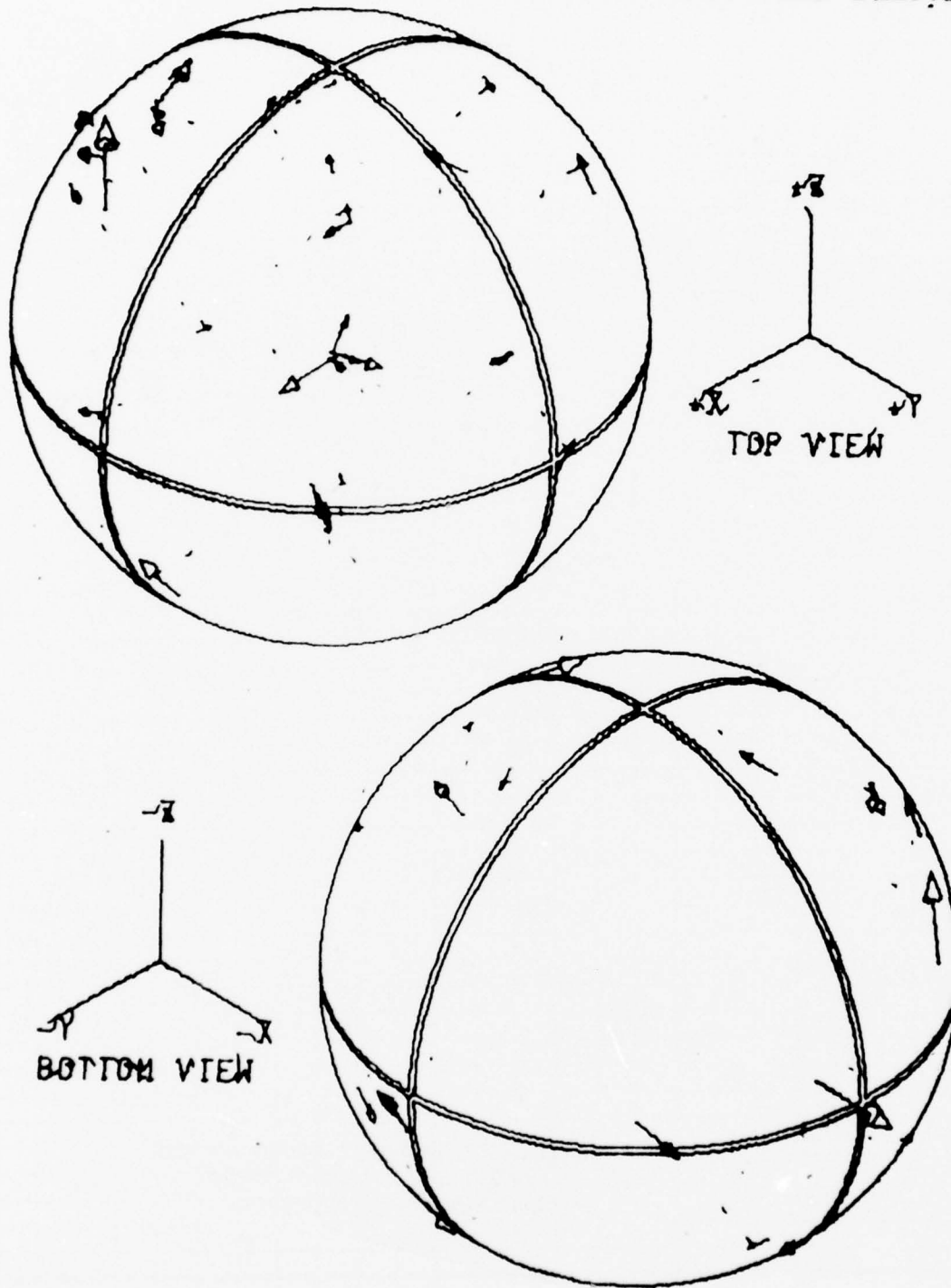


Figure 79. Gyro No. 2 Drift Calibration Residuals Using Drift Model K73

Under this task, the Y-level compensation program was modified and integrated into the drift calibration program. (The drift data must be compensated for angle readout errors). Also, the sub-program for computation of the measurement sensitivity matrices for the K73 model was modified from the specialized version used in derivation of the model, and this was integrated into the drift calibration program and checked out. This same sub-program was integrated into the angle calibration program. It is used for compensating the deterministic gyro drift during the time (about 1-1/2 hours) that data are being sampled for angle calibration. Both calibration programs were then checked out and verified by comparison of compensation residuals from calibration data which had been compensated independently with the "old" models.

#### 2.4.2.3 Change the Mechanization for Estimating Angle Readout Compensation Parameters

2.4.2.3.1 Background. Because the MESH is a "whole-angle" instrument, the angle readout biases must be computed as functions of the whole-angle readout. This functional relationship is approximated by a vector-valued polynomial with 56 polynomial coefficients. These are the 56 independent parameters that are used in compensating the angle readout biases of the MESH. Simultaneous estimation of 56 parameters is a formidable computational problem. Earlier attempts to mechanize this with a Kalman filter in 48-bit floating-point arithmetic were unsuccessful. The covariance matrix became non-positive definite, and the estimational accuracy went awry.

A method which did prove successful for the computational problem was a least-squares solution using Cholesky decomposition of the augmented matrix. This is a computational procedure for solving an overdetermined system of linear equations. The least-squares problem for angle calibration can be posed in general terms as that of minimizing the vector magnitude squared:

$$\|Ax-b\|^2$$

where

$x$  is the 56-rowed column vector of calibration constants (to be determined)

$b$  is the 420-rowed column vector of calibration data measurements

$A$  is a 420-by-56 matrix, composed of computed measurement sensitivity matrices

Cholesky decomposition consists of forming the matrix product

$$\begin{bmatrix} A \\ b \end{bmatrix}^T \begin{bmatrix} A \\ b \end{bmatrix} = \begin{bmatrix} A^T A & A^T b \\ b^T A & b^T b \end{bmatrix}$$

and taking its upper-triangular square root,  $R$ . That is,  $R$  is an upper triangular matrix (no non-zero terms below the main diagonal) and

$$R^T R = \begin{bmatrix} A^T A & A^T b \\ b^T A & b^T b \end{bmatrix}$$

(The algorithm for computing R is efficient. It requires in the order of 500 multiplies, whereas the product of two 56-by-56 matrices takes 175,616 multiplies.) It turns out that, by partitioning,

$$R = \begin{bmatrix} Q & z \\ 0 & s \end{bmatrix}$$

where

$$x = Q^{-1}z$$

and "s" equals the rss residual compensation error resulting from the estimate of "x" (the calibration parameters). The matrix square root and the inversion of the upper-triangular matrix "Q" each require in the order of 500 multiplies and adds. This is considerably fewer operations than the Kalman mechanization requires. This may be the reason that the Cholesky decomposition method is computationally more stable for this application.

Another advantage of the Cholesky decomposition (and one that was particularly important during development of the angle readout compensation models) is that the "z" vector corresponds to the calibration coefficients with respect to a Gram-Schmidt orthonormalization of the individual model terms. That is, the units of the z-coefficients are in radians of rss compensation, the total rss compensation is the RSS of all these coefficients, and the Kth coefficient represents the marginal rss compensation resulting from adding the Kth model term to the "composite model" of the previous (K-1) model terms. This type of information is particularly useful during model development for evaluating the relative compensation afforded by candidate model terms.

Besides the 56 model parameters, there are four other parameters which must be determined during angle calibrations. Two of these parameters are bias errors for the intermediate axis of the precision tilt table, because the vernier readouts on two setting positions of this axis are not sufficiently accurate and must be estimated from the data. The other two parameters define the inertial position of the spin axis, which must also be estimated from the data. However, due to drift, this direction does not remain constant. One drawback of the least-squares approach is that it has no provisions for optimal estimates of non-constant parameters.

The method that has been used for "open-loop" updating the estimates of the inertial direction of the spin axis is to repeat a tilt table orientation occasionally, so that the accumulated drift since the last repetition of the orientation can be measured directly. However, no attempt is made to infer the time-history of drift between repeated orientations. As a result, variations have been observed in the estimated parameters with different methods of drift compensation.

The Kalman filter mechanization with state vector dynamics is the correct model for problems of this type. It has provisions for allowing "drift" of states that are being estimated. The problem is to overcome the computational errors that make the Kalman covariance matrix meaningless. Square-root filtering is functionally equivalent to Kalman filtering, and the Carlson algorithm for covariance update is exceptionally efficient in reducing the number of computer operations which erode accuracy. The Carlson algorithm had been programmed for the drift calibration program under an IR&D task in Company Fiscal Year 1972, and programmed for covariance analysis of angle readout errors under Phase 2A. In both cases, no computational problems were encountered.

2.4.2.3.2 Approach. A Kalman filter model for the angle calibration process was developed to include: (1) random drift of the spin axis direction, and (2) residual unmodeled angle readout errors in addition to angle readout noise. The random drift is modeled by adding "process noise" variance to the variances of the two states which model the uncertainty in the true direction of the spin axis. That is,

$$\sigma_i^2(t_{n+1}) = \sigma_i^2(t_n) + \sigma_v^2(t_{n+1} - t_n)^2$$

where

$\sigma_v^2$  is the variance of net drift rate between the (n)th and (n+1)th samples of angle calibration data

$t_n$  is the time at which the (n)th sample is read

$\sigma_i^2$  is the variance of the uncertainty in the (i)th component of a unit vector along the rotor spin axis

The basis directions for components of the rotor spin axis are chosen so that the first two components are normal to the nominal direction of the rotor spin axis and the third component is parallel to the nominal direction of the rotor spin axis. Because the spin axis direction is represented by a unit vector, the first-variation of the third component with respect to spin axis direction is zero. Consequently, the first two components are sufficient for characterizing the problem.

In order to mechanize this model as a square-root model, it is important that the states with process noise be the first elements of the state vector. This is so that the "rss" algorithm for adding process noise to the square root of the covariance matrix can be made more efficient. That is, if the upper triangular square root of the covariance matrix can be partitioned as shown below:

$$\begin{bmatrix} A & B \\ O & C \end{bmatrix}$$

so that "A" is the square root of the covariance matrix of the states with process noise, and if

$$D = (AA^T + E)^{1/2} \text{ (upper triangular)}$$

where E is the process noise covariance, then

$$\begin{bmatrix} D & | & B \\ \hline O & | & C \end{bmatrix}$$

is the upper-triangular square-root of the covariance after adding process noise. That is,

$$\begin{bmatrix} D & | & B \\ \hline O & | & C \end{bmatrix} \begin{bmatrix} D & | & B \\ \hline O & | & C \end{bmatrix}^T = \begin{bmatrix} A & | & B \\ \hline O & | & C \end{bmatrix} \begin{bmatrix} A & | & B \\ \hline O & | & C \end{bmatrix}^T + \begin{bmatrix} E & | & O \\ \hline O & | & O \end{bmatrix}$$

By having the states with process noise in an upper-left sub-matrix, one can avoid having to square, add process noise covariance and take the square-root of all but the affected upper-left sub-matrix. In this case, the upper-left sub-matrix is dimensioned two-by-two. The algorithm for adding process noise in this case can be simplified to the following equations

$$A_{22}(t_{n+1}) = \left[ A_{22}^2(t_n) + \sigma_v^2 (t_{n+1} - t_n)^2 \right]^{1/2}$$

$$A_{12}(t_{n+1}) = \frac{A_{12}(t_n) A_{22}(t_n)}{A_{22}(t_{n+1})}$$

$$A_{11}(t_{n+1}) = \left[ A_{11}^2(t_n) + A_{12}^2(t_n) + \sigma_v^2 (t_{n+1} - t_n)^2 \right]^{1/2}$$

where "A<sub>ij</sub>" is the element in the (i)th row and (j)th column of the upper triangular square-root of the covariance matrix of state uncertainty.

The reason for wanting to treat angle readout noise separately from unmodeled angle readout bias errors is to be able to use this extra piece of information whenever a calibration sample is repeated. Whenever a calibration sample is repeated, the unmodeled angle readout bias errors for that sample will also be repeated, whereas the angle readout noise error will not be repeated. The rms magnitude of unmodeled biases is in the order of 0.05 milliradians per axis, and the rms noise is in the order of 0.01 milliradians per axis. Consequently, whenever a sample is repeated, the accumulated drift since the sample was last taken should be determinable to within the level of the 0.01 mrad noise. If the unmodeled biases error for a repeated sample are included as state variables, then these can be estimated also. This model is a true representation of the physical situation during angle calibration, and it removes the correlation that would otherwise exist between the measurement errors on repeated samples.

Actually, there is only one sample that is repeated throughout the data collection, but there are several samples that are repeated once. The sample that is repeated more than once is with the rotor spin axis nominally in the center of the No. 1 suspension electrode. The other repeated samples occur when a series of samples are taken between constant increments of the angle setting of the innermost tilt table rotation axis. In these cases, the last sample is taken after a complete rotation about the rotation axis, and is a repeat of the conditions on the first sample of the series. These "rotational closure point" samples are used only twice, and no other repeated samples are taken in between. Consequently, the states added for all the rotational closure points (RCP) can be shared in the Kalman filter. That is, the two components of the unmodelled bias errors for the first RCP can be modelled in the filter. After the repeat of that RCP, they can be replaced by the unmodelled bias errors of the second RCP. They can later be replaced by the third, fourth, fifth, etc. RCP's. Each time that the states are swapped, the estimated a priori value must be reset to zero, and the estimated covariance must be re-initialized to be uncorrelated with the other states. This covariance re-initialization is mechanized in the square-root filter more efficiently by putting these temporary RCP unmodelled bias error states next after the two states with process noise. Then the upper triangular square root of the covariance matrix can be partitioned as shown below:

$$\begin{bmatrix} \bar{A} & \bar{B} & \bar{C} \\ \bar{O} & \bar{D} & \bar{E} \\ \bar{O} & \bar{O} & \bar{F} \end{bmatrix}$$

where the sub-matrices "B", "D" and "E" contain the information for the covariances of the "temporary states." It may be shown that, if A is replaced by the upper-triangular square root

$$A \leftarrow [AA^T + BB^T]^{1/2}$$

and

$$B \leftarrow O$$

$$E \leftarrow O$$

$$D \leftarrow I_{\sigma} \text{ unmodelled}$$

Then the associated covariance matrix will have been re-initialized as required.

The treatment of drift and unmodelled errors are the only modifications needed for adapting the square-root filter for the angle calibration problem. The covariance update for measurements and the state estimation update use the algorithm of N. A. Carlson (Ref 6).

**2.4.2.3.3 Results.** The approach described in the previous section was coded and checked out. The results were verified on angle calibration data that had been processed by the Cholesky decomposition method, and the resulting parameters were compared to the "Cholesky" parameters by the comparison program CMPZE. The results show agreement to within 0.04 mrad rms per axis. This is within the expected variation due to drift effects. The method was further verified by comparing navigational performance of N57A-2 with parameters derived by both methods from the same data.

#### 2.4.2.4 Calibration Software Modifications

The instrument mounting orientations of all EPM sensors (2 FSG's and 3 EMA's) are different from those of any previous systems. The two FSG's have been rotated about five degrees from the N57A (and Gyro Test Station) orientations, in order to decrease overall system packaging height. The accelerometers were re-oriented with two input axes near the horizontal plane to minimize the impact of ESG scale factor errors on system navigational accuracy.

The calibration programs were modified to calibrate the sensors in the new orientations. The programs were modified in such a way that the same program can calibrate N73 (EPM) systems, N57A systems and single instruments on a Gyro Test Station.

The programs which collect the calibration data were modified for the EPM-to-HP2100 interface. The EPM system uses a new calibration approach, in which all high-rate real-time data smoothing computations are performed in the EPM dedicated processor, and the smoothed data are transmitted at a slow rate (a few words per second) to the Test Station Computer. This approach is much simpler to implement, and permits simultaneous calibration of several systems with one Test Station Computer. The resulting changes in the test station software decreased the size and complexity of each data collection program, making it possible to collect drift calibration data from two FSG's and calibration data from three EMA's simultaneously. There are now two data collection programs: "ANGLE" (which collects angle calibration data) and "DATA" (which collects drift data from the ESG's and/or smoothed calibration data from the EMA's). Both programs control the Goerz automatic tilt table or, if the system is mounted on a manual tilt table, request specific angle settings from a table operator.

The following modifications were also made in the test station software:

1. Data reasonableness testing was added for checksum of all HP2100/FPM data transmission, for word count verification, for FSG readout saturation, and for Goerz table settings.
2. "Retransmission request" modes were added to all HP2100/FPM transmissions, in the event of transmission errors being detected by the data reasonableness tests.
3. The FPM sequence counter value was made the standard time reference for all data. (The HP2100 clock had been used as the time reference.) This ensures that the same time reference will be used in compensation of errors as in evaluation of the relevant compensation parameters.

#### 2.4.2.5 Formatting and Scaling of Calibration Constants

A program was developed and checked out for generating calibration parameter tapes for FPM. This program uses five parameter files on magnetic disks (two of angle readout parameters, two of drift parameters and one of EMA parameters), scales and reformats them for EPM memory storage, and generates a punched paper tape for loading into DPU memory. The program also generates a magnetic disk file that can be loaded into DPU memory via the HP2100-to-EPM data link, and a printed software control document identifying all data and processing used in generating the parameter tape.

#### 2.4.2.6 1553A Data Bus Software

Software was developed and checked out for using the HP2100 computer on the test station to control a terminal on the 1553A Data Bus. The Data Bus hardware had previously been checked out with special test equipment. The test equipment was used for controlling the Data Bus for checkout of the HP2100 program. When this program had been checked out, it was then used for checking out the DPU program for transmitting on the Data Bus via the Data Terminal Unit.

#### 2.4.2.7 ESG Noise Diagnostic Software

A program named "LOOKC" was developed for a "look-see" at the noise characteristics of ESG data. This program was used in verification of the noise characteristics of the ESG angle readout electronics. The noise characteristics are determined from data collected by the DATA program, which is described in Para 2.4.2.4. LOOKC options include plots generated on the printer of angle readout noise, its Fourier content, or spatial characteristics. Other options include plots of signal magnitude and print-outs of direction cosines and smoothed  $\alpha$ - $\beta$ -data. The program was modified from a program developed for N77. Modifications were necessary for using the new data file formats. Other modifications were made for ease of operation of the program, so that less operator input and control is required for generating standard outputs.

#### 2.4.2.8 Real-Time Data Diagnostic Software

Three programs were developed for real-time collection of EPM data, and storage of the data on standardized files for plotting. One program ("RAWX") has the capability for simultaneous sampling of 512 consecutive samples of each of 20 different raw data variables in EPM memory. The specific variables which are sampled are specified by a block of addresses of the respective variables in DPU memory. Consequently, the RAWX program could be used for a number of purposes. It was used during software/hardware integration for verification of polhode damping control and demodulator frequency control, and for noise elimination in the angle readout electronics during hardware integration testing. It was also used for verification of the delays in control of the rotating element.

Another program was developed for collecting consecutive readings (at 64/sec) of the rotating element encoder for about 2-1/2 minutes (10240 samples). This program was used for verification of rotation control software. A sample output plot is shown in Figure 80. This plot shows the encoder readout values (in degrees) while the rotating element was turned around twice, and then turned off. Another output plot is shown in Figure 81. This is a "blow-up" of a turn-around sequence, with units as shown on the plot.

A third program (AVRAW) was developed for diagnosis of fast reaction test data. This program averages raw accelerometer outputs for five-second periods, and saves these smoothed values to standard data files for plotting. The program also saves 15 other variables, sampled at the mid-points of the 5-second intervals. The other variables include measured temperatures, ESG rotor-to-cavity gaps, and temperatures predicted by software thermal models. The AVRAW program was used for development and verification of fast reaction software.

#### 2.4.2.9 Assembler Development

INU software development was somewhat hampered by the complexity of its supporting assembly language. This language uses 372 3- and 4-letter mnemonics for op-codes, one for every machine instruction. This is unwieldy for software development. It was particularly limiting during software checkout, when it was necessary to scan lines of mnemonic code to find errors. It was decided to investigate the possibility of developing a new assembler before the problem arose. It was found to be feasible by going to outside sources, and a consultant (James Dean Smith) was retained for that purpose. The assembler was developed in time to support the development schedule, and a translator program was developed for translating code previously developed on the "old" assembler to the new assembly language. This software is now operational.

Some features of the new software which make it especially useful are the following:

1. The language uses only 110 mnemonic op-codes (versus 372 for the previous assembler), and the op-codes are truly mnemonic (which makes them easier to remember).
2. The language uses 21 assembler directives, many of which were not available before. New directives include MACRO, which defines a macro-assembly, and EXT, which defines external labels.
3. The assembler generates re-locatable modules, which can be linked and loaded by the linking loader program. This permits modularization of the system software so that one module can be modified without re-assembling the entire program.

The assembler is documented in the following publications which were prepared during this reporting period.

1. C76-1184/201, "MICRON Assembler User's Manual," Dec 1976
2. C76-1185/201, "MICRON Assembler Design Document," Dec 1976

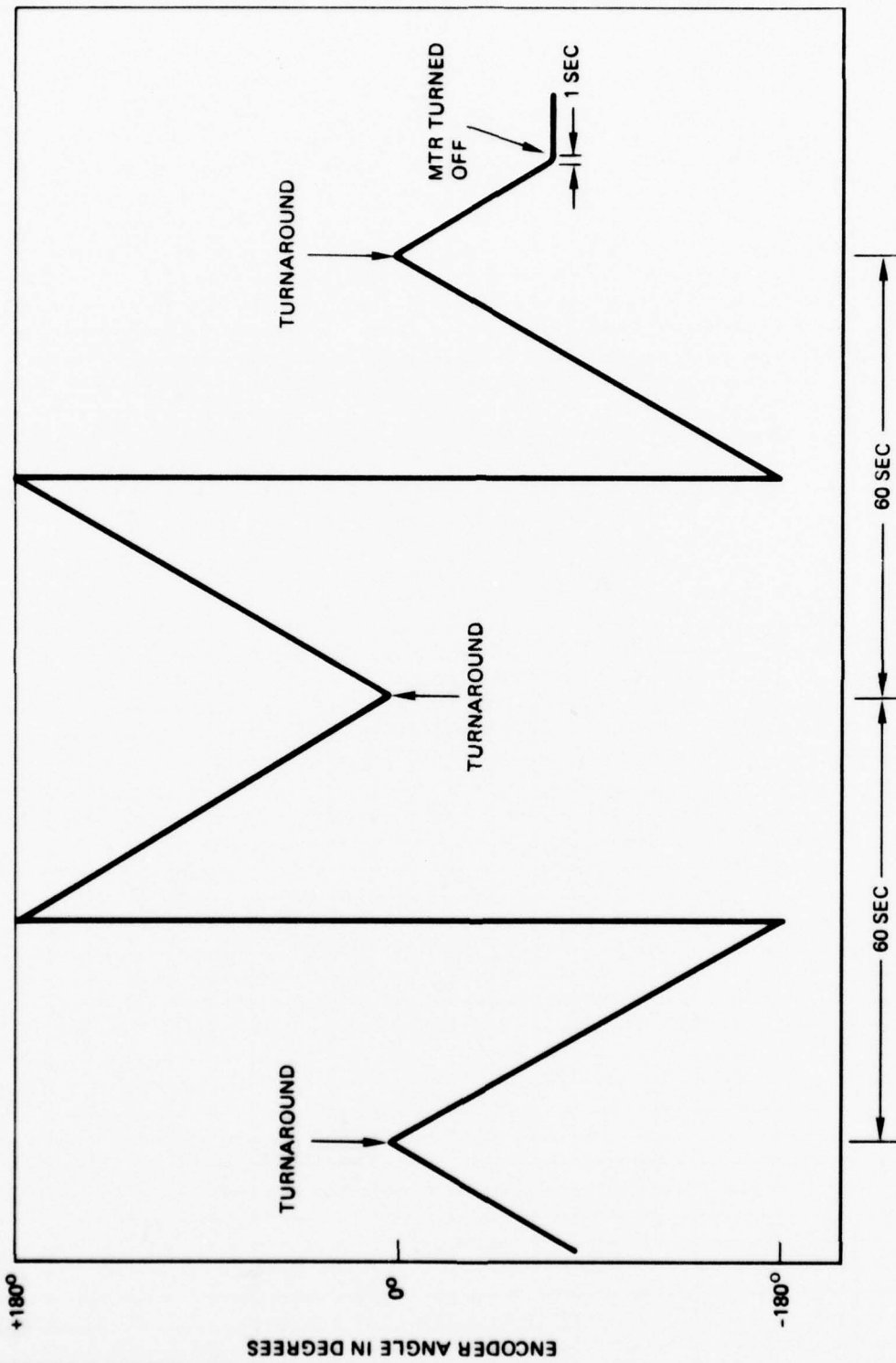


Figure 80. Encoder Readouts - First Run

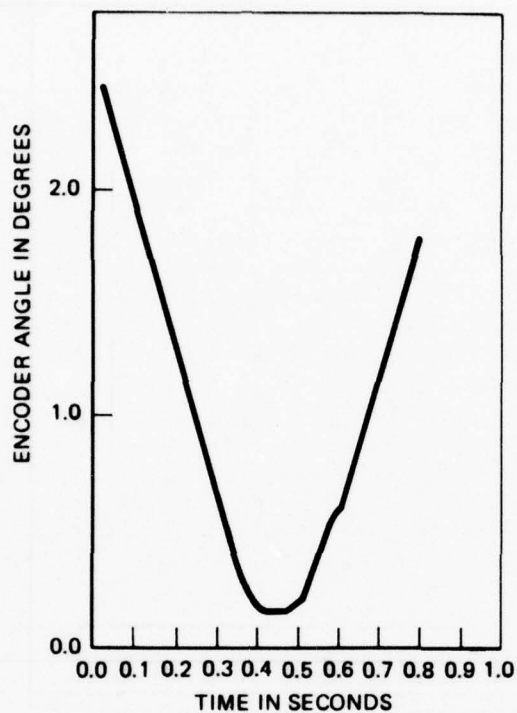


Figure 81. Encoder Readout During Turnaround

3. C76-1186/201, "MICRON Macro Assembler: MICRON Assembler Language Definition Reference Manual," Dec 1976
4. C76-1187/201, "MICRON Assembler Interpreter Description Manual," Dec 1976
5. C76-1188/201, "MICRON Linking Loader Description Document," Dec 1976
6. C76-1189/201, "MICRON Absolute Tape Punch Description Document," Dec 1976

#### 2.4.3 FPM System Data Analysis

This task was deleted from the contract per Reference 5.

## 2.5 TASK 1.5, INTEGRATION

The purpose of this task was to integrate the EPM to establish compatibility and operability of the INU, INBU, BU, CDU, STS, and software in accordance with the test plan developed in Task 2.1. This testing also included two demonstration navigation runs as defined in the Statement of Work, Para 4.1.5.

A summary of the tasks worked on during the period covered by this final report is as follows:

<u>Integration Task</u>	<u>Date Started</u>	<u>Date Completed</u>
Test Equipment Checkout	7 June 1976	11 June 1976
Integrated Wiring Test	15 June 1976	21 June 1976
INU Mechanical Interface Test	22 June 1976	22 June 1976
Power Verification Test	22 June 1976	23 June 1976
Timing and Sequencing Test	23 June 1976	23 June 1976
DPU and System Electronics Verification	24 June 1976	30 Sept 1976
Flight Tape Checkout	24 June 1976	25 February 1977
Rotating EPM Integration	2 August 1976	12 August 1976
Thermal Control Tests	30 August 1976	30 Sept 1976
BITE Verification	30 Sept 1976	2 Oct 1976
Spin Motor Electronics Checkout	2 Oct 1976	12 Oct 1976
MUM Demod and A/D Converter Checkout	11 Oct 1976	21 Oct 1976
Rotating IAU Integration	12 Oct 1976	30 Oct 1976
EMA Verification	13 Oct 1976	29 Oct 1976
Fast Warm-up Heater Checkout	16 Oct 1976	19 Oct 1976
System Computer Operation without Control Panel	21 Oct 1976	28 Oct 1976
MESG Verification	27 Oct 1976	8 Nov 1976
Calibration and Navigation Software Checkout	3 Nov 1976	19 Dec 1976
Calibration Verification Testing	3 Dec 1976	11 Dec 1976
Initialization, Alignment and Navigation Verification	21 Dec 1976	30 Dec 1976
Multi-Heading Navigation Testing	23 Dec 1976	25 February 1977

A detailed account of each of the above tasks is given in the following paragraphs.

#### 2.5.1 Test Equipment Checkout

Checkout and integration of the EPM and associated test equipment was begun on 7 June 1976.

During the checkout of the EPM Test Console, all test equipment functions and cabling were verified. Concurrently, all the applicable drawings were checked and red lined as appropriate. The Test Console checkout was completed on 11 June 1976.

#### 2.5.2 Integrated Wiring Test

On 15 June the EPM non-rotating housing was received in the integration area for checkout and subsequent system integration.

As defined in the MICRON EPM Integration Test Plan, C76-545/201, the first task undertaken was to verify all signal paths. Additionally, all signal paths were checked for isolation from one another, from the INU housing and from the ground paths. These tests were performed with the EPM INU housing and appropriate cabling and test equipment connected. When all circuits had been checked, the INU Housing was returned to the wiring area on 18 June for necessary corrections and/or additions.

Wiring corrections were accomplished and the INU Housing was again received in the integration area on 21 June. The corrections were verified and a megohmmeter was used to verify isolation of the high-voltage circuits.

#### 2.5.3 INU Mechanical Interface Test

A mechanical fit check was completed on 22 June. This included checking mechanical compatibility of the INU housing and the electronic modules, the inertial instruments, the INBU and mount, and all cabling not previously checked.

#### 2.5.4 Power Verification Test

Prior to performing the Power Verification Tests, the correct operation of all components integral with the INU Housing was verified. These tests included checking the power relays and the running time meter. At this point, 400 Hz, 3 $\phi$  power was applied to the system before any of the power supply modules were installed. The system was manually turned on and the presence of the 400 Hz power at the proper connectors was verified.

With the power off, the three power supply modules were installed. With the system on, the remainder of the connectors were checked to verify the voltages at the appropriate pins. In addition, all the connectors were checked to further insure that no power was applied to a pin not intended for that purpose.

As a part of the Power Verification Tests, the High Voltage Supply was installed and checked for proper operation. The Power Verification Tests were completed on 23 June 1976.

#### 2.5.5 Timing and Sequencing Test

Timing and Sequencing Verification Tests were begun in preparation for DPU Verification. The Timing and Sequencing Module, SEU No. 3, was installed and the signals generated by this module were verified. This task was accomplished on 23 June 1976.

#### 2.5.6 DPU and System Electronics Verification

On 24 June, DPU verification was initiated. The first objective was to successfully load and execute the Self Test Program. The primary problem encountered was the noise level on some of the critical signal lines. This problem was corrected in part by (1) eliminating ground loops introduced when using auxiliary test equipment to study the signals, (2) isolating various signal lines to eliminate noise pick-up, and (3) twisting signal lines with a ground line over its entire length.

The entire month of July was devoted entirely to DPU Verification. The major problem being worked was the inability to successfully run the CPU self-test program on the EPM, which verifies CPU operation and communication with the memory.

The first problem attacked was electrical noise on the ground and signal lines. By eliminating ground loops introduced when using auxiliary test equipment, isolating signal lines to minimize noise pickup, and verifying that the original system grounding scheme was optimum, the electrical noise was significantly reduced but the self-test program would still not run.

At this time, an alternate plan was instituted to replace functions, signals and power supplied by the EPM components and as close as possible duplicate the CPU bench level test configuration. With (1) an external commercial core memory, (2) an external oscillator providing the 9 MHz, (3) an external +5 vdc supply for the CPU, and (4) bypassing the CDU/Memory Adapter, successful running of the self-test program was accomplished on 16 July 1976.

Integration of the CDU/Memory Adapter was begun on 16 July. This effort continued through 22 July. It was found that noise on the CDU/Memory Adapter power supplies was coupling into the signals on the I/O and support modules. By changing the ground wiring within the CDU/Memory Adapter power supply, the self-test program would run with the CDU/Memory Adapter connected to the EPM and the I/O and support modules installed.

As a result of the noise levels observed on some of the signal lines, the design of all the cables carrying the critical signals was reviewed. On the basis of this review, it was decided to modify the spare cable which connected the Processor Control Panel to the CDU/Memory Adapter by twisting each memory address, memory input, and memory output line with a separate ground line. This cable modification was begun on 23 July.

In spite of a concentrated effort, continuous running the self-test program using the SEMS-9 memory could not be accomplished. On 26 July, the decision was made to proceed with integration using the external commercial core memory and investigate the SEMS-9 memory problem when the N73 EPM system began integration. This would free the EPM Hot Mockup to be used to solve the SEMS-9 problem.

Integration continued with the successful incorporation of all the internal power supplies and the 9 MHz signal being supplied by SEU 3.

On 27 July, the modified cable was completed and installed in the EPM. As a result of the improved transmission lines, successful operation with the SEMS-9 memory was accomplished. DPU verification continued with successful CDU and Printer integration. This effort was essentially complete on 30 July. It should be noted that

CDU and Printer integration required successful use of selected portions of the EPM Flight Program. The last problem encountered with the CDU integration manifested itself as very noisy CDU displays and random indications of a unintentional data transfer from the CDU to the system. The problems were solved by optimizing the CDU-EPM grounding and by adding decoupling capacitors to the CDU electronics boards.

On 3 August, integration of the Signal Generator and Memory Module, SEU No. 4, with the EPM Hot Mock-up was begun. It was found that the EPM Flight Program would not run when the 64 Hz interrupt was allowed to initiate a data transfer from the Processor Input/Output Module into the Computer Memory. While investigating the 64 Hz interrupt problem and during periods of minimal systems activity in this area, other portions of SEU No. 4 integration were accomplished. The SDO discrete operation was verified. The computer controlled rotor liftoff timing sequence as well as the signal outputs, i.e., 10 kHz, 40 K pps, etc., were also verified. These verifications were completed by 10 August.

After integration of the rotating EPM as reported in Para 2.5.8, Turn Off/On Sequence verification was resumed on 16 August. The problem of the PIO module not operating successfully in the DMA Mode, as described earlier, was now attacked. An intensive test effort was initiated and continued until the problem was isolated and corrective action taken. In summary, the problem can be stated as follows: there was a carry-borrow logic problem in the CPU in that if a cycle steal request occurred during the last bit time of an instruction with a carry bit generated out of the adder simultaneously, the logic incorrectly handled the carry bit. This caused the program counter to be incremented by one too many. The problem was solved by incorporating a logic change on the CPU module. This fix was verified on 25 August.

During the course of the carry-borrow investigation, another logic problem was identified and corrected. The problem was, briefly, that when the Processor Control Panel was in the "halt" mode and one wanted to command a register display mode, the PIO module was not prevented from initiating a DMA cycle. A logic change on the PIO module corrected this problem and was installed and the fix verified on 23 August.

In spite of the high level of effort on the above problems, there were still periods during which the EPM system was available for integration of functions not requiring the DMA capability of the PIO Module. These items are listed chronologically as follows:

<u>Date</u>	<u>Function</u>
13 August	Integrated EPM Test Connector Box with EPM and Test Console
13 August	Verified proper operation of the Processor Discrete Outputs (PDO)
17 August	Verified correct system turn-off sequence and proper rotor braking signals
18 August	Verified correct rotor suspension sequence
19 August	Verified correct operation of the Sequencer Discrete Outputs (SDO)

With the ability to run the Self Test program with the PIO DMA enabled, integration of those functions which require PIO DMA were initiated. The correct operation of the MUM Demod Reference Generators on SEU No. 4 was verified. The HP2100 Computer was integrated with the EPM Computer via the CDU/Memory Adapter. In addition the proper functioning of the MDO discrettes were verified on 28 August.

On 30 August a DPU problem was encountered which manifested itself as numerous illegal instructions during execution of the Nav program. As was the case when other computer problems were encountered, a concentrated effort was initiated to identify and correct this problem. On 3 September the problem was identified and the appropriate modifications were made on the CPU module. Briefly stated, the problem was that the program counter was not being incremented when an interrupt and cycle steal request occurred on successive cycles while executing an instruction fetch. Correct CPU operation was verified on 3 September.

In parallel with the work on the illegal instruction problem, continuity checking of the test IAU (the one without the twist capsule) was initiated. This task, including correction of wiring errors, was completed on 11 September. During the week of 7 September, the following items were accomplished:

1. Successful integration of SEU No. 1 and SEU No. 2
2. Integration of the High-Voltage Switch
3. Installation of the IAU including verification of the correct signals through the cabling and up to the Charge Amplifier connectors.
4. Integration of the Charge Amplifier modules up to and including successful suspension of the rotor on each channel.
5. Continued closed loop thermal control checkout.

On 14 September two rotors were successfully suspended simultaneously. The Battery Unit was installed and the Battery Test and Battery Fast Charge functions were reverified. Rotor suspension verification tests continued through the remainder of the week of 14 September with attempts to apply a torque disturbance to the gyro and monitor the charge on the rotor following a liftoff. Numerous hardware and software problems in both the HP and EPM computers were encountered and solved. Also, a problem of high resistance shorts between portions of the triax cables, which connect the suspension electrodes of the gyro to the Charge Amplifier outputs, was corrected.

On 30 September, successful power interruptions were accomplished. Both the 400 Hz power and the 28 vdc power can be interrupted with no effect on rotor suspension or system operation.

#### 2.5.7 Flight Tape Checkout

Flight tape checkout began on 24 June 1976 when it was first used during DPU integration. Clearly this was a tool to aid DPU integration but, nevertheless, selected portions of the tape had to function for the tape to be an effective tool.

Several times during the integration period, a new flight program computer tape was received. Each new version of the computer tape incorporated necessary changes identified while utilizing the previous version in addition to newly coded segments of

the full-up flight tape. For each updated tape, a short time was devoted to tape verification at the system level. This verification was done to ensure that those functions previously checked out still operated correctly.

In actuality, flight tape checkout is a continuous process. As additional hardware and/or functions are encountered in the normal sequence of system integration, the appropriate portions of the flight program are also exercised. Although all components of the flight program are checked out on the simulation station, final program verification is required at the system level.

Updated versions of the flight tape were integrated throughout the test period. On each occasion a short time was devoted to tape checkout.

#### 2.5.8 Rotating EPM Integration

In parallel with DPU and Electronics Verification, integration of the N73 EPM (rotating EPM) housing was begun. The housing was received in the Systems Test Laboratory on 2 August at which time continuity and Megger checks were initiated. The wiring continuity testing was completed on 6 August and the N73 EPM housing was returned to the Electronics Lab to correct the wiring errors. At the same time, continuity checking of the IAU and the IAU extender cabling was begun.

On 10 August, the N73 EPM housing was returned to the Systems Test Laboratory for verification of wiring corrections and resumption of system integration. The wiring corrections were verified and it was determined that the N73 EPM housing could then replace the EPM Hot Mock-up housing in the system integration effort. This change-over occurred on 10 August.

In order to bring the N73 EPM system up to the current status of the Hot Mock-up, the integration sequence and procedures employed during the Hot Mock-up integration were repeated with the N73 EPM housing. This orderly integration was again performed in accordance with the integration test plan developed in Task 2.1. The integration included (1) mechanical fit check of all modules, (2) verifying correct operation of all components integral with the EPM Housing, (3) power verification testing, (4) Timing and Sequencing Model, SEU No. 3, integration, (5) Processor Input/Output Module integration, (6) Signal Generator and Memory Module, SEU No. 4, integration, and (7) CPU integration. Integration continued with the addition of the CDU/Memory Adapter and the Processor Control Panel and with the successful execution of the self-test program. The EPM Flight program was loaded into the computer and the CDU and printer interfaces were reverified on August 12.

At this time, integration of the N73 EPM was essentially at the same point as was integration of the EPM Hot Mock-up on 10 August when the effort was shifted to the N73 EPM. It is significant to note that due to the experience gained and the problems solved during the integration of the EPM Hot Mock-up from 21 June 1976 through 10 August 1976, the same integration was accomplished on the N73 EPM in two days. The time accumulated on the Running Time Meters were 507 hr and 10 hr for the EPM Hot Mock-up and N73 EPM systems, respectively.

#### 2.5.9 Thermal Control Tests

The first function to be verified was the operation of the fast warm-up heater relays. This was completed on 30 August 1976. Thermal control loop checkout was begun on 30 August with open loop tests to verify the correct functioning of the various

individual hardware components and software functions which comprise the total thermal control system. These open loop tests were successfully completed on 30 August.

Closed loop thermal control was operationally checked and found to be correct. In preparation for further thermal control testing with the EPM housing closed, a Converter module was installed on 21 September. With the Converter module installed, rotor liftoffs could not be initiated. This problem was traced to incorrect installation of a signal inverter. The installation was corrected and normal system operation restored.

On 27 September closed loop thermal control tests were resumed. Several thermocouples were installed within the EPM housing at strategic points to establish the thermal control loop set points. By 30 September, long term rotor suspension with torque disturbance and charge monitoring was completed. During this time the thermal control loops operated successfully. In addition, the thermal set points were varied in order to determine the control thermistor scale factor.

#### 2.5.10 BITE Verification

BITE verification was initiated on 30 September. This task was successfully completed on 2 October after all the BITE functions applicable at this point in the integration had been verified.

#### 2.5.11 Spin Motor Electronics Checkout

Spin Motor Electronics checkout was initiated on 2 October 1976. After successful application of power to the spin motor power amplifier electronics, the correct functioning of the control discretes was verified. These discretes include (1) Spin Motor Enable, (2) Heat, (3) Damp, and (4) Brake Enable.

While attempting to verify the long shutdown and rotor braking sequences, it was found that the rotor braking sequence did not operate properly. The problem was that braking currents were applied only to the X and Y motor coils and no current to the Z coil. For proper operation, braking current should be flowing in all three coils sequentially, two at a time. This problem was perplexing in that the braking signals had been correctly verified on 17 August 1976. In addition, all the components were removed and tested in the electronics lab and found to be operating correctly.

Further system testing showed that the signals were correct when support power was on but were incorrect when a Power Control shutdown was initiated which turned off support power and accomplished the shutdown with critical power only. It might be noted that the 17 August testing was performed with the support power on.

The problem was traced back to the design of the three braking signals which are generated on SEU No. 4. All of the voltages and signals used to generate the braking signals were monitored with the support power both on and off. These tests showed a large noise spike on clock phase 1+2 of the 4-phase clocks. It was ultimately found that the noise spike was caused by using +5 v support on the PIO module for devices generating the 4-phase clocks instead of +5 v critical. The PIO module was modified to use +5 v critical and this action corrected the clock phase 1+2 noise spike problem, however, it did not correct the braking signal problem.

Testing continued to solve the braking problem. Ultimately it was found that by increasing the value of four resistors that were in series with the 4-phase clock lines going from the PIO module to SEU No. 4, the correct braking sequence was achieved.

The effect of the increased resistance was to slightly decrease the rise time of the 4-phase clock signals. The braking sequence was verified for both conditions, i.e., support power on and support power off, on 6 October 1976.

Testing of the Spin-up, Heat, and Damp functions was initiated on 6 October 1976. Initial attempts at commanding any kind of spin motor action other than braking resulted in program scrambles. This problem was worked continuously until its resolution on 11 October 1976. The solution consisted of (1) grounding the cases of the relays which enable the spin motor power and which select the motor coils to be energized and (2) removal of four wires from the cable between the EPM and the test point box which were no longer required at this level of system integration. These wires carry signals which are associated with initiating the A/D conversion of various signals and with initiating a PIO Direct Memory Access (DMA) cycle. Evidently noise spikes generated on other lines in the cable were coupling in and causing erroneous A/D conversions and/or PIO DMA cycles.

On 12 October 1976 operation of the Z-coil heat mode was verified as planned. Further checkout of the spin motor electronics is considered part of MESH verification, discussed in Para 2.5.17.

#### 2.5.12 MUM Demod and A/D Converter Checkout

MUM Demod and A/D Converter testing began on 11 October 1976. The intent of this testing was to determine the MUM readout noise due to the suspension and MUM electronics, the signal multiplexers, and the A/D converter. The technique employed was to ground the input signals at various points in the signal flow path and measure the readout noise at each step. This testing showed that a filter with a 1  $\mu$ sec time constant was required at the input to the A/D converter. This was necessary to suppress high frequency ringing occurring when the multiplexers switched the various signals into the A/D converter. The final test results indicated the RMS noise level to be acceptable and less than one least significant bit. This testing was completed on 21 October 1976.

#### 2.5.13 Rotating IAU Integration

Integration of the rotating IAU (including twist capsule) was initiated on 12 October 1976. The intent of this testing was to evaluate the performance of components peculiar to the rotating IAU, i.e., the IAU drive motor and the position encoder, and to evaluate rotor suspension integrity through the twist capsule.

The first item to be checked out was the IAU rotational drive motor and associated electronics. During the course of this checkout, three problems were identified and corrected. Drive motor overheating was resolved by adding a heat sink to promote better heat transfer to the cooling air. Computer halts due to reversing the IAU rotation direction were eliminated by adding a filter capacitor on the computer alive signal on the PIO module. The third problem encountered was noise coupling which caused the IAU drive motor to turn off when the direction was reversed. This problem was isolated to the IAU drive motor electronics board and the solution included redesign of the logic functions on that board. Checkout of this function was completed on 30 October 1976.

Testing of rotor suspension integrity through the twist capsule began on 15 October 1976 with successful lift-off being accomplished on both dummy loads and non-inertial grade gyros. On 24 October 1976 long term suspension integrity with a rotating IAU was begun while the rotors were being TD'ed and charge monitored. This testing was successfully completed on 26 October 1976 with no suspension electronics problems being encountered.

On 23 October 1976, encoder performance was successfully evaluated.

#### 2.5.14 EMA Verification

EMA verification was initiated on 13 October 1976. At this time, the intent was to verify EMA operation and correct functioning of the associated software. The software was checked by substituting an EMA simulator which outputs a known pulse rate and then monitoring the measured pulse rate via the software. The EMA's themselves were checked by monitoring the EMA pulse rate for three orientations of the EMA's with respect to gravity. This phase of EMA verification was completed on 14 October 1976.

After installation of the EPM on the Imperial table, EMA verification was resumed on 28 October 1976. A short version of the EMA calibration data acquisition sequence was performed. The results of this calibration indicated correct EMA hardware and associated software operation. EMA verification was completed on 29 October 1976.

#### 2.5.15 Fast Warm-up Heater Checkout

On 30 August 1976, the fast warm-up heaters were activated for the first time. The intent of this initial checkout was only to verify correct functioning of the heaters. A problem was encountered in that operation of the fast warm-up heaters caused computer resets. Due to other system problems, this checkout was terminated on 31 August and resumed on 16 October 1976. During this testing, the fast warm-up heaters were activated and deactivated numerous times with no computer halts. It is felt that steps taken to eliminate troublesome noise sources or otherwise desensitize the system to noise also eliminated the computer halts due to cycling the fast warm-up heaters. Fast warm-up heater verification was completed on 19 October 1976.

#### 2.5.16 System Computer Operation Without Control Panel

In order to perform system calibration and any system testing where space and/or conditions do not allow the processor control panel to be in close proximity, the system must operate without the control panel. Verification of this capability was initiated on 21 October 1976.

The first attempt at operation without the control panel revealed two problems. First, it was noted that after the computer was loaded and the control panel disconnected, only one successful power cycle with a short shutdown could be accomplished without a computer scramble. It was also noted that if a long shutdown was commanded with the computer alive circuit enabled, multiple power cycles could be performed with no computer scrambles. The difference is that during a long shutdown, the Support Power is turned off automatically while Critical Power remains on during the rotor braking period. When the Support Power goes off at least 30 ms before the Critical Power the memory protect function in the computer is enabled, thus preserving the computer program.

When a short shutdown is initiated, Critical and Support Power are turned off simultaneously. This problem was identified on 26 October 1976 and a sequencer design change was initiated which maintains Critical Power at least 30 ms after Support Power is turned off for any type of shutdown.

The second problem manifested itself as computer scrambles when communication with the HP2100 data acquisition computer was linked to the EPM computer. This link is required for calibration and functions correctly when the processor control panel is connected to the EPM. Upon reviewing the control panel and CDU/Memory Adapter drawings it was noted that the shield grounds on some of the computer signal lines were grounded in the control panel and, therefore, were floating when the panel was disconnected. By moving the shield ground point into the CDU/Memory Adapter, successful operation without the control panel was achieved. This was accomplished on 28 October 1976.

#### 2.5.17 MESG Verification

MESG verification was begun on 27 October 1976 with installation of the system on the Imperial 3-axes table. The move to the table was required because it is necessary to position the system at various attitudes during spin-up and damping checkout. After the move, all system functions were again verified on 28 October 1976. In addition, the stand alone MUAR (Mass Unbalance Attitude Readout) console was integrated on 28 October 1976. The MUAR console is required to provide visibility during spin-up and damping testing.

The first rotor was spun up on 28 October. During the time in which checks were being made to determine the spin axis attitude, an erroneous shutdown signal initiated a system shutdown. It was noted that rotor braking was not occurring and after the normal 64 second braking period, the system was turned off with the rotor at approximately full speed. The gyro was damaged and replaced.

A thorough investigation showed that the reason for the lack of rotor braking was that the 4 $\Omega$  clock load resistors had not been installed on the PIO module in the system. Prior to rotor spin-up, the braking sequence had been verified but only with the Support Power on.

In order to preclude the braking problem from recurring, all PIO modules were checked to insure that the 4 $\Omega$  loading resistors had been installed. In addition, a modification was added to the sequencer which would allow inhibiting of the 64 sec braking sequence, if required, so the rotors could be despun manually prior to shutdown. These modifications were implemented on 29 October 1976.

Rotor spin-up and damping checkout was resumed on 30 October 1976 with initial testing of the gap sensing hardware and software. The spin motor power waveforms as commanded by the computer and then generated by the Spin Motor Power Amplifier (SMPA) Electronics were verified for both the spin and damp functions. A gyro rotor was spun to operating speed and after preliminary damping signal phasing measurements, the first successful rotor damping was accomplished on 1 November 1976.

In order to characterize the spin motor regarding gain and phase of the torques applied by the three motor coils, the rotor was subsequently spun up at all eight plate centers in addition to along the X, Y, and Z axes. During this motor characterization,

the signals generated by the SMPA as well as the actual current waveforms in the motor coils were also verified.

Spin and damp function checkout was completed on 4 November 1976 with the successful spin-up and damping of both gyros. Rotor spin-ups required approximately seven seconds each and polhode damping required approximately 30 sec each. These times are comparable to those required to support the reaction time requirements.

In order to continue with the Z-coil heating and rotor temperature stabilization (fine heating) portions of MESH verification, it was necessary to establish the steady state gap between the rotor and the cavity. This also required verifying the correct operation of the control heaters on the Instrument Assembly Unit (IAU). The IAU was instrumented with a number of thermocouples so that an independent temperature measurement of the various components could be obtained. Thermal control checkout was initiated on 4 November 1976 with installation of the IAU in the EPM Housing. The thermal control loops were enabled sequentially so each heater circuit could be monitored continuously until thermal control was obtained. With all thermal control circuits operating, the system was allowed to seek thermal equilibrium. At that point the thermal set points were established to achieve approximately a 50 percent duty cycle on all heaters. This closed loop thermal control testing was completed on 5 November 1976.

During the above thermal control testing, the rotors had been left desuspended to allow them to also reach the steady state temperature. Preliminary checkout of the gap sensing circuitry had been accomplished on 31 October 1976. At this time the suspended and desuspended rotor gaps were established with the rotors at their operating temperature of 160°F. It should be noted that a gap measurement is peculiar to a given gyro and must be reestablished when a gyro is changed.

With steady state gap measurements determined, checkout of the Z-coil heating and fine heating functions resumed on 6 November 1976. The first function verified was Z-coil heating. A rough measurement indicated the rotor heating rate to be approximately 114°F/min. This is well above the required minimum heating rate of 80°F/min. The fine rotor heating and degaussing functions were also verified. With the successful verification of all the spin motor functions, MESH verification was completed on 8 November 1976.

#### 2.5.18 Calibration and Navigation Software Checkout

This integration task was initiated on 3 November 1976 with checkout of the adapter cables required to enable EPM installation on the Goerz 3-axes tilt table. The cable checkout was completed on 7 November 1976 including the correction of identified deficiencies.

On 8 November 1976 the EPM to Goerz mounting hardware was installed in the Goerz. During a period when the EPM was off, the power cables were attached to the Goerz adapter cables and the EPM power transmission through the Goerz sliprings was verified.

Prior to installing the EPM on the Goerz, three drift data samples were obtained. Reduction of the data gave an rms angle readout noise measurement of between 0.02 mr and 0.03 mr. All of the noise measurements were less than the 0.03 mr rms required for acceptable system navigation performance.

The EPM was installed on the Goerz on 9 November 1976. During preliminary checkout and while power was applied to the system bypassing the Goerz sliprings, the system experienced a rotor drop while spinning, thus damaging the gyro. Subsequent investigation showed the rotor drop was due to lack of preload. The preload was lost due to a short on the 10 kHz signal used in the generation of the preload signal. When the system was disassembled, a small sliver of wire was found lodged under one of the 10 kHz signal lines. Apparently the wire moved while the rotor was spinning, shorting out the 10 kHz signal to ground.

The gyros were replaced with non-inertial grade instruments, and the system was thoroughly checked out prior to installation of inertial grade gyros.

On 14 November 1976 inertial grade gyros were installed in the system and system operation was verified prior to reinstallation in the Goerz. Steady state gap readings were determined and another 30 minute drift sample was obtained. Again, all of the angle readout noise measurements were less than the required 0.03 mr rms.

The system was reinstalled on the Goerz on 17 November 1976. After balancing the Goerz table, system operation was again verified while bypassing the Goerz sliprings.

The first attempts to apply power to the EPM through the Goerz sliprings were unsuccessful. It was found that there was a large voltage drop through the sliprings on the 28 vdc power being supplied to the CDU/Memory Adapter Box. This problem was corrected by installing a variable voltage power supply capable of outputting 40 vdc. It was found that the supply had to be set to 34 vdc in order to supply 28 vdc at the CDU/Memory Adapter connector. Successful operation on the Goerz was achieved on 18 November 1976.

The first EMA calibration was performed on 18 November 1976. The data was reduced and the results indicated that the X-EMA was not operating correctly. In order to do an initial checkout of the gyro data collection and reduction programs, it was decided to spin-up the gyros prior to replacing the EMA. When polhode damping was attempted it was found that the No. 1 Gyro rotor could not be successfully damped. Repeated attempts also were unsuccessful. It was determined that the mass unbalance on this particular rotor was such that it was difficult if not impossible for the computer program to recognize the polhode family in which the rotor has been spun-up. The system was removed from the Goerz and both the No. 1 Gyro and the X-EMA were replaced. Subsequent testing of the EMA at the component level verified the failure.

The system was reinstalled on the Goerz on 20 November 1976. An EMA calibration was performed with acceptable results. It was intended to spin and damp the gyros in order to resume drift and angle calibration checkout. However, an oscillation on one of the Charge Amplifier boards was again present. This oscillation had been noted on two previous occasions but had disappeared when the Charge Amplifier modules reached operating temperature. The problem had already been isolated to poor feed-through holes on the teflon based Charge Amplifier multilayer boards. Fiberglass based boards were being fabricated as replacements. The fiberglass boards were not to be ready until approximately 27 November 1976 and rather than delay testing until that time, the decision was made to continue integration testing if the oscillation was not present. On this occasion the oscillation did not disappear when thermal stabilization was achieved. This required changing the Charge Amplifier.

The next three days were devoted to reestablishing good system operation to allow resumption of calibration checkout.

On 23 November 1976 the system was again operating on the Goerz. An EMA calibration was performed with acceptable results.

The remainder of November was devoted to resolving problems associated with angle and drift data acquisition and reduction. The programs which provide the communication link between the EPM Computer and the HP2100 data acquisition computer were debugged. In addition, a similar effort was underway on the gyro angle and drift data acquisition and reduction programs.

The gyro angle readout and drift data acquisition and data reduction programs checkout effort was somewhat interrupted due to an oscillation on one of the Charge Amplifier modules. The oscillation had previously been isolated to a poor feedthrough hole on the teflon based multilayer board. Fiberglass based Charge Amplifier modules were received on 24 November 1976 and, since the system had been off during the Thanksgiving holidays, these new Charge Amplifier modules were installed on 29 November 1976. The IAU was reassembled and the system installed on the Goerz 3-axis table for resumption of the software checkout.

From time to time during November, the triax cables which connect the Charge Amplifiers to the suspension electronics had to be changed or repaired. These problems resulted largely from handling and were mostly mechanical in nature. To eliminate this type of problem, the triax assembly was modified so that the cables were significantly more flexible.

On 3 December 1976, the first EMA data acquisition and calibration was successfully completed. The calibration results compared favorably to those obtained at the component level.

After identifying and correcting several software errors in both the data acquisition and data reduction programs, the first successful gyro angle readout calibration was completed on 4 December 1976.

From time-to-time, beginning on 30 November 1976, it was noted that for short periods it appeared that the EPM thermal control loops were acting like a full-on/full-off system rather than a proportional control system. Great difficulty during polhode damping of the rotors was experienced occasionally. Also, other problems periodically appeared which were related to portions of the software which had been previously operating correctly. On 4 December 1976 these problems were all attributed to a problem associated with one of the data transmission lines between the A/D converter and the computer. The data line in question would, on occasion, remain "one" set. The data line was instrumented and monitored. However, after instrumentation, the problem never reoccurred. It is felt that the work done to instrument the data line corrected the problem.

On 9 December, after being up and spinning for several hours, the gyro rotor in the No. 1 channel incurred a full-speed drop. The P2 connector on Charge Amplifier No. 1 was found to be not fully engaged although it was tightly secured. Disengagement revealed that the teflon sleeves inside the connector halves were misaligned and damaged showing evidence of interference when trying to engage. The center conductors

had apparently only made a point contact when assembled (there is a continuity check at assembly) and, due to thermal conditions within the IAU, had become intermittent. This intermittent condition affected signal transmissions from the Charge Amplifier output to the -2 plate of the gyro. The connector was repaired, the IAU reassembled, and the suspension servo operation successfully reverified.

At this time, the software checkout was temporarily suspended in order to rework a portion of the EPM wiring. Several wiring connections had been broken while system rework and/or repair was being accomplished. Since a full up system calibration was essentially next, this opportunity was taken to rework all wiring which had caused problems and/or were potential problem areas. The wiring rework was completed on 9 December 1976.

The first total system calibration was completed on 11 December 1976. This included EMA calibration, gyro angle readout calibration, gyro drift calibration, and generation of instrument parameters to be used with the navigation program. At this time, checkout of the navigation program on the system commenced. It should be noted that considerable navigation program checkout had been accomplished prior to this time utilizing a system simulator program. During the initial checkout numerous navigation runs were attempted. Several program corrections and/or modifications were accomplished as a result of these navigation tests. Since it was advantageous to compare the EPM results against the performance obtained on the earlier N57A systems, these checkout navigation runs were performed without employing the IAU rotation capability.

On 13 December 1976, it was noticed that the rotor speed on the gyro in position No. 2 was changing up to 4 Hz as the attitude of the EPM housing was changed. This necessitated changing the servo notch hybrid on the gyro No. 2 suspension servo module.

After verifying rotor speeds with the new module, a calibration sequence was initiated on 14 December 1976. Navigation program checkout continued with the identification and correction of several navigation program errors. These errors included improper mechanization of the vertical velocity compensation and improper positioning of the rotor spin axes during spin-up and damping.

In spite of correcting all identified errors in the software, navigation data continued to exhibit large errors due to gyro drift. It was speculated that these drift errors might be due to a magnetic sensitivity associated with the IAU rotational motor and electronics and, hence, EPM housing fixed. A special test was performed to test this hypothesis. The results of this test indicated that the uncompensated drift rate was IAU fixed and not a housing fixed magnetic effect. Since the drift rate was IAU fixed and also similar in nature on both gyros, three terms were added to the drift calibration model which effectively eliminated the large uncompensated drift errors.

A set of calibration data was reprocessed with software updated to include the three additional drift terms and on 19 December 1976 the first successful navigation run was obtained. The run duration was 3 1/2 hours with 90° heading changes every 40 minutes. This nav run was made without the IAU rotation feature. The results were as follows:

<u>Duration (hours)</u>	<u>Position Error (nm/hr)</u>	<u>Time RMS per Channel Velocity Error (ft/sec)</u>
0 - 2	0.78	3.58
0 - 3 1/2	1.17	3.63

Non-rotating navigation checkout continued through 20 December 1976 although Calibration and Navigation Software Checkout was completed on 19 December 1976 when the first successful navigation run was achieved.

#### 2.5.19 Calibration Verification Testing

Although this task is identified separately in the integration test plan, the very nature of what was required to complete the Calibration and Navigation Software checkout included the requirements of this task. This task was essentially initiated on 3 December 1976 with the first successful EMA calibration and was completed on 11 December 1976 with the successful generation of a set of instrument navigation parameters.

Calibration Verification required (1) comparison of instrument level calibration data with equivalent data at the system level, (2) computing the calibration residuals by compensating the calibration data with the calibration coefficients, and (3) verifying instrument navigation parameter scaling in the navigation software.

Instrument parameter comparison and calibration residual computation were two vital tools used to effect Calibration Software Checkout. Until the system level calibration results agreed closely with those obtained at the instrument level, one could not be assured that the system level calibration software was indeed performing as required.

Parameter scaling was verified by the successful generation of a set of instrument navigation parameters. This could not have been accomplished if the parameters exceeded predetermined limits.

#### 2.5.20 Initialization, Alignment, and Navigation Verification

This task was initiated on 21 December 1976. During the angle calibrations performed prior to the alignment and navigation testing, it was noted that the repeatability of selected angle parameters on gyro No. 2 were poor. Further, it appeared that each parameter in question toggled between two distinct values. Numerous angle calibrations across power cycles were performed in an attempt to isolate the problem. During these calibrations, hybrids on SEU No. 2 most likely to produce the phenomenon were interchanged. In all cases the parameter instability remained. The conclusion was that the problem was associated with the gyro No. 2 Charge Amplifier. Since it was deemed that the parameter instability was not too large to jeopardize the navigation performance, this task was resumed on 23 December 1976. The system was calibrated and after performing two short non-rotated navigation runs, the first rotated navigation run was attempted on 27 December 1976. Several alignments followed by short navigation runs were performed at headings of both 0 degrees and 90 degrees. It was noted that during all the alignments an oscillation with a period of approximately two minutes was noted on the estimates of drift rates. This is also the period of the IAU rotation. In addition, all except one of the navigation runs following the alignments were aborted

at various intervals prior to the normal two hour termination due to computer resets and/or program scrambles. In almost all cases the navigation performance would have been well within the required levels if the run had continued for the normal two hours.

In spite of the truncated navigation runs, this testing did show that there was little or no effect due to aligning at different headings. Also, since most of the navigation runs were performed across shutdowns, system initialization was verified whenever the system was powered up. This task was essentially completed on 30 December 1976.

The computer resets and/or scrambles encountered during this testing were attributed to noise pulses generated by the IAU rotation motor power supply and switching module. All during this testing steps were taken to eliminate the noise source or at least desensitize the system to the noise. On 30 December 1976, two successful navigation runs were obtained with no resets. It appears that the problem was solved.

The drift estimate oscillation noted during the alignments was minimized by incorporating the five state alignment filter in the navigation program. The original alignment filter had three states, namely drift rate, velocity, and tilt. The two additional states are used to estimate EMA and gyro angle readout cyclic effects due to the IAU rotation. It should be noted that the five state filter was always planned for use with the rotating system. However, the three state filter (N57A design) was originally used on the EPM for comparing EPM test data with N57A test data and to preclude the introduction of additional variables during the early integration stages.

#### 2.5.21 Multi-Heading Navigation Testing

On 23 December 1976 multi-heading navigation testing was initiated. The plan was to perform these tests concurrently with the tests required to accomplish the requirements outlined in the previous two sections. However, most of the navigation runs were inadvertently aborted prior to two hours. After desensitizing the system to the noise produced by the IAU rotation system, navigation runs were accomplished on 30 December 1976.

During a navigation run on 2 January 1977, Gyro No. 2 experienced a high-speed drop thereby damaging the instrument. All diagnostic tests performed at the time indicated the rotor drop was due to a faulty Charge Amplifier. The gyro and Charge Amplifier were replaced and the system was recalibrated. The navigation runs, starting with the 0 deg heading run, were resumed on 6 January 1977. About one hour into this first navigation run, Gyro No. 2 again suffered a high-speed drop.

This rotor drop had all the characteristics of the previous drop. A thorough review of the test sequence showed that the major difference between system operation during the navigation runs and all other testing such as calibration, etc, was that the IAU was rotating only during navigation. With this in mind, that function including the twist capsule circuits were thoroughly evaluated. It was found that one of the circuits carrying a signal to Gyro No. 2 was intermittent at a particular position of the twist capsule. All the other circuits through the twist capsule were checked and no other problems were identified. A spare circuit was used to replace the faulty circuit and correct system operation was verified.

Another gyro was installed in the No. 2 position on 9 January 1977 and system calibration began. It is felt that this twist capsule was in fact the cause of both rotor drops. After completion of system calibration, navigation testing was resumed.

On 12 January 1977 a third high-speed rotor drop occurred. A thorough investigation showed that this drop was due to a failure in the High Voltage Switch module. The High Voltage Switch failure was verified at the component level.

On 14 January 1977 the gyro and the high voltage switch were replaced and the system prepared for recalibration.

In parallel with the recalibration preparation, fast warm-up testing was initiated. Initial tests were conducted to verify the component heating rates. Z-coil rotor heating was also verified. This effort continued through 21 January 1977.

A problem with the No. 1 Charge Amplifier was noticed on 21 January 1977 and the Charge Amplifier was subsequently replaced. In addition, several problems with rotor suspension were encountered and ultimately traced to an intermittent signal required during the rotor suspension sequence. The suspension problem was resolved on 28 January 1977.

While the system was being checked prior to recalibration, fast warm-up and automatic sequencing testing was resumed. The first fully automatic start sequence from power-on through rotor spin-up, damping, etc, to the point where the system was ready to begin alignment was accomplished on 28 January 1977.

The system was calibrated and nav performance testing started. Nav runs obtained on 3 and 4 February as well as nav runs being obtained on another EPM system (non-contract effort) indicated a problem associated with the alignment mechanization. Numerous alignments followed by short nav runs were made to identify and correct this problem. Simply stated, the problem occurred in the transition from the nav standby mode to the alignment mode. During this transition, the routine which normalized the spin frame to nav frame transformation would overflow if the initial vectors were significantly different from unit length. This problem was eliminated by including protection against this overflow in the software.

During the investigation of the alignment mechanization problem, a gyro drift which was caused by a beat frequency between one gyro rotor and the demod reference of the other gyro was encountered. The system had already been mechanized such that the two rotors ran at frequencies different by approximately 7 Hz. Since the demod reference frequencies were 5 Hz less than rotor speed, one of the demod frequencies was very close to the other rotor speed, causing the beat frequency. Although the exact coupling mechanism was not isolated, the problem was solved by setting the demod frequency of the higher speed rotor to 5 Hz above that speed. With this software modification, all the rotor and demod reference frequencies are separated by at least 5 Hz thereby eliminating any beat phenomenon.

On 14 February, nav performance verification runs were made with the corrected software program. These runs demonstrated that the problem had been corrected.

On 15 February, a change was incorporated on the SEU 3 Sequencer Module based on EPM 2 (non-contract) experience. This change provided a more positive means of insuring that once the gyros have been spun-up a long shutdown (with rotor braking) rather than a short shutdown (without rotor braking) will be initiated by the system sequencer when it receives a shutdown command from either the CDU or the system computer.

Previous shutdown problems had been experienced due to noise transients caused by other equipment power cycles and by test equipment being connected/disconnected. The system was moved to a van where the power transfer and test equipment configuration is much more representative of an aircraft configuration. Initial checkout and power transfer tests were successful. However, on 17 February, a full speed rotor drop occurred on the No. 1 gyro after a van power circuit breaker opened.

Subsequent investigation revealed that, when the circuit breaker opened, the 400 Hz motor-generator began to coast down. The system properly sensed the power loss and transferred to battery power. (The normal sequence for the system is to wait 10 seconds and if the 400 Hz power has not been restored, an orderly shutdown sequence will be started. However, during this particular test start sequence the 10 second shutdown was not enabled for test reasons and the system stayed on battery power.) About 30 seconds after loss of power, the circuit breaker was closed by an operator. The system did not transfer off battery back onto line power as expected. (This was determined to be because as line voltage and frequency are slowly brought back up, the power sensing logic circuitry will not detect that line power is back on.) The system shut down dropping the No. 1 gyro rotor (it was the only gyro spinning) when the battery was drained and could no longer support the system. The gyro was replaced and the system had started calibration when the contract period of performance was terminated.

#### 2.5.22 Fast Reaction Summary

Although the contract period of performance limitation precluded completion of the fast reaction testing, initial test results looked promising. Start up (suspension, spin, polhode damping and heating) times were 3 1/4 minutes versus the three minute budget for room ambient start ups. This testing did show uneven heating rates between the two Charge Amplifiers. A short term solution has been to adjust the heating by changing the software controlled fast warm up heater cut-off temperature. Eventually, however, a change in fast warm up heater sizing is indicated.

Gyro Compass alignment times (five minute budget) are between five and six minutes from a thermally stable warmed up condition. Thermal transient effects were not able to be evaluated within the Integration testing time period.

#### 2.5.23 Navigation Performance Summary

This section of the report summarizes the navigation performance data obtained during integration testing of the contract system (EPM 1). In addition, during this same test period (through 25 February 1977) a second unit of the same design (EPM 2) was fabricated and tested with non-contract funds. Performance data from EPM 2 testing has been included in this report for comparison purposes and to provide a broader statistical base for evaluation of the inherent navigation performance capabilities of this EPM design. A summary table is included in this section of the report. Individual navigation plots as well as ensemble CEP and velocity error curves are contained in Appendix N.

Two demonstration navigation runs were required by the contract. One run was to be made from an initial 0 degree heading during gyrocompass alignment with two 90 degree heading changes during the two hour navigation period. The second run was to be made from a 180 degree heading during gyrocompass alignment with two

90 degree heading changes during the two hour navigation period. The position error (CEP) for these two runs (No. 1230761825 and No. 1230762239) was 0.71 nmph as compared to the 1.0 nmph requirement and the 0.8 nmph goal.

During the test period, a number of navigation runs were made for performance evaluation on both EPM 1 and EMP 2. These runs were made under varying conditions e.g. some were with heading changes and some were with tilts made during the navigation period. Data from these runs is summarized in Table 42. These twenty eight navigation runs demonstrate performance well within the contract requirements.

TABLE 42. EPM NAVIGATION PERFORMANCE SUMMARY

	Contract		EPM 1	EPM 2	EPM 1 & EPM 2
	Requirement	Goal			
Position Error Rate CEP (nmph)					
1st Hour	1.0	0.8	0.36	0.25	0.28
Total Run	1.5	1.0	0.41	0.27	0.33
Time RMS Velocity Error (fps)					
North Channel	3.9	2.5	1.66	0.79	1.36
East Channel	3.0	2.5	1.06	1.54	1.31

## SECTION III

### TASK 2, TEST AND EVALUATION

#### 3.1 TASK 2.1, TEST PLANS

This task included the development of test plans for integrating the FPM and for testing the FPM in the laboratory. Test plans were also developed for second-source rotor and cavity tests, for non-destructible rotor and cavity tests, MESH prefunctional tests and accelerometer performance and environmental tests. The task to develop test plans for testing the FPM in the van and at LAX was deleted from the contract per Ref 5.

The following test plans were completed and submitted in April 1976 as CDRL Item A00D:

1. MICRON EPM Integration Test Plan (C76-545/201)
2. MESH Test Plan (C76-273/201)
3. A77M Accelerometer Test Plan (C76-566/201)

The MICRON EPM Integration Test Plan defined the tests required to integrate the modules/subassemblies of the INU and to integrate the INU, INBU, BU, CNP, and STS. *The orderly manner for integration established in the test plan was based upon the functions and partitioning within the INU.* The INU integration tests defined in the test plan were as follows:

1. Subassembly/Subsystem Integration Tests
2. System Software and Calibration Verification Tests
3. Navigation Performance Tests
4. External Interface Verification Tests
5. Reliability Screen Tests

The MESH Test Plan defined the prefunctional tests to be performed on all MESH units fabricated during the Phase 2B contract. This document also outlined the tests to be conducted on second-source and non-destructible rotor and cavity sets.

The A77M Accelerometer Test Plan defined the tests to be performed on the A77M accelerometers fabricated during the Phase 2B contract. The tests defined in the test plan were the functional test, performance test, and environmental test.

A test plan for FPM laboratory testing was prepared. This test plan (C76-1578/201) consisted of four parts and included plans for the following tests:

1. Stability, heading sensitivity, and tilt sensitivity testing

2. Scorsby and rate testing
3. Fast reaction, hot and cold soak testing
4. Vibration and shock testing

A draft copy of Part 1 (Stability, heading sensitivity, and tilt sensitivity testing) was provided to AFAL in December 1976. The final version of Part 1 was submitted in February 1977 as CDRL Item A00D. Draft copies of Parts 2, 3, and 4 were provided to AFAL in February 1977. The final versions of Parts 2, 3, and 4 were in final type at contract completion and consequently were not formally submitted as CDRL data items.

### 3.2 TASK 2.2, DEVELOPMENTAL TEST

The purpose of this task was to test rotors and cavities fabricated by the second source. The task to conduct non-destructible rotor and cavity tests was deleted from the contract per Ref 5.

#### 3.2.1 Second Source Rotor and Cavity Tests

Autonetics responsibility under this task, with respect to Second Source, included component testing of four rotors and cavity sets and testing of two MESH instruments containing Second Source rotors and cavities.

The items in Table 43 were received from Northrop for evaluation. All units were evaluated and reports submitted to AFAL, WPAFB. The Master Parts listed below were evaluated at Autonetics and then returned to Northrop.

TABLE 43. NORTHROP ITEMS RECEIVED FOR EVALUATION

Cavities Sets	Rotors	Master Cavity	Master Rotor
N0007	NA11	B-1	No. 2
N0008	NA16	B-2	No. 7
N0009	NA14	No. 7	
N0010	NA22	BeO	

Two sets of rotors and cavities were received at Autonetics, Anaheim in January 1976 and two sets were received in February 1976. All parts were component evaluated prior to selecting the best two asset sets to build into the final gyro configuration. All parts were good for instrument use with regard to size, roundness, surface finish, and general integrity. The last sets of cavity parts (N0009 and N0010) and rotors (NA11 and NA22) were selected for assembly into the gyro configuration because they had a somewhat better surface finish than the other sets.

MESH Unit N0009/NA11 and MESH Unit N0010/NA22 completed assembly in April 1976 and successfully passed prefunctional testing, bake out, and cold soak. No problems of any kind were encountered. However, functional test of the units on Test Station IV revealed some discrepancies in the desired rotor parameters. Table 44 summarizes the initial measurements of parameters.

2. Scorsby and rate testing
3. Fast reaction, hot and cold soak testing
4. Vibration and shock testing

A draft copy of Part 1 (Stability, heading sensitivity, and tilt sensitivity testing) was provided to AFAL in December 1976. The final version of Part 1 was submitted in February 1977 as CDRL Item A00D. Draft copies of Parts 2, 3, and 4 were provided to AFAL in February 1977. The final versions of Parts 2, 3, and 4 were in final type at contract completion and consequently were not formally submitted as CDRL data items.

### 3.2 TASK 2.2, DEVELOPMENTAL TEST

The purpose of this task was to test rotors and cavities fabricated by the second source. The task to conduct non-destructible rotor and cavity tests was deleted from the contract per Ref 5.

#### 3.2.1 Second Source Rotor and Cavity Tests

Autonetics responsibility under this task, with respect to Second Source, included component testing of four rotors and cavity sets and testing of two MESH instruments containing Second Source rotors and cavities.

The items in Table 43 were received from Northrop for evaluation. All units were evaluated and reports submitted to AFAL, WPAFB. The Master Parts listed below were evaluated at Autonetics and then returned to Northrop.

TABLE 43. NORTHROP ITEMS RECEIVED FOR EVALUATION

Cavities Sets	Rotors	Master Cavity	Master Rotor
N0007	NA11	B-1	No. 2
N0008	NA16	B-2	No. 7
N0009	NA14	No. 7	
N0010	NA22	BeO	

Two sets of rotors and cavities were received at Autonetics, Anaheim in January 1976 and two sets were received in February 1976. All parts were component evaluated prior to selecting the best two asset sets to build into the final gyro configuration. All parts were good for instrument use with regard to size, roundness, surface finish, and general integrity. The last sets of cavity parts (N0009 and N0010) and rotors (NA11 and NA22) were selected for assembly into the gyro configuration because they had a somewhat better surface finish than the other sets.

MESH Unit N0009/NA11 and MESH Unit N0010/NA22 completed assembly in April 1976 and successfully passed prefunctional testing, bake out, and cold soak. No problems of any kind were encountered. However, functional test of the units on Test Station IV revealed some discrepancies in the desired rotor parameters. Table 44 summarizes the initial measurements of parameters.

TABLE 44. MESG PARAMETER MEASUREMENTS

	Mum. Amp. (Volt P <sub>K</sub> P <sub>K</sub> )	Axial Mass Unbalance Deg/hr/g	Polhode Period (seconds)	Angle Cal Residual (Blind) mrad	Polhode Signature	Rotor Speed Hz
Northrop N0009/NA11	1.3	0.04	0.82 ( $\omega = 2430$ )	0.121	See Fig 82	2419
Northrop N0010/NA22	3.6	0.78 Approximate (Special Test)	0.68 ( $\omega = 2432$ )	0.557	See Fig 83	2434
MICRON A015Y Series	3.4	0.009	0.64 ( $\omega = 2433$ )	0.225	See Fig 84	2434



Figure 82.  
Polhode Signature  
Northrop N0009/NA11

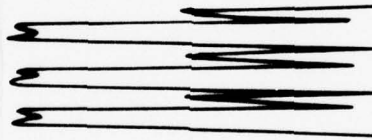


Figure 83.  
Polhode Signature  
Northrop N0010/NA22



Figure 84.  
Polhode Signature  
MICRON A015Y Series

There were two anomalies revealed by the data analyses: (1) Rotor characteristics were vastly different from those observed on standard MICRON three wire rotors and (2) the rotor characteristics were vastly different between NA11 and NA22, even though the rotors were fabricated from material which came from near vicinities in the extrusion.

Two possible explanations for the observed behavior of the rotors and the deviations between the Northrop rotors are as follows:

1. Homogeneity of the originally purchased beryllium material.

Because of the good results of the tests and evaluation of the geometry of the rotors (via x-ray, wire length measurements) it is thought that the most probable cause of the discrepancies was the non-uniformity of the material which Northrop procured. The large variation between rotor NA11 and NA22 gave a very strong indication that this was the probable cause. The

extreme variation in both MUM amplitude (radial mass unbalance) and axial mass unbalance indicated an uncontrolled, unpredictable center of gravity of each rotor. In the earlier MMSG developmental stages, Autonetics purchased material from one other vendor which had similar characteristics. Indeed, without any intentional mass unbalance, the mass unbalance of the finished rotor was so large it precluded full spin up of the rotor.

2. Other than "Choice Cut."

Northrop's first effort of rotor material extrusion did not produce the desired geometry in the long uniform midsection of the extruded rod. In order to get rotors of the desired geometry (wire location), it was necessary for Northrop to use material closer to an end section. There were unknown characteristics in the material from such a section (transition phase in the extruding process) and Autonetics had no experience with those sections. It is noted however that if such were the case, it would still be expected that NA11 and NA22 would show similar characteristics.

Four complete sets of Angle and Drift Calibrations were performed on each of the two MMSG's containing Northrop rotor and cavity sets. The tests were conducted in the following sequence:

1. Two sets of Angle and Drift Calibrations without an intermediate shutdown
2. A third set after a gyro shutdown
3. The fourth set after an additional shutdown

A tabulation of the Angle and Drift Calibration residuals is given in Table 45.

A computer program was prepared to compare and analyze the drift parameters between calibrations. The drift parameters for the two sets of four calibrations were then processed through the parameter comparison program. A tabulation of the parameter comparisons, together with overall mean differences, is given in Tables 46 and 47 listed by parameters.

The comparison program ranks the parameters by their RMS drift rate effect, in descending order, for each individual calibration and intercalibration comparison. Table 48 lists the overall parameter ranking, for each gyro, for the observed intercalibration differences.

The parameters themselves, or their variations, do not present a clear picture of the gyro performance; however, their equivalent RMS drift rates do provide an insight. Accordingly, the equivalent RMS drift of the individual parameter differences were tabulated, together with their overall RMS value as shown in Tables 49 and 50. The equivalent RMS drift rate changes were ranked, in descending order, for each gyro and the listings are shown in Table 51.

TABLE 45. RESULTS OF ANGLE AND DRIFT CALIBRATION TESTS;  
 SERIES OF FOUR CONSECUTIVE TESTS  
 (Gyros NA0009 and NA0010)

Test	Results	Test 1	Test 2	Test 3	Test 4	Overall rms
NA-0009						
Angle	Calib Residual mrads rms/axis	.113	.107	.111	.102	.108
Calib	Total Residual mrads rms/axis	.173	.167	.159	.140	.160
Drift	Calib deg rms/axis	.017	.014	.017	.018	.016
Calib	Total Rate deg rms/axis	.049	.047	.045	.047	.047
NA-0010						
Angle	Calib Residual mrads rms/axis	.071	.073	.072	.073	.072
Calib	Total Residual mrads rms/axis	.100	.096	.096	.111	.100
Drift	Calib deg rms/axis	.008	.009	.008	.009	.008
Calib	Total Rate deg rms/axis	.704	.714	.706	.711	.708

TABLE 46. DRIFT PARAMETER COMPARISONS BETWEEN  
SUCCESSIVE DRIFT CALIBRATIONS, GYRO NA-0009

Parameter No.	Parameter Differences			Mean Difference	Error Source
	1 To 2	2 To 3	3 To 4		
1	- .0078	.0015	- .0086	- .0050	Case-Fixed Bias (X)
2	- .0029	.0012	- .0027	- .0015	Case-Fixed Bias (Y)
3	- .0021	- .0015	.0069	- .0022	Case-Fixed Bias (Z)
4	- .0158	- .0377	.0257	- .0093	Acceleration-Squared
5	- .0062	.0471	- .0677	- .0089	"Cavity Prolateness"
6	.0011	.0109	- .0117	.0003	X-Y Cavity Shape*
7	- .0103	- .0065	.0255	.0029	Y Cavity Misalignment
8	- .0025	.0169	- .0124	.0007	X Cavity Misalignment
9	.0048	- .0084	.0109	.0024	Cavity Shape Term*
10	-1.1050	.1428	1.9017	.3132	Z-Groove & 12th Harm
11	.0000	.0000	.0000	.0000	Vertical Magnetic Field*
12	-2.3512	2.3128	1.2497	.4038	Z-Groove & 14th Harm
13	- .0034	- .0026	.0080	.0007	T.S. Azimuth Error
14	.0161	.0078	- .0148	.0030	Z-Servo Unbalance
15	.0021	- .0003	- .0035	- .0006	X-Y Servo Unbalance
16	- .0025	- .0102	.0155	.0009	X-Servo 4-Sp Pattern
17	- .0113	- .0013	.0029	- .0032	Y-Servo 4-Sp Pattern
18	- .0068	.0047	- .0102	- .0041	Z-Servo 4-Sp Pattern
19	- .8154	.7985	.1192	.0341	Z-Groove & 6th Harm
20	- .1650	.0119	.2440	.0303	Z-Groove & 4th Harm
21	- .0243	.0578	- .0854	- .0173	Pear-Shape & Preload
22	.8945	.0312	-1.5484	- .2076	Z-Groove & 8th Harm
23	2.8578	-2.6144	- .1212	.0407	Z-Groove & 10th Harm
24	- .0280	.0015	.0071	- .0153	Axial Mass Unbalance
25	- .0124	- .0649	- .0567	- .0819	Grooves & 4th Harm
26	- .3785	.0130	- .3289	- .2315	Grooves & 6th Harm
27	.2041	.7642	- .5533	.1383	Grooves & 8th Harm
28	1.2769	- .9360	1.0402	.4604	Grooves & 10th Harm
29	- .1944	-1.7398	1.2722	- .8528	Grooves & 12th Harm
30	- .0135	1.2221	-1.1418	.0223	Grooves & 14th Harm
31	.1052	1.3424	-1.1432	.1015	Grooves & 16th Harm
32	.0029	- .0005	- .0199	- .0655	Pear Shape & Acceler
33	- .1114	- .0306	.1952	.0177	Grooves, G & 3rd Harm
34	- .0347	- .1680	.3558	.0510	Grooves, G & 5th Harm
35	.0415	- .1595	.1683	.0168	Grooves, G & 7th Harm

\*Error source listed is theoretical; i. e., not confirmed by experiment.

TABLE 47. DRIFT PARAMETER COMPARISONS BETWEEN  
SUCCESSIVE DRIFT CALIBRATIONS, GYRO NA-0010

Parameter No.	Parameter Differences			Mean Difference	Error Source
	1 To 2	2 To 3	3 To 4		
1	.0085	- .0026	- .0007	.0017	Case-Fixed Bias (X)
2	.0063	- .0030	.0000	.0011	Case-Fixed Bias (Y)
3	.0053	.0015	.0015	.0028	Case-Fixed Bias (Z)
4	- .0080	- .0098	- .0477	-.0552	Acceleration-Squared
5	.0050	.0471	- .0944	-.0141	"Cavity Prolateness"
6	- .0061	.0049	- .0054	-.0022	X-Y Cavity Shape*
7	- .0082	.0053	- .0026	-.0018	Y Cavity Misalignment
8	- .0039	- .0049	.0135	.0016	X Cavity Misalignment
9	- .0101	.0106	.0045	.0017	Cavity Shape Term*
10	.0331	- .1293	.2473	.0504	Z-Groove & 12th Harm
11	.0000	.0000	.0000	.0000	Vertical Magnetic Field*
12	.1960	- .0895	- .0890	.0327	Z-Groove & 14th Harm
13	.0064	.0011	.0000	.0025	T. S. Azimuth Error
14	- .0046	- .0041	.0034	-.0018	Z-Servo Unbalance
15	- .0118	.0024	.0046	-.0016	X-Y Servo Unbalance
16	- .0061	.0007	- .0003	-.0019	X-Servo 4-Sp Pattern
17	.0009	.0005	- .0084	-.0275	Y-Servo 4-Sp Pattern
18	- .0055	- .0021	.0084	.0003	Z-Servo 4-Sp Pattern
19	.2721	- .0661	- .1476	.0195	Z-Groove & 6th Harm
20	.0349	- .0941	.0500	-.0031	Z-Groove & 4th Harm
21	.0037	- .0015	.0068	.0030	Pear-Shape & Preload
22	- .1387	.2922	- .2886	-.0450	Z-Groove & 8th Harm
23	- .5172	.1818	.2099	-.0418	Z-Groove & 10th Harm
24	.0212	- .0003	- .0051	.0053	Axial Mass Unbalance
25	.0734	.0976	- .0915	.0265	Grooves & 4th Harm
26	- .2040	.1843	.2913	.0905	Grooves & 6th Harm
27	.6506	- .5275	.5424	.2218	Grooves & 8th Harm
28	.4014	- .3327	-1.1059	-.3457	Grooves & 10th Harm
29	-1.2079	1.0191	-1.1125	-.4338	Grooves & 12th Harm
30	- .1071	.1672	.8159	.2920	Grooves & 14th Harm
31	.7122	- .6404	.6997	.2572	Grooves & 16th Harm
32	- .0011	- .0033	.0009	-.0012	Pear Shape & Acceler
33	- .0062	.0000	.0123	.0020	Grooves, G & 3rd Harm
34	- .0333	- .0342	.0818	.0048	Grooves, G & 5th Harm
35	- .0097	- .0450	.0332	-.0072	Grooves, G & 7th Harm

\*Error source listed is theoretical; i. e., not confirmed by experiment.

TABLE 48. OVERALL RANKING OF PARAMETERS BY RMS DRIFT EFFECT,  
GYROS NA-0009 AND NA-0010

Rank	Gyro NA-0009		Gyro NA-0010	
	Para- meter	Error Source	Para- meter	Error Source
1	24	Axial Mass Unbalance	24	Axial Mass Unbalance
2	5	"Cavity Prolateness"	27	Grooves & 8th Harm
3	13	T.S. Azimuth Error	6	X-Y Cavity Shape*
4	33	Grooves, G & 3rd Harm	5	"Cavity Prolateness"
5	6	X-Y Cavity Shape*	25	Grooves & 4th Harm
6	35	Grooves, G & 7th Harm	26	Grooves & 6th Harm
7	20	Z-Groove & 4th Harm	13	T.S. Azimuth Error
8	34	Grooves, G & 5th Harm	20	Z-Groove & 4th Harm
9	25	Grooves & 4th Harm	7	Y Cavity Misalignment
10	21	Pear-Shape & Preload	8	X Cavity Misalignment
11	27	Grooves & 8th Harm	9	Cavity Shape Term*
12	7	Y Cavity Misalignment	21	Pear-Shape & Preload
13	3	Case-Fixed Bias (Z)	34	Grooves, G & 5th Harm
14	14	Z-Servo Unbalance	3	Case-Fixed Bias (Z)
15	22	Z-Groove & 8th Harm	19	Z-Groove & 6th Harm
16	10	Z-Groove & 12th Harm	35	Grooves, G & 7th Harm
17	31	Grooves & 16th Harm	11	Vertical Magnetic Field*
18	12	Z-Groove & 14th Harm	16	X-Servo 4-Sp Pattern
19	4	Acceleration-Squared	29	Grooves & 12th Harm
20	8	X Cavity Misalignment	32	Pear Shape & Acceler
21	19	Z-Groove & 6th Harm	4	Acceleration-Squared
22	9	Cavity Shape Term*	22	Z-Groove & 8th Harm
23	18	Z-Servo 4-Sp Pattern	23	Z-Groove & 10th Harm
24	1	Case-Fixed Bias (X)	12	Z-Groove & 14th Harm
25	17	Y-Servo 4-Sp Pattern	30	Grooves & 14th Harm
26	23	Z-Groove & 10th Harm	14	Z-Servo Unbalance
27	29	Grooves & 12th Harm	1	Case-Fixed Bias (X)
28	2	Case-Fixed Bias (Y)	18	Z-Servo 4-Sp Pattern
29	30	Grooves & 14th Harm	15	X-Y Servo Unbalance
30	32	Pear Shape & Acceler	31	Grooves & 16th Harm
31	16	X-Servo 4-Sp Pattern	2	Case-Fixed Bias (Y)
32	28	Grooves & 10th Harm	10	Z-Groove & 12th Harm
33	26	Grooves & 6th Harm	17	Y-Servo 4-Sp Pattern
34	15	X-Y Servo Unbalance	33	Grooves, G & 3rd Harm
35	11	Vertical Magnetic Field*	28	Grooves & 10th Harm

\*Error source listed as theoretical; i. e., not confirmed by experiment.

TABLE 49. EQUIVALENT DRIFT RATE CHANGES BETWEEN SUCCESSIVE  
DRIFT CALIBRATIONS, GYRO NA-0090

Parameter No.	Error Source	Differences: Deg/Hr rms - Equiv.			Overall Equiv. Deg/Hr
		1 to 2	2 to 3	3 to 4	
1	Case-Fixed Bias (X)	-.0031	.0008	-.0048	.0033
2	Case-Fixed Bias (Y)	-.0025	.0006	-.0012	.0016
3	Case-Fixed Bias (Z)	-.0053	-.0045	.0028	.0043
4	Acceleration-Squared	-.0017	-.0034	.0021	.0025
5	"Cavity Prolateness"	-.0038	.0036	-.0147	.0090
6	X-Y Cavity Shape*	.0004	.0040	-.0033	.0030
7	Y Cavity Misalignment	-.0045	-.0027	.0094	.0063
8	X Cavity Misalignment	-.0006	.0052	-.0068	.0050
9	Cavity Shape Term*	.0026	-.0032	.0036	.0032
10	Z-Groove & 12th Harm.	-.0036	.0013	.0017	.0024
11	Vertical Magnetic Field*	.0000	-.0081	.0000	.0047
12	Z-Groove & 14th Harm.	.0041	.0041	-.0110	.0072
13	T. S. Azimuty Error	-.0027	-.0015	.0046	.0032
14	Z-Servo Unbalance	.0046	.0023	-.0029	.0034
15	X-Y Servo Unbalance	.0009	-.0001	-.0014	.0010
16	X-Servo 4-Sp. Pattern	.0011	-.0042	.0069	.0047
17	Y-Servo 4-Sp. Pattern	-.0050	-.0005	.0027	.0033
18	Z-Servo 4-Sp. Pattern	-.0030	.0026	-.0047	.0036
19	Z-Groove & 6th Harm.	-.0051	.0050	.0008	.0041
20	Z-Groove & 4th Harm.	-.0027	.0016	.0034	.0027
21	Pear-Shape & Preload	-.0042	.0068	-.0096	.0072
22	Z-Groove & 8th Harm.	.0015	-.0001	-.0026	.0017
23	Z-Groove & 10th Harm.	.0056	-.0043	-.0035	.0045
24	Axial Mass Unbalance	-.0083	.0003	.0038	.0053
25	Grooves & 4th Harm.	-.0004	.0098	-.0013	.0057
26	Grooves & 6th Harm.	-.0012	-.0042	-.0020	.0028
27	Grooves & 8th Harm.	.0020	.0050	-.0145	.0089
28	Grooves & 10th Harm.	.0009	-.0027	.0035	.0026
29	Grooves & 12th Harm.	.0059	-.0032	.0039	.0045
30	Grooves & 14th Harm.	-.0035	.0059	-.0079	.0060
31	Grooves & 16th Harm.	.0018	.0017	-.0043	.0029
32	Pear Shape & Acceler	.0008	-.0002	-.0048	.0028
33	Grooves, G & 3rd Harm.	-.0066	-.0020	.0184	.0113
34	Grooves, G & 5th Harm.	-.0041	-.0078	.0092	.0074
35	Grooves, G & 7th Harm.	.0018	-.0031	.0109	.0066

\*Error source listed is theoretical; i. e., not confirmed by experiment.

TABLE 50. EQUIVALENT DRIFT RATE CHANGES BETWEEN SUCCESSIVE DRIFT CALIBRATIONS, GYRO NA-0010

Parameter No.	Error Source	Differences: Deg/Hr rms-Equiv.			Overall Equiv. Deg/Hr
		1 to 2	2 to 3	3 to 4	
1	Case-Fixed Bias (X)	.0030	-.0016	-.0004	.0020
2	Case-Fixed Bias (Y)	.0023	-.0019	.0000	.0017
3	Case-Fixed Bias (Z)	.0024	.0026	.0007	.0021
4	Acceleration-squared	-.0011	-.0015	-.0076	.0045
5	"Cavity Prolateness"	-.0065	.0121	-.0217	.0148
6	X-Y Cavity Shape*	-.0026	.0030	-.0034	.0030
7	Y Cavity Misalignment	-.0020	.0023	-.0009	.0018
8	X Cavity Misalignment	-.0013	-.0023	.0044	.0030
9	Cavity Shape Term*	-.0024	.0028	.0024	.0025
10	Z-Groove & 12th Harm	-.0016	.0017	.0007	.0014
11	Vertical Magnetic Field*	.0000	.0000	.0000	.0000
12	Z-Groove & 14th Harm	.0004	.0010	-.0002	.0006
13	T. S. Azimuth Error	.0027	.0006	.0000	.0016
14	Z-Servo Unbalance	-.0010	-.0014	.0010	.0011
15	X-Y Servo Unbalance	-.0043	.0010	.0032	.0031
16	X-Servo 4-Sp. Pattern	.0022	.0003	-.0001	.0013
17	Y-Servo 4-Sp. Pattern	.0005	.0002	-.0031	.0018
18	Z-Servo 4-Sp. Pattern	-.0023	-.0008	.0045	.0030
19	Z-Groove & 6th Harm	.0014	-.0005	-.0017	.0013
20	Z-Groove & 4th Harm	.0006	-.0018	.0007	.0012
21	Pear-Shape & Preload	.0005	-.0002	.0009	.0006
22	Z-Groove & 8th Harm.	-.0004	.0010	-.0015	.0011
23	Z-Groove & 10th Harm	-.0023	-.0009	.0009	.0015
24	Axial Mass Unbalance	.0093	-.0001	-.0014	.0054
25	Grooves & 4th Harm.	.0028	.0013	-.0028	.0024
26	Grooves & 6th Harm.	-.0014	.0013	.0031	.0021
27	Grooves & 8th Harm.	.0018	-.0008	.0010	.0013
28	Grooves & 10th Harm.	.0010	-.0014	-.0066	.0039
29	Grooves & 12th Harm.	-.0015	.0018	-.0007	.0014
30	Grooves & 14th Harm.	.0022	.0005	.0018	.0017
31	Grooves & 16th Harm.	.0018	-.0014	.0018	.0017
32	Pear Shape & Acceler	-.0029	-.0011	.0002	.0018
33	Grooves, G & 3rd Harm	.0046	.0000	.0025	.0030
34	Grooves, G & 5th Harm	-.0022	-.0021	.0061	.0039
35	Grooves, G & 7th Harm	-.0005	-.0014	.0016	.0013

\*Error source listed is theoretical; i. e., not confirmed by experiment.

TABLE 51. OVERALL RANKINGS OF PARAMETERS BY EQUIVALENT DRIFT RATE CHANGES, GYROS NA-0009 AND NA-0010

Rank	Gyro NA-0009		Gyro NA-0010	
	Parameter	Error Source	Parameter	Error Source
1	33	Grooves, G & 3rd Harm	5	"Cavity Prolateness"
2	5	"Cavity Prolateness"	24	Axial Mass Unbalance
3	27	Grooves & 8th Harm	4	Acceleration-Squared
4	34	Grooves, G & 5th Harm	28	Grooves & 10th Harm
5	12	Z-Groove & 14th Harm	34	Grooves, G & 5th Harm
6	21	Pear-Shape & Preload	15	X-Y Servo Unbalance
7	35	Grooves, G & 7th Harm	6	X-Y Cavity Shape*
8	7	Y Cavity Misalignment	8	X Cavity Misalignment
9	30	Grooves & 14th Harm	18	Z-Servo 4-Sp Pattern
10	25	Grooves & 4th Harm	33	Grooves, G & 3rd Harm
11	24	Axial Mass Unbalance	9	Cavity Shape Term*
12	8	X Cavity Misalignment	25	Grooves & 4th Harm
13	11	Vertical Magnetic Field*	3	Case-Fixed Bias (Z)
14	16	X-Servo 4-Sp Pattern	26	Grooves & 6th Harm
15	23	Z-Groove & 10th Harm	1	Case-Fixed Bias (X)
16	29	Grooves & 12th Harm	7	Y Cavity Misalignment
17	3	Case-Fixed Bias (Z)	17	Y-Servo 4-Sp Pattern
18	19	Z-Groove & 6th Harm	32	Pear Shape & Acceler
19	18	Z-Servo 4-Sp Pattern	2	Case-Fixed Bias (Y)
20	14	Z-Servo Unbalance	30	Grooves & 14th Harm
21	1	Case-Fixed Bias (X)	31	Grooves & 16th Harm
22	17	Y-Servo 4-Sp Pattern	13	T.S. Azimuth Errors
23	9	Cavity Shape Term*	23	Z-Groove & 10th Harm
24	13	T.S. Azimuth Error	10	Z-Groove & 12th Harm
25	6	X-Y Cavity Shape*	29	Grooves & 12th Harm
26	31	Grooves & 16th Harm	16	X-Servo 4-Sp Pattern
27	26	Grooves & 6th Harm	19	Z-Groove & 6th Harm
28	32	Pear Shape & Acceler	27	Grooves & 8th Harm
29	20	Z-Groove & 4th Harm	35	Grooves, G & 7th Harm
30	28	Grooves & 10th Harm	20	Z-Groove & 4th Harm
31	4	Acceleration-Squared	14	Z-Servo Unbalance
32	10	Z-Groove & 12th Harm	22	Z-Groove & 8th Harm
33	22	Z-Groove & 8th Harm	12	Z-Groove & 14th Harm
34	2	Case-Fixed Bias (Y)	21	Pear-Shape & Preload
35	15	X-Y Servo Unbalance	11	Vertical Magnetic Field*

\*Error source listed is theoretical; i. e., not confirmed by experiment.

In summary, the tabulated data ensemble appears normal when compared to similar data ensembles, and the two gyros successfully met the repeatability test requirements. The overall repeatabilities are summarized in Table 52.

TABLE 52. OVERALL SUMMARY OF ANGLE AND DRIFT CALIBRATIONS, GYRO NA0009 AND NA0010

Gyro No.	Angle Calibrations MRADS/Axis - RMS		Drift Calibrations Deg/Hr/Axis - RMS	
	Mean	Std. Dev	Mean	Std. Dev
NA-0009	.1083	.0049	.0165	.0025
NA-0010	.0723	.0012	.0085	.0006

### 3.2.2 Non-destructible Rotor and Cavity Tests

The task to conduct non-destructible rotor and cavity tests was deleted from the contract per Ref 5.

### 3.3 TASK 2.3, SYSTEM LABORATORY TEST

The purpose of this task was to functionally test the EPM to demonstrate compliance with the requirements of the system specification. Updates of hardware, software, and/or documentation as a result of changes necessitated by these laboratory tests were to be performed under this task.

This task was deleted from the contract per Ref 5.

### 3.4 TASK 2.4, MOBILE TEST

The purpose of this task was to conduct mobile tests on the EPM to determine the sensitivity of the INU performance to low speed translation over the earth's surface.

This task was deleted from the contract per Ref 5.

### 3.5 TASK 2.5, CONTRACTOR FLIGHT TEST

The purpose of this task was to flight test the EPM to determine the sensitivity of the INU performance to a "high performance" aircraft environment.

This task was deleted from the contract per Ref 5.

SECTION IV  
TASK 3, SUPPORT HARDWARE

4.1 TASK 3.1, ENGINEERING TEST EQUIPMENT

The purposes of this task were to design, develop, fabricate, and procure the engineering tooling and test equipment required to design, fabricate, integrate, and test the EPM.

4.1.1 Software Test Station

The Software Test Station is required for the development and checkout of MICRON operational software prior to MICRON system level testing.

The MICRON Processor Test Console and the MICRON Processor, both developed under AF Contract F33615-72-C-1674 were modified for this purpose in order to minimize the Phase 2B contract costs and to provide software testing facilities prior to the availability of MICRON DPU hardware.

The MICRON Processor Test Console is a two-bay console containing a Processor Control Panel, Processor Power Supply, Core Memory Power Supply, MICRON Processor (CPU), and interconnect cabling. In addition, a 16K Core Memory and a Paper Tape Reader, both *Autonetics capital equipment*, are used with the MICRON Processor Test Console.

A block diagram of the Software Test Station is shown in Figure 85 and a photograph of the Test Station is shown in Figure 86. The Processor Control Panel, shown in Figure 87, is the heart of the test console and provides many functions. Some of the major functions are described below:

1. Tape Reader Control. Control Switches are provided to start, stop, and rewind the tape. Two verify modes are available. In "Load Verify", the data is read from the tape stored into memory, then reread and compared with the data read from tape. The "Tape Verify" mode causes the data previously loaded from tape to be read and compared against the data being read from tape on the second pass. An error in either mode will stop the reader and light an error lamp.
2. Power Control. The control panel has the switches and controls to sequence power on/off to the processor and to provide initialization signals.
3. Halt/Compute. The control panel has a HALT/COMPUTE switch. When in "COMPUTE" the processor operates normally except that data entry into main memory can be accomplished from the keyboard. When in "HALT," the processor is automatically stopped at the completion of the execution of an instruction. When in "HALT," the operator may read/write main memory and display CPU registers.

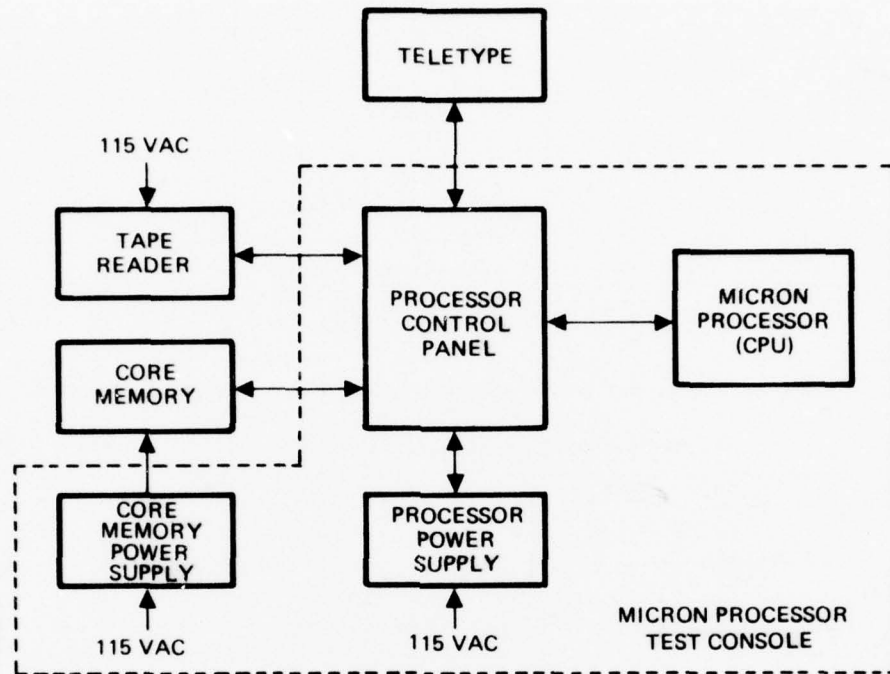
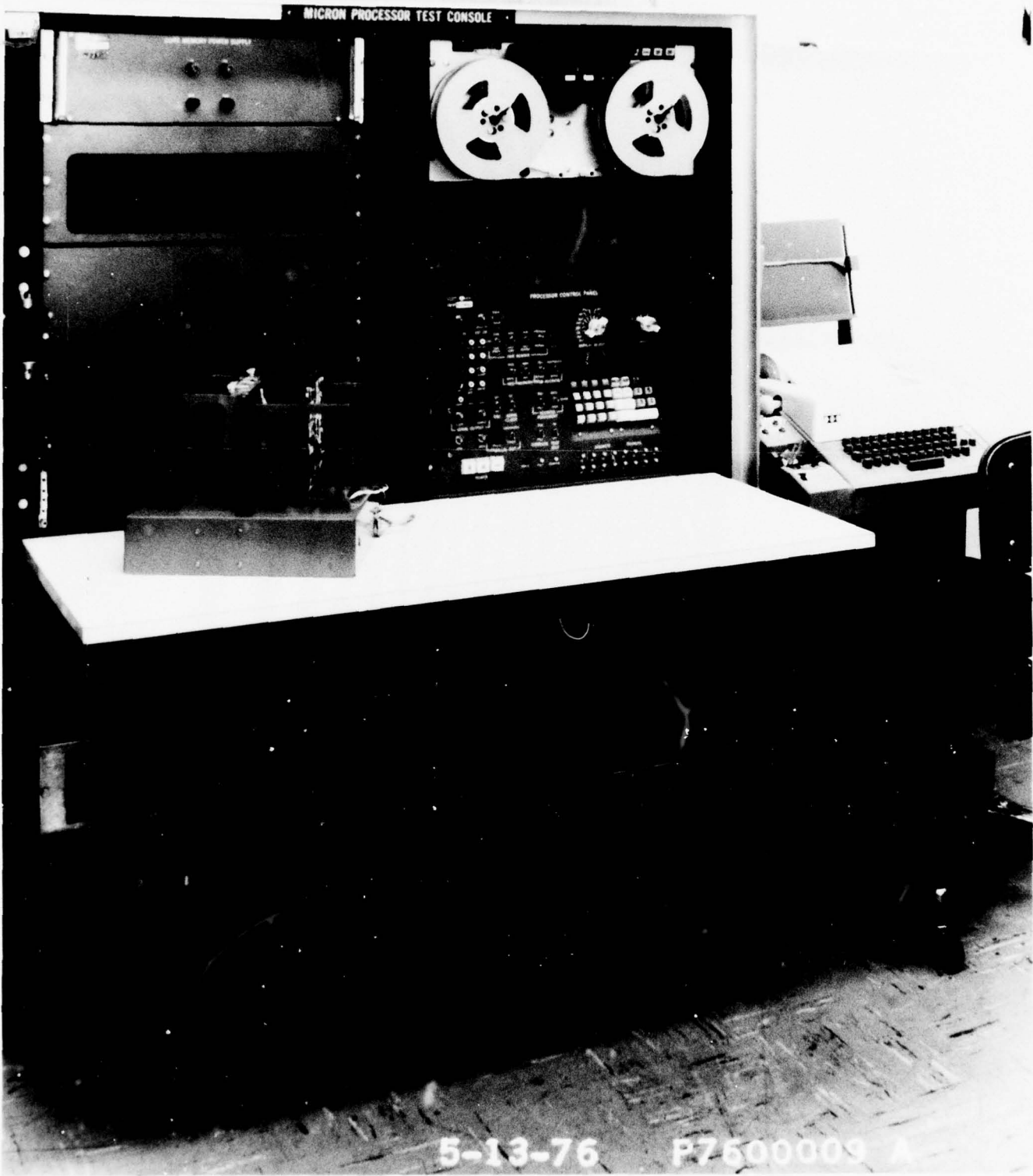


Figure 85. Software Test Station Block Diagram

4. Single Instruction Stepping. While in "HALT", the control panel can cause the processor to execute exactly one instruction for each activation of a pushbutton switch.
5. CPU Register Display. The control panel contains the necessary controls and sequencing to display the CPU registers. In addition, the control panel can display memory address, memory data, and keyboard entries as they are keyed.
6. Direct Memory Access. The control panel has the capability to read from or write into the processor main memory. Initial program loading is over this DMA channel.
7. Memory Address Trapping. The control panel includes a stop on address agreement mode. When the selected address is encountered, a scope synchronizing pulse is generated, or the processor is halted and the "HALT" lamp turned on. The selection between these two options can be made by the operator.

Fig 86  
~~Fig 94~~ HIT  
~~PHOTO~~  
~~480~~

Figure 86. Software Test Station

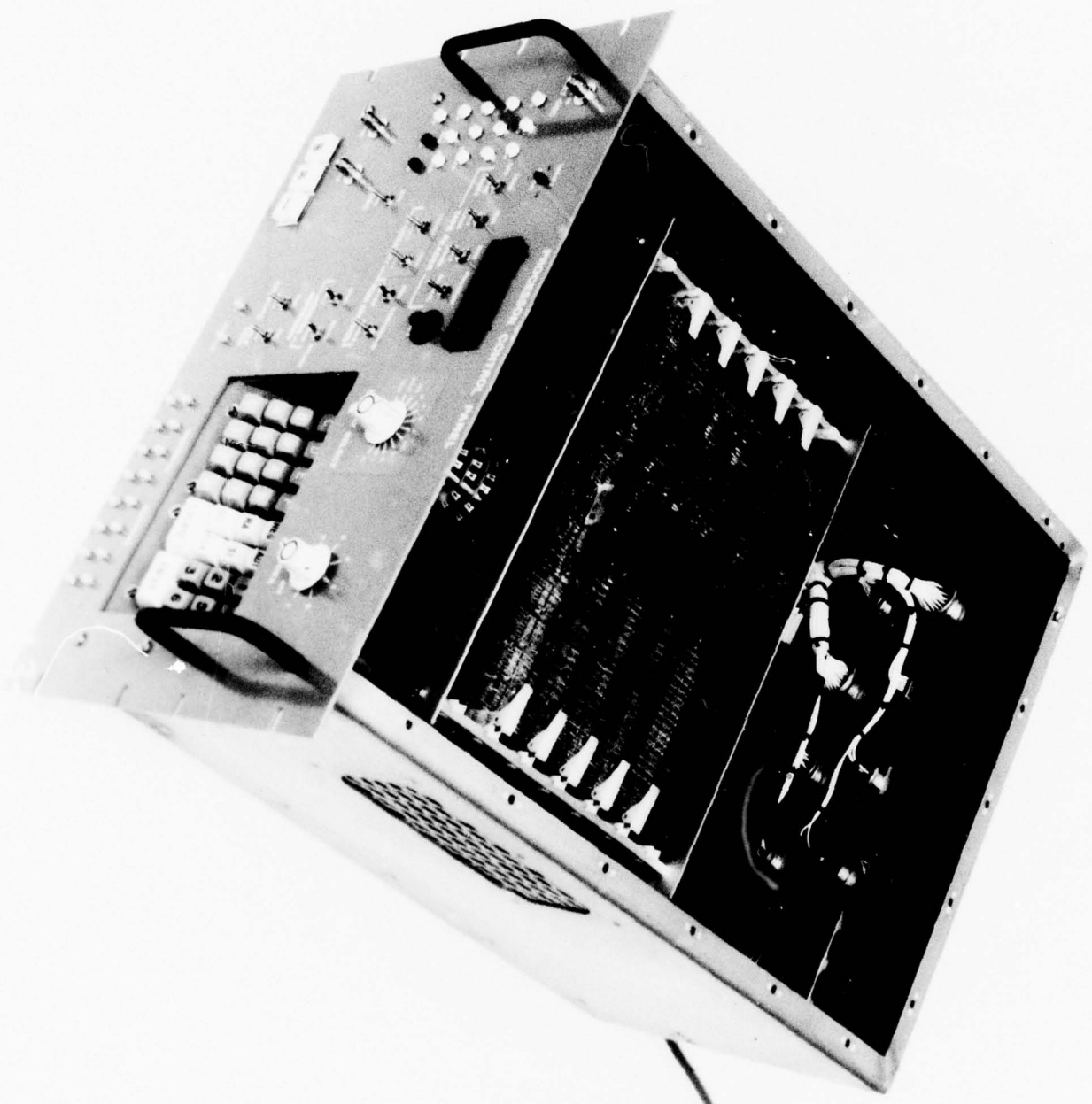


94

197215



Figure 87. Processor Control Panel



Handwritten markings at the bottom of the page include a large 'A' on the left, a '6'' in the center, and another large 'A' on the right, with a horizontal line extending from the first 'A' across the page.

The Test Console was updated to include functions 4 (single instruction execution) and 5 (CPU register display). The MICRON Processor was refurbished, updated and checked out for proper operation in the Test Station. Major modifications were: (a) replacement of five microprogram ROM's with ROM's containing updated DPU instruction set; (b) changes in the input/output section to make it compatible with the new PIO design. Both changes required modifications not only in the CPU but also in the Processor Control Panel. In addition, circuitry was designed and added to the Processor Control Panel to provide hard copy printout capability via Teletype Terminal.

The processor (CPU) used in the Software Test Station had been mechanized with beam lead devices on 2 in. by 2 in. open hybrids, and, therefore, presented continuous maintenance problems. Therefore, it was decided to accelerate testing of the spare MICRON CPU and use it to replace the existing CPU in the Software Test Station until completion of the first DPU. This required the fabrication of an additional test fixture for the CPU. In addition to alleviating maintenance problems, this changeover offers another significant advantage in that the Software Test Station and the DPU Test Console have identical capability and can, therefore, support either activity. The modification, including the fabrication and test of the test fixture was completed in less than three weeks, resulting in minimal down time of the Software Test Station.

#### 4.1.2 Electronics Test Equipment

This task includes all the tooling and test equipment design, fabrication and test for functional and screen tests of 26 hybrid module types, functional test of the Charge Amplifier MLB's, SEU's 1, 2, 3, 4, the Converter Module MLB's and the Power Supplies. Table 53 gives a list of the special tooling fabricated for module assembly. A summary of all the test fixtures fabricated is shown in Table 54.

Each hybrid test unit provides the capability of testing the hybrids at  $-55^{\circ}\text{C}$ ,  $25^{\circ}\text{C}$  and operating temperature ( $63^{\circ}\text{C}$  for some hybrids and  $71^{\circ}\text{C}$  for others). Actual system loads and signals have been simulated as closely as possible in the test fixtures. Test specifications, which provide instructions for the use of the test equipment, are listed in Appendix C.

TABLE 53. SPECIAL TOOLING FABRICATED FOR MODULE ASSEMBLY

Item	Description
Lead Form Tool (244-1)	Forms leads for butterfly - type hybrid packages
Hand Form Tool (244-2)	Forms leads for transformers
Hand Form Tool (244-3)	Forms leads for commercial MOS and integrated circuits
Alignment fixture and domino for hybrid packages	Aligns package, preform and cover while sealing and keeps package from moving.

TABLE 54. HYBRID AND MLB FUNCTIONAL AND SCREEN TEST EQUIPMENT

Item	Qty	Comments
Power Distribution and Temperature Control Unit	6	Interfaces with Load and Signal Generator Test Modules for all Hybrid types except Charge Amplifiers
Hybrid Temperature Control Heater Blocks	8	Interfaces with Load and Signal Generator Test Modules and Power Distribution and Temperature Control Unit
Power Distribution, Temperature Control, and Signal Generator for Charge Amp Hybrids	1	Interfaces with Charge Amplifiers Load and Signal Generator Test Module.
A/D Converter MOS Circuit Test Unit	1	Utilized for special tests associated with the packaged MOS A/D Converter circuits
Spin Motor Power Amp MOS Circuit Test Unit	1	Utilized for tests on Spin Motor Power Amplifier MOS circuits
QRFG&METG MOS Circuit Test Unit	1	Utilized for functional tests on QRFG & METG MOS circuits
Ladder Network Test Unit	1	Utilized to evaluate accuracy of 13-bit 50K/100K ladder networks which are used with the A/D Converter
Charge Amplifier Electronics Assy MLB Test Unit	1	Utilized to functional test Charge Amplifier Electronics Assy MLB which contains 8 Charge Amplifiers and 10 transformers
Spin Motor Electronics Assy Test Unit	1	For functional test of Spin Motor Electronics Assy
High Voltage Switch MLB Test Unit	1	For functional test of High Voltage Switch MLB
SEU 1 and 2 MLB Test Unit	1	For functional test of SEU 1 and 2 MLB's
SEU 3 MLB Test Unit	1	For functional test of SEU 3 MLB
SEU 4 MLB Test Unit	1	For functional test of SEU 4 MLB

TABLE 54. (Cont)

<u>Item</u>	<u>Qty</u>	<u>Comments</u>																
Converter Electronics MLB Test Unit	1	For functional test of Converter Module MLB																
Power Supply Test Unit	1	For functional test of Power Supply Modules. Contains load banks simulating system loads.																
Burn-In Module No. 1	1	Burns in 18 Charge Amp hybrids simultaneously with power applied.																
Burn-In Module No. 2	1	Burns in the following hybrids sim- ultaneously with power applied:  <table style="margin-left: 40px;"> <thead> <tr> <th><u>Hybrid</u></th> <th><u>Qty</u></th> </tr> </thead> <tbody> <tr> <td>Suspension Timing Generator</td> <td>2</td> </tr> <tr> <td>MUM Demodulator</td> <td>2</td> </tr> <tr> <td>MUM Demod Sample &amp; Hold</td> <td>2</td> </tr> <tr> <td>Spin Motor Controller</td> <td>2</td> </tr> <tr> <td>Sample &amp; Hold Gap Sum.</td> <td>4</td> </tr> </tbody> </table>	<u>Hybrid</u>	<u>Qty</u>	Suspension Timing Generator	2	MUM Demodulator	2	MUM Demod Sample & Hold	2	Spin Motor Controller	2	Sample & Hold Gap Sum.	4				
<u>Hybrid</u>	<u>Qty</u>																	
Suspension Timing Generator	2																	
MUM Demodulator	2																	
MUM Demod Sample & Hold	2																	
Spin Motor Controller	2																	
Sample & Hold Gap Sum.	4																	
Burn-In Module No. 3	1	Burns in the following hybrids simultaneously with power applied:  <table style="margin-left: 40px;"> <thead> <tr> <th><u>Hybrid</u></th> <th><u>Qty</u></th> </tr> </thead> <tbody> <tr> <td>Suspension Timing Generator</td> <td>1</td> </tr> <tr> <td>Precision Xtal Osc/Gap Monitor</td> <td>1</td> </tr> <tr> <td>Differential Amp/Notch Filter</td> <td>2</td> </tr> <tr> <td>Modulator</td> <td>4</td> </tr> <tr> <td>A/D Converter</td> <td>1</td> </tr> <tr> <td>Sequencer No. 2</td> <td>1</td> </tr> <tr> <td>D. C. Ref at Preload Modulator</td> <td>1</td> </tr> </tbody> </table>	<u>Hybrid</u>	<u>Qty</u>	Suspension Timing Generator	1	Precision Xtal Osc/Gap Monitor	1	Differential Amp/Notch Filter	2	Modulator	4	A/D Converter	1	Sequencer No. 2	1	D. C. Ref at Preload Modulator	1
<u>Hybrid</u>	<u>Qty</u>																	
Suspension Timing Generator	1																	
Precision Xtal Osc/Gap Monitor	1																	
Differential Amp/Notch Filter	2																	
Modulator	4																	
A/D Converter	1																	
Sequencer No. 2	1																	
D. C. Ref at Preload Modulator	1																	
Burn-In Module No. 4	1	Burns in the following hybrids simultaneously with power applied:  <table style="margin-left: 40px;"> <thead> <tr> <th><u>Hybrid</u></th> <th><u>Qty</u></th> </tr> </thead> <tbody> <tr> <td>Temperature Controller</td> <td>1</td> </tr> <tr> <td>EMA Signal Filter</td> <td>1</td> </tr> <tr> <td>Spin Motor Power Amp &amp; Logic</td> <td>1</td> </tr> <tr> <td>Sequencer No. 1</td> <td>1</td> </tr> <tr> <td>Multiplexer</td> <td>2</td> </tr> </tbody> </table>	<u>Hybrid</u>	<u>Qty</u>	Temperature Controller	1	EMA Signal Filter	1	Spin Motor Power Amp & Logic	1	Sequencer No. 1	1	Multiplexer	2				
<u>Hybrid</u>	<u>Qty</u>																	
Temperature Controller	1																	
EMA Signal Filter	1																	
Spin Motor Power Amp & Logic	1																	
Sequencer No. 1	1																	
Multiplexer	2																	

TABLE 54. (Cont)


Item	Qty	Comments												
Burn-In Module No. 5	1	Burns in the following hybrids simultaneously with power applied: <table data-bbox="797 491 1295 688" style="margin-left: 40px;"> <thead> <tr> <th data-bbox="938 491 1029 520"><u>Hybrid</u></th> <th data-bbox="1247 491 1295 520"><u>Qty</u></th> </tr> </thead> <tbody> <tr> <td data-bbox="797 533 971 562">Synchro Bite</td> <td data-bbox="1263 533 1279 562">2</td> </tr> <tr> <td data-bbox="797 562 1068 592">Synchro Buffer Amp</td> <td data-bbox="1263 562 1279 592">3</td> </tr> <tr> <td data-bbox="797 592 1182 621">Synchro Reference Generator</td> <td data-bbox="1263 592 1279 621">2</td> </tr> <tr> <td data-bbox="797 621 971 651">Synchro DAC</td> <td data-bbox="1263 621 1279 651">2</td> </tr> <tr> <td data-bbox="797 651 932 680">DAC Amp</td> <td data-bbox="1263 651 1279 680">1</td> </tr> </tbody> </table>	<u>Hybrid</u>	<u>Qty</u>	Synchro Bite	2	Synchro Buffer Amp	3	Synchro Reference Generator	2	Synchro DAC	2	DAC Amp	1
<u>Hybrid</u>	<u>Qty</u>													
Synchro Bite	2													
Synchro Buffer Amp	3													
Synchro Reference Generator	2													
Synchro DAC	2													
DAC Amp	1													
Charge Amplifier MLB Burn-In and Transient Glitch Detector Unit	1	Burns in two Charge Amp Charge Amp Electronics Assy MLB's Simultaneously												
Power Supply Burn-In Unit	1	Burns in a complete set of power supply boards including High Voltage Switch												
Charge Amplifier Load and Signal Generator Test Module	1	Interfaces with hybrid circuit and pwr Dist & Temp Cont for functional test.												
Servo Network Load and Signal Generator Test Module	1													
Diff Amp/Notch Filter Load and Signal Generator Test Module	1													
MUM Demod Load and Signal Generator Test Module	1													
MUM Demod Filter Load and Signal Generator Test Module	1													
Modulator Load and Signal Generator Test Module	1													
Multiplexer Load and Signal Generator Test Module	1													
MUM Demod S/H Load and Signal Generator Test Module	1													
Sample & Hold/Gap Summation Load and Signal Generator Test Module	1		Interfaces with hybrid circuit and pwr Dist & Temp Cont for functional test.											

TABLE 54. (Cont)


Item	Qty	Comments	
A/D Converter Load and Signal Generator Test Module	1	Interfaces with Hybrid Circuit and Pwr Dist & Temp Cont for Functional Test.	
Suspension Timing Generator Load and Signal Generator Test Module	1		
Sequencer No. 1 Load and Signal Generator Test Module	1		
Sequencer No. 2 Load and Signal Generator Test Module	1		
Precision Crystal Osc. / Gap Monitor Load and Signal Generator Test Module	1		
D. C. Ref. and Preload Modulator Load & Signal Generator Test Module	1		
EMA Signal Filter Load & Signal Generator Test Module	1		
Spin Motor Controller Load & Signal Generator Test Module	1		
Temp. Controller Load & Signal Generator Test Module			
Synchro Bite Load & Signal Generator Test Module	1		
Synchro Buffer Amp Load & Signal Generator Test Module	1		
Synchro Buffer Amp Load & Signal Generator Test Module	1		
Synchro DAC Load & Signal Generator Test Module	1		Interfaces with Hybrid Circuit and Pwr Dist & Temp Cont for Functional Test.

TABLE 54. (Concluded)

Item	Qty	Comments
DAC Amplifier Load & Signal Generator Test Module	1	Interfaces with hybrid circuit and Pwr Dist & Temp Cont for functional test.
Spin Motor Power Preamp & Logic Load & Signal Generator Test Module	1	Interfaces with hybrid circuit and Pwr Dist & Temp Cont for functional test.
Ladder Network Test Fixture	1	Utilized for checking accuracy of ladder networks.

#### 4.1.3 DPU Engineering Test Equipment

The DPU Engineering Test Equipment designed and fabricated under the Phase 2B contract consists of:

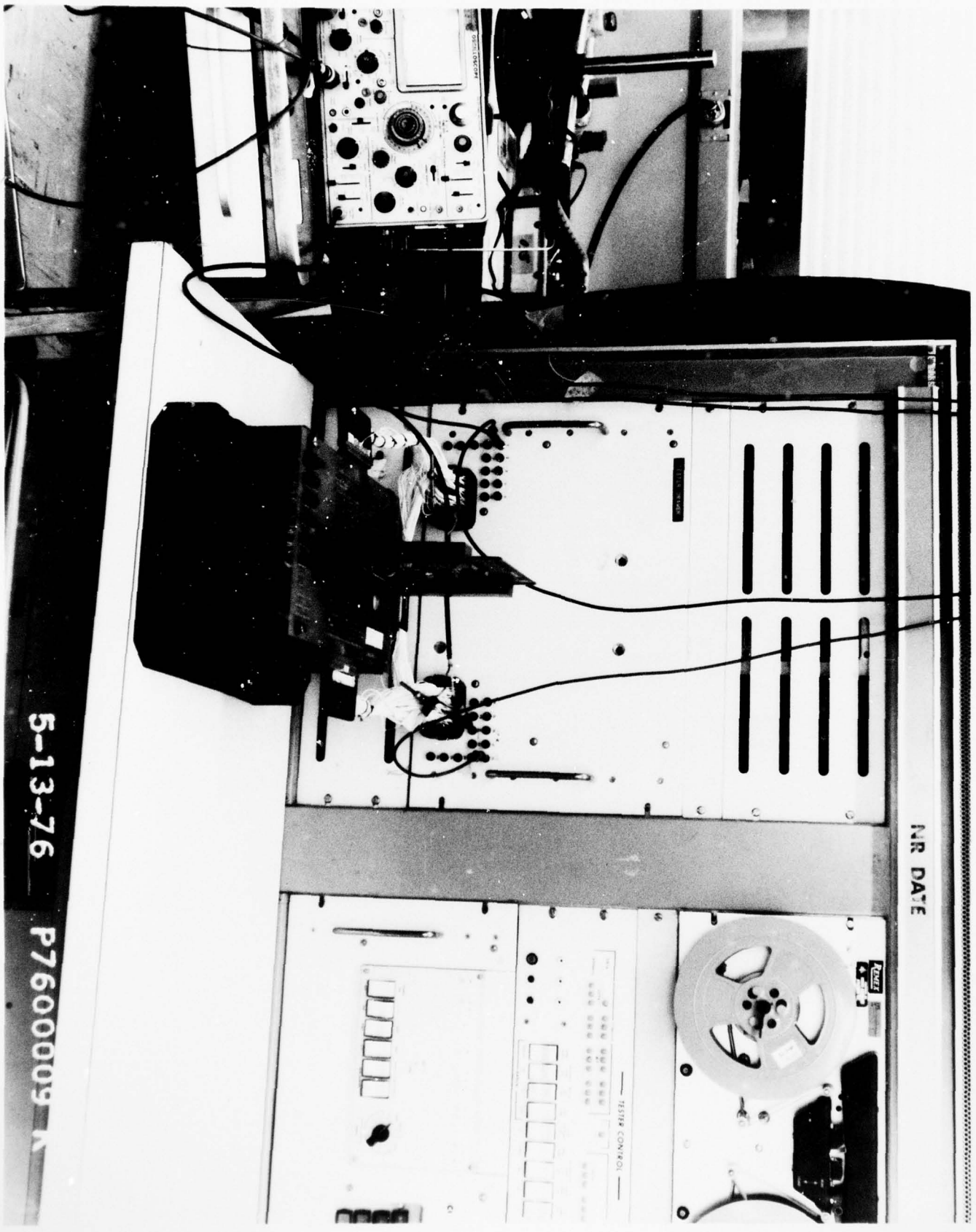
1. Performance boards for each DPU module to adapt these modules to an existing *Digital Automatic Test Equipment (DATE)* and a common test adapter.
2. DPU Test Console similar to the test console in the Software Test Station with a test fixture for mounting the DPU boards and the interface boards.

The engineering checkout of the three DPU modules was accomplished using the existing *Digital Automatic Test Equipment (DATE)*. This piece of test equipment is an Autonetics built tester which was designed specifically for testing MOS components and modules. It provides up to 96 channels of stimuli and can test for 96 channels of responses. These stimuli and response lines are grouped into 12-bit bytes. Each stimuli byte is programmable for both "zero" and "one" logic amplitudes, and timing relative to the four clock phases may be stipulated. Each response byte is also programmable as to minimum "1" levels, maximum "0" levels, and sampling period. In addition, voltage levels, clock amplitude, turn-on and turn-off times of all required clocks, frequency, and test length are all programmable. The tester can interface with either TTL or MOS circuits.

Three performance cards for module test were designed, one for each DPU module. These cards contain buffering for selected signals, and other interface circuitry unique to the module under test. A common adapter cable was designed to interface the performance cards with the DATE system. Figure 88 shows the performance card and the Memory Module in use with DATE.

88  
96  
Aug  
4/17  
~~Handwritten signature~~

Figure 88. Performance Card in Use with DATE



5-13-76 P76000009 K

*[Handwritten marks and scribbles at the bottom of the page]*

The DPU Test Console is functionally identical to the one used in the Software Test Station. A system test fixture providing mechanical support and electrical interconnection for DPU modules and their interface modules was designed, fabricated and tested. The two interface modules (CPU interface and I/O interface) were also designed, fabricated and tested. Both boards contain TTL circuits in DIP packages plugged into a wire wrap module. The CPU interface module provides clock circuitry and interface between the CPU and the control panel. It is used in the CPU and CPU/memory testing of the DPU. The I/O interface board is used only when the PIO board is plugged into the test fixture. It provides wraparound of DPU outputs to inputs to facilitate DPU self tests. Figure 89 shows the test fixture with DPU and the interface boards. Both interface boards use wide temperature components so as to allow the complete test fixture to be installed in the temperature chamber for temperature testing of the DPU.

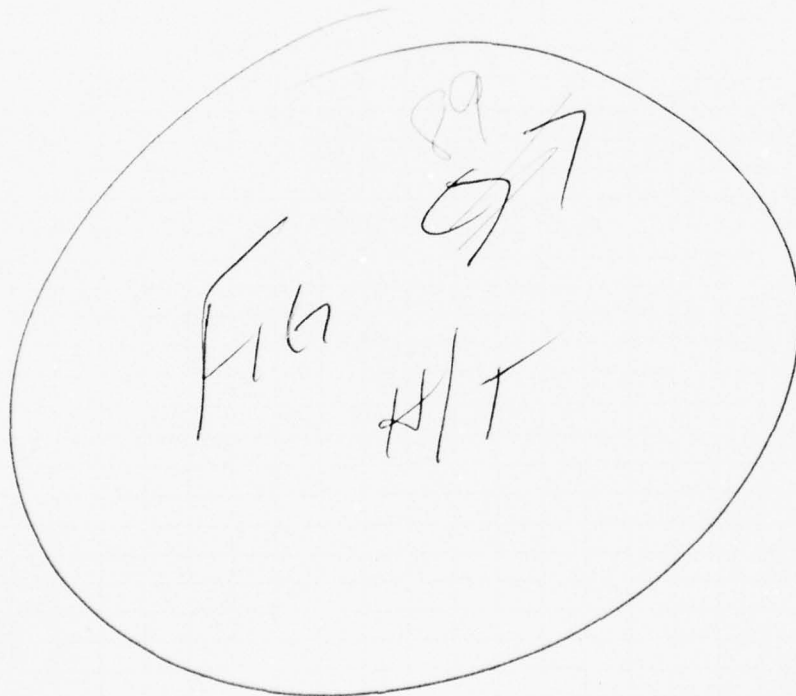
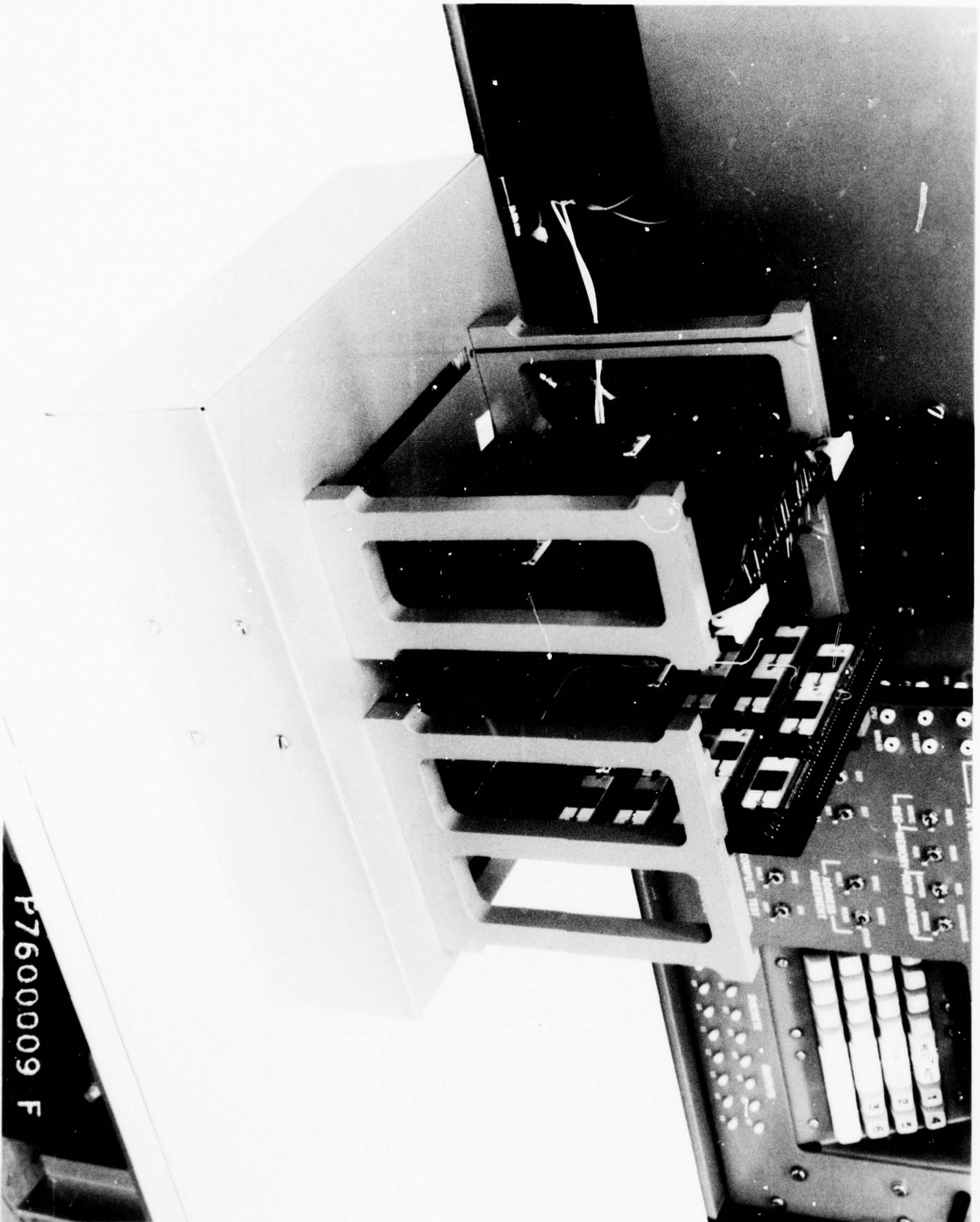


Figure 89. DPU System Test Fixture with DPU and Interface Boards



P7600009 F

5 1/2



The design, fabrication, and testing of the DPU Engineering Test Equipment was completed in April 1976 and was successfully used in DPU module checkout and DPU integration testing. In December 1976, the DPU system test fixture (shown in Figure 89) was modified to allow more accurate testing of the DPU at high temperature. The DPU temperature tests are discussed in Para 2.1.7 along with a more detailed discussion of the test fixture modification.

#### 4.1.4 Test Aids

The Test Aids designed and fabricated to support EPM integration are listed in Table 55.

TABLE 55. TEST AIDS

<u>Qty</u>	<u>Part No.</u>	<u>Description</u>
3	10070-727-1	Module Extender
1	02861-727-1	Module Extractor
1	02861-727-11	Module Extractor
1	10062-727-1	Goerz Cable (Gimbal)
1	10063-727-1	Goerz Cable (Base)
1	10518-727-1	CPC Pin Straightener
1	10517-727-1	CPC Removal Tool
1	10510-727-1	Power Supply Extender
1	10511-727-1	H. V. Switch Extender

#### 4.2 TASK 3.2, INU TEST STATION

The purposes of this task were to prepare a specification for an EPM System Test Station (STS) and to design, develop, fabricate, and integrate one EPM STS.

##### 4.2.1 STS Specification

A CI specification, AJ00093, was prepared to define the EPM STS configuration and signal interface. This activity was completed in December 1975.

##### 4.2.2 EPM STS Configuration

Design, development, fabrication, and integration of the EPM System Test Station was completed and the EPM STS was successfully used in integration of the EPM.

The EPM STS and its interface with the avionics and capital equipment is depicted in Figure 90, EPM System Test Station. Government furnished equipment (GFE),

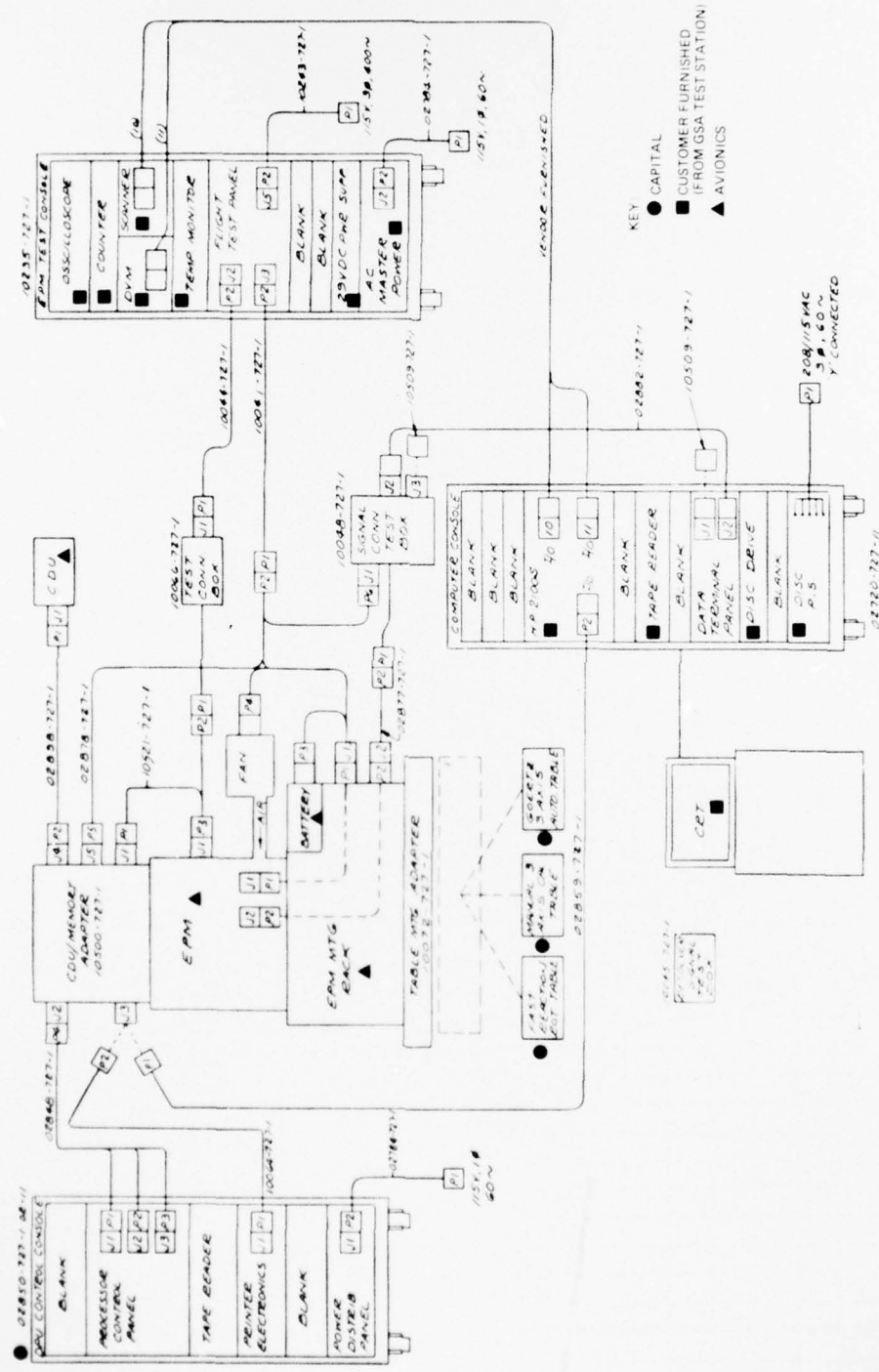


Figure 90. EPM System Test Station

taken from the Phase 2A GSA Test Station, is also identified since one of EPM STS objectives was to make maximum utilization of GFE from prior MICRON contracts.

The EPM, Flight Rack, Battery, Cooling Fan, and CDU/Memory Adapter are physically mounted together on a table mounting adapter which is compatible with either the manual or automatic (Goerz) tables. Short adapter cables are permanently attached to the flight rack in order to facilitate wiring and to provide a quick disconnect capability.

A discussion of the major components of the STS is given in the following paragraphs.

#### 4.2.2.1 CDU/Memory Adapter (also see Para 2.3)

The CDU/Memory Adapter provides:

1. A 16K word (16 bit) core memory and the necessary adaption circuitry required to make the memory electrically compatible with the EPM.
2. A bit parallel channel which can drive either a printer (located in the DPU Control Console) or a HP2100S Computer. This channel allows for data gathering and EPM calibration without depending on the 1553 data bus interface.
3. A compatible serial 100K bit serial channel capable of interfacing with the N57A CDU.
4. A continuation of the signals required for operation of the Computer Control Panel (CCP) located in the DPU Control Console.
5. A power supply and power control for all internal circuitry including the memory plus the power required by the CDU. The INU ON/OFF discrete is wired, internal to the EPM, to the CCP connector as well as the normal signal connector to allow for ON/OFF control from the CDU via the External Memory.

#### 4.2.2.2 DPU Control Console

The DPU Control Console contains a CCP for use with the DPU, a paper tape reader, and a printer and printer electronics. This console was built with capital funding.

#### 4.2.2.3 Data Terminal

The data terminal is physically packaged in a self contained panel which is mounted in the Computer Console (same Computer Console procured for use with the GSA Test Station under Phase 2A). The data terminal allows the HP2100S Computer to act as a system controller to test the data terminal function in the INU.

#### 4.2.2.4 Connector Test Boxes

The Connector Test Boxes provide test point signal access as required and the routing of signals required for display on the EPM Test Console. The test boxes are the prime interface for signals to be routed to the transient recorders (Biomations).

#### 4.2.2.5 EPM Test Console

The EPM Test Console consists of:

1. A Flight Test Panel which contains the prime power control and distribution to the EPM, cooling fan, and External Memory as well as display of critical signals.
2. A Temperature Monitor Panel obtained from the GSA Test Station.
3. Commercial equipment obtained from the GSA Test Station consisting of the scope and preamps, counter, DVM/Scanner, and 28V Power Supply.

#### 4.3 TASK 3.3, REPAIR

The purpose of this task was to repair in-house, as necessary, the EPM and STS. This task also included repair, as necessary, of the N57A-1, N57A-2, HAFB GSA, and the Phase 2A residual hardware.

All failures at the system level were recorded on FRR (Form for Removal Reporting) forms. The failures were then analyzed by the responsible engineer, the reliability engineer and appropriate people from fabrication and Material and Processes (M&P) laboratories. When the failure was isolated, the failed component was sent to the M&P laboratories for analysis if deemed necessary by the reliability engineer and the responsible engineer. The FRR's were closed out by the signature of the reliability engineer.

Repair of gyros was accomplished for failures due to rotor drops (11), improper polhode signature (1), MUM amplitude too high (1), large leak (1), vac ion pump high voltage feedthrough pin (1) and spark damage of inertial grade and suspender type gyros. Seven rotor drops occurred on the EPM system. The causes for these were identified. (See Integration Para 2.5.) A dual rotor drop, caused by operator error, occurred on the N57A-2. One rotor drop (cause not established) occurred on the Holloman Gyro subassembly. One rotor drop occurred on Test Station IV. The cause for the drop was not clearly established. It is noted, however, that the table was being moved at the time of the drop and it is suspected that a mechanical shock of the table as it was being moved could have been the cause. Table shock transients of very high g levels could be experienced if the table hits its hard stops. The Biomation fault monitors indicated no power or suspension electronics problems. The test station has been operating reliably since the drop.

EMA repair activity consisted of repair of two digitizers. In November 1976, EMA A77M-7604-002Y was removed from the EPM when its scale factor became excessively high. Diagnostic test isolated the cause to a zener diode in the precision current generator section of the digitizer. This digitizer was exposed to -100°F and the stress frame epoxy shrinkage could have caused the failure. The temperature cycle

process has been changed and the low temperature exposure is now -65°F which is the temperature limit recommended by the supplier of this part. The digitizer was replaced and EMA A77M-7604-002Y was acceptance tested. In December, EMA A77M-7604-003Y was repaired by replacing a zener diode in the digitizer. This instrument, along with A77M-7604-002Y, underwent long-term testing to insure that the zener diode failure will not occur again when the instruments are placed in the system.

Activity under the repair task also included repair of electronics hardware. A chronological summary of the electronics repair activity is given in the following paragraphs.

In July 1976, the Central Processor Unit (CPU) was repaired six times. Of these six failures, four were results of failures of ROM A0917 devices, one required replacement of a clock driver which was accidentally shorted in system test, and one was due to a cold solder joint on the MLB. The ROM A0917 failures were traced to a charge buildup in three output gates which were left floating when the wafers were reworked to improve the operating voltage range. ROM A0916s were also subject to this type of potential failure, since they were reworked using the same technique. The problem was corrected by fabricating new ROM A0916s and A0917s, using new masks, which eliminated the specific failure mode in the device.

In September, a CPU failure was experienced at the system level which was traced to the AB devices. This problem was corrected by replacing all the AB devices with devices containing the latest design changes. The AB device problem is discussed further in Para 2.1.7.

In September, a CCS No. 2 hybrid circuit was returned for repair. The failure was traced to a 54128 line driver which had inadequate current protection. Consequently, the design was changed to a 5433Y quad-2 NOR buffer (open collector) with a pull-up resistor. The new parts were ordered in September but were not received until December. The failed part was replaced in December and the hybrid was satisfactorily retested.

Also in September, a Charge Amplifier Assembly was returned for repair of an open circuit on the MLB. This was corrected by adding a jumper on the MLB.

In September and October, two replacement spin motors were fabricated and assembled. One was used to replace the motor which was apparently damaged during installation. The other was used to replace a motor which was inadvertently overheated during integration testing.

Repair of electronics during October consisted of the following:

An SEU 3 was returned for repair when a "power on" condition could not be maintained. The problem was isolated to a failed Sequencer 1 hybrid. Transistor Q1 had failed, probably from a negative transient on the collector lead. Diodes have now been placed in all collector leads to prevent similar occurrences.

An SEU 4 was returned for repair when the Channel 3 control output was found to be a sawtooth instead of a squarewave during the heat mode. The failure was isolated to a Spin Motor Controller hybrid which was subsequently replaced to correct the problem.

A PIO module was returned for repair which required replacement of three bi-polar devices. The cause of the failed devices is not known.

A Spin Motor Power Amplifier Heat Sink Assembly was returned for repair. Transistors Q13 and Q14 shorted. These failures resulted in overloading diode CR1, and resistors R32, R33, and R14 and caused a circuit line to open.

Power Supply Board No. 1 was returned for repair. A shorted output transistor, Q10, (2N6322) was found in the switching preregulator. The cause was most likely an overload or inadvertant short on the unregulated power output from Power Supply Board No. 's 2 and 3.

Power Supply Assembly (Boards 2 and 3) was returned when a 2 ohm short between the chassis and primary ground was observed on the system. The problem was found to be due to a short between the shield under transistors and the chassis. The unit was repaired and returned to integration.

Repair of electronics during November consisted of the following:

An SEU No. 1 Module was returned for repair because the preload signal intermittently disappeared during system operation. A loose wire, about 0.25 inches long was found lodged under the sleeving of the 10 kHz line which feeds modulator pin 15 and calibration line pin 20. The wire was removed and the module was returned to the system test laboratory.

On an SEU No. 2 Module, the multiplexer hybrid failed due to physical damage to Z<sub>2</sub> (Harris CF506A multiplexer chip). Channel 8B on Z<sub>2</sub> line was fused on the chip. This indicates high input current flow which was probably induced. The Z<sub>2</sub> chip was replaced to repair the unit.

On a Spin Motor Electronics Assembly, the circuit line from relay K1-B1 to A3J4-20, 21 and 22 was burned open. It was found that a short external to the Spin Motor Electronics Assembly induced the failure. The module was repaired and returned to the system test laboratory.

Defective feedthrough connections were found on a Charge Amplifier assembly teflon board. Jumpers were added on the MLB to correct this problem. The Charge Amplifier teflon boards were ultimately replaced with glass epoxy boards.

In December, a Charge Amplifier hybrid was found to be slew rate limited on negative slopes (positive to negative transition). The hybrid was delidded and a capacitor was found to be making a poor connection to the bonding pad due to the insufficient use of conductive epoxy during assembly. Repair of this hybrid was completed in December.

Repair of electronics during January 1977 consisted of the following:

A Charge Amplifier Assembly, which was suspected to have caused a rotor drop during EPM integration testing, was removed and tested. During exposure to high temperature testing, one of the 27059-404-1 transformers utilized on the module failed. (An intermittent twist capsule wire was subsequently found to be the cause of the rotor drop.) A failure analysis of the transformer was performed by de-potting the transformer and examining the transformer internally. The

failure analysis revealed that conduction had occurred between the secondary windings and the core. In order to prevent a similar occurrence on the remaining transformers in the system, all the transformers were removed from the Charge Amplifiers and tested with an excess of 1000 volts. Also, drawing changes were made specifying changes in the fabrication which should reduce the likelihood of this occurrence.

Intermittent operation of another Charge Amplifier Assembly was due to an open contact between the transformer lead and the MLB which was caused by a lead extension cut too short from the transformer pin to the MLB pad. The lead was extended to correct the problem.

The failure of a High Voltage Switch module caused a high speed desuspension. The failure was due to an internal open in the transformer winding which was intermittent at the system level. The transformer failure analysis and depotting revealed that a secondary winding had been burned open. This could only occur by application of excessive current in the secondary winding, possibly due to operator error during subassembly testing.

Repair of electronics during February 1977 consisted of the following:

A failure of a DPU discrete input was observed in EPM testing and was traced to a low impedance input in one of the Multiplexer (MXF) MOS devices. Further analysis revealed that the device had been damaged by static charges. The part was removed and replaced with another MXF from inventory. Retest of the module revealed that the replacement part had also been damaged. After replacement of several MXF parts, it was concluded that a significant percentage of the MXF parts inventory had been damaged by static charges, and the remaining inventory of MXF's was submitted to functional retesting. The tests yielded six good devices from an inventory of thirteen. The module was repaired with a retested good device and operated satisfactorily. In order to prevent similar occurrence with MXF's or other MOS devices, the personnel handling MOS devices were reminded of proper handling and storage procedures for MOS devices.

During EPM integration testing in the Van, a loss of 60 Hz occurred. This, in turn, caused the 3 phase 400 Hz generator to slow down. When this occurred, the power supply switched onto battery. When 60 Hz turned on again, the 400 Hz generator spun up, but the power supply did not transfer from battery. This occurs because the preregulator latches into the off state with this mode of operation. The power supply was not designed to operate in this mode since MIL-STD-704 does not require operation with less than 320 Hz input. In future EPM van tests, this will not be a problem since the computer alive discrete will not be disabled and the system will shutdown when transfer to battery is in excess of 10 seconds.

In the process of evaluating the above problem, a second Power Supply No. 1 was used. This power supply (transistors Q<sub>10</sub>, Q<sub>12</sub>, Q<sub>13</sub>, Q<sub>15</sub>) failed when transfer to battery occurred.



SECTION V

TASK 4, AIR FORCE FLIGHT TEST

No Air Force flight test requirements were included in Phase 2B.



AD-A048 000

ROCKWELL INTERNATIONAL ANAHEIM CALIF AUTONETICS GROUP  
MICRO NAVIGATOR (MICRON) PHASE 2B VOLUME I. TECHNICAL REPORT.(U)  
AUG 77 J M MILLER, A P ANDREWS, T F BRASHER F33615-75-C-1301  
C75-787/201-VOL-1 AFAL-TR-77-138-VOL-1 NL

F/O 17/7

UNCLASSIFIED

4 OF 4

AD  
A048000



END  
DATE  
FILMED  
-78  
DDC

**SECTION VI**  
**TASK 5, SYSTEM MANAGEMENT**

**6.1 TASK 5.1, PROGRAM MANAGEMENT**

The purposes of this task were to provide program management and project engineering for Phase 2B, conduct formal and informal design reviews, develop a detailed work breakdown structure (WBS) and a Phase 2B Program Plan, and modify as necessary the personnel, marketing, financial, and facilities plans prepared under Phase 2A.

**6.1.1 Design Reviews**

**6.1.1.1 Phase 2A Final Fee Evaluation/Design Review Meeting**

The Final Fee Evaluation Board Meeting and Design Review of the Phase 2A contract was held at Autonetics on 6 through 8 October 1975. This meeting was prepared and conducted on Phase 2A funding and is discussed in this report since it has not been previously documented in any final report. (The meeting was conducted after publication of the Phase 2A Final Report.)

The following personnel from organizations other than Autonetics Anaheim attended this meeting:

<u>Name</u>	<u>Organization</u>
Mr. J. W. Chin	USAF/AFAL
Capt. R. E. Janosko	USAF/AFAL
Mr. P. W. Eignor	USAF/AFAL
Maj. R. C. Brandt	USAF/AFAL
Mr. G. E. Himes	USAF-ASD/PPMEB
Capt. W. G. Peterson	USAF/AFAL/RWM
Fran Rockvam	AFPRO/TMD
J. W. Caldwell	AFPRO/PD
G. Atkisson	AFPRO/TMD
M. Pidhayny	AFPRO RI/EO
R. A. Holtz	(MMC)

The agenda for the Phase 2A Final Fee Evaluation and Design Review meeting is presented below:

Monday, 6 October 1975

8:15	Introduction	Capt. W. Peterson J. A. Schwarz
9:15	Overview	G. E. Runyon
10:15	Gyro Design Improvements/Testing	H. L. Bump A. G. Gross

11:15	VacIon Pump Elimination/Getter	A. G. Gross
1:30	Second Source Rotors/Cavities Support	H. L. Bump
1:45	Test Planning/Developmental Testing	T. F. Brasher
3:00	N57A-1/N57A-2 Flight Test Data Analysis	D. W. Holmes
4:00	N57A-2 Flight Test at HAFB	D. W. Holmes

Tuesday, 7 October 1975

8:15	Software Development	A. P. Andrews
8:30	Mechanization/Modeling Improvements	A. P. Andrews
9:30	Gyro Subassemblies	C. C. Whang, Jr. J. F. Klinchuch
11:00	Gyro Subassembly Test Station	J. D. Courtier
1:30	4-Plate GSA Test Results	T. F. Brasher
1:30	8-Plate GSA/MESGA Test Results	R. B. Hall
2:15	DPU Memory and Interface	W. P. Thoennes
4:00	Electronics Improvements/Simplifications/Tradeoffs	J. F. Klinchuch
4:30	Parts Program	A. L. Sattler

Wednesday, 8 October 1975

8:00	Cost of Ownership	M. J. Rupert F. R. Hall K. J. Gibson L. E. Johnsen R. A. Holtz (MMC)
11:30	Data	J. M. Miller
1:00	Technical Summary	G. E. Runyon
	Contract Administration	
1:45	Cost	F. E. Loftus

2:30	Administrative	L. C. Renold
3:00	Summary	J. A. Schwarz

6.1.1.2 Phase 2B Fee Evaluation/Design Review Meeting

The MICRON Phase 2B Fee Evaluation/Design Review Meeting was held at Autonetics on 7 through 9 June 1976.

The following personnel from organizations other than Autonetics Anaheim attended this meeting:

<u>NAME</u>	<u>ORGANIZATION</u>
Maj. Roger C. Brandt	RWA/666A
Maj. D. E. Culler	4950/PMEB
Capt. R. E. Janosko	RWA/666A
George Himes	4950/PMEB
Ronald L. Ringo	RWA
Philip W. Eignor	RWA/666A
Capt. Robert F. Lemon, Jr.	AFLC
Lt. Col. J. A. Pasalevich	AFPRO/EN
Capt. C. L. Moore	AFPRO/EN
Myron Pidhayny	AFPRO/EN
Capt. Gary Howe	AFPRO
Lt. Gary Luebbers	AFPRO
Dr. John Niemela	Army ECOM
G. A. Farrell	AGMC
Don Hardy	AGMC
J. H. Gilmore	Rockwell Northeastern District Office
Lew Jobe	Program Management Representative

The agenda for the Phase 2B Fee Evaluation/Design Review Meeting is presented below:

Monday, 7 June 1976

1:45	Introduction	G. Himes/ Capt. Janosko/ J. E. Menzel
2:15	Overview	G. E. Runyon
3:15	System Engineering	T. F. Brasher
4:00	Error Analysis and Budget	A. P. Andrews
4:30	EPM System Software	J. H. Mitzel
5:00	Test Station Software	A. P. Andrews

Tuesday, 8 June 1976

8:15	EPM	R. L. Rumbold/ H. Kamei
9:15	INBU	C. C. Whang
9:35	Data Terminal	J. N. Gayer
10:20	EPM Electronics	J. F. Klinchuch
11:30	A/D Converter and Spin Motor MOS	J. F. Klinchuch
11:45	INU MOS	J. Jurison
1:15	DPU	J. Jurison
2:00	EMA	D. J. Key
2:30	MESG	H. L. Bump
3:15	Getter Gyro	A. G. Gross
3:45	Associate Contractor MESG Fab/Testing/Support	H. L. Bump
4:00	Test Equipment	
	INS Test Station/Test Aids	J. D. Courtier
	CDU	G. L. Lawson
4:30	Parts and Beam Lead Carrier	A. L. Sattler

Wednesday, 9 June 1976

8:15	Data	J. M. Miller
8:30	Cost of Ownership	M. J. Rupert
	Acquisition Cost	L. E. Johnsen
	Reliability	F. R. Hall
	Life Cycle Cost	K. J. Gibson
10:15	Contract Cost Performance	F. E. Loftus
10:45	Contract Administration	L. C. Renold
11:00	Summary	J. E. Menzel
1:15	Government Only Caucus	

6.1.1.3 Informal Design Reviews

A total of ten (10) informal design reviews were conducted during the course of the Phase 2B contract. All these design reviews were held at Autonetics.

6.1.1.3.1 First Informal Design Review. The first informal design review was held on 18 through 20 August 1975. Personnel in attendance from organizations other than Autonetics were Capt. W. Peterson and Mr. D. Pleva, both of AFAL. The agenda for this design review was as follows:

Monday, 18 August 1975

8:00	Autonetics Organization	J. A. Schwarz A. P. Truban G. E. Runyon
1:30	High Accuracy MICRON	G. W. Sargent
2:00	Rotated N57A for Holloman Flight Tests	G. E. Runyon

2:15	Parts Program Status/Plans/ Approach	A. L. Sattler
3:30	Navy ESG Programs	H. J. Engebretson
4:30	Phase 2B Budgets	J. A. Schwarz F. E. Loftus
4:45	Accelerated GFY 76 and 77 Expenditures	J. A. Schwarz A. P. Truban F. E. Loftus

Tuesday, 19 August 1975

8:15	Electronics Design Status/ Plans/Approach	J. F. Klinchuch
9:45	Accelerometer Vendor Discussions	A. P. Truban
10:15	Autonetics EMA Status/Plans/ Approach	D. J. Key
11:00	Reaction Time	J. C. Pinson D. T. Friest
1:30	MESG Status/Plans/Approach	H. L. Bump J. C. Boltinghouse
2:30	MESG Lab Tour	J. C. Boltinghouse H. L. Bump A. G. Gross
3:15	Getter Status/Plans/Approach/ Lab Tour	A. G. Gross H. L. Bump J. C. Boltinghouse
4:00	Cost of Ownership Team Status/Plans/Approach	M. J. Rupert L. E. Johnsen K. J. Gibson F. R. Hall R. A. Holtz (MMC)

Wednesday, 20 August 1975

8:15	Cost of Ownership (Cont)	
9:00	DPU Status/Plans/Approach	W. P. Thoennes A. P. Truban
10:00	N77 Status/Plans/Approach	A. P. Truban

10:30	MICRON Lab Tour	G. E. Runyon
11:00	EPM System Design	R. L. Rumbold

6.1.1.3.2 Second Informal Design Review. The second informal design review was held on 10 October 1975. Personnel in attendance from organizations other than Autonetics were Mr. G. Himes, Maj. R. Brandt, Capt. W. Peterson, Capt. R. Janosko, Mr. J. Chin, and Mr. P. Eignor, all of AFAL and Mr. M. Pidhayny of AFPRO. The agenda for this design review was as follows:

8:15	Overview Schedule	G. E. Runyon
8:25	System Engineering	T. F. Brasher
9:00	Software and Analysis	A. P. Andrews
9:30	ESG Fabrication Tour	H. L. Bump J. Boltinghouse
10:45	DPU	W. Thoennes
11:15	Electronics Design	J. F. Klinchuch
1:00	EMA Technology and Lab Tour	D. J. Key
2:00	Cost of Ownership	M. J. Rupert F. R. Hall R. A. Holtz (MMC) L. Johnsen K. J. Gibson
3:00	Need Firm EPM Requirements Definition	A. P. Truban
4:00	MICRON Lab Tour	A. P. Truban

6.1.1.3.3 Third Informal Design Review. The third informal design review was held on 9 through 11 December 1975. Personnel in attendance from organizations other than Autonetics were Maj. R. Brandt, Maj. Raroha, Capt. W. Peterson, Capt. R. Janosko, and Mr. P. Eignor all of AFAL and Mr. M. Pidhayny of AFPRO. The agenda for this design review was as follows:

Tuesday, 9 December 1975

8:30	Phase 2B Overview	G. E. Runyon
9:00	System Specification	T. F. Brasher
9:30	INU Specification	T. F. Brasher
10:30	INU Packaging	C. C. Whang
11:30	INBU	C. C. Whang
1:00	DPU Specification	P. W. Hinman
1:30	DPU Memory	P. W. Hinman

2:00	Preliminary Error Budget	A. P. Andrews
2:45	Self Calibration Mechanization	J. C. Wauer
3:30	Getter Gyro	A. G. Gross
		H. L. Bump
		J. C. Boltinghouse

Wednesday, 10 December 1975

8:15	Parts Standardization	A. L. Sattler
8:30	Beam Lead Carrier	A. L. Sattler
9:00	Electronics	J. F. Klinchuch
10:15	EMA	D. J. Key
11:15	EMA Lab Tour	D. J. Key
1:00	Ring Laser Gyro Development	H. J. Engebretson
		P. L. Anthony
		S. G. Shutt
3:15	RLG Lab Tour	P. L. Anthony
3:45	Phase 2B Cost Status/Plan	F. E. Loftus

Thursday, 11 December 1975

8:15	MICRON Future Planning	T. K. Shuler
		G. W. Sargent
		J. A. Schwarz
9:30	N77 INS Status Review	J. T. Chapman
10:45	Army High Accuracy MICRON Status	J. A. Schwarz
11:00	Discuss Ø2B/IR&D Hardware Interchangeability	J. T. Chapman
1:00	Use of N57A for Navy Radar Stabilization Demo	W. R. Knight
2:00	High Accuracy Development Program to Production and Hardening Thereof	A. P. Truban
		J. A. Schwarz
		P. Y. Joe
		J. F. Klinchuch
3:00	AFAL/AFPRO (Gov't only mtg)	Capt W. Peterson
		M. Pidhayny
4:00	Mobil Evaluation Lab Availability for N77 Testing in June/July 1976	J. T. Chapman
		A. P. Truban

6.1.1.3.4 Fourth Informal Design Review. The fourth informal design review was held on 10 through 12 February 1976. Personnel in attendance from organizations other than Autonetics were Capt. W. Peterson and Mr. P. Eignor of AFAL, Mr. R. Clodfelter of AGMC, Mr. J. Niemela and Mr. R. Clark of USA/ECOM, Mr. R. Holtz and Mr. R. Burrows of MMC, Capt. Moore and Mr. J. Caldwell of AFPRO, and Mr. J. Gilmore of RI/N. E. District Office. The agenda for this design review was as follows:

Tuesday, 10 February 1976

8:30	Organization	J. A. Schwarz
8:45	Ø2B Overview	G. E. Runyon
9:15	INU Packaging	C. C. Whang
9:45	INBU	C. C. Whang
10:15	DPU	J. Jurison
11:00	Electronics	J. F. Klinchuch
1:15	Parts/Beam Lead Carrier	A. H. Fanzoi
1:45	MESG	H. L. Bump
2:30	Getter Gyro	A. M. Kinan
3:15	EMA	D. J. Key
3:45	MUX	J. N. Gayer

Wednesday, 11 February 1976

8:30	Velocity Accuracy	A. P. Andrews
9:15	Software	A. P. Andrews
9:45	N77 and N77R Status	J. T. Chapman
10:45	Hardened High Accuracy MICRON	P. Y. Joe
1:15	Phase 2B Cost Status Plan	F. E. Loftus
1:30	B-52 RFI	G. J. Campos
2:00	Standard Nav Spec	H. J. Engebretson M. J. Rupert
3:00	Cost of Ownership	M. J. Rupert L. E. Johnsen F. R. Hall K. J. Gibson
4:00	Martin-Marietta Reliability Presentation	R. Holtz
4:30	N77 Holloman Support Plan	J. T. Chapman T. F. Brasher

Thursday, 12 February 1976

8:15	Navy ESG Tour	H. J. Engebretson
9:15	MICRON System Lab Tour	T. F. Brasher
10:00	MOS/Hybrid Tour	J. F. Sexton
1:15	Ring Laser Gyro Briefing	H. J. Engebretson
2:00	MESG Factory Tour	J. C. Boltinghouse
2:30	EMA Lab Tour	D. J. Key

6.1.1.3.5 Fifth Informal Design Review. The fifth informal design review was held on 5 through 8 April 1976. Personnel in attendance from organizations other than Autonetics were Capt. R. Janosko, Mr. P. Eignor, and Mr. D. Pleva of AFAL and Lt. Col. J. Pasalevich, Capt. C. Moore, and Mr. J. Caldwell of AFPRO. The agenda for this design review was as follows:

Monday, 5 April 1976

1:00	Air Force Caucus	
2:00	High Accuracy Schedule	E. Menzel
2:15	F-4E Study Approach	C. Homolka
3:15	Non-Contract Activity Overview	E. Menzel
3:20	B-52 RFI Summary	G. Campos
3:45	N77, N77R & EPM #2 Status	J. Chapman
4:15	Rotated EPM Packaging	C. Whang

Tuesday, 6 April 1976

8:30	Gyro Factory	J. Boltinghouse
9:15	System Lab Tour	T. Brasher
9:45	EMA Lab Tour	D. Key
10:30	EMA	D. Key
11:00	Getter Gyro	A. Gross
1:15	IUS Summary	Schwarz Chapman

1:45	Parts/Beam Lead Carrier	A. Fanzoi
2:30	N77 and N77R Software	G. Andrews
3:15	Rotation Technical Discussion	J. Pinson
4:00	IR&D/Contract Hardware Interchangeability	L. Renold

Wednesday, 7 April 1976

8:30	System Schedule Options	
1:15	Ø2B Overview	G. Runyon
1:45	MIB Status	T. Brasher
2:00	Integration Support Plan	Brasher Klinchuch
2:15	INU Packaging	C. Whang
2:45	INBU	C. Whang
3:15	DPU	J. Jurison
3:45	Electronics	J. Klinchuch
4:15	Ø2B Test Equipment	J. Courtier

Thursday, 8 April 1976

8:30	Ø2B Cost Status	F. Loftus
9:15	Cost of Ownership	M. Rupert J. Johnsen F. R. Hall K. Gibson
10:15	Martin-Marietta Reliability Presentation	R. Holtz
10:30	MESG	P. Bump
11:00	EMA	D. Key
11:30	MUX	F. Gulde

1:15	Velocity Accuracy	A. Andrews
1:40	EPM Software	A. Andrews
2:00	Doppler Aided Flight Test Cost/Schedule	A. Andrews
2:20	PDP11 Computer in Bus	D. Pleva
2:45	Bus Schedules	J. Chapman
3:15	Standard Nav Spec	Engebretson Rupert
3:45	Summary	J. Schwarz
4:30	Air Force Recap	Capt. Janosko

6.1.1.3.6 Sixth Informal Design Review. The sixth informal design review was held on 10 June 1976. Personnel in attendance from organizations other than Autonetics were: Maj. Brandt, Capt. Janosko, R. Ringo, and P. Eignor of AFAL; Maj. Culler and G. Hines of ASD; Capt Lemon of AFLC; Capt. Moore and M. Pidhayny of AFPRO; and G. Farrell and D. Hardy of AGMC. There were no formal agenda for this design review.

6.1.1.3.7 Seventh Informal Design Review. The seventh informal design review was held on 13 and 14 July 1976. Capt. R. E. Janosko (AFAL) and M. Pidhayny (AFPRO) were in attendance at this meeting. The agenda for this meeting was as follows:

Tuesday, 13 July 1976

1:00	Schedule Review	G. E. Runyon
1:45	Integration Testing	T. F. Brasher
2:15	MHU/IAU	C. C. Whang
2:35	DPU	J. Jurison
3:05	Cost Performance	F. E. Loftus
3:30	Software	J. H. Mitzel
3:50	Magnetic Sensitivity Test Results	A. P. Andrews
4:20	MESG	H. L. Bump
4:40	Getter Gyro	A. G. Gross

Wednesday, 14 July 1976

8:15	EMA	D. J. Key
8:45	Electronics	J. F. Klinchuch
9:15	Col. Ziernicki Briefing	
1:15	Lab Test Discussion	Janosko/Runyon/Brasher
1:35	Program Schedules/Holloman Delivery	Janosko/Menzel/Runyon

6.1.1.3.8 Eighth Informal Design Review. The eighth informal design review was held on 11 August 1976. Capt. R. Janosko and Mr. P. Eignor of AFAL and Mr. M. Pidhayny from AFPRO were in attendance at this meeting. The agenda for this meeting was as follows:

8:15	Schedule Overview	G. E. Runyon
8:45	Integration Testing	T. F. Brasher
9:15	DPU	J. Jurison
9:30	Rotated MHU/LAU	C. C. Whang
9:45	Electronics	J. F. Klinchuch
10:15	Software	J. H. Mitzel
10:30	MESG	J. Boltinghouse
10:45	Cost of Ownership	
	Producibility	L. E. Johnsen
	Reliability	F. R. Hall
11:15	Martin-Marietta	R. A. Holtz
1:15	EMA	D. J. Key
1:30	Contract Cost Performance	F. E. Loftus
1:45	Standard Nav Spec/EPM Differences	J. A. Schwarz
2:15	EPM Ownership Swap	L. C. Renold
2:30	Contract Proposal Discussion	Menzel/Runyon
3:15	System Lab	T. F. Brasher

6.1.1.3.9 Ninth Informal Design Review. The ninth informal design review was held on 21 October 1976. Personnel in attendance from organizations other than Autonetics were: Maj. Raroha, Maj. Brandt, Capt. Janosko, and Mr. P. Eignor of AFAL; Mr. G. Lewis of ASD; and Mr. M. Pidhayny of AFPRO. The agenda for this meeting was as follows:

8:15	Ring Laser Gyro	H. H. Engebretson
8:45	Schedule Overview (EPM 1 and 2)	G. E. Runyon
9:15	Integration Testing	T. F. Brasher
9:45	DPU	J. Jurison
10:10	Electronics	J. F. Klinchuch
10:20	Software	J. H. Mitzel
10:30	MESG	H. L. Bump
10:40	Getter Gyro	A. G. Gross
10:50	EMA	K. K. Jin
1:00	Martin-Marietta Reliability	R. A. Holtz
1:00	Van Tour	R. B. Clark
1:30	System Lab	T. F. Brasher
1:50	Contract Cost Performance	F. E. Loftus
2:05	Pre-Production/Production Planning	J. A. Schwarz
2:20	Proposal Discussion	J. E. Manzel/L. C. Renold/ G. E. Runyon

6.1.1.3.10 Tenth Informal Design Review. The tenth informal design review was held on 14 and 15 December 1976. Personnel in attendance from organizations other than Autonetics were: Capt. Janosko and Mr. P. Eignor of AFAL; Mr. G. Lewis of ASD; and Mr. M. Pidhayny of AFPRO. The agenda for this meeting was as follows:

Tuesday, 14 December 1976

1:15	Proposal Discussion	All
------	---------------------	-----

Wednesday, 15 December 1976

8:15	Schedule Overview (EPM 1 & 2)	G. E. Runyon
8:35	Integration Testing	T. F. Brasher

9:05	Data Review	A. P. Andrews
9:45	Software	J. H. Mitzel
10:15	DPU	J. Jurison
10:35	Electronics	J. F. Klinchuch
10:45	MESG	H. L. Bump
10:55	EMA	D. J. Key
11:10	Martin Marietta Reliability	R. A. Holtz
11:30	Contract Cost Performance	F. E. Loftus

#### 6.1.2 Program Plans

The MICRON Phase 2B Program Plan was completed and submitted to AFAL in September 1975. This plan covered the work efforts as well as a technical description and schedule of events supporting the Phase 2B program.

The personnel, marketing, financial, and facilities plans prepared in Phase 2A were reviewed and it was determined that these plans were generally directly applicable to Phase 2B. Therefore, no specific update was made since the associated costs did not appear to be warranted.

#### 6.1.3 Work Breakdown Structure

A detailed work breakdown structure was prepared and submitted on 28 August 1975 as CDRL Item A003.

### 6.2 TASK 5.2, ASSOCIATED CONTRACTOR SUPPORT

The purpose of this task was to support the second source for MESG rotors and cavities and the non-destructible rotor and cavity effort, and provide office space and data to the reliability associate contractor's representative.

#### 6.2.1 Drawings and Specifications

Early in Phase 2B, two revised drawings and three revised specifications were forwarded to Northrop and CSDL via AFAL. These were revisions to documents submitted during Phase 2A. Drawing 12699-302 (cavity) was revised to add Megger test requirements between cavity plates. Drawing 12504-302 (rotor) was revised to increase major and minor diameters (for small gap MESG configuration). Specifications AA0109-009 (Deposition of an Electrical Nickel-Phosphorous Plating) and ST 0115A A0010 (Machine Parts: Tolerances, Surface Finish and Standard Configurations) were revised to reflect minor process changes and the most recent rotor configuration. The rotor fabrication specification (AL70030) was revised to more clearly define rotor fabrication operations and/or procedures, to incorporate the larger rotor size, and to revise operations to reduce flow time. Flow time was reduced by removing the 0.000050 lap operation between the 900° F oven bake and the temperature cycle thereby making two cleaning and handling operations unnecessary. The removed 0.000050 lap operation is now included in the final rough lap operation.

Drawings, specifications, and manuals describing the Autonetics owned Automatic Cavity Grinder, were submitted on 9 February 1975 as CDRL Item A00H. The documents accompanying the drawings consisted of the procurement specification which was used for design criteria for the cavity grinder (designed and fabricated by Pneumo-Precision Products, Inc.) and the maintenance and operating manuals.

#### 6.2.2 Associate Contractor Visits to Autonetics

Several visits to Autonetics were made by the associate contractors. The more significant visits are discussed in the following paragraphs.

##### 6.2.2.1 CSDL Visit (3 December 1975)

Mr. Ken Taylor of Charles Stark Draper Laboratories, conferred with Messrs. Joe Boltinghouse, Pete Bump, Al Benussi, and Al Gross, of Autonetics, on 3 December 1975. The subject was destruction-resistant materials for ESG electrodes. The topics discussed were as follows:

1. The significance of the argon content of sputter-deposited coatings. It was agreed that this must be evaluated in an ESG.
2. The acceptable level of magnetic susceptibility was discussed. Other than zero, Autonetics doesn't know where the acceptable to unacceptable value lies. It was agreed, however, that CSDL and Autonetics should both measure the same selected specimens to get the scale factor between their respective tests.
3. It was agreed that the scotch tape test for adhesion was the best repetitive test and that a small number of epoxy-bonded cleavage tests are useful.
4. The requirements for substrate surface geometry and finish were discussed.
5. The degree to which the electrical conductivity of the electrode material is important was reviewed.
6. The procedures and sequences for the machining and lapping of cavity surfaces were reviewed. Mr. Taylor was given a detailed shop tour.
7. The various candidate coating materials from both Autonetics and CSDL investigations were discussed. None of the currently identified candidates could be disqualified on an "a priori" basis.

##### 6.2.2.2 Northrop Visit (5 through 15 January 1976)

Northrop personnel were at Autonetics from 5 January 1976 through 15 January 1976. The purpose of the visit was: (1) coevaluate ESG parts which Northrop had processed; and (2) to review, in detail, ESG fabrication, assembly, and prefunctional test processes and techniques. The effort related to the ESGM program and the MICRON program. The following paragraphs document the activity of the two week period to update those concerned as to the full scope of Northrop activity and current capability.

In summary, Messrs. Bill Merritt, Bob Westhaver, Ken Milo and Paul Richardson were at Autonetics for almost two weeks. Hardware, which was brought for evaluation included two sets of rotors and cavities which Northrop had fabricated from their own purchased raw material (MICRON) and two preassembled spinners (ESGM) which Northrop had fabricated from piece parts as supplied by Autonetics. (The cavities were ready for plating and an extruded rotor bar was provided for rotor fabrication by Northrop.) Other hardware fabricated by Northrop and brought for evaluation included a stainless steel cavity master, A BeO cavity master, a mechanical cavity alignment tool, and "O" ring forming fixture and a fixture which aligns the support ring and Mu-metal shield to the ESG base. Two inductors and three suspension transformers (wound by Northrop) were also brought for Autonetics' evaluation.

All hardware was evaluated during the two week period in the presence of the Northrop personnel. There were no problems with the evaluation activity or the integrity of the parts with the following exceptions: (1) one spinner unit persisted as a slow charger. The diagnostic disassembly revealed a small contaminate on the rotor surface. The unit was recleaned, reassembled and placed back on prefunctional test. The unit then passed without problem; (2) the Northrop built cavity alignment fixture did not locate on the 0.680 in. dia. spotface of the twelve hole cavity half and did prove to be a problem for the mechanical alignment of the reworked spinner. The misalignment did cause some sparking on initial lift-off attempts of the reworked unit.

It is pointed out here that the cavity and rotor parts looked very good: measurements at Northrop agreed with measurements at Autonetics within the resolution of the equipment used ( $\pm 1\mu$ -inch). The surface finish of the MICRON cavity halves were observed to have somewhat "deeper than normal" lapping scratches and it was agreed that evaluation of the two sets to be delivered in February would be performed and the two best sets would be chosen from the four sets for full up instrument assembly and evaluation.

There was considerable activity while Northrop personnel were at Autonetics. Numerous meetings were held. Discussions included extrusion processes, fabrication techniques, shop tours, metrology measurements and prefunctional test and evaluation processes and techniques. Northrop personnel did much of the prefunctional test, cleaning and assembly of their own instruments. Northrop personnel took all hardware back with them with the exception of the two sets of rotors and cavities which were delivered on the MICRON program.

#### 6.2.3 Support to Reliability Associate Contractor (Martin Marietta Corporation)

A representative from Martin Marietta Corporation (MMC), was resident at Autonetics until January 1977. MMC, under separate contract with AFAL, provided assistance in performing reliability studies, predictions, failure reporting/analysis and independent reliability analyses in support of this program. Design and reliability data were provided to MMC to assist them in their various analyses.

#### 6.2.4 Other Associate Contractor Support Activities

Other activities in support of Associate Contractors are discussed in the following paragraphs of this report:

Para 2.1.10 Fabrication of MESH's for Second Source

Para 3.2 Development Tests

In addition, support to CSDL for the non-destructible rotor and cavity efforts also included the following activities:

Six BeO flat blanks, which were received from CSDL in June 1976, were nickel plated in July in support of magnetic susceptibility tests to be conducted on the plating material at CSDL. During August, the blanks were processed by Autonetics to render the units susceptible (with variations between units). Evaluation revealed that two of the units should be exposed to additional baking in order to establish a greater range of susceptibility. This was also accomplished during August 1976. Following subsequent retesting of these two units, it was decided to bake one of the two for an additional ten days at 3000F. This baking and characterization was completed in September. The flats were returned to CSDL in January 1977.

### 6.3 TASK 5.3, COST OF OWNERSHIP

The purposes of this task were to update as necessary the Phase 2A cost of ownership model and support the EPM analysis and design task through 30 September 1975 by trading off producibility, reliability, and maintainability parameters to arrive at a MICRON design which will result in low cost of ownership.

Cost of ownership support of the Engineering Prototype MICRON (EPM) resulted in several producibility, reliability, and maintainability tradeoffs as described in the following paragraphs.

Although this effort continued through the duration of the Phase 2B contract, only the cost of ownership activity performed under contract (5 August 1975 through 30 September 1975) is reported here. Consequently, the following paragraphs reflect status as of 30 September 1975.

#### 6.3.1 Producibility

The process flow, application of standards, material cost estimate, and cost predictions for the "Preliminary Hybrid Electronics Definition" were completed. The same "Preliminary Hybrid Electronics Definition" package was submitted to the Hybrid Microelectronics Division of Collins Radio Group, Dallas, Texas for a "B&P" cost estimate. Evaluation of the above data indicated a potential savings of >\$3,000 per system in recurring and non-recurring costs by utilizing the Collins facility.

It should be noted that the Collins estimate was for hybrids fabricated on thin film substrates. At the time, Collins was setting up a hi-rel thick film process facility with plans to be in production by April 1976. This capability would allow the continuation of present hybrid design for MICRON and the advantage of utilizing that process which is most cost effective for each hybrid circuit. Additionally, production set up costs are reduced by utilizing the existing process, assembly, and test facility.

The MESG drawing package (5/21/75 configuration) was processed through the work measurement group for application of standards to all details and assembly operations. All possible buy type items were processed through Purchasing for quotes from suppliers. Cost projections developed for the standard labor content and then compared against the "buy" costs indicated a 15 to 20 percent cost savings by utilizing those specialty suppliers for approximately 30 percent of the details. Fifteen drawings were "red lined", evaluated for cost tradeoff (50 percent labor reduction in these parts) and returned to the design group for analysis and changes.

A study to make SEU modules into four modules instead of two was completed. In the two module concept hybrids are mounted on both sides of an eight-layer aluminum core board. In the four module version hybrids are mounted on one side of a four-layer board with a surface heat sink. The study indicated a system savings of approximately \$250 for the four-module configuration.

### 6.3.2 Reliability

#### 6.3.2.1 Reliability Apportionment

Analysis of the Phase 2B ACF reliability requirement was initiated with the apportionment of the production INU specified MTBF ( $\theta_0$ ) to the subassembly level (i.e., SEU, DPU, etc). The apportioned MTBF value for each subassembly and the corresponding MTBFs predicted at the end of Phase 2A are shown in Table 56. This apportionment was considered preliminary; and was updated to reflect the results of the prediction study and trade-offs examined by the Cost of Ownership team during Phase 2B.

#### 6.3.2.2 Reliability Prediction

At the beginning of Phase 2B an initial prediction for the MICRON INU was projected for completion during the month of September 1975. However, activity on this effort was being paced by the release of a firm product description containing detail information on system partitioning, circuit design, board layout, and parts lists. The preliminary issue of the product description occurred on 29 September 1975 which resulted in the start and completion of the actual prediction effort to occur after the contract period for this task. (Note: The prediction study was continued and the initial Phase 2B prediction completed in early December 1975.)

TABLE 56. PHASE 2B RELIABILITY MTBF APPORTIONMENT - MICRON (ACF) INU

		APPORTIONED SPEC RQMT	PHASE 2A PREDICTION
MECHANICAL HOUSING UNIT	(MHU)	22,000	29,155
INSTRUMENT ASSEMBLY UNIT	(IAU)	4,444	6,329
SUPPORT ELECTRONICS UNIT	(SEU)	8,333	11,500
DEDICATED PROCESSOR UNIT	(DPU)	4,000	4,235
POWER SUPPLY UNIT	(PSU)	26,666	10,000
MULTIPLEX TERMINAL UNIT	(MTU)	10,000	16,025
CONVERTER UNIT	(CU)	44,444	53,475
INU SYSTEM TOTALS	MTBF	1,250	1,436
	FAIL. RATE (%/10 <sup>3</sup> HR)	80.00	69.65

#### 6.3.2.3 Specification Development (Support)

Reliability design and quality assurance verification requirements were generated for inclusion in the power subsystem specification. The reliability provisions of this specification were utilized as a basis for drafting the remaining subsystem specifications developed during Phase 2B.

The draft specification, entitled "Characteristics for an Inertial Navigation System (INS)," was reviewed and reliability comments generated for inclusion in Autonetics response. This document, dated July 1975, was prepared and distributed by ASD, AFSC, WPAFB for comment by potential INS suppliers.

#### 6.3.2.4 Autonetics' Reliability Study Activities

6.3.2.4.1 Beam Lead Reliability Survey. Beam lead device reliability was the subject of a telephone survey conducted for the MICRON program. By way of an introduction, each of the individuals contacted were advised of Autonetics intentions to utilize BLSJ devices in the design of hybrid electronic circuits for the MICRON. Also, the survey was being conducted to gain additional insight into the actual experience data of other users in sufficient detail to permit a continuing evaluation of the beam lead risks associated with achieving MICRON goals. A response was also solicited from BL users possessing data to compare their results and conclusions with those expressed by the Hughes reliability study.

Telephone contacts were initiated and completed with representatives of 12 separate companies and agencies concerned in one way or another with beam lead device reliability. Since experience data was the main concern of this survey, most of those individuals contacted represented the "user" as opposed to the "manufacturer" side of the BL community. Survey contacts are listed below:

- Bendix Corporation, Kansas City Division, Kansas City, Mo.
- Collins Radio Company, Avionics Division, Cedar Rapids, Iowa
- Collins Radio Company, Hybrid Electronics Division, Dallas, Texas
- IBM Corporation, Federal Systems Division, Owego, New York
- Martin-Marietta Corporation, Denver Division, Denver, Colorado
- Raytheon Company, Industrial Components Division, Quincy, Massachusetts
- Raytheon Company, Missile Systems Division, Bedford, Massachusetts
- Raytheon Company, Semiconductor Division, Mt. View, California
- Rome Air Development Center (RADC), R&M Engineering, Rome, New York
- Rome Air Development Center (RADC), Reliability Analysis Center (RAC), Rome, New York
- U.S. Army Electronics Command (ECOM), Ft Monmouth, New Jersey
- Sandia Corporation, Sandia Labs, Albuquerque, New Mexico

## Survey Results

### Availability

- Availability problem will be around awhile
- Industry demand not large enough at present
- Allow 40-50 weeks lead time for high reliability devices
- Select parts carefully - avoid complex custom circuits
- Continuous BL production currently at Texas Instruments, RCA, and Raytheon
- Be prepared to commit resources for development

### Reliability

- Manufacturer/user assessments agree that BLSJ device reliability is superior to chip and wire (C&W)
- Lots of Bell Laboratories data - but little otherwise:
  - IC failure rate (communication equipment)  
0.00011 - 0.0021%/1000 hours
  - IC failure rate (SAFEGUARD Life Tests)  
0.004 - 0.008%/1000 hours
- Bendix/Sandia claim Trident experience compares with Bell Laboratories
- Bendix/Sandia claim some new failure modes but indicate they are predictable, screenable and controllable
- Texas Instruments, RCA, Motorola and Raytheon using Bell Laboratories BLSJ process
- Careful attention to detail in procurement, screening, handling, assembly and rework essential to success
- Devices may require a protective coating to guard against particle contamination during assembly/rework; moisture protection may *not be required for normal use*
- Manufacturers/users do not support reliability conclusions of the Hughes BL study

### Testability

- BL carrier to improve testability - available soon
- Bendix/Sandia require visual, DC probe and temperature acceleration testing of an expanded wafer; and electrical characterization tests of die samples mounted on open header

- Bendix/Sandia, Raytheon and Collins claim >90% yield of BL devices (including rework) through final electrical tests of hybrids
- Provide for test point pads on hybrid for fault isolation

#### Cost

- Raytheon study indicates simple circuits (6 active devices) may be less cost effective if BLSJ devices are used rather than C&W.
- Costs are high; but attention to detail can yield savings

#### Survey Conclusions

A review of the survey results and published information obtained suggests that Autonetics is proceeding on a course of minimum risk with regard to implementing the beam lead technology. For example:

1. Careful attention has been given to development of the MICRON Item Identification Document testing requirements.
2. Parts are being selected carefully to maximize standardization, cost effectiveness and availability.
3. Beam lead carrier development is continuing and looks promising.
4. The majority of the beam lead active devices in the current MICRON SEU and IAU electronics design are transistors and diodes which have proven to be reliable and cost effective per Bendix and Collins experience.

6.3.2.4.2 Reliability Improvement Warranty (RIW) Investigation. A review of available F-111 Avionics and, in particular N-16 INS field performance data, was initiated. The purpose of this effort was to establish a basis from which to formulate a proposed reliability improvement warranty (RIW) MTBF for the MICRON INS.

#### 6.3.3 Maintainability

Life cycle cost studies were completed to provide guidelines for power supply redundancy (secondary rotor drop prevention) and module (SRU) size/value. The studies in both areas were accomplished using the July 75 stand-alone MICRON definition. Maintainability characteristics were varied from this configuration to define the various alternatives applicable to the questions in point. These values were input to the LCC model to determine cost sensitivities and potential savings. In all cases the recurring hardware cost to effect the alternative was not considered. The resultant guidelines were then used to evaluate specific design approaches by subtracting implementation costs from the predicted savings of that approach.

Replaceable module size (value) has a direct impact on spares and corrective maintenance costs. A larger number of lower priced assemblies decreases the cost of items in the repair pipeline. It also decreases condemnation costs in the event a module becomes beyond economical repair. Opposing these savings are increased spares management costs and more difficult fault isolation to the failed module. The

net effect for MICRON was evaluated by dividing some of the modules in the July 1975 stand-alone system. The module divisions used and predicted results are identified in Table 57. In summary this study showed that the reduced module sizes could have up to \$1,700 savings per system.

Sensitivity of the items listed in Table 57 to price and reliability was defined by also varying these parameters for the one and three unit power supply approaches. These results are graphed in Figure 91. This shows that if the goals of \$4,000 and 40,000 hr MTBF are met the module division no longer offers much advantage.

Secondary power drops caused by power supply failures may be reduced by either improving the primary failure rate or including redundant power sources and isolation circuitry. The latter alternative defeats itself to a certain extent, however, by generally increasing the primary failure rate and unit price. Figure 92 was developed to be used as a tool in selecting the best combination of these two approaches. As an example of how this curve may be used assume a 40,000 hr MTBF unit which causes two drops per failure. The curve shows that this is worse than a 10,000 hr unit with no secondary failures. However it is better than a 20,000 hr supply with one drop per failure.

All studies performed on MICRON to date showed that a Base Shop IMU repair and calibration maintenance philosophy is less costly than Depot Repair. This is due to the additional test equipment and other resources required at each base shop being more than offset by spares in a long depot pipeline. Because of these conclusions there was minor concern from time to time (based on experience with gimbale systems) that the lower skill levels and working conditions at the base shop might not really allow IMU repairs involving instrument replacement and calibration. One solution proposed was a single shop replaceable unit consisting of the instruments and all electronics associated with the calibration constants. This would allow a simple remove and replace function at the base shop deferring calibration and detailed repair to the depot.

An indication of the life cycle costs associated with a calibratable SRU alternative was developed. This was done by simply rearranging the July 1975 system data in the LCC model. The instruments and support electronics which affect calibration as defined for that system were arranged into one SRU. This approach does not consider any volume, weight, or additional price impacts which in reality will probably be required. Its purpose was only to provide insights into potential logistics costs and savings. The conclusion of the study was that a calibratable SRU concept does not offer LCC savings comparable to a total base repair and calibration maintenance concept. Quantitatively these savings are as follows compared to a total depot repair concept.

<u>Packaging/Maintenance Concept</u>	<u>LCC Savings per System</u>
Calibratable SRU	\$12K
Total Base Repair	18K

The physical constraints not quantified at this point also favored the total base repair approach. As a result the maintainability emphasis was continued toward hardware features allowing for ease of base maintenance.

TABLE 57. REDUCED MODULE SIZE IMPACT ON LIFE CYCLE COST

Proposed Design Change	Potential Dollar Savings from Design Change		
	Initial Spares	Average Cost Per INU Repair	Total Life Cycle Cost per System
Divide the Suspension Module Into Two Identical Modules	\$298,000	\$ 7.87	\$ 480
Divide the 2 SEU Modules into 4 Modules (3 types)	\$324,000	\$ 9.55	\$ 450
Divide the Power Supply Assembly into 3 Separate Plug-in Modules	\$226,000	\$26.49	\$ 786
<b>Total</b>	<b>\$848,000</b>	<b>\$43.91</b>	<b>\$1,716</b>

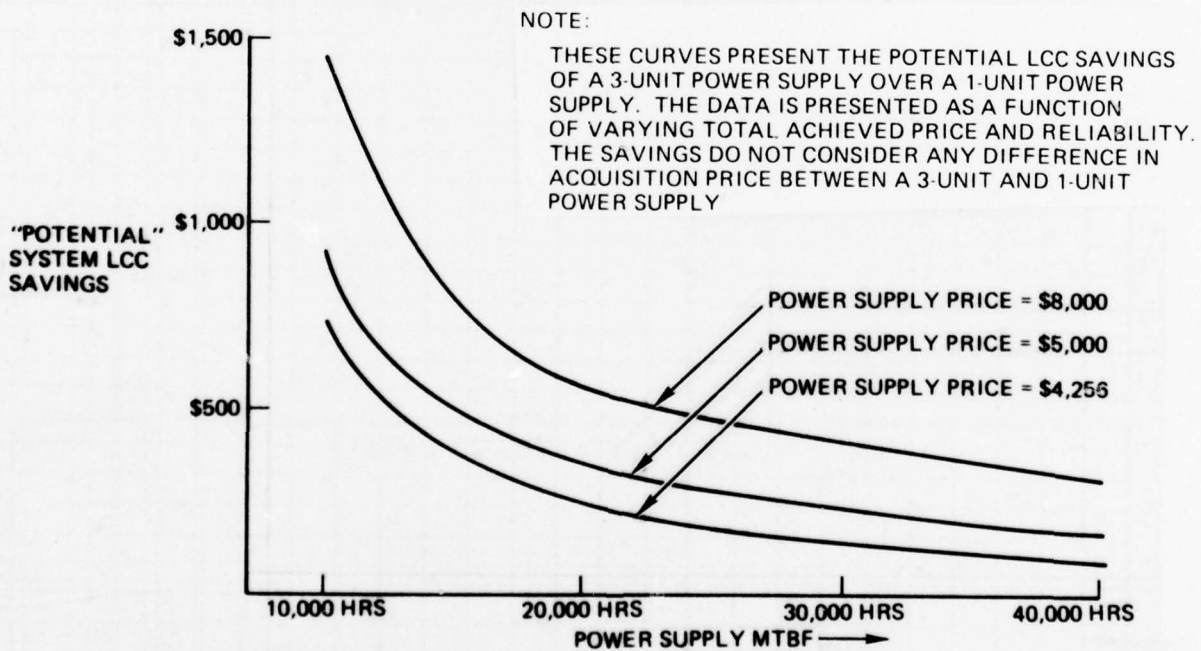


Figure 91. Power Supply Packaging Sensitivity Study

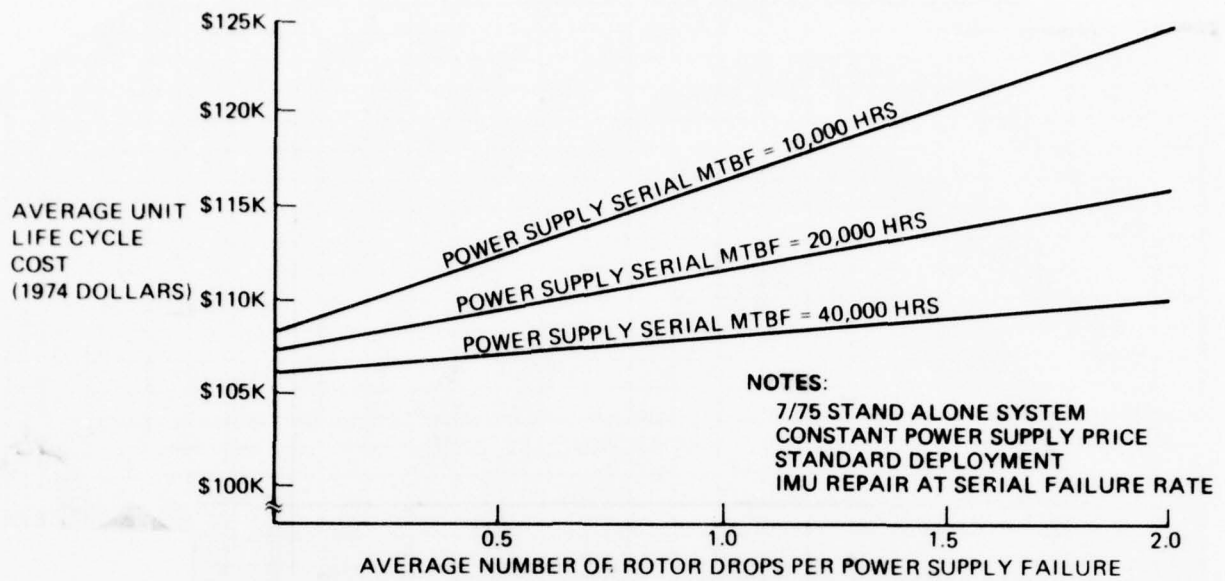


Figure 92. Power Supply Redundancy Guidelines

The sensitivity of the above dollar differences to varying achieved calibration stability periods and failure rates, was also investigated. The results are plotted in Figures 93 and 94. It is interesting to note that at a failure rate about 30 percent of that predicted, depot repair becomes the least costly but that a calibratable SRU approach never becomes the lowest.

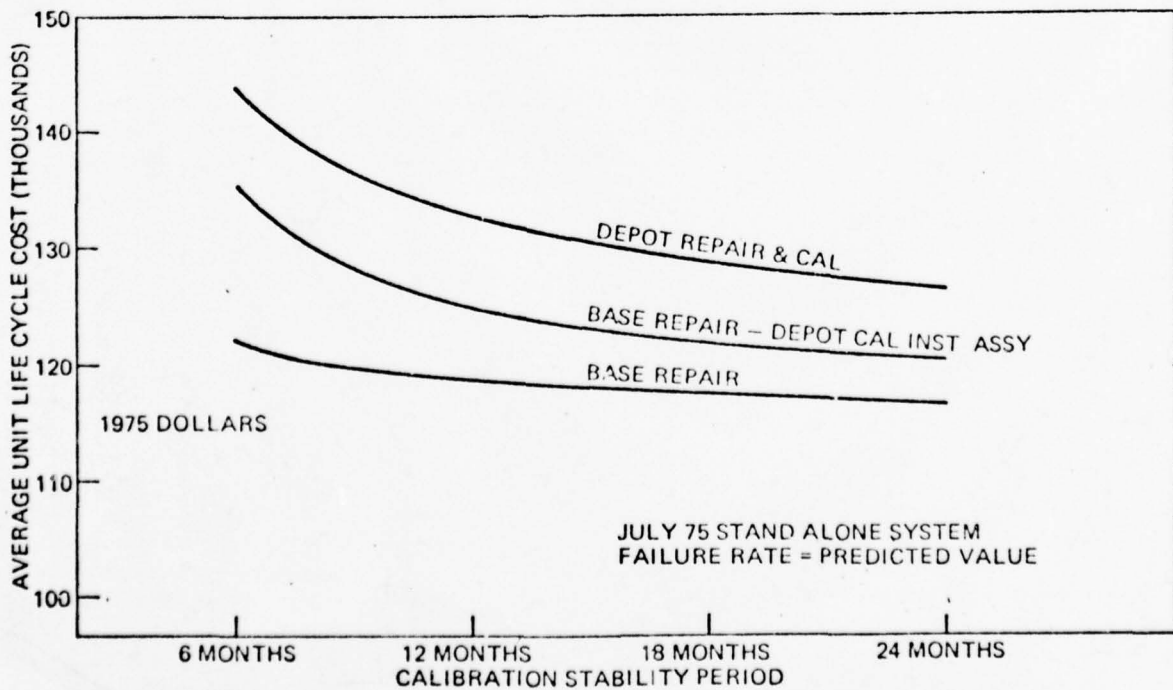


Figure 93. Life Cycle Cost vs Calibration Stability

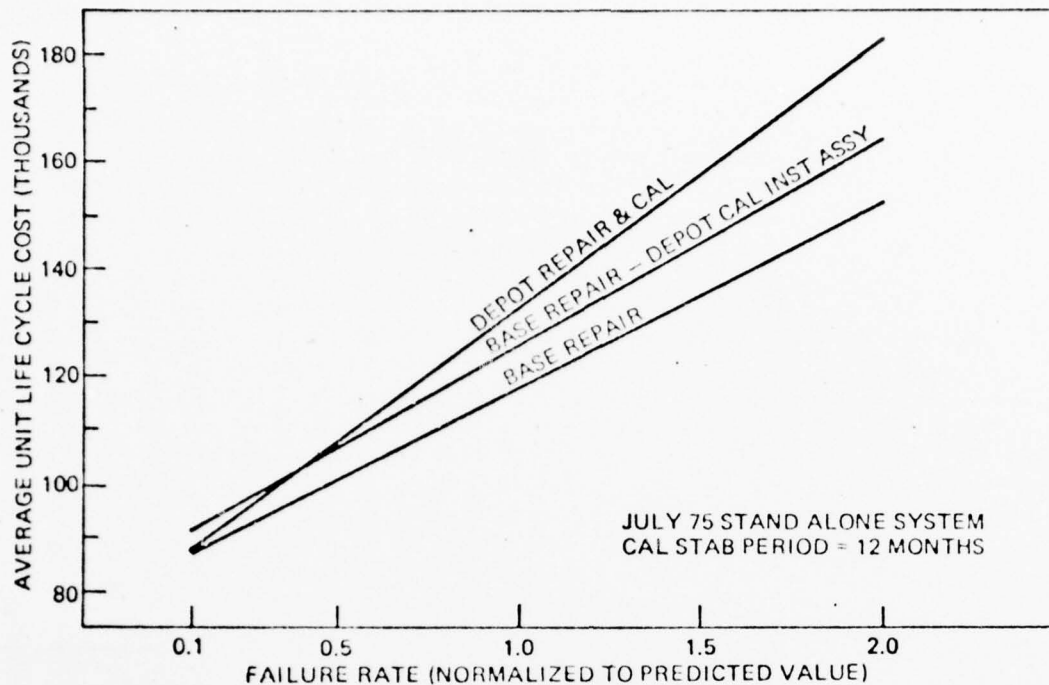


Figure 94. Life Cycle Cost vs Failure Rate

#### 6.4 TASK 5.4, PARTS PROGRAM

The purposes of this task were to support the producibility and reliability engineers through 30 September 1975 in the area of selecting parts for the EPM and to complete the development of the MOS A/D converter, spin motor control, and INU MOS chips initiated under Phase 2A.

##### 6.4.1 Parts Selection

Component Engineers supplied parts cost, application and reliability to the appropriate MICRON personnel in support of EPM design and parts procurement. Tradeoff of performance, cost, and reliability were evaluated and recommendations provided.

The 400 volt transistor chips (to be evaluated for use with the small gap gyro Charge Amplifier) were received from Fairchild and RCA and were subjected to performance probe tests. However, extensive testing, including packaged devices, was not performed, as planned, because of the late receipt of the RCA parts. The probe tests were satisfactory.

The electrical characterization of five different operational amplifiers (packaged versions) was completed and the data was submitted to Design Engineering to support final design and selection of parts.

Carriers for 16 beam integrated circuits were received and evaluation of the carriers commenced. Initial results indicated that the oversize hole for the device was creating beam electrical contact problems. Subsequent evaluation using automatic loaders with the parameter measuring equipment revealed relative movements of die, retaining glass, springs, etc. Further design modifications were recommended to improve these carriers.

#### 6.4.2 A/D Converter MOS Circuit

The A/D Converter MOS Circuit (P/N 65008) was designed to reduce the component count, reduce cost, and improve the speed and performance of the 13-bit A/D converter required for the system. The new MOS converter reduces cost by about \$170 from the previous configuration.

A functional block diagram of the A/D Converter MOS circuit is shown in Figure 95. The 65008 chip has a die size of 0.199 x 0.230 inches. There are 7,000 transistors on the chip. The process used is the LVN-5.

In the EPM System, a maximum of 63 analog signals can be converted to a binary code. The multiplexer is addressed and one of the 63 signals passes through the MUX to the A/D Converter. When the A/D is presented with a start conversion pulse, SC, the conversion begins. The switches in the A/D are sequentially set to a one and then they are evaluated by monitoring LVDT. Operation is as follows:

Before conversion begins SW1 is set to a one (-5V) and all others are set to a zero (+5V). Two bit times after the SC pulse arrives SW1 is evaluated, i. e. if LVDT is a zero then SW1 is reset to a zero. If LVDT is a one then SW1 remains a one. Next SW2 is set to a one. The following bit time it is evaluated and so on thru SW13. After all switches have been evaluated the MSB (SW1) is transferred directly to the output register. All other bits are inverted before they are transferred to the output register. The binary number in the output register is the binary equivalent to the analog voltage at the input.

There was one design and one redesign of the 65008 chip. After the original design, it was discovered that the active pull-up transistors (depletion mode) were too slow for the clocks to function properly at 125 kHz. It was also found that a FET was misconnected. The chip of the original design would not convert properly. It would convert only to even binary numbers.

Switch impedances were measured on the 65008 chip at 70°C and at room temperature. These data were used to compute an average switch impedance value to be used in making the A/D resistance ladder. The A/D Resistance Ladder Network was fabricated by Hallex Corp.

All of the A/D Converter hybrids have performed better than specification requirements. The maximum allowable standard deviation for linearity is 1.22 mV.

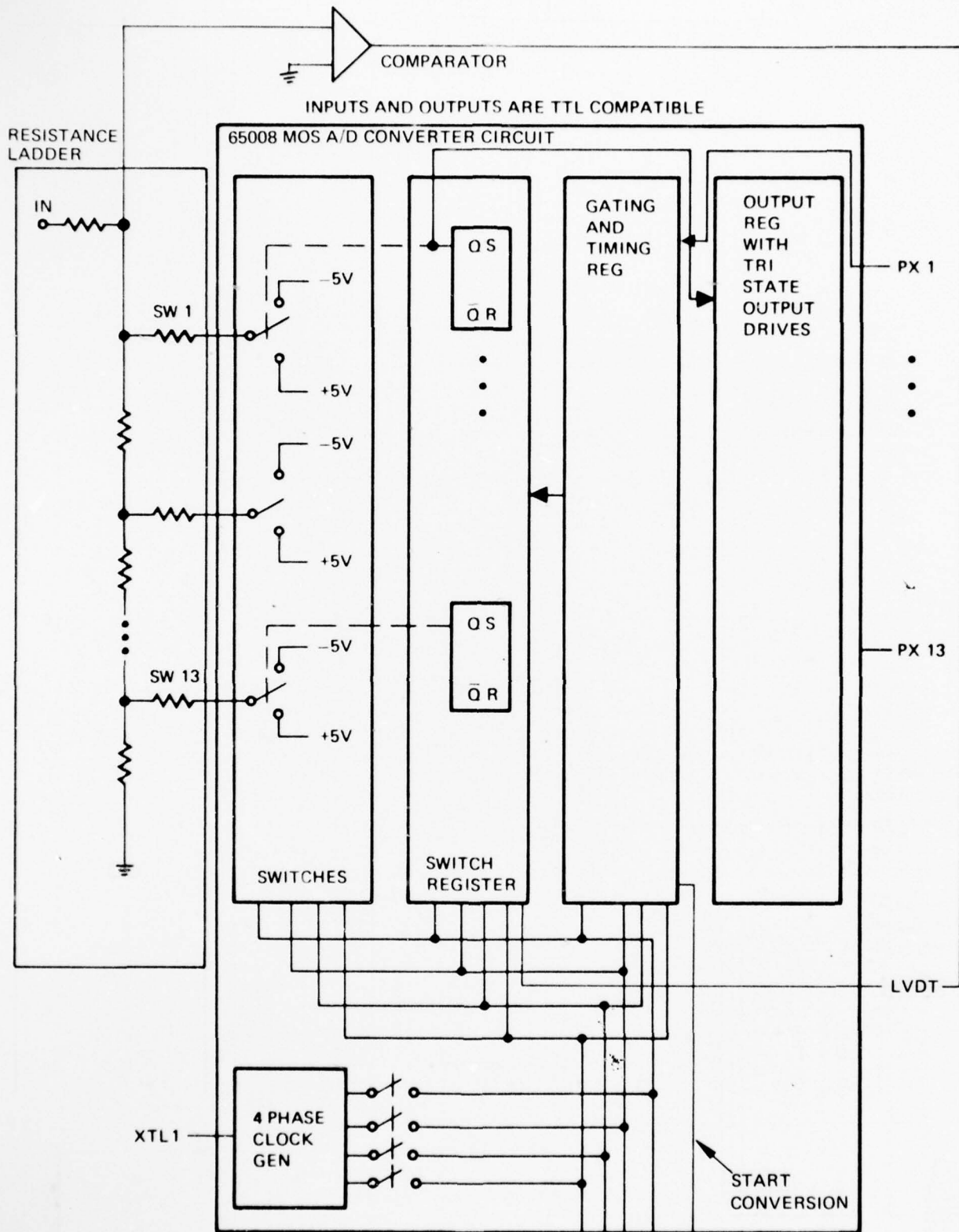


Figure 95. Functional Block Diagram of 65008 Chip

### 6.4.3 Spin Motor MOS Circuit

The Spin Motor MOS Circuit was designed to reduce the number of components and hybrid circuits required for spin motor control and for temperature control. The result is a reduction in cost and improvement in reliability. The cost savings is \$400 - \$500 per system with the MOS device utilized in both the temperature control and spin motor control applications.

A block diagram of the Spin Motor Control MOS circuit is shown in Figure 96. This device can provide the following output signals:

$$V_{mx} = A_{dex} + A_x (-\cos 2 \omega t) + B_x (-\sin 2 \omega t) + S_x \cos \omega t,$$

$$V_{my} = A_{dey} + A_y (-\cos 2 \omega t) + B_y (-\sin 2 \omega t) + S_y \cos \omega t,$$

$$V_{mz} = A_{dez} + A_z (-\cos 2 \omega t) + B_z (-\sin 2 \omega t) + S_z \cos \omega t.$$

The coefficients  $A_{dex}$ ,  $A_x$ ,  $B_x$ ,  $S_x$ ,  $A_{dey}$ ,  $A_y$ ,  $B_y$ ,  $S_y$ ,  $A_{dez}$ ,  $A_z$ ,  $B_z$  and  $S_z$  can be changed via the computer data bus. The output signal modulation can be deleted by tying the input modulation signals to DC levels.

The Spin Motor MOS circuit is fabricated with a bulk PMOS process (IPN-50, 20/30 D). The nominal value of the depletion devices is +5 v and -2 v for the enhancement devices. The minimum value of the field inversion voltage is 30 volts. The die size is 170 mils x 90 mils.

Several redesigns were required to improve yields and reduce the width of a transient spike that appeared on the output which was about 7 microseconds wide. The transient resulted in signal distortion in the polhode damping mode. The problem was alleviated by providing a better driver for the most significant bit to speed up the switching time. The width of the transient spike was reduced to one microsecond which is satisfactory.

Fifty MOS devices were packaged and test results showed that the Spin Motor MOS Circuits (65010) meet system requirements.

### 6.4.4 INU MOS Circuits

This effort covered the design, fabrication and test activity of MOS/LSI devices which were identified during the Phase 2A contract as contributors to significant cost reductions. These devices were:

1. Timing and Reference Generator Control (TRGC), later redesignated as MUM and EMA Timing Generator (METG)
2. Counter and Sequencer (CASC)
3. Quasi Reference Generator (QRFG)
4. Direct Memory Access Control (DMAC).

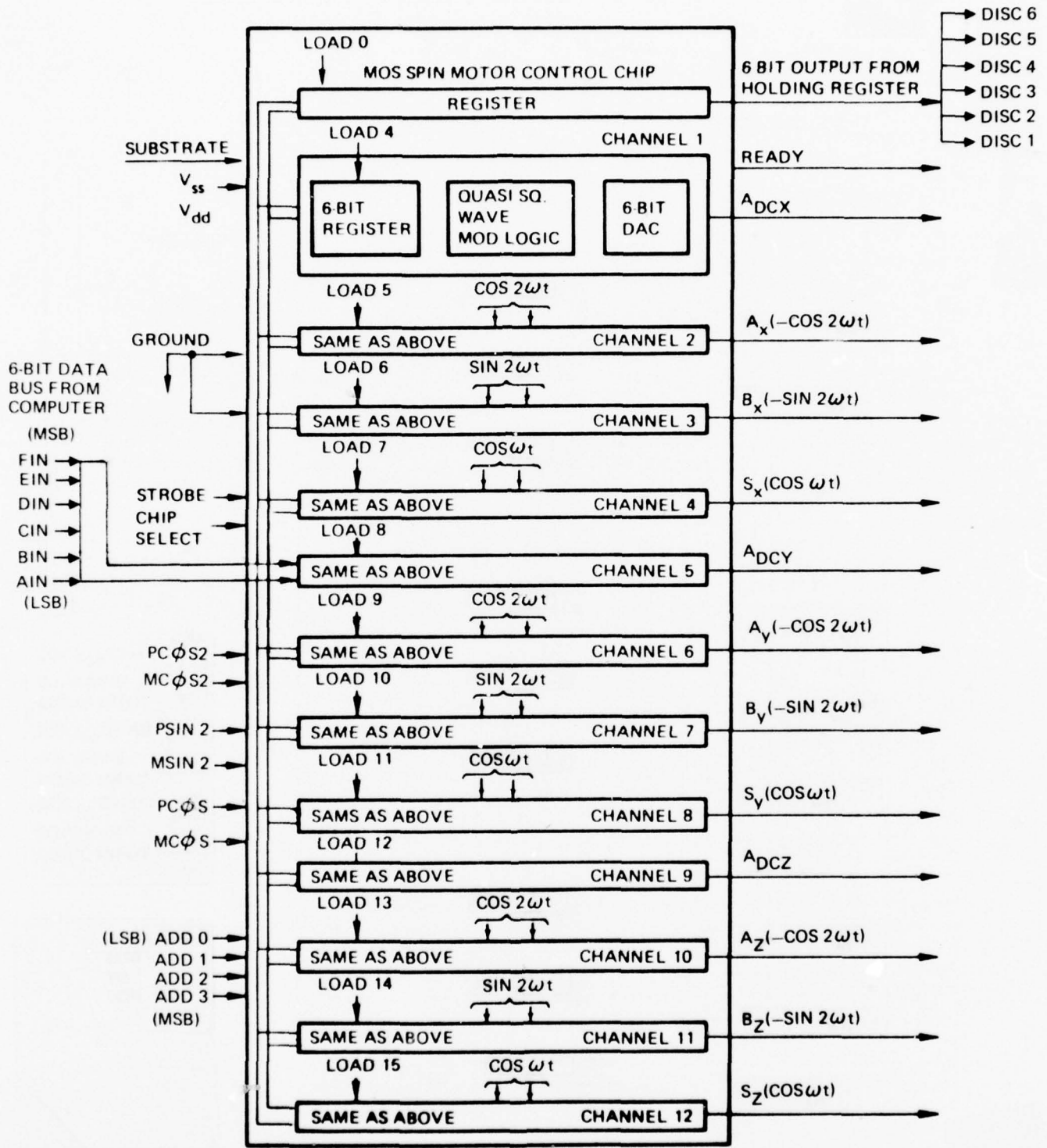


Figure 96. Functional Block Diagram of Spin Motor Control MOS Chip

The development of two of the MOS devices (CASC and DMAC) were stopped. In the EPM, these functions are implemented with bipolar MSI/SSI integrated circuits. This decision was made to eliminate the high schedule and cost risk which would have resulted from premature commitment of these functions to LSI design.

The remaining two devices were designed, fabricated and tested. Block diagrams of the METG and QRFC devices are shown in Figures 97 and 98, respectively.

The METG chip provides the brake control logic, signals which drive the X, Y, and Z accelerometer integrators, MUM Demod timing controls, and EMA timing pulse trains. The logic in this device consists primarily of frequency dividing counters used to generate fixed frequencies and timing signals. The 1 MHz clock frequency is divided down to provide outputs of 33-1/3 kHz (square wave), 40K PPS and a 3200 Hz signal. The dividing continues to 32 Hz. A strap input is used to select whether the 32 Hz or 64 Hz will be used for the fast cycle interrupt. Three other signals are generated with fixed delays from the selected fast cycle interrupt. These signals are used to control the sampling of the MUM demod signals. Finally, a small block of logic is included which is used to condition the asynchronous EMA signals to synchronous increment commands for the EMA counters.

The QRFG provides the quasi reference frequency generator for one ESG. Two devices per system are used. This logic consists of a 12-bit register and a 12-bit rate multiplier. The output from this section is a pulse train whose period is not generally symmetrical, but is a frequency whose average rate is equal to  $f_c X$  where  $f_c$  is the clock frequency (1 MHz) and  $0 \leq X < 1$ . In particular,  $X = N/4096$  where N is a 12-bit binary number  $0 \leq N \leq 4095$ . This pulse train is an input to a divide-by-16 counter whose output drives a modulo 24 counter. The outputs of the modulo 24 counter, together with  $\overline{SP}$ ,  $\overline{SN}$ , CM Discrete, and HEAT are used to generate sine, cosine waveforms. One device is used for each ESG frequency, and the SELECT GYRO 1/2 input selects which device will drive the spin motor control signals.

Because of the complexity of the METG and QRFG circuits, a recycling effort was anticipated and scheduled for both devices. The recycling was indeed necessary. Test results on devices from the first wafer lot indicated that each device had a logical design problem. The recycling permitted the incorporation of a design change on the METG which allowed the deletion of one phase locked loop circuit from the SEU No. 4 module. The recycling efforts were completed, initial deliveries of both device types were made in April 1976 as scheduled, and the devices were satisfactorily tested.

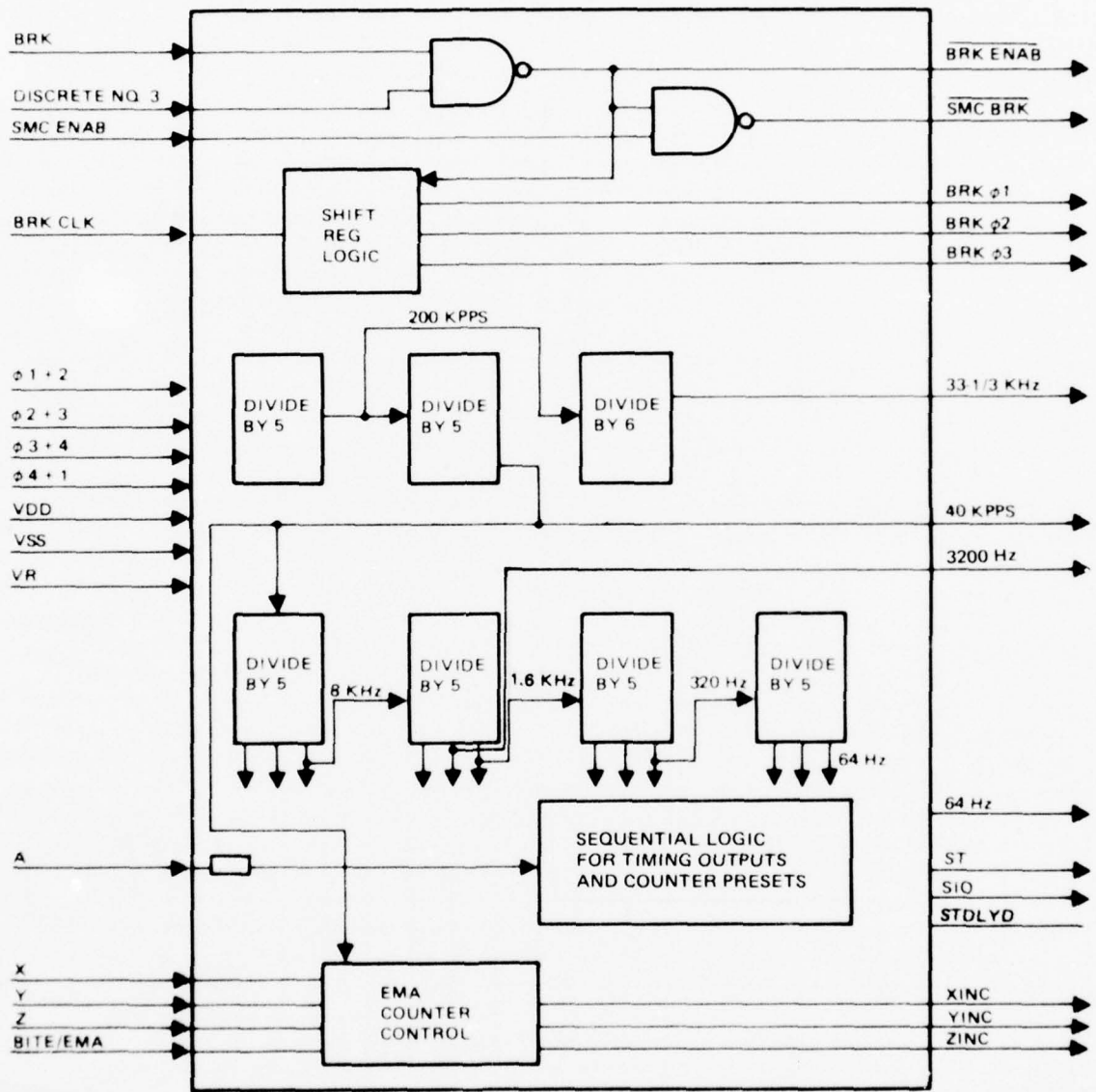


Figure 97. Block Diagram of METG Device

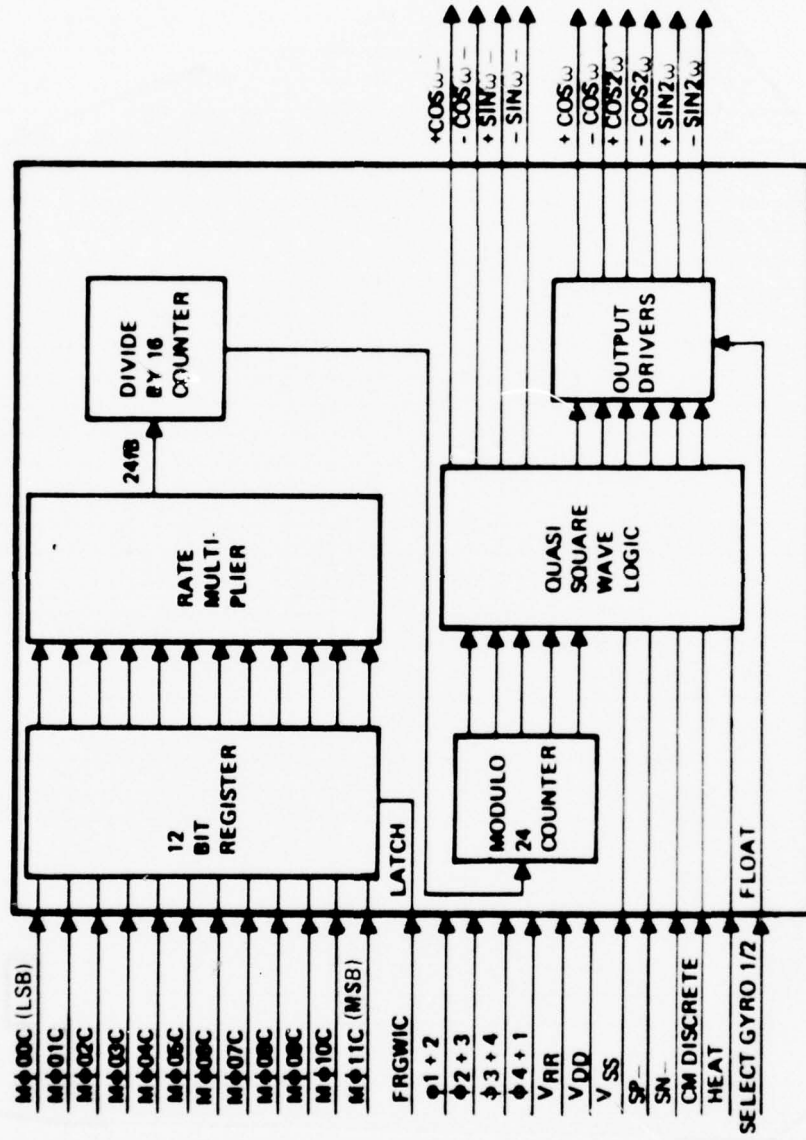


Figure 98. Block Diagram of QRFG Device

## SECTION VII

### TASK 6, DATA

The purpose of this task was to prepare and deliver data in accordance with the Contract Data Requirements List (CDRL).

The CDRL data items are shown in Figure 99. The numbers in the arrows represent the scheduled submittal dates for each data item. The shaded arrows indicate the completed items that were submitted to the Air Force. Figure 99 reflects the contract negotiations of Ref 5.

During Phase 2B, Autonetics submitted eighty-two data items. The actual submittal dates of these data items were as follows:

	<u>CDRL Item</u>	<u>Date Submitted</u>
A001	R&D Status Report	19 September 1975
		17 October 1975
		18 November 1975
		19 December 1975
		16 January 1976
		19 February 1976
		19 March 1976
		19 April 1976
		18 June 1976
		19 July 1976
		19 August 1976
		17 September 1976
		19 October 1976
		19 November 1976
		17 December 1976
		19 January 1977
		23 February 1977
A002	Program Schedule	19 September 1975
		17 October 1975
		19 November 1975
		19 December 1975
		16 January 1976
		19 February 1976
		19 March 1976
		19 April 1976
		19 May 1976
		18 June 1976
		19 July 1976
		19 August 1976
		17 September 1976
		19 October 1976
		19 November 1976
		17 December 1976
		19 January 1977
		23 February 1977

	<u>CDRL Item</u>	<u>Date Submitted</u>
A003	Contract Work Breakdown Structure	28 August 1975
A004	Data Accession List/Internal Data	28 May 1976 29 October 1976 24 November 1976 20 December 1976 14 January 1977 23 February 1977 24 April 1977 29 April 1977
A006	CI Development Spec (DPU)	14 November 1975
A007	CI Development Spec (INU)	14 November 1975
A008	System Specification	14 November 1975
A009	Cost Performance Report	26 September 1975 27 October 1975 25 November 1975 23 December 1975 27 January 1976 26 February 1976 26 March 1976 28 April 1976 26 May 1976 23 June 1976 29 July 1976 26 August 1976 29 September 1976 28 October 1976 29 November 1976 21 December 1976 27 January 1977 25 February 1977 30 March 1977 19 April 1977 20 May 1977 17 June 1977 22 July 1977
A00A	TRACE	27 May 1977
A00B	Interim Technical Report	28 May 1976
A00C	Final Technical Report (Draft) (Final)	27 May 1977 August 1977
A00D	General Plan/Procedure, MICRON MESG Test Plan EMA Test Plan EPM Integration Test Plan Test Plan for EPM (Part 1) Test Plan for EPM - (Parts 2, 3, 4 - Draft)	15 April 1976 30 April 1976 30 April 1976 3 February 1977 10 February 1977

	<u>CDRL Item</u>	<u>Date Submitted</u>
A00E	Process Spec, Second Source Rotors and Cavities	11 February 1976*
A00F	Material Spec, Second Source Rotors and Cavities	11 February 1976*
A00G	Drawings, MIL-D-1000 Form 3, Second Source Rotors and Cavities	11 February 1976*
A00H	Drawings, MIL-D-1000 Form 3, Automatic Cavity Grinder	9 February 1976
A00J	Contract Data Management Plan	20 November 1975

\*As part of the continued effort in support of second-source development for rotor and cavity fabrication, all documents required by CDRL Items A00E, A00F, and A00G were submitted to AFAL and ACO prior to the schedule 11 February 1976 submittal date. Therefore, no separate submittal of these items was made on this date. (Reference: Autonetics letter 76AN68557, dated 11 February 1976)

Fig 99

#

LINE

Figure 99. Phase 2B MICRON Data Schedule

**MICRON DATA SCHEDULE**  
DATA AS OF: August 1977

	1975												1976												1977											
	A	S	O	N	D	J	F	M	A	M	J	J	A	S	O	N	D	J	F	M	A	M	J	J	A	S	O	N	D							
A001 R&D STATUS REPORT	▲	▲	▲	▲	▲	▲	▲	▲	▲	▲	▲	▲	▲	▲	▲	▲	▲	▲	▲	▲	▲	▲	▲	▲	▲	▲	▲	▲	▲							
A002 PROGRAM SCHEDULE	▲	▲	▲	▲	▲	▲	▲	▲	▲	▲	▲	▲	▲	▲	▲	▲	▲	▲	▲	▲	▲	▲	▲	▲	▲	▲	▲	▲	▲							
A003 CONTRACT WORK BREAKDOWN STRUCTURE					▲																															
A004 DATA ACCESSION LIST/INTERNAL DATA																																				
A005 ABSTRACT OF NEW TECHNOLOGY (ANT)																																				
A006 CI DEVELOPMENT SPEC CRITICAL ITEM (DPU)																																				
A007 CI DEVELOPMENT SPEC PRIME ITEM (INU)																																				
A008 SYSTEM SPECIFICATION																																				
A009 COST PERFORMANCE REPORT																																				
A00A TRACE																																				
A00B TECHNICAL REPORT INTERIM																																				
A00C TECHNICAL REPORT FINAL																																				
A00D GENERAL TEST PLAN/PROCEDURE MICRON																																				
A00E PROCESS SPEC SECOND SOURCE ROTORS & CAVITIES																																				
A00F MATERIAL SPEC SECOND SOURCE ROTORS & CAVITIES																																				
A00G DRAWINGS MIL-D-1000 FORM 3 SECOND SOURCE ROTORS & CAVITIES																																				
A00H DRAWINGS MIL-D-1000 FORM 3 AUTOMATIC CAVITY GRINDER																																				
A00J CONTRACT DATA MANAGEMENT PLAN																																				

DRAFT

FINAL

**SECTION VIII**  
**CHANGES IN KEY PERSONNEL**

The following changes in key personnel were made during Phase 2B:

In November 1975, Mr. J. E. (Ed) Menzel was added to the MICRON Program Management Office as Assistant Program Manager. Mr. Menzel had held key project engineering and program management positions on Minuteman improvement programs. He had been responsible for new hardware and software development programs in these previous positions and this experience is directly applicable to MICRON Phase 2B development.

In November 1975, Mr. Jaak Jurison replaced Mr. Walt Thoennes as Supervisor of the MICRON DPU efforts. Mr. Thoennes was reassigned to supervise a new radiation hardened computer development effort. Mr. Jurison had long been associated with Autonetics MOS computer developments and is very familiar with the MICRON DPU. In view of Mr. Jurison's familiarity with the MICRON DPU, this change in the DPU supervisory responsibility did not cause any transient in the DPU efforts.

In January 1977, Mr. John D. Courtier replaced Mr. C. C. Whang, Jr. as supervisor of the MICRON System Design and Test Equipment Group. Mr. Whang accepted a position with the Space Division of Rockwell International. Mr. Courtier had long been associated with the MICRON program as the responsible engineer for all MICRON contract and capital system level test equipment. During this period he worked under the direction of Mr. Whang whom he replaced. As a result of this close association with Mr. Whang, he is familiar with the MICRON program history and decision making with respect to the MICRON system mechanization and packaging as well as the system testing activities and required test equipment.

272

CLASSIFICATION

## SECTION IX

### TRIPS, MEETINGS, AND CONFERENCES

On 7 August 1975, Mr. Ray Clark, U.S. Army ECOM, visited Autonetics for a program update. The agenda for this visit was as follows:

9:15	Phase 2B Overview	J. A. Schwarz
9:45	Getter Gyro	A. Gross
10:45	XN77 Status/Lab Tour	A. P. Truban
11:15	High Accuracy MICRON	J. A. Schwarz
1:30	USA/ECOM Participation in High Accuracy MICRON	G. E. Runyon
2:30	Ring Laser	P. Anthony

On 18 through 20 August 1975, Capt. Walter Peterson and Mr. David Pleva of AFAL/WPAFB visited Autonetics for the first Phase 2B informal design review. This meeting is discussed further in Para 6.1.1.3.1 of this report.

On 25 August 1975, Mr. Russell Shorey, Director, Acquisition and Support Planning, Office of Secretary of Defense, visited Autonetics for a general overview of the MICRON program. The agenda for this visit was as follows:

2:00	Arrival	D. A. Sackett
2:15	MICRON Review	J. A. Schwarz
2:45	ESG Factory Tour	H. L. Bump
3:15	MICRON Laboratory Tour	J. A. Schwarz
3:30	Cost of Ownership Team	K. J. Gibson F. R. Hall
5:00	Adjourn	

Due to numerous requests by the B-1 Division of Rockwell, SAC Headquarters, and ASD/RW, briefings were given on techniques to construct a high accuracy navigation system utilizing ESG. MICRON status briefings were given as background information to show growth to precision navigation systems. Although not MICRON funded, the following visits are related here due to their relationship to MICRON.

1. Mr. R. M. Schubert, Mr. G. W. Sargent, and Dr. W. West visited the B-1 Division of Rockwell and briefed the following personnel:

Buz Hello - President  
H. Raikland - VP Eng.  
L. Rose - Eng.  
J. Pierro - Eng.  
J. Paccassi - Eng.  
P. A. Otte - Eng.  
A. Wehmeyer - Eng.  
R. Frohman - Eng.  
E. Center - Procurement

2. Mr. G. W. Sargent and Mr. D. B. Freeland visited Washington, D. C. and briefed the following personnel:

AFSC

L/Col R. Lewis - XRTO  
L/Col Warner  
Col. Eddington  
Maj. R. Basso

Pentagon

Co. P. Fredrick, AFRDQSA  
L/Col M. Hatch, AFRDQSA  
Mr. R. O'Donohue, DDR&F  
L/Col R. Ziernicki - Air Staff  
L/Col C. Ewald - Air Staff  
L/Col R. Lavoie - Air Staff  
Col. E. DeAvies, USAF DDR&F  
L/Col T. Woods, F-16/AFRD  
Mr. D. McKanna, HQ. USAF

Mr. J. A. Schwarz attended AGARD's 30th Avionics Panel Technical Meeting on "Medium Accuracy Low Cost Navigation" September 8 through 11 1975 in Sandefjord, Norway. A paper on MICRON was presented to this meeting on September 8. Considerable interest was shown by the audience in the performance data on the N57A and in the low cost potential of the system. A contact was established with an electrostatic technologist (Mr. Joseph Taillet) from France which may lead to further information/insight into the breakdown voltage gradient of the vacuum in the rotor/plate gap. The implication from Mr. Taillet was that we should be able to significantly increase the voltage gradient above the 1 volt per micro-inch value without experiencing breakdown. If this is so, we may be able to increase the "g" capability of the MESH for higher "g" applications. Further discussion of this characteristic with Mr. Taillet is being pursued.

On September 23 ASD hosted a government/industry meeting on the Standard Navigation Specification. A. P. Truban, D. E. Shorridge, and J. A. Schwarz (along with Pete Pappas from our Dayton office) attended this meeting. The purpose of the meeting was for ASD to familiarize industry with how they expect to evolve the Std Nav Spec in an "open forum" method similar to the method employed on the ARINC Spec for commercial airline navigators. Our comments on the current version of the Std Nav Spec were prepared for submittal to ASD by October 24.

Mr. Dave Klein, of NAVAIR, visited the plant on 30 September 1975, primarily for the purpose of reviewing our ring laser gyro efforts. While here, he requested and received a tour of the MICRON laboratory. Points of discussion on MICRON were the Getter gyro status and the Holloman flight test results.

On 1 October 1975, Mr. T. K. Schuler and Mr. G. W. Sargent visited Brigadier General Patterson at ASD in Dayton, Ohio. The purpose of this visit was to discuss the applicability of MICRON to the F-16 Program and the Standard Navigator Program and associated schedules. AFAL personnel participated in this discussion.

Lt. Col. Roy White and Mr. Bob Baker, both of the U.S. Army at Ft. Monmouth, New Jersey, visited Autonetics on 2 October 1975. The discussion centered on the high-accuracy MICRON system and potential Army participation. It was generally agreed at this meeting that the rotated N77 system was the better alternate (relative to a rotated N57 system) for a high accuracy flight test demonstration. This alternate offers fast reaction and long-term stability capability as well as more compact system packaging. The rotated N57 alternate offers approximately a 5-month earlier demonstration, however, the Army, has no requirement for an earlier demonstration.

The Final Fee Evaluation Board Meeting and Design Review of the Phase 2A contract was held at Autonetics on 6 through 8 October 1975. This meeting was prepared and conducted on Phase 2A funding. The agenda for this meeting and the list of attendees is presented in Para 6.1.1.1 of this report.

A monthly informal review of the Phase 2B status was held on 10 October 1975. The AFAL and AFPRO attendees at this review were Mr. George Himes, Maj. Roger Brandt, Capt. Walt Peterson, Capt. Ron Janosko, Mr. Jin Chin, Mr. Phil Eignor, and Mr. Myron Pidhayny. The agenda for this review is presented in Para 6.1.1.3.2.

Mr. Ray Clark, from the U.S. Army ECOM, visited Autonetics on November 12, 1975 to discuss the high accuracy MICRON and possible Army participation in that development program. Subsequently a trip was made to Ft. Monmouth, New Jersey, by J. A. Schwarz, D. B. Freeland, and J. C. Barron (all of Rockwell) along with Capt. Peterson and Major Brandt (of AFAL) to brief the NAVCON and ECOM personnel on MICRON and further discuss Army participation in the high accuracy program. The Army personnel have indicated a desire to participate in the N77R system development this fiscal year and in the testing of that system next year. Final determination of their participation will depend on the outcome of their current search for GFY76 funding that they could apply to high accuracy MICRON.

On November 17, 1975 Mr. G. W. Sargent presented the general MICRON familiarization/status briefing to a group of British Royal Air Force visitors who were touring the country and reviewing current aerospace new technology developments.

On 8 December 1975, Dr. David Charvonia of DDR&E visited the plant for an update on several technology areas, including MICRON. He was given a general orientation briefing on the MICRON Program and the MESH technology. He was especially interested in the MESH information since he worked here with Joe Boltinghouse 10 to 12 years ago on the early ESG efforts.

A monthly informal Phase 2B status review was held at Autonetics on 9-11 December 1975. The agenda for this review is included in Para. 6.1.1.3.3 of this report. The agenda included some non-contractual efforts (RLG, N77, etc) at AFAL's request. The AFAL attendees at the review were Major Brandt, Major Raroha, Capt. Peterson, Capt. Janosko, and Mr. Phil Eignor.

A group of Aerospace Corporation personnel visited the Anaheim facility on 12 December 1975. The purpose of the visit was to get an update of the MICRON program and other programs/technologies as they might relate to the Interim Upper Stage (IUS) Program. They were given an overview briefing, shown through the laboratory, toured through the MESH factory, and given a detailed briefing on the MESH suspension electronics. Considerable interest seems to have been generated at Aerospace Corporation in MICRON for IUS.

On 8 January 1976 Mr. J. A. Schwarz visited Washington, DC to update and/or acquaint several DoD offices with current MICRON Program status. Lt. Col. Bosking and Lt. Col. Johnson in the Department of the Army were acquainted with the MICRON Program. Discussion centered mostly around the high accuracy system for Army applications. Lt. Col. Bosking's attitude was that if an order of magnitude accuracy improvement can be acquired for only a 10 percent increase in cost, the Army would buy the high accuracy version. However, on the opposite side of the coin, he indicated they would have significant headwinds in convincing their superiors to buy any piece of avionics that costs  $\approx$ \$50,000 for an Army aircraft.

Two U.S. Navy offices were visited. Capt. Seibert (OPNAV) was acquainted with MICRON and indicated an interest in being kept updated on the status. He was candid in stating that he didn't foresee Navy money going into MICRON development (in view of the Navy pursuit of RLG systems), but he seemed objective toward the RLG/MICRON programs and indicated that the Navy would buy production MICRONS for Navy programs if the MICRON development program is successful and if the system satisfies Navy requirements. Mr. McHale and Mr. Burns (both of NAVAIR) were updated on MICRON. Mr. McHale appeared interested in MICRON for the F-18 application. It turns out that the N77 IMU is almost exactly the same form factor as the Litton IMU (LN40) which Mr. McHale had a mockup of in his office and which appeared to be the planned INS for the F-18. Mr. McHale indicated that McDonnell Douglas is coming out with their F-18 INS spec in March and that we could obtain a copy from McDonnell Douglas then.

Col. Ziernicki and Lt. Col. Ewald (Hdqtrs USAF) were visited to let them know we had acted on their suggestion to acquaint Lt. Col. Bosking and Capt. Seibert (Col. Ziernicki's counterparts in the U.S. Army and U.S. Navy respectively) with the MICRON Program. While there, a brief update on program status was given to Col. Ziernicki and Lt. Col. Ewald.

On 9 January 1976, Mr. T. K. Shuler, Mr. J. N. Schmidt, Mr. G. W. Sargent, and Mr. J. A. Schwarz attended a meeting with ASD/RW, AFAL, ASD/ENA, and ASD/XR to present our plans for MICRON development up to production and to discuss how this fits with USAF planning. The outcome of the meeting was that ASD/RW indicated they were not recommending a 6.4 funded MICRON Program, but that they had to get that recommendation approved by Hdqtrs AFSC and Hdqtrs USAF before it became an AF position. In subsequent USAF only meetings on this subject on 29 January 1976 ASD/RW was apparently unable to sell their recommendation. The outcome of the 29 January 1976 meetings was to postpone a decision on this matter for a few months.

Mr. Lew Jobe has recently been assigned as a technical representative of Autonetics in the Dallas-Ft Worth area. He visited the plant 22-29 January 1976 for a technical acquaintance with the MICRON Program. Mr. Jobe will represent MICRON to General Dynamics, LTV, and others in that area. He will also help interface with Boeing, Wichita, and McDonnell-Douglas, St Louis as required.

On 9 February, Mr. K. J. Gibson and Mr. J. A. Schwarz participated in a meeting at Oklahoma City Air Logistics Center. Capt. Peterson, AFAL, also participated as did representatives of AGMC, hdqtrs AFLC, and OC/ALC. The purpose of the meeting was to provide coordination toward AFLC participation in the MICRON development programs. MICRON overview presentations were made as well as a MICRON Cost of Ownership/maintainability presentation. OC/ALC made presentations regarding some of their current programs/concerns. The result of the meeting was agreement that OC/ALC would support MICRON. Mr. Robert Callaghan will be our point of contact at OC/ALC. This will provide MICRON with:

1. An AFLC sounding board for our logistics/maintenance philosophy and considerations
2. A means to get AFLC comments on logistics related documentation
3. AFLC inputs to our life cycle cost parameters in our model
4. A means to keep abreast of maintenance/support problems on other fielded INS's so we can avoid the same mistakes on MICRON that the AF is experiencing on current systems

A monthly status meeting was held on 10, 11, and 12 February 1976. The list of attendees and agenda for this meeting is covered in Para. 6.1.1.3.4 of this report.

Dr. Eppers, Director of AFAL, visited Autonetics on 17 February 1976. A brief overview of Phase 2B status as well as IR&D program status was presented. Included in his agenda was a MICRON System Lab tour and an MESH fabrication area tour.

On 27 February, Mr. Sid Wright of Martin Marietta Corp (Denver) visited Autonetics to discuss the IUS program. MICRON overview and background information was presented as well as detailed discussions of the MESH. The same lab tours as Dr. Epper's (above) were included.

Systron Donner personnel visited Autonetics on 27 February to discuss potential application of their accelerometer to MICRON and to discuss a sensor package for use with MICRON to satisfy the Electronically Agile Radar requirements. Further discussion in both areas is expected.

Colonel Bush, Commander of AGMC, visited Autonetics on 3 March 1976. While here, he was briefed on many of our programs, including MICRON. A general overview of MICRON was presented and a system lab tour was conducted.

On 11 March 1976, Mr. David Kahn of the Institute for Defense Analysis, visited Autonetics. He is conducting a study for DoD on the exportability of various technologies/systems. MICRON is one of the systems/technologies he is considering in his study. He had previously provided us with a copy of his preliminary report. In this preliminary report, he implied that the only export allowable would be technical papers on MICRON and that no export of hardware (either separately or in a weapon system) would be allowed. Mr. Kahn was here to solicit our ideas and opinions on the exportability of MICRON and indicated that the preliminary report contained only "sample" information rather than his recommendations. We recommended that MICRON export be allowed both separately and in weapon systems. Further we recommended that MICRON repair be allowed in friendly foreign countries under the constraint that the critical gyro parts (rotors and cavities) not be released for fabrication in foreign countries. It is felt that this approach would maintain adequate control of the MICRON hardware since the rotor and cavities are significantly advanced in design, fabrication, and processing technology such that it would be many years, if ever, before any foreign country could produce adequate replacement parts. This approach should be acceptable to both the U.S. and the foreign countries since a dual source capability already exists (Northrop and Rockwell). It is not known how many of our recommendations will be accepted by Mr. Kahn, but he seemed receptive to our thoughts and rationale.

On 16 March Capt. Sandlin and Capt. Krumm, of CIGTF, were here for an orientation to the N77, N77R, and EPM hardware and planned flight test schedules. They were familiarized with the various hardware configurations by briefings, drawing review, and hardware/lab tours. CIGTF has contacted Air Training Command (ATC) regarding the training class we will conduct for the CIGTF test personnel prior to them flying our hardware. Since this visit, ATC has contacted us for coordination of the contract to cover the training class. Capts Sandlin and Krumm are to identify the CIGTF test engineer for us to coordinate with regarding what interface drawings, etc, CIGTF will need prior to system delivery.

Mr. David Kaye, from Electronics Design magazine, visited Autonetics on 19 March to review the status of several of our programs, including MICRON.

On 1 April 1976 several Cubic Corporation personnel were at Autonetics to explore the possibility of Cubic providing the warranty repair/maintenance of future MICRON RIW contracts. This possibility is being explored since Cubic has provided this type of effort on other programs.

On 5 April, Mr. Bill Storey, Director of Tactical Systems in DDR&E, was briefed on the MICRON program, its status, and its potential applications. This briefing was at Mr. Storey's request for an update since he recently moved into his current job and since the MICRON program was in a division of Autonetics which Mr. Storey was vice-president and general manager of a few years ago.

F-4 INS replacement discussions were held on 5 and 6 April at Autonetics with Capt. Ron Janosko and Mr. Dave Pleva (from AFAL), Capt. Neil Thomas (PRAM office), Mr. Tom Summers (Ogden ALC), and Capt. Carl Moore (AFPRO) in attendance. The discussion topics included (a) F-4 requirements and interface information, (b) potential schedules for high accuracy MICRON, and (c) the content of a potential study of incorporation of MICRON into the F-4. MICRON system laboratory and MESH factory tours were also included.

On 7 and 8 April a Phase 2B informal monthly status review was conducted. Capt. Ron Janosko, Mr. Phil Eignor and Mr. Dave Pleva attended from AFAL. Lt. Col. John Pasalevich, Capt. Carl Moore, and Mr. Joe Caldwell attended from AFPRO. The agenda for this design review is given in Para. 6.1.1.3.5 of this report. It was during this meeting that the decision to rotate the IAU was made in order to meet the accuracy requirements of the contract and to better match the Standard Navigator Specification requirements.

On 7 April, Capt. Warzynski, of SAMSO, visited the Autonetics facility to discuss the MICRON approach to electronic parts and the MICRON DPU. He was interested in updating himself on the MICRON approach in these areas for his consideration in laying out plans for the SAMSO ACT I computer program.

Mr. Cliff Loomis and Mr. Steve Jackson, of the USAF Standard INS Procurement Agency, visited Autonetics on 13 and 14 April. Since their primary interest was toward production plans and capabilities for MICRON, almost the entire visit was spent on lab and production facility tours. The tours included were: MICRON System Laboratory, MESH fabrication area, Production Inertial Instrument Factory, Production INS Factory, Irvine Electronics Production Facility, and the Military MOS/LSI Facility. Presentations were made on the Maine Facility and West Virginia Facility since they are not conveniently available for a tour.

Mr. Hy Shulman, Mr. Anthony Robinson, and Mr. Ted Garber, of Rand Corporation, visited Autonetics on 14 April. While here they were briefed on both MICRON and Minuteman programs. The MICRON briefing was an overview type briefing including high accuracy.

On 22 April Dr. Parker, Deputy Director of DDR&E, visited Autonetics for update/discussion on many of our programs. The only MICRON related portion of his visit was approximately 5 minutes spent going quickly through the MICRON System Laboratory.

On 28 April Mr. Jerry Schwarz, Mr. Ed Menzel, Mr. Lowell Renold, and Mr. Fred Langan visited WPAFB to discuss our response to the 22 April PCO letter. Mr. George Himes, Mr. Ron Ringo, Major Roger Brandt, Capt. Ron Janosko, Mr. Phil Eignor, and Mr. Dave Pleva attended the meeting for the Air Force. Most of the AFAL concerns have been answered as a result of our 27 April response letter and this visit to WPAFB. Two action items resulted from this meeting. The first action item was to identify the quantities of each type of government hardware listed in our 27 April response letter. This action item was completed on 4 May. The other action item was to provide written information explaining why a strapdown inertial system has worse accuracy performance than a gimbaled inertial system during the first hour of free inertial navigation mode. Dr. John Pinson, Chief Scientist, generated the answer to this action item in May.

Mr. Fred Corey, Mr. Bob Baker, and Mr. Merrill Stone of the Northrop (Hawthorne) F-18L and F-5 programs visited Autonetics on 13 May 1976 for an update on MICRON. A general status briefing was given along with tours of the MICRON system lab and the MESH rotor/cavity fabrication area.

On 17 May, Mr. J. A. Schwarz visited Air Staff in Washington D. C. to meet Maj Tom Swartz who is replacing Lt Col Chuck Ewald who is leaving for War College. A general MICRON Orientation briefing booklet and the MESH parts in the display case were reviewed with Maj Swartz.

Mr. Schwarz visited WPAFB on 18 May 1976. A meeting was held with Capt Ron Janosko (AFAL), Capt Neil Thomas (PRAM office), and Mr. Tom Summers (Ogden ALC) regarding the possibility of retrofitting MICRON into the F-4 fleet as a life cycle cost savings approach. The PRAM office is conducting a study to assess the feasibility of saving life cycle cost dollars by replacing the current F-4 INS. They indicated they would welcome a MICRON input on this subject and that they plan to consider MICRON in their study. Our input to the PRAM office is planned for approximately 10 June 1976.

A meeting was also held on 18 May with Mr. Ron Ringo, Maj Roger Brandt, and Capt Ron Janosko from AFAL to discuss the FDL AFTI-16 Program and the possibility of flight testing MICRON as a part of the AFTI-16 program. Mr. Ralph Shannon, Mr. Lew Jobe, and Mr. Schwarz reviewed a briefing on the AFTI-16 program and MICRON's potential involvement therein. As a result of this meeting, AFAL concluded they would talk to FDL to assess the advantages of MICRON being flight tested as a part of the AFTI-16 program.

On 25 May, Lt Gen Slay visited Autonetics. During this visit he was given short overviews on many programs. Mr. G. W. Sargent gave a 15 min presentation on MICRON during this visit.

Also on 25 May, Col Charles Hudson (AFAL) visited Autonetics. The MICRON portion of his visit consisted of attending the same briefing presented to Lt Gen Slay, visiting the MICRON system laboratory, and touring the MESH rotor and cavity fabrication area.

The MICRON Phase 2B Fee Evaluation/Design Review Meeting was held at Autonetics on 7 through 9 June 1976. The agenda for this meeting and the list of attendees is given in Para 6.1.1.2 of this report.

An informal monthly design review was held on 10 June 1976. Those in attendance from organizations other than Autonetics were: Maj. Brandt, Maj. Culler, Capt. Janosko, Capt. Lemon, G. Himes, R. Ringo, and P. Eignor of AFAL; Capt. Moore and M. Pidhayny of AFPRO; and C. Farrell and D. Hardy of AGMC.

Mr. Blake Reid and Mr. J. Ernest Smyth of the Canada Centre for Remote Sensing visited Autonetics on 16 June 1976. They were given an overview of the MICRON status and capabilities. The specific application the Canadian Government is interested in is an inertial reference for Canadian coastal surveying by airplane between land check points.

Mr. Ron Kaehr and Mr. Wiley Marsh from AFAL visited Autonetics on 16 June 1976. They were here to discuss ASALM with the Missile Systems Division of Autonetics. They had time for only a very fast (about 10 minutes) review of MICRON status.

Mr. Ron Duncan of Autonetics visited Lockheed Missile and Space Company, Sunnyvale, California on 17 June 1976. Lockheed is one of two main contractors on the Precision Emitter Location Strike System (PELSS); the other is Boeing. The program is in the study phase with various subcontractors looking at details of the communication and navigation requirements of the mother locator aircraft, the vectored strike aircraft and their guided weapons. Lockheed had requested that we brief the PELSS engineering staff on the capabilities of the high accuracy MICRON. Lockheed attendees were C. Wilson, J. Golden, K. Yenkere, J. Pope, D. Simcox, J. Krakar, J. Files, and J. Neenan.

Mr. Ron Duncan visited McDonnell Douglas in Long Beach, California on 21 June 1976. An updated medium accuracy, high accuracy and nuclear hardening MICRON briefing was presented. The audience was F. Wilson, B. Singleton, G. Nichols and D. Taylor.

Mr. E. Menzel, Mr. G. Runyon, and Mr. L. Renold visited AFAL on 23 June 1976. The purpose of the meeting was to discuss the Autonetics recommended accelerated integration schedule and several program alternatives subsequent to integration testing. The accelerated integration schedule was approved. The post integration effort was discussed but no decision reached. It is expected to be resolved by the end of July. Government attendees were Capt. R. Janosko, Maj. R. Brandt, Maj. G. Raroha, Mr. P. Eignor, Mr. D. Pleva, and Mr. G. Himes. Subsequent to these discussions the Autonetics personnel visited Mr. C. Loomis for a few minutes to discuss the MICRON EPM configuration planned for Holloman verification flight testing.

On 30 June 1976, Mr. J. Daniell, R. De Grey, K. Hoff, and F. Schenk from the Lockheed Skunkworks visited Autonetics. They were interested in discussing interfaces and performance analysis for a classified reconnaissance aircraft.

On 8 July 1976, Carl Pilnick of Telecommunications Management Corporation visited Autonetics to obtain information of a general nature on inertial navigation technology of the future. The information was requested to support a study, with which he is involved, on the future needs of the Department of Defense with inertial navigation technology which is under development. Information was provided to him on MICRON and Laser Gyros.

Capt Janosko visited Autonetics on 13 and 14 July 1976 for a monthly status review meeting. The agenda is contained in Para 6.1.1.3.7 of this report. Col. R. Ziernicki, Headquarters USAF, also visited Autonetics on 14 July 1976. Col Ziernicki received a general update on MICRON and several other programs.

On 22 July 1976 Ed Menzel, Gil Campos, and Keith Gibson visited Ogden ALC for a meeting on the F4 application of MICRON. Government attendees were Jack Woods OOALC/MMI, Harold Haddock OOALC/MME, Capt Neil Thomas ASD/PRAM, and Robert D. Davis ASD/PRAM. The purpose of the meeting was to answer questions on MICRON RIW planning.

On 20-23 July 1976, Jerry Schwarz and Milt Rupert represented Autonetics at the final Standard Navigator open forum meeting at Wright-Patterson AFB.

On 28 July 1976, Bill Bauder, Lewis Reid, Dick Watt and Jack Marlow from the Cubic Corporation visited Autonetics. The purpose of the meeting was to explore the possibility of having cubic design and fabricate the Preproduction Fire Control/Navigation Panels needed for the Standard Navigator verification testing.

On 9 August 1976, Mr. Bob Baker from the Army NAVCON office at Fort Monmouth visited Autonetics. He was briefed on the status of the MICRON program. Potential Army participation in some high accuracy development was discussed.

On 10 August 1976, Mr. Gil Campos, Mr. Dave Freeland and Mr. Chuck Homolka briefed the ASD PRAM office on the MICRON approach to the F-4 INS Retrofit Program. Lt/Col Evans (ASD/PRAM), Capt Neil Thomas (ASD/PRAM), John Kallish (ASD/ENA), and Capt Ron Janosko were present for the briefing.

On 11 August, Capt Ron Janosko and Mr. Phil Eignor visited Autonetics for a monthly status review meeting. The agenda is contained in Para 6.1.1.3.8 of this report.

On 24 August 1976 Mr. Bob Norris and Mr. Bill Cowell from Boeing Seattle visited Autonetics. While here on Minuteman Program business, they were given a general MICRON Program Status.

On 8 September 1976, Messrs. J. A. Schwarz, J. E. Menzel, G. E. Runyon, and L. C. Renold met with AFAL and the contracting officer at Wright-Patterson AFB. The purpose of the meeting was to discuss restructuring the remainder of the Phase 2B contract.

On 9 September, Mr. J. A. Schwarz and Mr. D. B. Freeland visited ASD Engineering to present a MICRON program overview/update. Mr. Schwarz and Mr. Freeland also visited AFAL/Mr. L. C. Loomis to discuss Standard Navigator CIGTF system requirements.

On 16 September, Capt. Jack Krumm, Capt Scott Richey, and Mr. Pete Zagore from Holloman AFB visited Autonetics. They were given a briefing and lab tour to familiarize them with the hardware to be delivered in January 1977.

On 21 September, Mr. Bob Baker and Mr. John Niemela of the U.S. Army at Ft. Monmouth visited Autonetics to discuss a potential Army contract. The effort involved would be hardware and software development to flight test an EPM with a TACAN and central computer in an integrated system configuration in an Army aircraft.

On 30 September, three personnel from AFAL Fire Control (including Capt. W. Peterson) visited the MICRON lab for a status update of MICRON.

On 21 October 1976, an informal design review was held at Autonetics. The agenda and list of attendees is given in Para 6.1.1.3.9 of this report.

On 3 November 1976, Navy personnel (Lt Commander Mc Allister, Lt. Readhead, Lt Southworth, Lt Wise, Chief Buttrum and Chief Teemly) from the carrier Constellation toured the Autonetics facility. They were given a 30 minute MICRON familiarization briefing and a system lab tour.

On 4 November, Ling Temeo Vought of Dallas (C. McLean, L. McNulty, L. Shipley, M. Barnett and V. Ginnings) visited Autonetics Missile Systems Division. They were given a 15 minute MICRON overview and system lab walkthrough.

On 11 November, Messrs J. A. Schwarz and G. W. Sargent visited Col Dave Dempster. Capt Harvey Brock, Cliff Loomis, and Bill Laubendorfer were also present. The purpose of the meeting was to review Autonetics plans, questions, and problems regarding MICRON and the Standard Navigator Program. Subsequent to that meeting, a brief visit was made to AFAL, Capt Ron Janosko.

On 15 November, a Royal Air Force Team visited Autonetics for a briefing on many programs/topics. They were cleared through the State Department and Department of Defense. They had asked that a MICRON briefing be on the agenda.

On 18 November, Boeing IUS personnel were here surveying finalists in the IUS guidance system competition. They were briefed in the morning. Discussions were held in the afternoon answering numerous questions they had.

On 29 November, D. Freeland and J. Pinson visited Northrop to discuss MICRON applications for the F-5 and F-18.

On 8 December 1976, McDonnell-Douglas personnel and John Perdzoek from the Flight Dynamics Laboratory visited Autonetics. The purpose was to discuss the Air Force Multi-Function Inertial Reference Assembly (MIRA). While here, they asked for and were given a 30 minute MICRON status briefing.

On 14 December, Mr. G. W. Sargent visited Colonel Eaton (DOD/I&L). Col Eaton had requested a discussion of MICRON and how it relates to the Standard Nav program/Trident program. While on the East Coast, Mr. Sargent visited Grumman Aerospace Corporation and Fairchild Industries on 15 December. He provided a briefing update on MICRON status.

On 14 and 15 December 1976, an informal design review was held at Autonetics. The agenda and list of attendees is given in Para 6.1.1.3.10 of this report.

On 15 December, D. Freeland, S. Miller and R. Nason visited ASD/AEA. The purpose was to brief the Standard Nav Office on Autonetics logistics support experience/capabilities and to outline our support plans for the Standard Nav program.

On 21 December, Mr. Harry Downs (Holloman AFB) visited Autonetics. The purpose was to pick up interface/mechanization information on the EPM that will be going to Holloman for Standard Nav screening tests.

On 18 January 1977, a number of personnel from Northrop visited Autonetics for a technical evaluation of the MICRON Program. The purpose of this meeting was to provide a basis for Northrop's evaluation of MICRON application to the F-5 and F-18.

On 19 January, Mr. Bill Laubendorfer from ASD/AE visited Autonetics. He was provided a technical briefing and status update on MICRON.

On 20 January, Mr. Macki and Mr. Zuzolo from Republic Division of Fairchild Industries visited Autonetics. They were given a briefing on MICRON production plans and logistics approach.

On 20 January, Mr. Jerry Schwarz and Mr. Dave Freeland visited the Standard Navigation office (Major Rauley). The purpose of the meeting was to provide Autonetics' recommendation for the KC-135 program.

On 26 through 28 January, ten personnel from Holloman AFB visited Autonetics. They were provided a training course on MICRON in preparation for subsequent Standard Nav testing at Holloman.

On 10 February, Mr. J. A. Schwarz, J. E. Menzel and L. C. Renold of Autonetics visited AFAL Wright-Patterson AFB. The purpose of the visit was to discuss closing down the contract efforts.

**SECTION X**  
**PROGRAM SCHEDULE**

The MICRON Phase 2B Program Schedule is shown in Figure 100. The symbols used are the standard milestone symbols as shown in Figure 101.

The Figure 100 schedule reflects the contract negotiations of Ref 5; the duration of the line item tasks marked "\*" were shortened per Ref 5, the line item tasks marked "\*\*\*" were deleted per Ref 5.

*LINE*

Figure 100. Program Schedule (Sheet 1 of 6)

"FORGING MILITARY SPACEPOWER"

PROGRAM SCHEDULE	SYSTEM (Prj/act) NUMBER 666A	SUBSYSTEM MICRON PHASE 2B	TYPE OF SCHEDULE	AS OF DATE August 1977				COMPLETION DATES			
				1977	1978	19					
L I N E	PRIOR SCHEDULE DATES	FY 19 75	CY 19 75	FY 19 76	CY 19 76	FY 19 77	1977	1978	19		L I N E
		J F M A M J J A S O N D	J A S O N D J F M A M J J A S O N D	J F M A M J J A S O N D	J A S O N D J F M A M J J A S O N D	1 2 3 4	1 2 3 4	1 2 3 4	1 2 3 4		
1	TASK 5.0 SYSTEM MANAGEMENT										1
2	PROGRAM MANAGEMENT										2
3	PROGRAM MANAGEMENT SUPPORT *										3
4	PROGRAM MANAGEMENT SUPPORT *										4
5	PROJECT ENGINEERING SUPPORT *										5
6	PROJECT ENGINEERING SUPPORT *										6
7	FEE EVALUATION REVIEWS *										7
8	PROGRAM PLAN (EVENT NETWORK)										8
9	ASSOCIATE CONTRACTOR SUPPORT										9
10	COORD/SUPPORT ASSOCIATE CONTRACTORS FOR MESSG *										10
11	COST OF OWNERSHIP										11
12	PHASE 2A STUDIES CONTINUED										12
13	PARTS PROGRAM										13
14	PHASE 2A PARTS PROG CONT'D										14
15	DEVELOP MOS DEVICES										15
16	TASK 1.0 PRIME MISSION PRODUCT										16
17	DEVELOP MICRON SYSTEM SPEC										17
18	INU DEVELOPMENT										18
19	INU ERROR ANALYSIS & ERROR BUDGET										19
20	AUTHENTICATION										20
21											21
22											22
23											23
24											24
25											25
26											26
27											27
28											28
29											29
30											30
31											31
32											32
33											33
34											34
35											35
36											36

AFSC FORM MAR 67 103

PREVIOUS EDITION OF THIS FORM WILL BE USED UNTIL STOCK IS EXHAUSTED.

AFSC AATB WASH. D.C.

78

Figure 100. Program Schedule (Sheet 2 of 6)

*100*  
*100*

*113*

"FORGING MILITARY SPACEPOWER"

L I N E	PROGRAM SCHEDULE	SYSTEM (Project Number) 666A	SUBSYSTEM		TYPE OF SCHEDULE				AS OF DATE				COMPLETION DATES																										
			MICRON PHASE 2B						August 1977																														
			FY 1975	FY 1976	FY 1977	1977	1978	19	19	19	19																												
PRIOR SCHEDULE DATES																																							
1	INU DEVELOPMENT (CONT'D)		J	F	M	A	M	J	J	A	S	O	N	D	J	F	M	A	M	J	J	A	S	O	N	D	1	2	3	4	1	2	3	4	1	2	3	4	1
2	DEVELOP INU CI SPEC																								2												2		
3	DEVELOP INU DETAILED DESIGN SPECS																								3												3		
4	MECHANICAL HOUSING UNIT (MHU)																								4												4		
5	DESIGN & DEVELOP																								5												5		
6	DESIGN & DEVELOP (SEU)																								6												6		
7	DESIGN & DEVELOP (PS)																								7												7		
8	FAB/TEST & SPARES (SEU)																								8												8		
9	FAB/TEST & SPARES (PS)																								9												9		
10	FAB/TEST & SPARES (EMA)																								10												10		
11	DESIGN & DEVELOP (ELEC)																								11												11		
12	DESIGN & DEVELOP (ELEC)																								12												12		
13	DESIGN & DEVELOP (ELEC)																								13												13		
14	DESIGN & DEVELOP (ELEC)																								14												14		
15	DESIGN & DEVELOP (ELEC)																								15												15		
16	DESIGN & DEVELOP (ELEC)																								16												16		
17	DESIGN & DEVELOP (ELEC)																								17												17		
18	DESIGN & DEVELOP (ELEC)																								18												18		
19	DESIGN & DEVELOP (ELEC)																								19												19		
20	DESIGN & DEVELOP (ELEC)																								20												20		
21	DESIGN & DEVELOP (ELEC)																								21												21		
22	DESIGN & DEVELOP (ELEC)																								22												22		
23	DESIGN & DEVELOP (ELEC)																								23												23		
24	DESIGN & DEVELOP (ELEC)																								24												24		
25	DESIGN & DEVELOP (ELEC)																								25												25		
26	DESIGN & DEVELOP (ELEC)																								26												26		
27	DESIGN & DEVELOP (ELEC)																								27												27		
28	DESIGN & DEVELOP (ELEC)																								28												28		
29	DESIGN & DEVELOP (ELEC)																								29												29		
30	DESIGN & DEVELOP (ELEC)																								30												30		
31	DESIGN & DEVELOP (ELEC)																								31												31		
32	DESIGN & DEVELOP (ELEC)																								32												32		
33	DESIGN & DEVELOP (ELEC)																								33												33		
34	DESIGN & DEVELOP (ELEC)																								34												34		
35	DESIGN & DEVELOP (ELEC)																								35												35		
36	DESIGN & DEVELOP (ELEC)																								36												36		

*78*

*6"*

*7*

Figure 100. Program Schedule (Sheet 3 of 6)

"FORGING MILITARY SPACEPOWER"

PROGRAM SCHEDULE	SYSTEM (P/N) NUMBER	SUBSYSTEM	MICRON PHASE 2B		TYPE OF SCHEDULE		AS OF DATE																							
			FY 19 75	FY 19 76	FY 19 77	19 77	19 78	19	COMPLETION DATES																					
LINE	666A		J	F	M	A	M	J	J	A	S	O	N	D	1	2	3	4	1	2	3	4	1	2	3	4	1	2	3	4
1	INSTRUMENT ASSY (CONT'D)																													
2																														
3	DESIGN & DEVELOP																													
4	(MECH)																													
5																														
6	FAB/TEST																													
7	(MECH)																													
8	FAB/TEST ROT. IAU																													
9	DEDICATED PROCESSOR UNIT (DPU)																													
10																														
11	CI SPEC																													
12																														
13	DESIGN & DEVELOP																													
14																														
15	FAB/TEST & SPARES																													
16																														
17	INPUT-OUTPUT UNIT (IOU)																													
18																														
19	DESIGN & DEVELOP																													
20																														
21	FAB/TEST & SPARES																													
22																														
23	FAB MESSG PARTS TO SUPPORT																													
24	2ND SOURCE																													
25																														
26	ROTOR & CAVITIES																													
27																														
28	MESG's (less Rotors & Cav)																													
29																														
30	INERTIAL NAV MOUNT																													
31	DEVELOP DETAIL DESIGN																													
32	SPEC																													
33																														
34	DEV/FAB/PROCURE																													
35																														
36	AUTHENTICATION																													

Figure 100. Program Schedule (Sheet 4 of 6)

"FORGING MILITARY SPACEPOWER"

L I N E N O	PROGRAM SCHEDULE	SYSTEM (Project) NUMBER 666A	SUBSYSTEM MICRON PHASE 2B				TYPE OF SCHEDULE	AS OF DATE August 1977																																		
			FY 1975	CY 1975	FY 1976	CY 1976		1977	1978	19	COMPLETION DATES																															
1	CONTROL/NAVIGATION PANEL(CNP)		J	F	M	A	M	J	J	A	S	O	N	D	J	F	M	A	M	J	J	A	S	O	N	D	1	2	3	4	1	2	3	4	1	2	3	4	1	2	3	4
2	DESIGN/MOD N57A CDU																																									
3	SOFTWARE DEVELOPMENT																																									
4	INU																																									
5	TEST STATION																																									
6	DATA ANALYSIS ON EPM SYSTEM	**																																								
7	INTEGRATION																																									
8	ELECTRONIC EVAL																																									
9	EPM INTEG PER PAR 4.2.1 TEST PLAN																																									
10	TASK 2.0 TEST & EVALUATION																																									
11	TEST PLANS																																									
12	DEVELOP TEST PLANS *																																									
13	DEVELOPMENTAL TESTS																																									
14	ROTOR & CAVITY																																									
15	NON DESTRUCT ROTOR & CAVITY *																																									
16	AUTHENTICATION																																									

98

6"

Figure 100. Program Schedule (Sheet 5 of 6)

100 (5410)

116

"FORGING MILITARY SPACEPOWER"

L I N E	PROGRAM SCHEDULE	SYSTEM (Project) NUMBER 666A	SUBSYSTEM MICRON PHASE 2B		TYPE OF SCHEDULE		AS OF DATE August 1977		COMPLETION DATES L I N E
			FY 19 75	FY 19 76	FY 19 77	1977	1978	19	
			PRIOR SCHEDULE DATES				1 2 3 4	1 2 3 4	
1	LABORATORY TESTS		J F M A M J J A S O N D	J A S O N D J F M A M J J A S O N D	J F M A M J J A S O N D	1 2 3 4	1 2 3 4	1 2 3 4	1
2									2
3	CONDUCT PER PARA. 4.2.1**								3
4	TEST PLANS								4
5									5
6	MOBILE TESTS								6
7									7
8	CONDUCT PER PARA. 4.2.1								8
9	TEST PLAN								9
10									10
11	CONTRACTOR FLIGHT TEST								11
12									12
13	TASK 3.0 SUPPORT EQUIPMENT								13
14									14
15	ENGINEERING TEST EQUIP								15
16									16
17	DESIGN/DEVEL/PROCURE								17
18	ENG'RG TOOLING & TEST								18
19	EQUIPMENT								19
20									20
21	INU TEST STATION (STS)								21
22									22
23	SPEC								23
24									24
25	DESIGN/DEVELOP								25
26									26
27	FAB/INTEG								27
28									28
29	REPAIR								29
30									30
31	PHASE 2A HDWE AS REQ'D								31
32									32
33	PHASE 2B HDWE AS REQ'D								33
34									34
35									35
36	AUTHENTICATION								36

78

6"

Figure 100. Program Schedule (Sheet 6 of 6)

PUB NO.

VOL NO.

FIG. NO.

PAGE No.

"FORGING MILITARY SPACEPOWER"

LINE	PROGRAM SCHEDULE	SYSTEM (Project) NUMBER	SUBSYSTEM				TYPE OF SCHEDULE	ASOF DATE				COMPLETE DATES																							
			MICRON PHASE 2B		CY 1976			August 1977																											
		666A	FY 1975	FY 1976	FY 1977	1977	1978	19	19	19	19																								
			J F M A M J J A S O N D	J F M A M J J A S O N D	J F M A M J J A S O N D	1 2 3 4	1 2 3 4	1 2 3 4	1 2 3 4	1 2 3 4	1 2 3 4																								
1	TASK 6.0 DATA		J	F	M	A	M	J	J	A	S	O	N	D	1	2	3	4	1	2	3	4	1	2	3	4	1	2	3	4					
2																																			
3	PREPARE & DELIVER DATA																																		
4	PER CDRL	*																																	
5																																			
6	INTERIM TECH REPORTS	*																																	
7																																			
8	FINAL TECH REPORT	*																																	
9																																			
10																																			
11																																			
12																																			
13																																			
14																																			
15																																			
16																																			
17																																			
18																																			
19																																			
20																																			
21																																			
22																																			
23																																			
24																																			
25																																			
26																																			
27																																			
28																																			
29																																			
30																																			
31																																			
32																																			
33																																			
34																																			
35																																			
36																																			

AFSC FORM 103

PREVIOUS EDITION OF THIS FORM WILL BE USED UNTIL STOCK IS EXHAUSTED.

AFSC AAFB WASH DC

Handwritten signature and number 666A

Handwritten number 1-2

Handwritten number 6













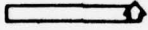
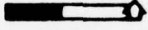
BASIC SYMBOL	MEANING
	Scheduled Completion
	Actual Completion
	Previous Scheduled Completion - Still in future
	Previous Scheduled Completion - Date passed
REPRESENTATIVE USES	MEANING
 	Anticipated Slip - Rescheduled Completion
 	Actual Slip - Rescheduled Completion
 	Actual Slip - Actual Completion
 	Actual Completion Ahead of Schedule
	Time Span Action
	Progress Along Time Span

Figure 101. Standard Milestone Symbols

## REFERENCES

1. Purchase Request No. FY11757510548, Attachment No. 1, Statement of Work, dated 16 July 1975, MICRON Phase 2B.
2. Micro Navigator (MICRON) Phase 2A, Technical Report, AFAL-TR-75-210, dated February 1976.
3. "SAMUS, A Program for State Space Analysis of Multisensor Systems," Autonetics Report No. T9-1735/501, August 1969. Vol 1, 2 and 3.
4. Purchase Request No. FY11757510548, Appendix I, Preliminary Development Specification, MICRON Inertial Navigation Unit, dated 16 July 1975.
5. Contract Modifications to MICRON Phase 2B, Contract F33615-76-C-1301, Autonetics Letter 77AN69052, dated March 11, 1977.
6. N. A. Carlson, "A Fast Triangular Formulation of the Square Root Filter," AIAA Journal, September 1973, pp 1259-1265.